CATALYTIC HYDRODEOXYGENATION OF DIBENZOFURAN IN A TRICKLE BED REACTOR: KINETICS, POISONING, AND PHASE DISTRIBUTION EFFECTS

by

Vito LaVopa

B.S.Ch.E., Tufts University
(1983)

M.S.C.E.P., Massachusetts Institute of Technology
(1985)

SUBMITTED IN PARTIAL FULFILLMENT

OF THE REQUIREMENTS OF THE

DEGREE OF

DOCTOR OF SCIENCE

IN CHEMICAL ENGINEERING

at the

MASSACHUSETTS INSTITUTE OF TECHNOLOGY

October 1987

Signature of Author_____
Department of Chemical Engineering
October 30, 1987

Certified by_____
Charles N. Satterfield
Thesis Supervisor

Accepted by_____
Robert C. Armstrong
Chairman, Departmental Committee on Graduate Students

CATALYTIC HYDRODEOXYGENATION OF DIBENZOFURAN IN A TRICKLE BED REACTOR: KINETICS, POISONING, AND PHASE DISTRIBUTION EFFECTS

by

VITO LAVOPA

Submitted to the Department of Chemical Engineering on October 30, 1987 in partial fulfillment of the requirements for the Degree of Doctor of Science in Chemical Engineering

ABSTRACT

The hydrodeoxygenation of dibenzofuran (DBF) was studied at 350-390°C and 7.0 MPa over a sulfided Ni-Mo/Al_2O_3 catalyst. The major products isolated were C_5-C single-ring hydrocarbons, cyclohexane predominating; the remainder were double-ring hydrocarbons, cyclohexylbenzene predominating. No organo-oxygen intermediates were isolated in any significant amount, as the initial reactions are rate-limiting. From studies of possible intermediates it appears that on a sulfided catalyst two pathways operate in parallel for the hydrodeoxygenation (HDO) of dibenzofuran: (1) hydrogenation of DBF to hexahydro-DBF, which reacts via 2-cyclohexylphenol to form single-ring hydrocarbons; (2) direct hydrogenolysis via 2-phenylphenol, without prior ring hydrogenation, to form biphenyl and cyclohexylbenzene (a minor route). The overall reaction is first order with respect to hydrogen and DBF and exhibits an apparent activation energy of 67 kJ/mol. The non-sulfided ("oxide") form of the catalyst is less active, and double-ring products predominate over single-ring products.

Inhibition of thiophene hydrodesulfurization (HDS) over the same Ni-Mo catalyst was studied at 7 MPa and 300-400°C. Poisoning by non-sterically hindered nitrogen compounds, expressed as adsorption equilibrium constants derived from Langmuir-Hinshelwood kinetics for thiophene HDS, correlated well with gas phase basicity (proton affinity). The order of adsorption strength agrees generally with that reported for poisoning of hydroprocessing catalysts and of acidic cracking catalysts. Model predictions of the poisoning of dibenzofuran HDO at 360°C, using inhibitor adsorption constants from the thiophene HDS study, agreed with the experimental results, even when the nitrogen compound underwent considerable reaction and inhibition by nitrogen intermediates was significant.

The distribution of reactants and inert liquid between the vapor and liquid phase in a trickle bed reactor used for hydrotreating is affected by H_2/feed ratio, relative volatilities, and temperature. The consequences of altering these variables are not always immediately obvious, although significant changes in conversion can result. Studies are reported for the HDO of dibenzofuran (b.p. 287°C) and the hydrogenation of n-butyl benzene (b.p. 183°C) dissolved in either n-hexadecane (b.p. 287°C) or in squalane (b.p. 350°C). Experimental results obtained at low conversions are compared with theoretical predictions.

Thesis Supervisor: Dr. Charles N. Satterfield
Title: Professor of Chemical Engineering

Dedication

To my parents, who encouraged me to attend college and enter a respectable profession. I am indebted to them for the values which they passed on to me.

Acknowledgements

- I am grateful to Professor Satterfield for attempting to share some of his wisdom with me and for teaching his philosophy of research. I will always remember his ready supply of anecdotes.

- I would also like to acknowledge my thesis committee: Prof. John Longwell for providing access to the g.c./m.s. facility in the department, Prof. James Wei for suggestions during the progess of the thesis, and Dr. Michael Manning for comments in the early stage.

- The National Science Foundation and the Department of Energy for providing funding through an NSF Fellowship for myself and a research grant for the project respectively.

- To my fellow graduate students at MIT with whom I shared the experience of MIT and from whom I learned more than just research.

  -Nancy and Robert King who also were crazy enough to take four courses in the first semester. They helped make it bearable.

  -To the Practice school group in the spring of 84: Rhonda, Kim, Ivan, Vijay, and Andy; we survived the Bethlehem station.

  -Barbara Smith, who always kept the lab cheerful with her Kiwi accent. I learned from her that I had it easy using a flow reactor.

  -Dave Matsumoto, for many perceptive comments about my work, a great sense of humor, and an unlimited supply of puns.

  -To some of my predecessors: Thom Bartos for advice on functioning in our research group, Bob "Moose" Hanlon for demonstrating the merits graduating early, and Morris Smith for building the box.

  -Erja Rautiainen for teaching us the Finnish language and for keeping us entertained with gas chromatography.

  -Kirk Limbach for providing a different view of grad school from one who has worked for a living.

  -To the newer crowd in the lab: Chung Lee, Tim Donnelly, and Ian Yates. Good luck and keep up the lab standards.

  -To all of the others who should be acknowledged but are not; I accept all responsibility for omissions.

TABLE OF CONTENTS

APPENDIX

LIST OF TABLES

LIST OF FIGURES

Chapter I

INTRODUCTION

I.A Importance of Hydrotreating

Large swings in the price of crude oil over the past decade have shown that forecasts of the long-term outlook for synthetic fuels cannot be made with any accuracy. Certainly the processes which have been developed for producing liquid fuels from tar sands, shale, or coal are not cost effective at present. However, it is also clear that discoveries of new petroleum supplies needed to replace reserves will require exploration in remote regions and drilling at greater depths. This additional expense, as well as political considerations, may eventually encourage greater utilization of available heavy petroleum crudes and synthetically derived fuels.

The available processes required to upgrade these heavier and dirtier feedstocks to acceptable transportation fuels include: hydrotreating for the removal of heteroatoms including sulfur, nitrogen, oxygen, and metals; catalyic cracking and hydrocracking for molecular weight reduction to lower boiling point liquids; and reforming for octane enhancement. Hydrotreating generally serves as the first step in any processing scheme in order to protect downstream catalysts from poisons in the feedstock. Ni and V in petroleum bottoms or Fe and Ti in coal-derived liquids can deposit on and deactivate refinery catalysts. A separate hydrodemetallation guard reactor therefore often precedes the main hydrotreating unit. Among the non-metallic poisons, basic organo-nitrogen compounds in the feed have been shown to strongly inhibit the activity of acidic cracking catalysts (Fu and Schaffer, 1985). The acidic supports of bifunctional

catalysts, used in hydrocracking and reforming, are also sensitive to nitrogen bases, while the active metals on these catalysts are poisoned by ppm levels of sulfur (Satterfield, 1980). Hydrotreating also improves the product stability by reducing the content of oxygenates.

Extensive upgrading of crude petroleum has produced a world-wide market for hydrotreating catalysts estimated at U.S. $190 million in 1987 (Hoffman, 1987), while catalyst replacement costs represent only a portion of the total cost for hydrotreating. The importance of hydrotreating heavier feedstocks is likely to increase further as environmental restrictions are tightened. Reduction of the sulfur content of catalytic cracker feeds limits the emission of sulfur dioxide during regeneration of the cracking catalyst, and current regulations in this area may be strengthened.

Refiners may also be faced with finding new ways to increase the octane of gasoline blending stocks, especially if the Environmental Protection Agency places limits on fuel volatility (Anderson, 1987). Refiners would then be forced to lower the butane content of gasoline and to recover the loss in octane through addition of oxygenates, more extensive reforming, or improvements in cracking selectivity. New cracking catalysts based on ultrastable Y type zeolites produce a gasoline with a high olefins content which improves the RON (research octane number). However, these highly dealuminated zeolites have relatively few active sites, making them especially sensitive to the presence of organo-nitrogen species (Corma et al., 1987).

I.B Process Description

During catalytic hydrotreatment of a feedstock, the sulfur, nitrogen, and oxygen containing compounds react with hydrogen to form hydrocarbons and either hydrogen sulfide, ammonia, or water respectively. These inorganic species are then removed from the product in downstream separation units, and the purified hydrogen is recycled to the process. Typical operating conditions for mild hydrotreating of a light feed and for residuals processing are listed in Table I.1 (Schuit and Gates, 1973). More severe operating conditions and lower space velocities are used for heavier feeds having high contents of heteroatoms and aromatics.

Commercial hydrotreating catalysts consist of molybdenum oxide supported on γ-alumina and promoted with either cobalt or nickel oxide. Cobalt promoted catalysts have generally been used for sulfur removal, while Ni promoted catalysts have higher hydrogenation activity and are recommended for nitrogen removal. All of these catalysts are generally pre-sulfided or become sulfided in use, and the species present on the surface can be quite complex. Several models have been proposed to describe the active desulfurization (sulfur removal) site and the mechanism of promotion, but these are described elsewhere (Topsoe and Clausen, 1984; Schuit and Gates, 1973; Delmon, 1977).

A fixed bed hydrotreating reactor is typically used with concurrent downflow of the hydrogen and liquid feeds. For volatile feeds, either vapor phase or trickle bed operation is attained depending upon the reaction conditions (see Section I.G). For either mode of operation the fixed bed catalyst consists of cylindrical extrudates having diameters in the range of 1.6 to 3.2 mm, with the size representing a compromise between pressure drop and internal mass transfer limitations. The catalyst bed is generally divided into stages, and interstage cold-shot

Table I.1

Typical Hydrotreating Process Conditions

Reactor Variable	Light Feeds	Residua
Temperature (°C)	300-400	350-450
Pressure (MPa)	1-10	3-20
Hydrogen Feed Ratio (std. m^3 H_2/m^3 oil)*	50-250	300-1500
Liquid Hourly Space Velocity (hr^{-1})	2-10	0.5-3

*where 1013 std. m^3 of H_2 / m^3 oil is equivalent to 6000 standard cubic feet per barrel

feeding of hydrogen is used to control the temperature rise resulting from the exothermic hydroprocessing reactions. Alternatively, slurry-bed reactors can be used to produce better temperature control and to allow continuous replacement of catalyst. Slurry-bed reactors are also favored when solids or coke buildup would plug a fixed bed reactor.

I.C Hydrodesulfurization

The main objective of hydrotreating carried out over the past 30 years has been sulfur removal, through hydrodesulfurization (HDS) reactions of the form:

$$\text{organic sulfur} + H_2 \longrightarrow H_2S + \text{hydrocarbons.}$$

As shown in in Table I.2, petroleum crudes can contain up to 1 wt % sulfur or higher, while oxygen and nitrogen are present at much lower levels. The obvious importance of HDS in petroleum processing has focused most of the hydrotreating catalysis research on optimizing the activity and selectivity for hydrodesulfurization. As the literature in this area is quite extensive and has been reviewed in the past (Schuman and Shalit, 1970; Schuit and Gates, 1973), only details of relevance to this work will be briefly discussed.

I.C.1 Model HDS reactions.

The sulfur compounds commonly found in petroleum are shown in Table I.3, listed in order of decreasing reactivity from the thiols to the thiophenic compounds (Schuit and Gates, 1973). Among these compounds, only the aromatic sulfur compunds are found to any extent in coal-derived liquids. Thiophene, benzothiophene, and dibenzothiophene have been studied extensively since these compounds are representative of the least

Table I.2

Typical Compositions of Petroleum and Synthetic Crudes

	Petroleum	Coal	Shale Oil	Tar Sands
Oxygen	0 - 0.5	3.8	1.4	0.4
Nitrogen	0.2	1.2	1.7	0.4
Sulfur	1.0	0.5	0.7	3.6

(from Furimsky (1983a))

TABLE I.3

Representative Sulfur Compounds Found in Petroleum

COMPOUND TYPE	STRUCTURES
THIOLS	R-SH
DISULFIDES	R-S-S-R'
SULFIDES	R-S-R'
THIOPHENES	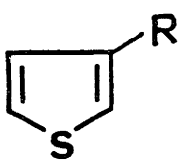
BENZOTHIOPHENES	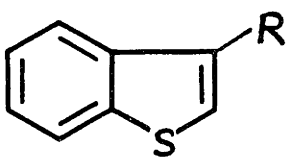
DIBENZOTHIOPHENES	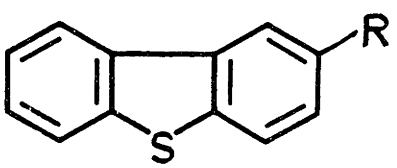

(from Schuit and Gates, 1973)

reactive compounds found in fuels. Several studies on the HDS of thiophene carried out in the vapor phase at amospheric pressure have proposed reaction pathways and developed reaction kinetics (Owens and Amberg, 1961; Satterfield and Roberts, 1968; Massoth, F.E., 1977; Lee and Butt, 1977); however, it is not clear if these results can be extrapolated to higher pressures. All of the studies indicate that H_2S is a significant poison for the HDS reaction of thiophene, and the work of Satterfield and Roberts (1968) showed that Langmuir-Hinshelwood kinetics were required to model the reaction in the form:

$$\text{(I.1)} \qquad \text{rate} = \frac{k\, P_T\, P_H^n}{(1 + K_T P_T + K_S P_S)^2}$$

where n equals 0 or 1 and H, S, and T refer to H_2, H_2S, and thiophene respectively.

The HDS of dibenzothiophene (DBT) has been studied extensively as a model reaction for the HDS of heavier distillates at realistic hydrotreationg conditions. Houalla and co-workers (1978) discuss the reaction networks for DBT and methyl-substituted dibenzothiophenes and review the previous literature. In a later study, Broderick and Gates (1981) studied the HDS of DBT over a Co-Mo catalyst at temperatures near 300°C and a total pressure ranging from 3.5 to 14 MPa. The reaction was carried out in a flow reactor, with the DBT dissolved at 0.15 mole % in a hydrogen saturated C_{16} carrier. The reaction network developed in this study is shown in Figure I.1. The main reaction pathway involves direct hydrogenolysis (C-S bond breaking) to form biphenyl, while the hydrogenation pathway through 1,2,3,4-tetrahyro-DBT is a minor route. Competitive adsorption effects were found to be significant, and the two pathways were described by separate Langmuir-Hinshelwood rate expressions.

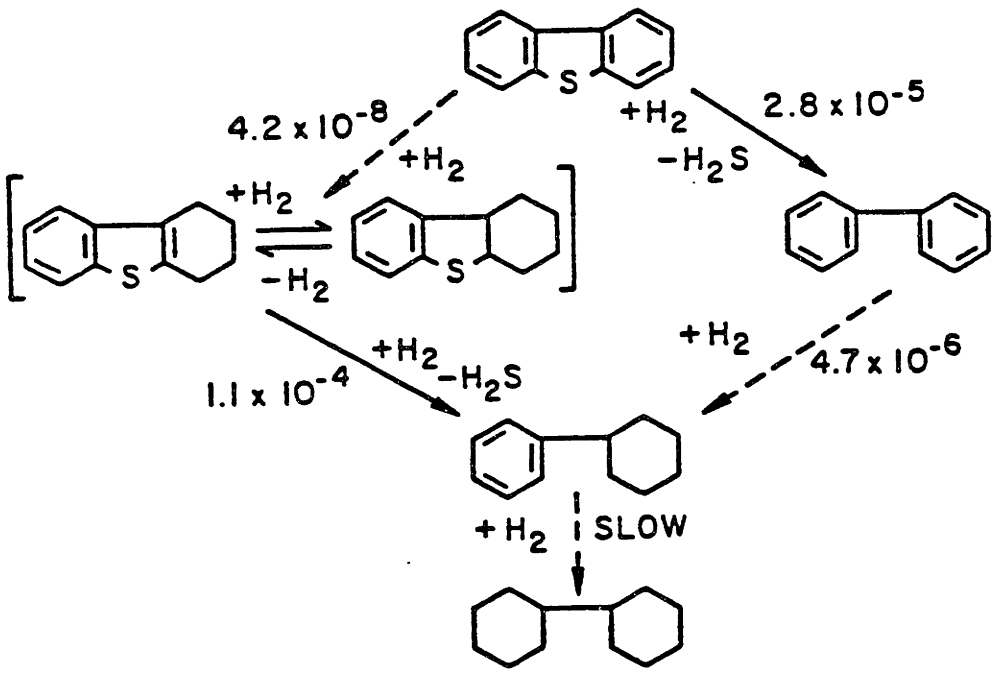

Figure I.1 Proposed reaction network for the HDS of dibenzothiophene. (from Broderick and Gates, 1981)

The recommended equation for the hydrogenolysis rate was:

$$(I.2) \qquad \frac{-d(DBT)}{dt} = \frac{k\, C_{DBT}\, C_{H2}}{(1 + K_{DBT}P_{DBT} + K_{H2S}P_{H2S})^2\,(1 + K_{H2}P_{H2})}$$

while for hydrogenation the best rate expression was:

$$(I.3) \qquad \frac{-d(DBT)}{dt} = \frac{k\, C_{DBT}\, C_{H2}}{(1 + K_{DBT}\, C_{DBT})}$$

Of particular interest here, the product hydrogen sulfide was reported to inhibit the hydrogenolysis step while having no effect upon hydrogenation.

A detailed study by Singhal and co-workers (1981a) reported on the HDS of dibenzothiophene and several probable intermediates at 300°C and 3-4 MPa total pressure. In a related study (Singhal et al., 1981b), they developed kinetics for the HDS reaction which accounted for the significant reactant and product inhibition observed over a Co-Mo catalyst. A number of kinetics models were tried, and the overall rate of disappearance of DBT was best described by:

$$(I.4) \qquad \frac{-d\,(DBT)}{dt} = \frac{k\, K_{DBT}\, K_{H2}\, P_{DBT}\, P_{H2}}{(1 + K_{DBT}\, P_{DBT} + K_{prod}\, P_{prod})\,(1 + K_{H2}\, P_{H2})} \,.$$

A higher concentration of DBT was used in this study (2-10 wt % in tetralin) at a hydrogen feed rate of 4000 SCF/bbl. These investigators also reported inhibition of the rate by H_2S, but they observed only a small increase in selectivity to hydrogenation with increasing H_2S concentration.

I.C.2 Inhibition of hydrodesulfurization by nitrogen compounds.

In some of the earliest work on model compound interactions, Desiken and Amberg (1964) reported on the poisoning of thiophene HDS by pyridine over a pre-sulfided Co-Mo/Al_2O_3 using an atmospheric pressure

pulsed reactor. Satterfield et al. (1975) investigated the simultaneous reaction of pyridine and thiophene over a pre-sulfided Co-Mo/Al_2O_3 catalyst under continuous flow conditions at 0.4-1.1 MPa. Later, Satterfield et al. (1980) reported further studies of pyridine inhibition over Ni-Mo/Al_2O_3 at higher pressures ranging from 1 to 7 MPa. These studies postulated the existence of two types of sites active for HDS which were poisoned to different extents.

Recently, Miciukiewicz et al. (1984) studied the inhibiting effects of several nitrogen compounds on thiophene HDS over a Co-Mo/Al_2O_3 catalyst at 350°C and 1 atm and compared them to inhibition of 1-hexene hydrogenation. For a given N-compound, inhibition of HDS was greater than that of hydrogenation in the absence of steric effects, and inhibition was generally greater for those N-compounds having higher pK_a values.

A few studies have also attempted to measure the relative poisoning effects of a variety of nitrogen compounds upon the HDS of dibenzothiophene (DBT). In an early study, Bhinde (1979) found that quinoline inhibited mainly the hydrogenation reactions in the network for the HDS of DBT. Nagai and Kabe (1983) studied the HDS of dibenzothiophene (DBT) in a flow reactor at 300°C and 10 MPa over Mo/Al_2O_3. Under some conditions heterocyclic N-compounds actually increased the rate of reaction of DBT (Nagai, 1985), an effect that we have confirmed and discuss in section V.A In the study by Nagai and Kabe, whether the DBT disappearance rate increased or decreased, the nitrogen compounds consistently inhibited the formation of partially hydrogenated products. Thus, the ratio of biphenyl to cyclohexylbenzene, the principal products isolated, increased and the amount of hexahydrodibenzothiophene, isolated in small amounts, decreased. Inhibition effects increased in the order: phenanthrene < carbazole < acridine, and aqueous basicity (pK_a) was found

to be a poor predictor of adsorption strength.

Later Nagai et al. (1986) continued the study of poisoning of the dibenzothiophene HDS reaction over Ni-Mo/Al_2O_3. Adsorption constants for several nitrogen bases were measured from the inhibition of the secondary reaction of tetrahydro-DBT to form hexahydro-DBT, both intermediates being present at relatively low concentrations. At 260°C and 10.1 MPa the adsorption strength increased in the order: aniline < pyridine < quinoline < acridine, and adsorption constants varied over two orders of magnitude. The adsorption constants determined from the kinetics increased linearly with gas phase basicity (proton affinity), but did not correlate well with solution basicity. Nagai and co-workers observed that cyclohexylamine and piperidine did not fit the correlation and suggested that they may have decomposed. However, the extent of reaction of the nitrogen compounds was not specified. Quinoline and acridine would rapidly attain chemical equilibrium with their partial hydrogenation products at the low temperature of this study. Moreover, the work was restricted to nitrogen levels below 1.5 kPa since higher levels somehow enhanced the HDS reaction of DBT (Nagai, 1985).

Inhibition effects on complex feedstocks have also been studied. Gutberlet and Bertolacini (1983) examined the poisoning effect of nitrogen compounds upon the hydrodesulfurization of a naphtha feed. Several alkylpyridines, 2,5-dimethylpyrrole, 4-methylaniline, and benzylamine were tested as catalyst poisons, using a magnesia supported Co-Mo catalyst at 292°C and 1 MPa. Calculated adsorption constants varied by a factor of 20 from the weakly adsorbed 4-methylaniline to strongly adsorbed 4-ethylpyridine. No inhibition was detected from 2,6-dimethylpyridine, and the results were interpreted largely in terms of the degree of steric hindrance of the nitrogen atom during adsorption.

I.D Hydrodenitrogenation

Nitrogen removal by hydrodenitrogenation (HDN) proceeds through reactions of the form:

$$\text{organic nitrogen} + H_2 \longrightarrow NH_3 + \text{hydrocarbons.}$$

As shown in Table I.2, liquid fuels derived from coal and shale can contain over 1 wt% of organically bound nitrogen. Recognition of the severity of catalyst poisoning caused by nitrogen bases has produced an extensive literature which was recently reviewed by Ho (1987).

The less reactive nitrogen compounds found in petroleum and synthetic fuels include the aromatic heterocyclic compounds and the anilines. Some representative nitrogen species are shown in Table I.4. The heterocyclic species can be conveniently divided into two groups: basic compounds containing a 6-membered pyridine ring and "non-basic" compounds containing a 5-membered pyrrole ring. The anilines are important as hydrogenolysis (C-N bond breaking) products formed from the aromatic heterocycles.

Among the basic heterocyclic compounds, pyridine and quinoline have been studied in the greatest detail, and the trends observed for these species appear to be quite general. McIlvried (1971) determined that the HDN of pyridine proceeds through an initial reversible hydrogenation to form piperidine, and this saturated species then undergoes irreversible hydrogenolysis (C-N bond scission). In agreement with this reaction scheme, Satterfield et al. (1975) found that the equilibrium between pyridine and piperidine limits the rate of hydrodenitrogenation at higher temperatures. Publications by Cocchetto and Satterfield (1976, 1981) present estimated and experimentally determined reaction equilibrium constants for the hydrogenation of several nitrogen heterocycles including pyridine and quinoline.

TABLE I.4

Representative Nitrogen Compounds in Synthetic Fuels

COMPOUND	STRUCTURE
Six-membered ring	
PYRIDINE	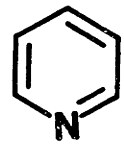
QUINOLINE	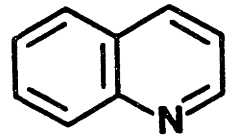
Five-membered ring	
PYRROLE	
INDOLE	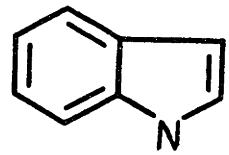
CARBAZOLE	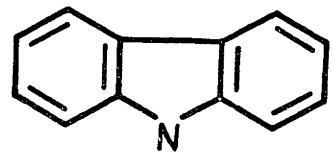
Non-heterocyclic	
ANILINE	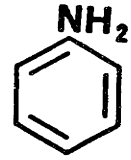

(from Ho, 1987)

The HDN of quinoline has been studied by many investigators (Satterfield and Cocchetto, 1981; Shih et al., 1977). As with pyridine, the nitrogen containing ring must undergo initial hydrogenation before C-N bond hydrogenolysis can occur. Hydrogenation equilibria therefore play an important role in determining reactivity and selectivity, as shown by the reaction network in Figure I.2 used recently by Satterfield and Smith (1986). The ring opening reactions of PyTHQ to form OPA and of DHQ represent hydrogenolysis reactions while the remainder are hydrogenations. Quinoline and 1,2,3,4-tetrahydroquinoline rapidly attain their equilibrium ratio at reaction conditions, so these two species can be lumped together as a single pseudo-species.

Langmuir-Hinshelwood kinetics have been used to model the reactions in the form:

$$\text{(I.5)} \qquad \text{Rate}_i = \frac{k_i K_R P_R}{1 + \Sigma K_N P_N}$$

where the expression represents the rate of the ith reaction in the network. The seven reaction steps are indicated in Figure I.3. K_R and P_R in equation I.5 represent the adsorption equilibrium constant and the partial pressure of the nitrogen containing reactant, while the summation in the denominator represents the adsorption of all of the nitrogen bases. In previous studies, adsorption of nitrogen species was assumed to be so strong that all sites on the catalyst were occupied and the "1" was neglected in the denominator.

Satterfield and Gultekin (1981) and Yang and Satterfield (1984) found that the presence of hydrogen sulfide significantly enhances the rate of hydrogenoysis of C-N bonds during the HDN of quinoline over a Ni-Mo catalyst. Hydrogenation reactions were mildly inhibited by the same

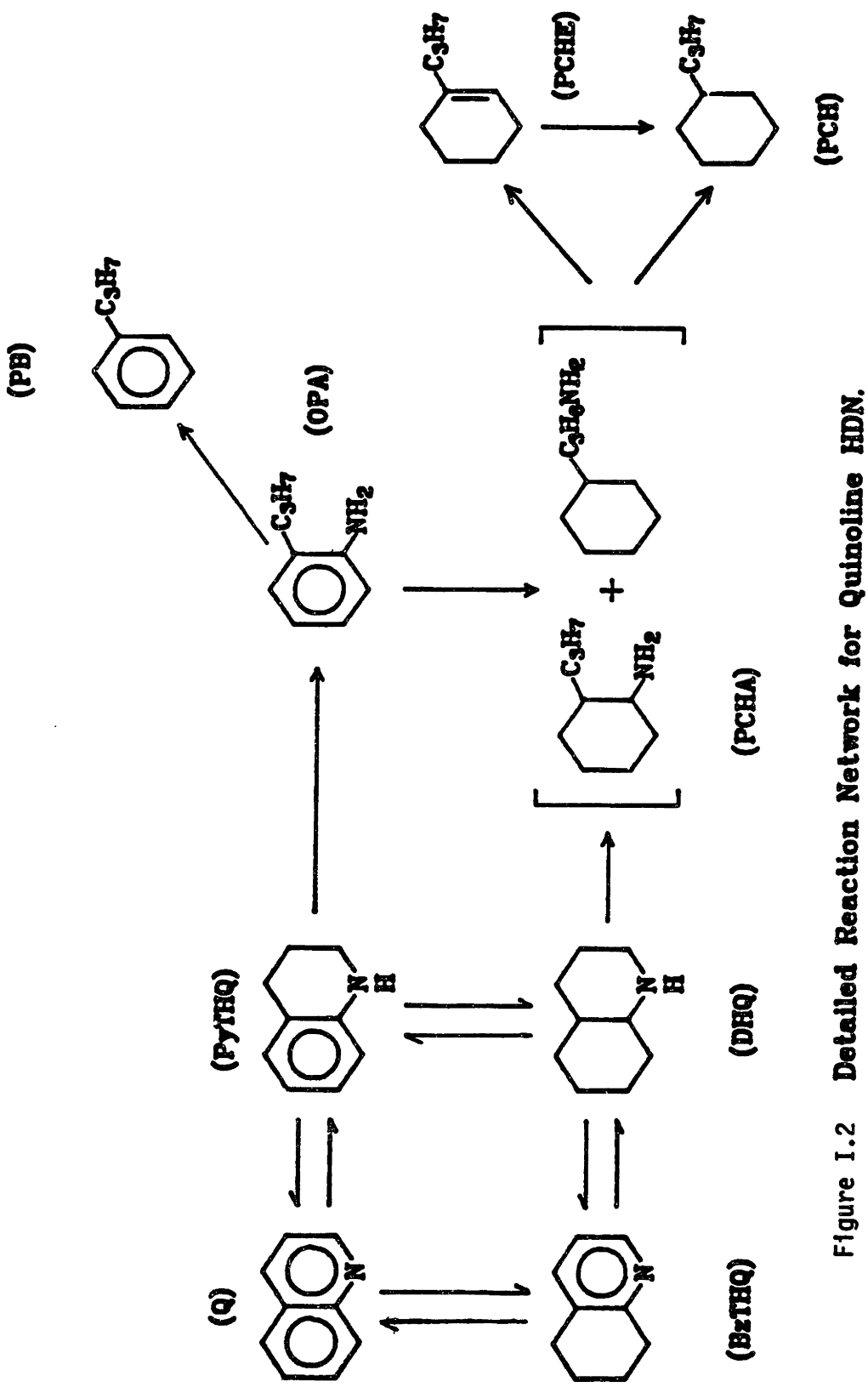

Figure I.2 **Detailed Reaction Network for Quinoline HDN.**

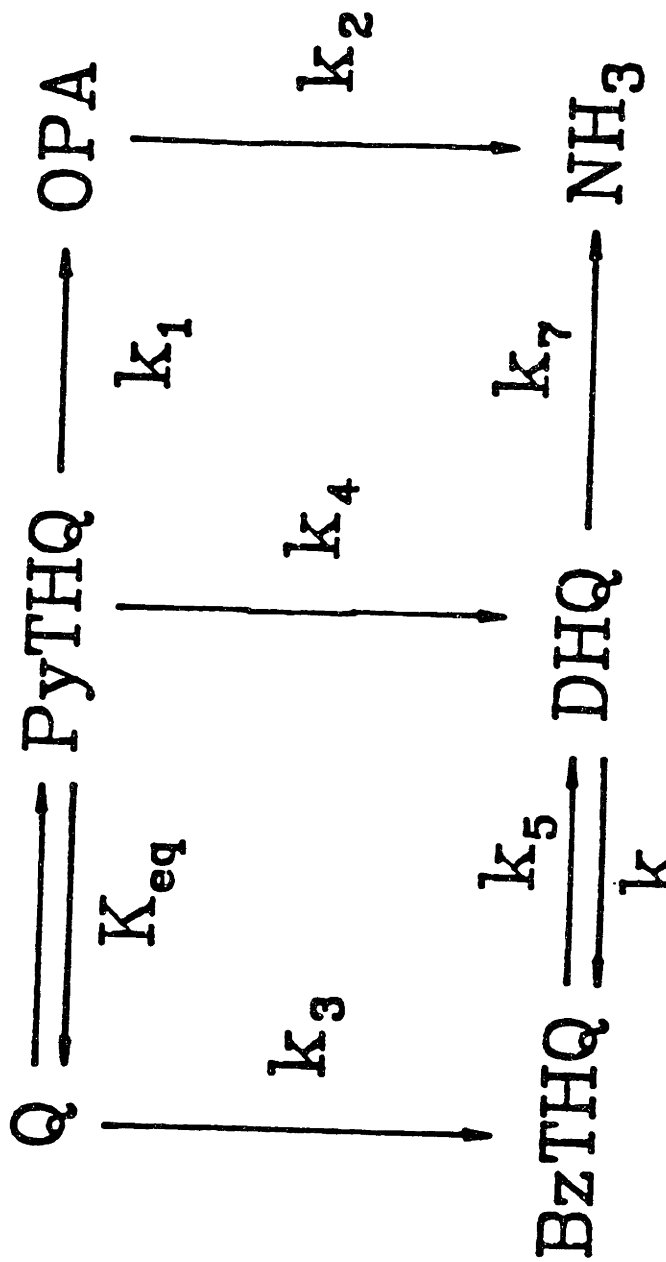

Figure I.3 Simplified Kinetic Scheme for Quinoline HDN.

levels of H_2S, leading to a net enhancement of the rate of HDN by hydrogen sulfide. This effect has also been observed with a real feed, an SRC-II middle distillate, processed with a Co-Mo catalyst (Hirschon et al., 1985). Satterfield and Smith (1986) observed similar enhancement of the rate of HDN in the presence of water, but the effect was small in the presence of H_2S.

Investigation of the reactions of "non-basic" heterocycles has been hindered by the low thermal stability and low solubilities of these compounds. Thakkar et al. (1981) found that the carbazole present in an SRC-I recycle solvent was less reactive than quinoline or indole. The reactions of indole and of the intermediate 2-ethyl aniline have been reported by Olive and co-workers (1985). This latter study was carried out using Ni-Mo, Co-Mo, and Ni-W catalysts at 250-350°C and total pressures ranging from 3.4 to 7 MPa. Hydrodenitrogenation of indole was found to proceed via hydrogenation to indoline followed by hydrogenolysis to 2-ethyl aniline. Hydrogenation of the heterocyclic ring prior to C-N bond hydrogenolysis therefore appears to be characteristic of the reactions of both 5 and 6 membered ring nitrogen heterocycles.

I.E Hydrodeoxygenation

The catalytic removal of oxygen, termed hydrodeoxygenation or HDO, proceeds by the following general reaction:

$$\text{organic oxygen} + H_2 \longrightarrow H_2O + \text{hydrocarbons.}$$

This class of reactions, unlike HDS or HDN, has limited impact upon petroleum refining because of the low oxygen content of typical crudes. As shown in Table I.2, however, the oxygen content of coal-derived liquids can reach almost 4 wt %, and liquids produced from shale and biomass are

also high in oxygen (Elliott, 1983). Oxygen removal must be effected for these synthetic crudes to promote fuel stability and to eliminate the presence of phenolics.

Several studies on the storage stability of coal-derived liquids have shown that compounds containing phenolic oxygen are responsible for the fuel aging process, in which the viscosity, oxygen content, and average molecular weight may increase. Work by Brown and Karn (1980) demonstrated that the exposure of a coal-derived liquid to oxygen led to the formation of a benzene insoluble fraction with a high oxygen content. A study by Hara and co-workers (1981) used IR analysis to track the decrease in phenolics concentration with time for a mixed SRC-I and II liquid. The authors asserted that oxidative coupling of phenolics causes fuel aging.

A more recent study by White et al. (1983) has supported this contention. Analysis of an aging SRC-II middle distillate by g.c.-m.s. showed that the concentrations of individual phenolic species decreased with time, and oligomers with molecular weights ranging from 200 to 470 were found in the aged samples. These oligomers were tentatively identified as polyphenylene ethers and C-C coupled diphenoquinones, structures consistent with formation by oxidative coupling of phenolics.

Since the majority of oxygen in synthetic fuels is present in phenolic groups (Schwager et al. 1978), the findings suggest that oxygen contents would have to be lowered to produce transportation fuels which are compatible with current distribution systems. There is also evidence that the presence of oxygen compounds can affect other hydrotreating reactions and can lower the performance of coal liquefaction units.

I.E.1 Processability of oxygen compounds.

Oxygen compounds are generally thought to be quite reactive under conventional hydrotreating conditions. However, published results indicate that the oxygen species present in coal liquids show more resistance to hydroprocessing than the sulfur and nitrogen species. For example, Cusumano et al. (1978) describe the catalytic hydrotreatment of a pyrolysis oil produced by the COED process. The liquid initially contained 2 wt % sulfur, 1 wt % nitrogen, and 5 wt % oxygen; and hydrotreatment at 13.8 MPa and 400°C over a Ni-Mo catalyst reduced the heteroatoms contents by the following percentages:

sulfur	95.0 %
nitrogen	99.9 %
oxygen	88.0 %.

Similarly, the thesis of Haider (1981) discusses experiments on the hydroprocessing of an SRC-II distillate with a boiling point range of 230-450°C. Hydrotreatment over a Co-Mo/alumina catalyst at 370°C eliminated virtually all of the sulfur, 90.9 % of the nitrogen, and only 75.9 % of the oxygen.

The low activity for oxygen removal may be due to the presence of refractory oxygen compounds or to inhibition by nitrogen bases. Haider (1981) found that single and double bridged phenolic compounds and ethers were extremely resistant to HDO. Satterfield and Yang (1983) have shown that nitrogen compounds, including quinoline and 2-ethylaniline, severely inhibited the HDO of benzofuran, 2- and 3-ethylphenol during simultaneous hydrotreating experiments.

I.E.2 Oxygenates found in feedstocks.

Most crude feedstocks will contain hydroxyl, carbonyl, carboxylic, etheric, and other functional groups, and the oxygen content can increase upon prolonged exposure to air (Furimsky, 1983). However, many of these groups are unstable and will decompose non-catalytically under the thermal or reductive conditions found in hydroprocessing.

After reviewing the literature, Weisser and Landa (1973) reported that most alcohols, benzyl ethers, aldehydes, ketones, and carboxylic acids decompose readily over sulfide catalysts. They also reported that aliphatic and aryl ethers, phenols, and furanic compounds appear to be considerably more resistant to HDO. This latter group of oxygenates would thus provide the most relevant model compounds for investigation.

The fraction of total oxygen represented by these various functional groups varies considerably in petroleum and synthetic fuels. Snyder (1970) analyzed a 200-370°C distillate from a California crude oil and found the compounds listed in Table I.5. The distillate fraction contained 0.25 wt % oxygen, and the percentages of the total oxygen assigned to various structures is indicated. Carboxyl groups accounted for the bulk of the oxygen, while phenols and furans accounted for 11% and 19% respectively.

Characterization of synthetic fuels has concentrated upon identifying the presence of various oxygen functionalities. Hertz et al. (1980) detected the presence of phenolic oxygen in liquids obtained by the retorting of oil shale. Petrakis et al. (1983) analyzed a heavy distillate from an SRC-II liquid and identified the presence of phenols, carboxyl groups, aryl ethers, and benzofuran-like structures. In addition, a significant quantity of the oxygen in the basic fraction was present as hydroxyanilines, hydroxyindoles, and hydroxypyridines. White

TABLE I.5

Oxygen Functional Groups Found in a California Petroleum Distillate (400-700°F fraction)

COMPOUND TYPE	PERCENT OF TOTAL OXYGEN
R-COOH	35
R-CO-R, $R-CO_2-R$, $R-CO-R-CO_2R$	27
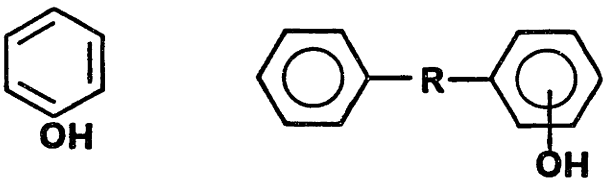	11
DIBENZOFURAN 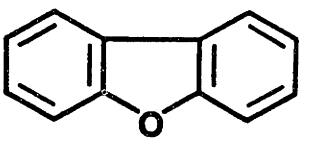	17
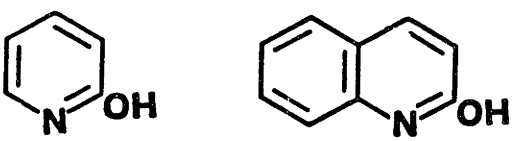	7
BENZOFURAN 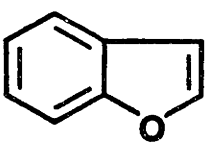	2
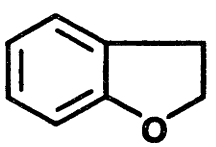	2

(from Snyder, 1970)

and Li (1982b) identified phenols and indanols, including 2-phenylphenol, in an SRC-II middle distillate. McClennen et al. (1983) detected phenols and indanols in coal liquids produced by the Exxon Donor Solvent and H-Coal processes.

With coal-derived liquids the relative importance of the oxygen compound classes depends upon the liquefaction process. Furimsky (1982) analyzed a primary product from coal hydrogenation; benzofuran, dibenzofuran, and phenols were detected, with methyl substitution predominating among the phenols. Schwager et al. (1978) analyzed the asphaltenes fractions obtained from several primary coal liquids. For the SRC-II process, approximately 95% of the oxygen was present in phenolic groups. By contrast, phenolics accounted for only 50-60% of the oxygen in a liquid obtained from coal hydrogenation. The authors postulated that the difference resulted from conversion of phenolic groups into ether linkages under the more severe conditions of the hydrogenation process. However, other studies have indicated that ether linkages are cleaved to form phenols at high pressures of hydrogen (Mallinson et al., 1980).

I.E.3 Thermodynamic stability of oxygen compounds.

In addition to being present in synthetic fuels, model oxygen compounds for hydroprocessing studies should also be resistant to HDO. Chemical equilibria for oxygen containing functional groups were calculated for the temperature range of 327 to 527°C and for reducing conditions with hydrogen and tetralin present (Messenger and Attar, 1979). Equilibrium constants predicted the removal of oxygen from all compound classes except for aryl ethers and dibenzofuran (DBF). Similar calculations, completed by Fishel and co-workers (1980), investigated the equilibrium for a system including phenol, phenylether, DBF, 2-

phenylphenol, and biphenyl. The results show that at 400°C in the absence of H_2, phenol should be converted mainly to DBF. Thermodynamic considerations, therefore, indicate that aryl ethers and dibenzofuran should be resistant to decomposition.

Non-catalytic reaction studies under reducing conditions have verified these predictions, although even the most stable compounds begin to react at high temperatures. Cronauer and co-workers (1979) investigated the reactivities of oxygen compounds in tetralin at 400 to 450°C. Substituted phenols were found to be unreactive at 450°C, and reactivities were found to increase in the order: furanic rings < phenols < ketones < aldehydes < alkylethers. Other studies in the presence of H_2 and hydrogen donors have shown that homogeneous reactions become significant at temperatures above 400°C. Mallinson et al. (1980) showed that at 400-450 °C in the presence of H_2 and tetralin, benzofuran was converted mainly to 2-ethyl and 2-methyl phenol. At about 500°C and a hydrogen pressure of 10 MPa, DBF was converted mainly to 2-phenylphenol (Huttinger and Kirrman, 1982). A study by Kamiya et al. (1979) investigated the stability of ethers in tetralin. At 450°C phenylether was found to be more stable than DBF, while aryl ethers with larger fused ring systems, such as naphthylether, were more reactive.

I.E.4 Previous Literature on Hydrodeoxygenation Reactions.

A considerable literature on HDO has developed since the early 1970's. Shah and Cronauer (1979) reviewed O, N, and S removal reactions from donor solvent coal liquefaction, and Furimsky (1983a) reviewed the chemistry of catalytic HDO. Only pertinent model compound studies carried out over conventional hydroprocessing catalysts are discussed below.

I.E.4.a Phenols - The HDO of phenols has been studied by numerous investigators since these compounds are prevalent in coal-derived liquids and are intermediates in the reaction of furans. Weisser and Landa (1973) reviewed the literature prior to 1971 and reported that two pathways are possible over sulfide catalysts. One pathway involves direct removal of the hydroxyl group from the aromatic ring, while the other pathway requires ring hydrogenation prior to C-O hydrogenolysis. The latter pathway was reported to predominate at pressures greater than 1 to 2.5 MPa, producing a cyclohexene as an intermediate and a cyclohexane as the final product.

Rollmann (1977) studied the HDO of several alkyl-substituted phenols, 2-phenylphenol, and 1-naphthol over a pre-sulfided Co-Mo catalyst. Reactivities for phenolics and other S, N, and O compounds in mixtures were found to decrease in the order: sulfides $\gg$ p-alkylphenols $>$ benzothiophenes $>$ quinolines $\sim$ o-alkylphenols $\sim$ indoles $\sim$ benzofuran $>$ dibenzofuran. The difference in reactivity of ortho and para substituted phenols was attributed to steric hindrance of the ortho form. In addition, selectivity for the formation of alkylbenzenes over alkylcyclohexanes (major product) was found to increase with temperature from 344 to 399°C for several alkylphenols.

A number of studies have also reported on the relative reactivities of phenolic compounds. Satterfield and Yang (1983) found that over a Ni-Mo catalyst, ethylcyclohexene was an intermediate in the HDO of 2- and 3-ethylphenol. This result suggested that ring hydrogenation occurs prior to C-O hydrogenolysis and explained the greater product selectivity to ethylcyclohexane over ethylbenzene. The relative reactivities of the compounds studied decreased in the order: 3-ethylphenol $>$ 2-ethylphenol $>$ benzofuran. An investigation by Furimsky et al. (1986) studied the HDO of

ortho-substituted phenols over a Co-Mo catalyst. At 350°C and 7 MPa total pressure, the order of reactivities found was: 2-t-butylphenol > phenol > 2-methylphenol > 2-ethylphenol > 2,6-dimethylphenol.

A detailed study of the HDO of cresols over Co-Mo was reported by Odebunmi and Ollis (1983a). The major products obtained from the HDO of cresols were toluene and methylcyclohexane, which disagrees with the report of Bredenberg and co-workers (1982) of 50% phenol production. A first order dependence upon hydrogen pressure was observed by Odebunmi and Ollis, and the reactivities were found to decrease in the order: meta- > para- > ortho- cresol.

Li et al. (1985a) investigated the hydroprocessing of 1-naphthol over a Ni-Mo catalyst and developed a reaction network. The major pathway for HDO proceeded through a ketone, followed by hydrogenolysis to form teralin; a parallel reaction pathway involved direct hydrogenolysis to form naphthalene. Mitchell (1980) found the HDO of 1-naphthol to be significantly easier than the HDO of p-cresol over a variety of catalysts.

Published work also indicates that the selectivity towards aromatic or alicyclic products depends upon the catalyst, with Ni-W catalysts favoring hydrogenated products. Haider (1981) observed a 76% selectivity towards benzene during the HDO of phenol over Co-Mo; cyclohexane was the major product over a Ni-W catalyst. Dalling et al. (1984) reported similar results, in which the aromatic character of an SRC-II middle distillate decreased more over a Ni-W than over a Co-Mo catalyst.

I.E.4.b Furans - The furans are aromatic ethers containing a 5-membered heterocylic ring, and this class of compounds represents the least reactive oxygen containing compounds. Grandy et al. (1984) studied the hydroprocessing of acidic fractions extracted from a coal-derived

liquid and found that the concentration of ethers remained constant while the phenols were extensively reacted. Haider (1981) also found evidence that the ethers present in an SRC-II liquid were especially resistant to HDO.

Furan - The hydrodeoxygenation of furan is a facile reaction at atmospheric pressure, producing a broad range of hydrocarbon products from C_1 to C_4 (Pratt and Christoverson, 1983). Furimsky (1983b) found that butadiene was detected in the product stream in trace amounts after several hours of catalyst operation. Likewise, butadiene formation during the HDO of tetrahydrofuran increased as the catalyst aged in atmospheric pressure experiments (Furimsky, 1983c).

Benzofuran - More relevant studies at industrial pressures have been reported for the multiple ring furans. Rollmann (1977) investigated the hydrodeoxygenation of benzofuran over a Co-Mo catalyst and proposed a reaction scheme involving hydrogenation of the heterocyclic ring, followed by C-O hydrogenolysis to form 2-ethylphenol. The final products obtained were ethylbenzene and ethylcyclohexane, and the reaction of 2-ethylphenol was thought to be rate limiting. Satterfield and Yang (1983) detected 2-ethylphenol and 2,3-dihydrobenzofuran as intermediates, with the latter species found in only trace amounts. Yang and Satterfield also reported that the HDO of benzofuran proceeded at a faster rate than the HDN of quinoline, while Rollmann found the reactivities of these two compounds to be approximately the same in mixtures.

Lee and Ollis (1984a) determined the kinetics for the HDO of benzofuran and found that hydrogenation of the heterocyclic ring is required prior to oxygen removal. 2,3-dihydrobenzofuran and 2-ethylphenol

were the only products detected below 260°C; oxygen removal occurred at temperatures above 310°C. However, when 2-ethylphenol was fed to the reactor alone, deoxygenation was found to occur at much lower temperatures. This effect was explained by the assertion that benzofuran and 2,3-dihydrobenzofuran may adsorb strongly and inhibit hydrogenolysis reactions.

Dibenzofuran - In an early study, Hall and Cawley (1939) reported on the HDO of dibenzofuran over supported and unsupported molybdena catalysts. At 10 MPa and 300-450°C, the main reaction pathway was postulated to proceed through 2-cyclohexylphenol. Enhanced production of biphenyl and 2-phenylphenol above 450°C indicated the existence of an alternate HDO pathway not requiring ring hydrogenation. High boiling point products were also produced over pelleted MoS_2 at 300 to 350°C as a result of condensation reactions.

Weisser and Landa (1973) also studied the HDO of dibenzofuran and proposed the reaction network shown in Figure I.4. According to this network, the main pathway proceeds with ring hydrogenation through either 2-cyclohexylphenol or 2-phenylcyclohexanol. The alternate pathway involves direct oxygen removal through 2-phenylphenol to form biphenyl.

Badilla-Ohlbaum et al. (1979a,b) and Rollmann (1977) found that dibenzofuran was the least reactive of a group of compounds tested in mixtures, including heterocyclic sulfur and nitrogen compounds. Rollmann also substituted several other phenol and furan derivatives one at a time for DBF in the mixture and showed that DBF was the least reactive of the group. Li et al. (1984, 1985b) reported that the phenols and dibenzothiophene present in an SRC-II liquid were at least an order of magnitude more reactive than dibenzofuran.

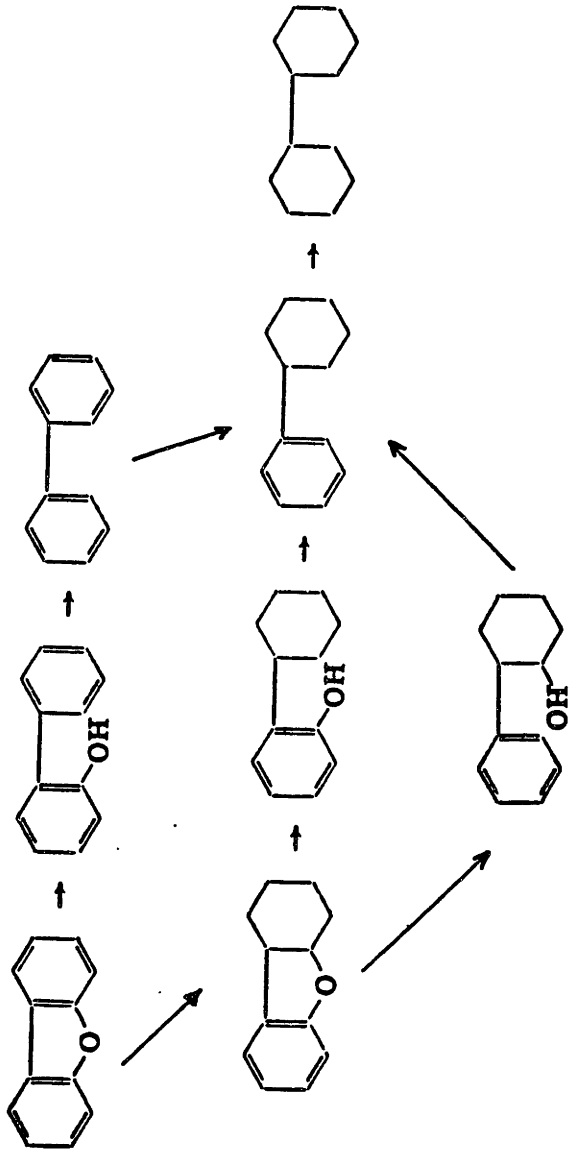

Figure I.4 Reaction network of Weisser and Landa (1973) for the HDO of dibenzofuran.

Krishnamurthy et al. (1981) reported on a detailed study of the products formed from dibenzofuran and its reaction network, done in a batch autoclave at 343-376°C and hydrogen pressures of 6.9 to 13.8 MPa. A presulfided Ni-Mo/alumina catalyst was used, and the DBF and CS_2, added to maintain a H_2S partial pressure, were dissolved in n-dodecane. Hydrogenation of DBF was assumed to be the rate limiting step since oxygenated intermediates were not found in significant amounts. The simplified first order kinetics used in this study is shown in Figure I.5. The best-fit rate constants from Table I.6 indicate that the main reaction path was through k_4 to form products. The rate constant for the hydrogenation of biphenyl was found to have the largest magnitude in the network, although other investigators have reported that biphenyl is very resistant to hydrogenation (Rollmann, 1977; Singhal et al., 1981b). Sapre and Gates (1982) have reported on the hydrogenation of biphenyl over a Co-Mo catalyst (1982).

Other significant aspects of the findings by Krishnamurthy and co-workers involve the effects of H_2S, hydrogen pressure, and initial feed concentration. Addition of CS_2 to the feed was found to enhance the activity of the sulfided catalyst slightly. Kinetics modelling showed that most of the first order rate constants increased with hydrogen pressure with only two exceptions. In addition, doubling the initial concentration of DBF was found to retard the reaction biphenyl ---> cyclohexylbenzene more strongly than other reactions such as DBF ---> biphenyl. The authors explained this last result by postulating a two site model, with strong adsorption of DBF on the hydrogenation site.

Krishnamurthy and co-workers (1981) also reported studies on 2-phenylphenol and 2-cyclohexylphenol, two possible intermediates in the reaction network for DBF. Both of these species were more reactive than

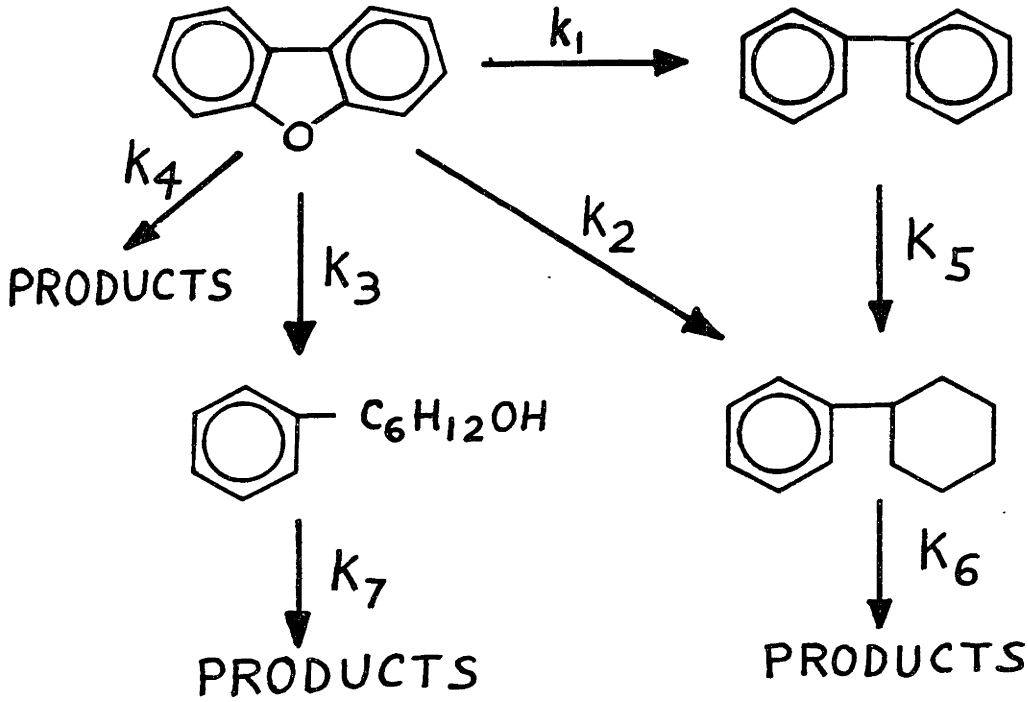

Figure I.5 Simplified Kinetics Scheme for the HDO of Dibenzofuran (from Krishnamurthy et al. (1981))

Table I.6

First-Order Rate Constants for DBF Kinetics at 365 °C and 10.34 MPa

Rate Constant	g. oil/g. catalyst, min
k_1	0.028
k_2	0.077
k_3	0.026
k_4	0.710
k_5	1.633
k_6	0.377
k_7	0.235

(from Krishnamurthy et al. (1981))

DBF, and experiments indicated that the reaction of the latter species could be non-catalytic. Li et al. (1984) also compared the reactivities of these species in fractions extracted from an SRC-II liquid. The reactivity of 2-phenylphenol in the weak acid fraction was estimated to be about a factor of 10 greater than that of DBF in the neutral oils fraction.

Shukla (1985) describes a study of the HDO of dibenzofuran over pre-sulfided Co-Mo and Ni-Mo catalysts. Reaction conditions were 230-350°C and 1.75-14 MPa total pressure, and high selectivity towards cyclohexane was observed over both catalysts. A compound identified as 6-phenyl-2,4-cyclohexadienone was detected by G.C./M.S. in the products tubing bomb experiments at low conversions of the undiluted 98% DBF. This species was proposed as the initial intermediate; however, it was not detected in experiments carried out in a stirred batch autoclave with the DBF dissolved in n-dodecane.

Recently Schulz et al. (1987) studied the HDO of dibenzofuran over pre-sulfided NiW/Al_2O_3 and $CoMo/Al_2O_3$ catalysts at 4.5 MPa and 250-400°C in a vapor phase flow reactor. High selectivity towards cyclohexane was observed. The main reaction pathway proposed by Schulz and co-workers is shown in Figure I.6. However, formation of the initial intermediate would destroy the aromaticity of three rings, and it is unlikely that such a reaction would occur.

I.E.5 Interactions in hydrodeoxygenation.

Sulfur, nitrogen, and oxygen compounds interact with each other during simultaneous reaction, and the products of hydrotreating (H_2S, NH_3, and H_2O) can also significantly affect the catalyst activity. Only interactions which directly affect hydrodeoxygenation are discussed below; the

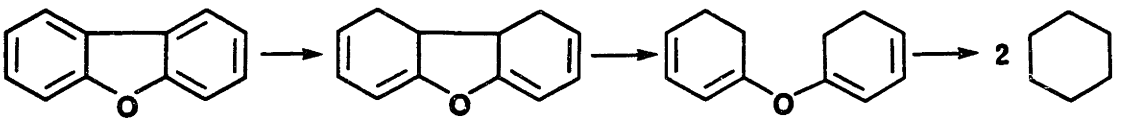

Figure I.6 A proposed reaction pathway for the HDO of DBF (Schulz et al., 1987).

interaction of HDN and HDS reactions have been discussed in previous sections.

I.E.5.a Effect of oxygenates on HDO - Several studies have shown evidence of competitive adsorption occurring between various oxygen compounds during hydrodeoxygenation. Lee and Ollis (1984a) observed inhibition of the HDO of 2-ethylphenol in the benzofuran system, and Krishnamurthy et al. (1981) reported on concentration effects in the DBF system. Li et al. (1984) found that the reaction of 2-phenylphenol was much slower in the acidic fraction from an SRC-II liquid than in a model feed; the results were attributed to inhibition by phenols.

I.E.5.b Effect of sulfur compounds and H_2S on HDO - Sulfur compounds also have a retarding effect upon the reactions of oxygen compounds during simultaneous HDS and HDO. The hydrodesulfurization of dibenzothiophene (DBT) has been shown to inhibit the reactions of phenol, xanthene, and dibenzofuran (Nagai and Kabe, 1983); dibenzofuran (Krishnamurthy and Shah, 1982); m-cresol (Odebunmi and Ollis, 1983b) and benzofuran (Lee and Ollis, 1984b). Odebunmi and Ollis demonstrated that low concentrations of DBT increased the HDO of cresol, while higher concentrations caused inhibition. Lee and Ollis observed the same effects with DBT and benzofuran. Their explanation for this behavior was that at low concentrations H_2S enhanced the activity, while higher concentrations of DBT adsorbed competitively. Gevert et al. (1987) reported that H_2S reduced the conversion of phenols and lowered the selectivity towards aromatics.

I.E.5.c Effect of nitrogen compounds on HDO - The inhibition of hydrodeoxygenation by the simultaneous HDN of nitrogen compounds has been shown to be even more drastic and may account for the apparent low reactivity of oxygen compounds in mixtures. Nitrogen compounds were found to inhibit the HDO of 2- and 3- ethylphenol and benzofuran (Satterfield

and Yang, 1983), and indole lowered the HDO rate of 3-cresol (Odebunmi and Ollis, 1983c). Satterfield and Yang found that quinoline produced greater inhibition than 2-ethylaniline; the effect was attributed to the higher reactivity of 2-ethylaniline. Krishnamurthy and Shah (1982) observed that 7,8-benzoquinoline, present at 0.25 wt%, lowered the rate of dibenzofuran HDO over Ni-Mo/Al_2O_3 by a factor of four. The effect of ammonia has been less well characterized. Weigold (1982) found that the addition of ammonia reduced the conversion of 2-cresol and lowered the toluene/methylcyclohexane selectivity, but this work was done with pure phenols. Recently Gevert et al. (1987) measured the inhibition produced by NH_3 on the HDO of a several phenols. Unlike H_2S, ammonia inhibited without changing the product selectivity.

Nitrogen compounds also inhibit the hydrogenation reactions of the hydrocarbon products formed during hydrodeoxygenation. Gultekin et al. (1984) studied the effects of H_2S and NH_3 upon the hydrogenation of propylbenzene over the HDS-3A Ni-Mo catalyst. Addition of H_2S was found to reduce the hydrogenation rate by a factor of 2, while additon of H_2S and NH_3 reduced the rate by a factor of 8 or more. Ho and co-workers (1984) also found that nitrogen compounds severely inhibited the hydrogenation of polyaromatics.

Lo (1981) studied the inhibition of naphthalene hydrogenation produced by simultaneous reactions including the HDS of dibenz-thiophene (DBT) and the hydrodenitrogenation of quinoline or indole. The study used a Ni-Mo/Al_2O_3 catalyst in a batch reactor at 350°C and 3.4 MPa. For naphthalene hydrogenation, inhibition effects increased in the order: DBT < NH_3 < indole and intermediates < quinoline and intermediates. The degree of inhibition was expressed in terms of adsorption constants derived from the kinetics, and these varied over two orders of magnitude.

I.F Catalyst Deactivation

Catalyst deactivation has a significant impact upon the economics of hydrotreating and coal liquefaction due to catalyst replacement costs. Thakur and Thomas (1984, 1985) review the subject of hydrotreating catalyst deactivation during direct coal liquefaction and heavy feed processing respectively. The reviews indicate that the various modes of deactivation: coking, metals deposition, nitrogen poisoning, and physical changes in the catalyst - all play a role in the loss of activity.

After a hydrotreating unit is brought on stream, the catalyst generally exhibits an initial period of relatively rapid deactivation, followed by a much longer period during which the catalyst deactivates slowly. This deactivation history is characteristic of all hydrotreating catalysts used under widely different processing conditions. In order to compensate for the loss in activity, the reactor temperature is often slowly increased. Once the temperature has reached the operational limits, the catalyst is removed from the reactor and is regenerated by oxidation.

The period of rapid initial deactivation has generally been attributed to coke deposition, since the maximum coke content of the catalayst (15-25 wt%) is attained in a short time (Thakur and Thomas, 1985). Although the coke content remains relatively constant during the remainder of the catalyst cycle, the hydrogen-to-carbon ratio of the coke has been found to decrease. Coke which has aged on the catalyst therefore probably has a more graphitic nature. Other investigators (Tamm et al., 1981) have postulated that the initial deactivation is due to the deposition of metals.

Thakur and Thomas (1985) discuss studies which indicate that the coke content of a catalyst changes from the inlet to the outlet of fixed bed

reactors. Intraparticle concentration profiles are also found in which the coke content is highest on the edge of catalyst particles.

Several studies have also postulated that Lewis acidity promotes coking on these catalysts. Ramaswamy et al. (1984) found that a Co-Mo/alumina catalyst which had been used for five regeneration cycles coked more rapidly than a sample of the fresh catalyst. The used catalyst was found to possess significantly higher Lewis acidity (as measured by ammonia adsorption) than the fresh catalyst. Bronsted acidity (as measured by the adsorption of 2,6-dimethylpyridine) was unaffected by the aging and regeneration cycles. Scaroni and Jenkins (1985) found that the presence of nitrogen bases (pyridine or acridine) inhibited the the coking of phenanthrene over a Co-Mo/alumina catalyst at high temperature in the absence of hydrogen. Nitrogen bases would be expected to adsorb on acidic sites, and the nitrogen species apparently adsorbed on and blocked sites responsible for coking.

Studies on commercially aged catalysts have demonstrated that significant changes in the physical properties of the catalysts also occur. Yoshimara et al. (1987) investigated the initial catalyst deactivation which occurred during processing of a coal-derived oil. In 50 hours of operation, pore volumes and surface areas were reduced, and carbonaceous deposits high in N and O formed on the catalyst. Bogdanor and Rase (1986) observed changes in intraparticle concentration profiles of the active metals on a commercially aged Ni-Mo/alumina catalyst. Ramaswamy et al. (1985) concluded that actual loss of MoO_3 had occurred after five regeneration cycles of a Co-Mo catalyst.

I.G Trickle Bed Reactor Studies

The observed activity of hydrodeoxygenation and other hydroprocessing reactions can also be affected by vapor-liquid equilibrium. The distribution of reactants, products, and inert species between the vapor and liquid phases in a trickle bed reactor can affect reaction selectivity, mask the intrinsic kinetics, and alter the observed activation energy.

Several models which account for partial vaporization of the liquid phase have been described in the literature, yet only a few experimental studies have been reported. Collins et al. (1985) simulated the hydrodesulfurization (HDS) of benzothiophene using the Soave-Redlich-Kwong equation of state to estimate vapor-liquid equilibrium. The reactor was modelled as a series of differential plug-flow reactors, with phase equilibrium calculated between each segment. They also presented further case studies of the model for various kinetic orders (Akgerman et al., 1985). Kocis and Ho (1986) used a similar model to simulate the HDS of dibenzothiophene under trickle bed conditions. Their model incorrectly reduced the LHSV used in the kinetics by a factor 1-f, where f is the fraction of the feed vaporized at reaction conditions. All of these studies used liquid phase kinetics and emphasized the effect of solvent volatility.

A few studies have attempted to experimentally verify a reactor model using reaction kinetics determined separately under complete liquid or vapor phase operation. Nalitham et al. (1985) compared the hydrogenation of naphthalene in cyclohexane at supercritical conditions to reaction in mineral oil. A reactor model applicable to slurry reactors was presented although it was not applied to the naphthalene system. Smith and Satterfield (1985) present results on the effect of changing gas to liquid

flow ratio for quinoline hydrodenitrogenation. This system is near zero order so the effect on conversion was small; however, changes in reaction selectivity were observed.

Smith (1985) also describes a trickle bed reactor model in which the reactor is divided into stages, with a flash calculation performed at each stage. The flash calculation was based on the vapor and liquid volumes present in the reactor (derived from hold-up data), rather than on the vapor and liquid streams. Moreover, the space time used in the kinetics was related to the estimated vapor phase residence time, similar to the space time adjustment of Kocis and Ho (1987). For a catalytic reaction, the space time used in the kinetics should actually be determined by the feed rate to the hydrotreater - not by the residence time in the reactor.

I.H Objectives and Approach

The pupose of this study was to determine the cause of the low activity for hydrodeoxygenation observed industrially. Dibenzofuran, an aromatic ether, was chosen for study since removal of the least reactive oxygenated compounds is the bottleneck for obtaining a high degree of conversion. The study had three major objectives:

(1) To investigate the reaction network of DBF and to determine the rate limiting steps for the hydrodeoxygenation of this species. -- Reaction pathways were determined from studies on possible intermediates in the reaction network, and the kinetics for DBF were measured.

(2) To measure the poisoning of hydrodeoxygenation reactions produced by a variety of nitrogen compounds and polyaromatic hydrocarbons. -- Previous literature suggested that proton affinity (gas phase basicity) might be useful for correlating the results and that steric hindrance could be important. The inhibition of hydrodesulfurization of thiophene, a representative sulfur compound, was studied first to allow experiments to be carried out with low conversion of the inhibitiors. Poisoning was interpreted in terms of competive adsorption of the inhibitor using Langmuir-Hinshelwood kinetics. The results for thiophene were then applied in modelling the poisoning of dibenzofuran HDO.

(3) To develop and test a model useful for predicting the consequences of altering H_2/liquid feed ratio, relative volatilities, and temperature in a trickle bed reactor. --
A model was used which accounted for the vapor-liquid equilibrium, and the predictions were compared with experimental results on the HDO of dibenzofuran (b.p. 285°C) and the hydrogenation of n-butylbenzene (b.p. 183°C) dissolved in either n-hexadecane (b.p. 287°C) or in squalane (b.p. 350°C).

Chapter II

EXPERIMENTAL DETAILS

II.A Reactor System

The reactor has been used for previous studies of hydrodenitrogenation and hydrodeoxygenation and is described in more detail elsewhere (Satterfield and Yang, 1984; Smith, 1985). Briefly, the reactor consisted of a vertical 0.52 cm ID tube immersed in a fluidized sand bath to maintain isothermal conditions. As shown in Figure II.1, the liquid containing the model compounds was fed by a high pressure HPLC pump. The liquid passed through a preheater coil immersed in the sand bath and then was fed to the top of the catalyst bed. Hydrogen was similarly fed through a preheater coil. The hydrogen and liquid feeds mixed at the reactor inlet, flowed downward through the catalyst bed, and flashed through a back-pressure regulator.

The reactor tube was 81 cm in length, with a 20 cm preheater zone packed with inert silicon carbide placed above the catalyst zone. It was found that use of large particle size SiC (36 grit) in the top few centimeters of the preheat zone reduced the incidence of reactor plugging by carbonaceous deposits. The 50 cm long catalyst zone was filled with a catalyst and silicon carbide mixture at a volumetric ratio of inert to catalyst of either 4:1 or 8:1. A 10 cm layer of SiC inert was placed below the catalyst zone at the bottom of the reactor tube.

Reactor effluent samples were collected at low pressure downstream of the back pressure regulator. Two stainless steel bombs in series served as a gas-liquid separator, and the liquid stream flowed continuously through a sampling loop to the waste container. The vapor exitting from

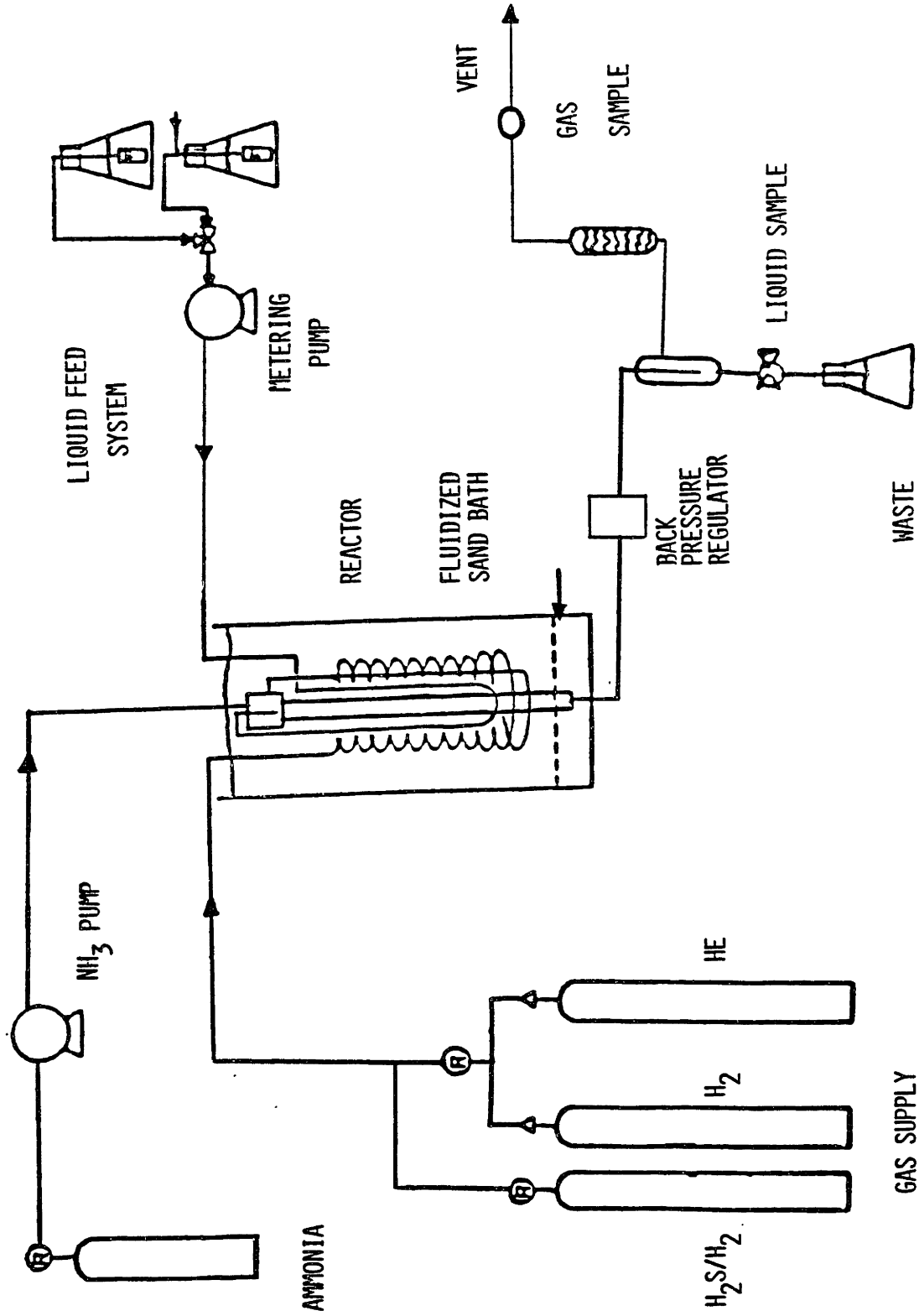

Figure II.1 Schematic diagram of the experimental apparatus.

the top of the separator passed through heated lines to a septum port. Samples were collected in a 0.25 ml gas-tight syringe and injected directly in the gas chromatograph.

The new addition to the apparatus was an anhydrous ammonia feed system, diagrammed in Figure II.2. The ammonia supply consisted of an anhydrous ammonia cylinder equipped with an internal eductor tube for withdrawal of liquid. A cross-tee purge valve arrangement allowed the ammonia manifold to be flushed with inert gas before a cylinder change. The liquid ammonia was used to fill the reservoir of an ISCO (Instrumentation Specialties Co.) model 314 piston-type metering pump. The metering pump was rated for 14 MPa service and could deliver flow rates ranging from 0.2 to 200 ml/hr. The ammonia was preheated before mixing with the other feeds at the reactor inlet.

During filling, the supply lines and reservoir were purged with ammonia vapor to remove any non-condensable inert gas. Using the manual crank on the pump, the piston was then withdrawn from the cylinder and the reservoir filled with ammonia. Since some vaporization of NH_3 was likely to occur, the liquid volume collected could be determined by closing the cylinder outlet valve and compressing the ammonia with the manual crank. The piston position at which the cylinder pressure rose above the vapor pressure of ammonia (approximately 114 psig at room temperature) identified the volume of liquid collected.

II.B Reactor Conditions

The reactor was normally operated with a liquid flow rate ranging from 0.17 to 2.72 mL/min and a catalyst loading of 1.6 grams. In this study space time is based on the reactant molar flow rate and not upon the total liquid volumetric flow rate. A liquid flow rate of 0.363 mL/min produced

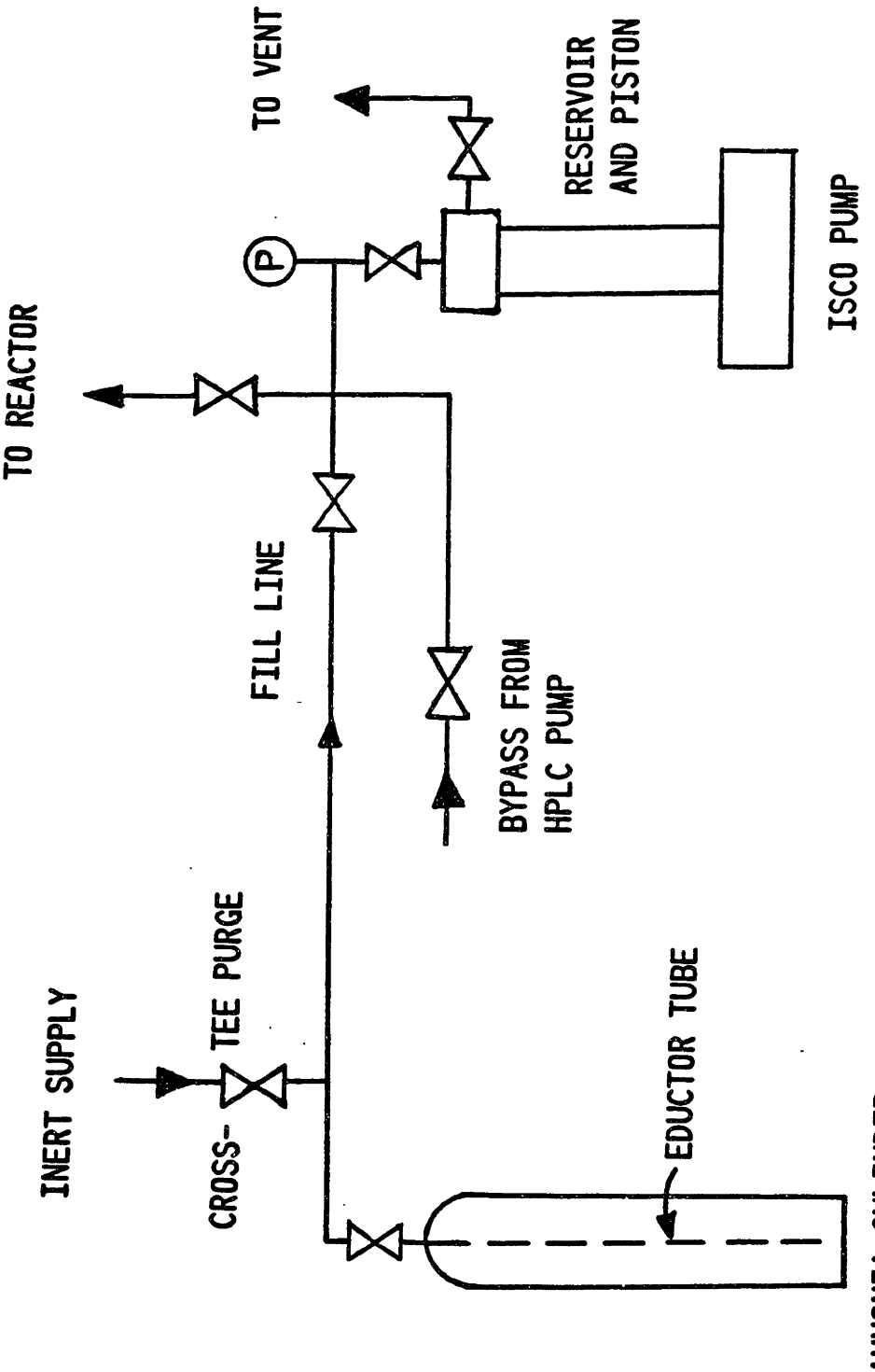

Figure II.2 Diagram of the Anhydrous Ammonia Feed System

a space time of 300 (hr g of catalyst)/(mol of reactant), at the usual liquid concentration (0.245 mols of reactant/liter). An equivalent industrial liquid hourly space velocity (LHSV) can be obtained from the weight of the crushed catalyst and the compacted bulk density of catalyst pellets (Appendix A1). A space time of 300 hr g catalyst/mol therefore corresponds to an LHSV of 10 hr^{-1} for all of the experiments.

The hydrogen flow rate was defined in terms the gas-to-liguid feed ratio measured in ml of hydrogen at STP fed per ml of liquid where STP refers to 1 atm and 0°C. A hydrogen to liquid feed ratio of 1520 ml at STP/ml liquid is equivalent to 9000 SCF/barrel where: SCF = standard cubic foot measured at 1 atm. and 60°F. The feed ratio was an important parameter for determin..g the phase behavior in the reactor. For operation with hexadecane as the solvent and a feed ratio of 9000 SCF/bbl, the work of Lin et al. (1980) indicates that complete vapor phase operation will be obtained at temperatures of 350°C and higher.

The hexadecane mixture used as the solvent for most of the experiments was purchased as C_{16} olefin from Chevron Gulf. The olefin was hydrogenated at room temperature and 60 psig of H_2 in reactor vessel equipped with a magnetic stirring bar. Catalyst loading was 12 g of a 1% palladium on activated carbon powder for 2 liters of olefin.

II.C Catalysts

The properties of the commercial hydrotreating catalysts used in this work are listed in Appendix A1. Most of the experiments were conducted using the same sample of a Ni-Mo/Al_2O_3 catalyst (American Cyanamid's HDS-3A) used in previous studies by our group. Ni-Mo catalysts have been found superior to Co-Mo or Ni-W catalysts for hydrodenitrogenation in the hydrotreatment of an SRC-I recycle solvent (Thakkar et al., 1981) and a

shale oil (Harvey et al., 1986). A few brief studies were also carried out on a Co-Mo/Al_2O_3 catalyst HDS-1442B and a Ni-Mo/Al_2O_3-SiO_2 catalyst (MHC-110), both from American Cyanamid. The catalyst pellets were crushed and sieved to a size range of 150-212 microns for all experiments except for one batch of catalyst used to study the HDS of thiophene at 400°C (batch 37). The particle size of the inert SiC used for dilution was 142 microns (120 grit) in the vapor phase experiments and 406 microns (60 grit) for the trickle bed experiments (batch 42).

The catalysts were pre-sulfided using a procedure recommended for HDS-3A by the manufacturer. After the catalyst was packed in the reactor, the system was purged under helium flow for 12 hr at 100°C. The catalyst was then sulfided using a 10 mol % H_2S in hydrogen mixture, at a flow rate of 40 ml/min (at STP) and a total pressure of 0.24 MPa (20 psig). Sulfiding temperature was maintained at 175°C for the first 6 hours, and the temperature was then raised to 315°C at a rate of about 1 °C/min. The gas flow rate was switched to helium after sulfiding had proceeded for one hour at 315°C. Brief histories of the catalyst batches are listed in appendix A2.

II.D Analytical Procedures

Reaction products were analyzed by gas chromatography, using a Perkin-Elmer Sigma 1B equipped with two FID detectors. This arrangement allowed a single sample injection to be analyzed simultaneously on two columns having stationary phases of different polarity. 30 meter fused silica capillary columns were used, and these had an ID of 0.25 mm and a film thickness of 0.25 microns.

Dibenzofuran - The reaction products from the HDO of dibenzofuran and the HDO of its intermediates were separated on a Supelcowax-10 (bonded

polyethylene glycol) column since this phase adequately separates the phenolics (White and Li, 1982a). The oven temperature program for the chromatographic method is listed in Table II.1. A typical chromatogram of a liquid phase sample (after reaction at 360°C, 7 MPa, and a space time of 160 hr g-cat/mol) is provided in Figure II.3. All of the reaction intermediates of DBF could be separated except for (cyclopentylmethyl)-benzene which is masked by the hexadecane solvent peak. The eicosane peak in Figure II.3 results from an unsuccessful attempt to use this high boiling paraffin as an internal standard in the feed. With this procedure great emphasis is placed upon the integration of the peak for the internal standard, and the method of external standards was used instead. Compounds were identified by comparing their retention times to those of pure standards, and carbon mass balances on total products compared to dibenzofuran disappearance ranged from 99 to 107%.

One representative liquid sample (produced at 360°C, 7 MPa, and 160 hr g-cat/mol of DBF) was also subjected to GC/MS analysis on a methyl silicone column (SE-30) for positive component identification. Mass spectra of individual species were compared with published spectra if these were available (Heller and Milne, 1980), and the species that were identified are listed in Table II.2. Cyclopentane was not detected by GC/MS, although an initial GC peak was always observed at a retention time corresponding to that of cyclopentane. This can be attributed to evaporation of the volatile cyclopentane from the particular sample during storage.

A product identified as (cyclopentylmethyl)-benzene (CPMB) was detected by GC/MS at 13% of the concentration of its isomer cyclohexyl-benzene. No published spectrum was found, and identification was based upon the fragmentaion pattern (see M.S. data in Appendix A3). A parent

TABLE II.1

Gas Chromatograph Oven Temperature Programs

Dibenzofuran products analyzed on a Carbowax column.

55°C (5 min)--------> 55°C 10°/min--------> 90°C 5°/min--------> 245°C (3 min)--------> 245 °C

Quinoline products analyzed on a Carbowax column.

85°C (3 min)--------> 85°C 5°/min--------> 150°C 10°/min---------> 200°C

(3 min)-------> 200°C 5°/min--------> 240°C

Thiophene products analyzed on a SPB-35 column.

55°C (5 min)--------> 55°C 10°/min----------> 220°C

RT (min)	Component
2.43	cyclopentane
2.52	methylcyclopentane
2.66	cyclohexane
2.84	methylcyclohexane
2.92	impurity in C_{16}
3.03	cyclohexene
4.40	benzene
A	xylenes
B	n-dodecane (from thiol)
14.43	cyclopentylmethyl-cyclohexane
14.76	tetradecane (in C_{16})
15.82	dicyclohexyl
C	C_{16} mixture
21.76	impurity in C_{16}
21.83	cyclohexylbenzene
D	octadecane (in C_{16})
28.94	eicosane
29.24	biphenyl
35.07	dibenzofuran

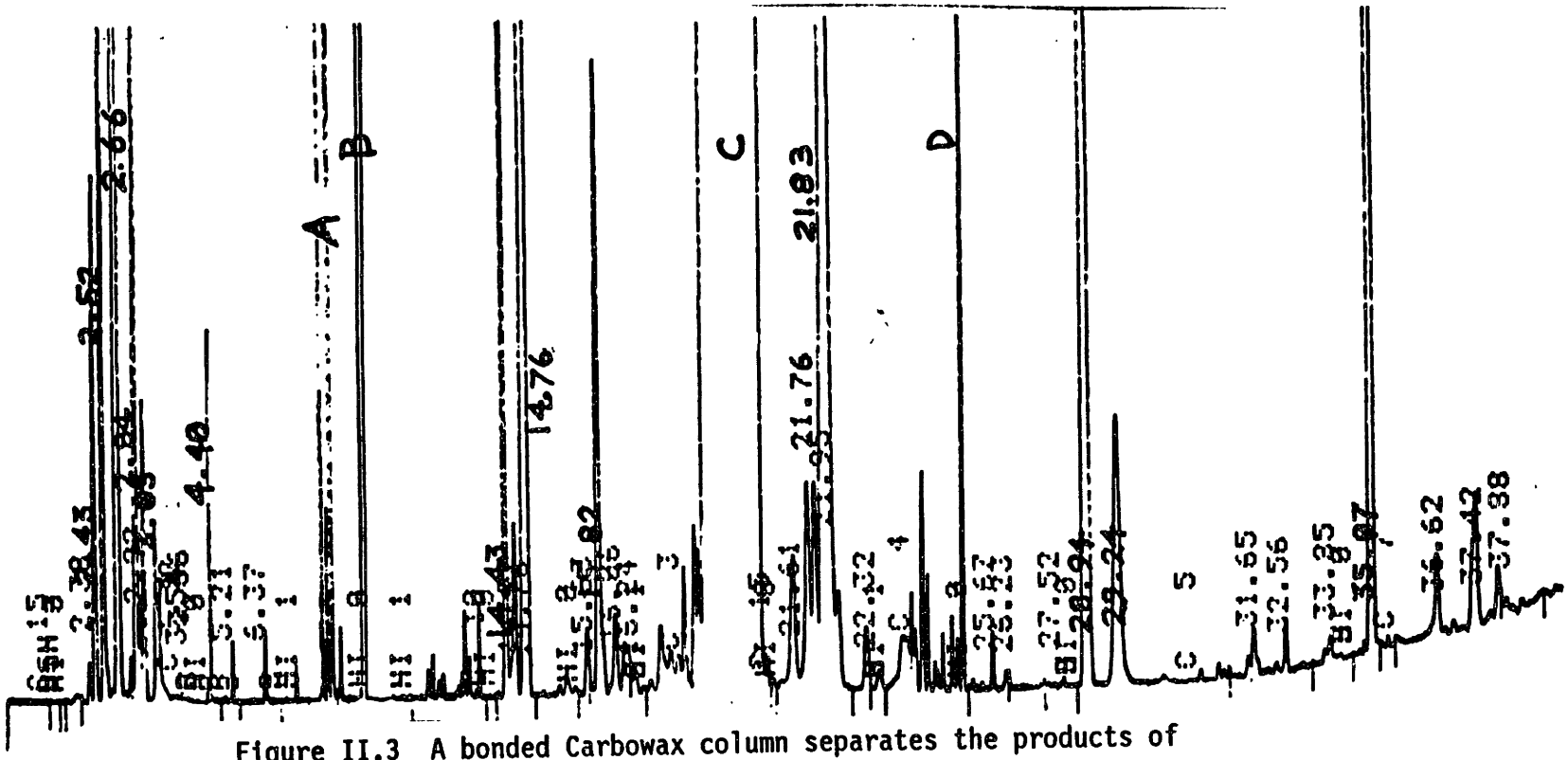

Figure II.3 A bonded Carbowax column separates the products of dibenzofuran HDO.

Table II.2 Species in the Reaction Network for Dibenzofuran Identified by GC/MS

Retention Time (min)	Component
1.78	methylcyclopentane
2.08	benzene
2.20	cyclohexane
2.46	cyclohexene
3.42	methylcyclohexane
33.32	cyclopentylmethyl-cyclohexane
34.10	cyclopentylmethyl-benzene
34.72	dicyclohexyl
34.94	cyclohexylbenzene
37.46	biphenyl
43.68	dibenzofuran
44.28	1,2,3,4-tetrahydro-dibenzofuran

Analyzed on at methyl silicone capillary column with the following oven temperature program:

35 °C ---(11 min)---> 35 °C ---5 °/min---> 90 °C ---(5 min)---> 90 °C

---3 °/min---> 170 °C ---10 °/min---> 265 °C ---(5 min)---> 265 °C

ion was observed at 160 amu, and a base peak was observed at 92 amu, characteristic of alkylphenyl compounds such as n-hexylbenzene. Since the CPMB was normally masked on a Carbowax column, inclusion of this species would have increased the mass balances by 1-2%.

A compound identified as tetrahydro-dibenzofuran was present in very low concentration and is not shown on any figures for the HDO of DBF. Its assignment is based on the similarity of its spectrum to that of tetrahydrodibenzothiophene, which has an analogous structure.

Quinoline - The high polarity of the Carbowax phase made it useful also for separation of the products from quinoline HDN. Figure II.4 shows a typical chromatogram obtained for the HDN of quinoline in the absence of H_2S at 360°C and 160 hr g-cat/mol. The two isomers of decahydroquinoline, a saturated amine, exhibited peak tailing on the Carbowax column, and these species were analyzed simultaneously on an SPB-1 (bonded methyl silicone) capillary column.

Thiophene - The products and nitrogen inhibitors in the thiophene hydrodesulfurization study were separated using either a Supelcowax-10 or an SPB-35 (bonded 35% phenyl- 65% methyl- silicone phase) capillary column. A typical chromatogram for the HDS of thiophene in the presence of pyridine is shown in Figure II.5, which represents a gas sample collected during reaction at 360°C on Batch 31. The various C_4 products which may have been present could not be separated at the initial oven temperature of 55°C, so the response factor for 1-butene was used for all products. Carbon mass balances on thiophene ranged from 94 to 101 percent.

RT (min)	Component
3.51	propylcyclohexane
4.22	propylcyclohexene
6.34	propylbenzene
A	tetradecane
B	DHQ
C	C_{16} isomers
D	n-hexadecane
18.73	BzTHQ
19.56	octadecane
21.95	OPA
22.31	quinoline
22.56	heavy product
22.80	eicosane
24.79	PyTHQ

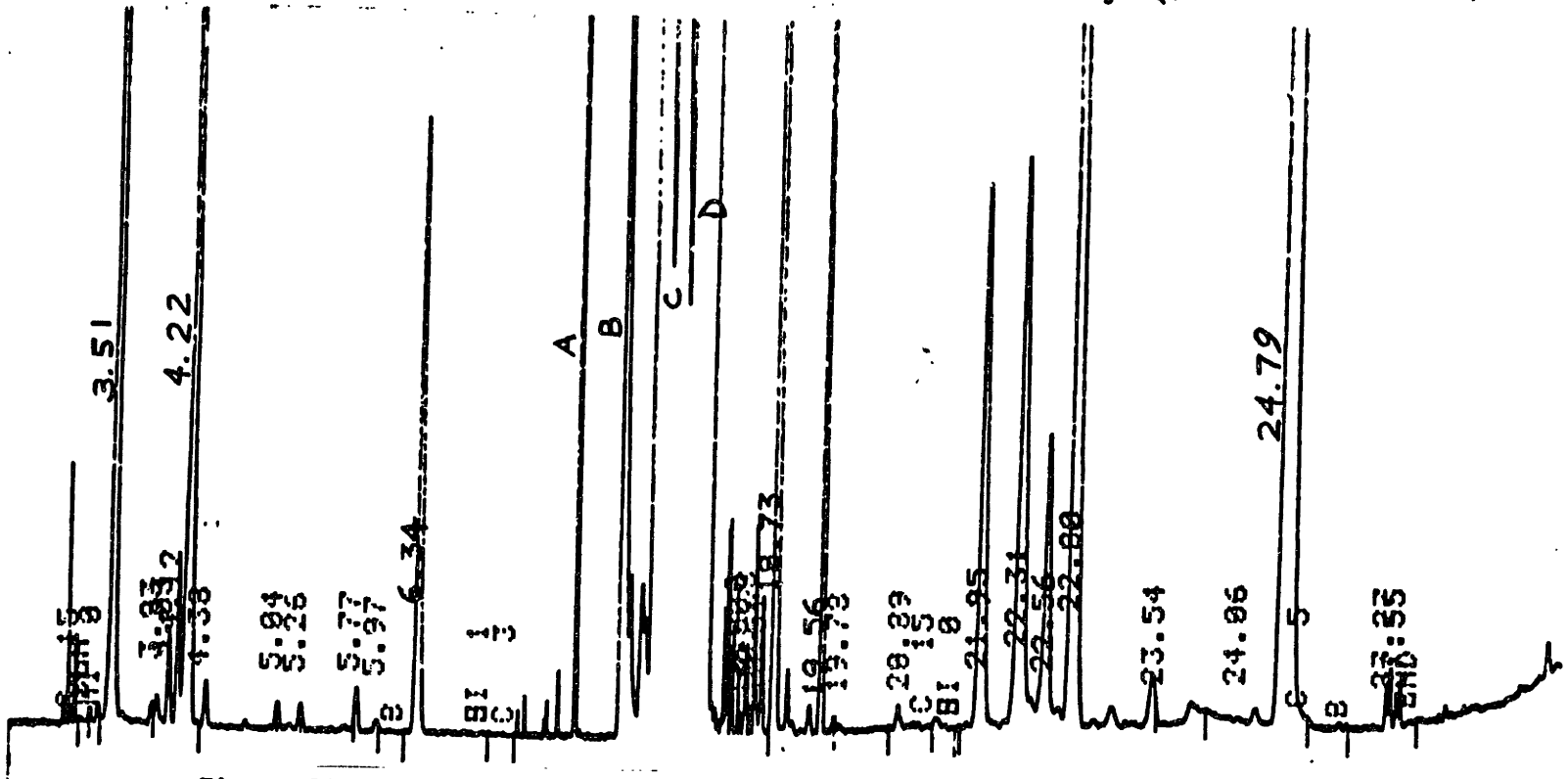

Figure II.4 Typical chromatogram for the HDN products of quinoline separated on a Carbowax column.

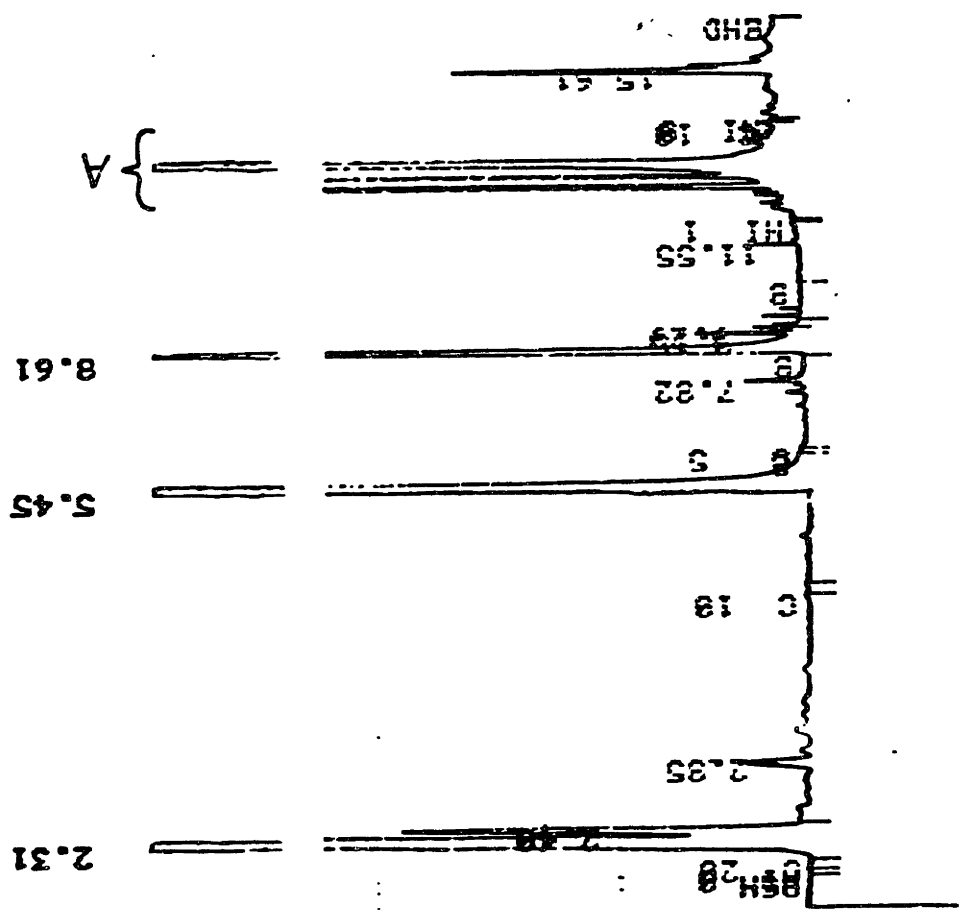

Figure II.5 Chromatogram for the hydrodesulfurization of thiophene.

II.E Laboratory Trickle Bed Reactor Design

In order to obtain intrinsic kinetics, it was desirable to minimize axial dispersion and to eliminate heat and mass transfer limitations. Data could then be analyzed using a simple isothermal plug-flow reactor model. Analysis of heat transfer limitations in this same reactor is described in detail in the thesis of Smith (1985). Insertion of a thermocouple into the center of the reactor tube above the catalyst bed showed that the preheater lengths were sufficient to bring the H_2/liquid mixture up to reaction temperature. Generally temperature variations between the catalyst and the fluid arise only after mass transfer limitations become important. Therefore, only axial dispersion and mass transfer limitations will be considered here.

II.E.1 Axial dispersion

Van Klinken and van Dongen (1980) found that dilution of catalyst pellets with inert particles of 200 micron diameter significantly increased the plug-flow behavior of a laboratory reactor. At a superficial liquid velocity of 1.9×10^{-4} m/s and a feed ratio of 800 ml H_2 at STP/ml liquid, dilution of the catalyst was found to increase liquid hold-up and to increase the mean residence time of the liquid.

Axial dispersion in the trickle bed reactor used here was reduced by diluting the catalyst particles (150-212 microns in diameter) with inert silicon carbide having an average particle size of 406 microns. This gives a reactor radius to particle radius of $r_R/r_p > 13$, which should be large enough to limit wall effects. Larger particles were required in this study to avoid excessive pressure drop at the liquid and H_2 flow rates used. A catalyst to inert volume ratio of 1 to 8 was used.

Trickle bed reaction experiments in this study were conducted at a superficial liquid velocity of 5.3×10^{-4} m/s. Using the dispersion coefficient from the study by van Klinken and van Dongen (Pe=69), a Peclet number for the system here can be estimated by adjusting for the higher superficial velocity and shorter reactor length L. This gives a Peclet number for the reactor $Pe = \mu L/D = 97$.

For small deviations for plug flow and for an irreversible first-order reaction, Levenspiel (1972) shows that the exit concentration ratio for equal volume reactors is:

$$\frac{C_A}{C_{Ap}} = 1 + \left[\ln \frac{1}{1-x} \right]^2 Pe^{-1} \qquad \text{(II.1)}$$

For the highest conversion observed in the trickle bed reactor, x=0.3, this expression indicates that the ratio of actual concentration to ideal plug-flow concentration (C_A/C_{Ap}) would be 1.001, and deviation from plug-flow behavior is negligible. Actual dispersion effects might be somewhat larger since the liquid partially vaporizes (reducing liquid flow rate) and the particle size of the inert was larger than in the experiments by van Klinken and van Dongen (1980).

For gas phase operation the criterion of Mears is used (Satterfield, 1980). In this case the catalyst to inert ratio was 1 to 4, and the inert particle size was 200 microns. Since the Reynolds number Re> 2, the Peclet number is set equal to 2, and the required length of the reactor is calculated from:

$$\frac{L}{d_p} > \frac{20}{Pe} \ln \frac{C_i}{C_f} \qquad \text{(II.2)}$$

For a conversion of 99% this expression indicates that the ratio L/d_p must be greater than 46. The actual reactor length to particle diameter ratio was almost 2500 so that plug-flow behavior can certainly be assumed.

II.E.2 Internal mass transfer limitations (liquid phase)

The catalyst particle size was chosen to eliminate any internal mass transfer limitations with the catalyst pores filled with either liquid or vapor. For the liquid phase reaction of dibenzofuran (the fastest reaction studied under trickle bed conditions), the liquid diffusivity for DBF in C_{16} was calculated from the Wilke-Chang correlation (Reid et al., 1987) in the form:

$$D_{12} = 7.4 \times 10^{-10} \frac{T\,(x\,M_2)^{1/2}}{\mu\,V_b^{0.6}} \qquad \text{(II.3)}$$

In this case: temperature T=623 K, x=1, molecular weight of C_{16} (M_2=226), and the viscosity of C_{16} at reaction temperature μ = 0.15 cP. Equation 1 gives a diffusivity of D_{12} = 0.00018 cm^2/s for these values. An effective diffusivity is calculated from typical values of the void fraction and tortuosity as:

$$D_{eff} = \frac{D_{12}\,\theta}{\tau} = 0.00003\ cm^2/s \qquad \text{(II.4)}$$

A generalized modulus can be calculated from the equation (Satterfield, 1981)

$$\Phi_s = \frac{R^2}{D_{eff}} \left[-\frac{1}{V_c} \frac{dn}{dt} \right] \frac{1}{C_s} \qquad \text{(II.5)}$$

where the expression in brackets is the observed rate of reaction per unit volume of catalyst pellets. The average catalyst particle radius is

R= 8.75×10^{-3} and the liquid phase concentration of reactant is estimated from the feed concentration C_s = 0.000245 mol/cm^3. A reaction rate per unit volume of catalyst is calculated from the observed conversion (30%) at a flow rate of 0.68 ml of feed/min and a catalyst loading of 0.8 g. This gives a value of 7.5×10^{-7} mols DBF/(s cm^3 catalyst).

The calculated modulus Φ_s = 0.01, this value being low enough to ensure that the catalyst effectiveness factor is close to unity. Similar results are found for reaction in squalane. Mass transfer limitations for hydrogen, which has a higher flux to the surface (from reaction stoichiometry), can also be shown to be insignificant.

II.E.3 Internal mass transfer limitations (gas phase)

The fastest reaction studied in the gas phase was the reaction of thiophene, studied over 25 mg of catalyst at 360°C. The catalyst diameter varied from 150-212 μm (use 181 μm) and the volume of catalyst was estimated to be 0.0243 cm^3. At a flow rate of 0.68 ml liquid/min the conversion of thiophene was 70%, which gives a reaction rate of 1.94×10^{-6} mols of thiophene/s. Thiophene was present in the reactor at 24 kPa under conditons of 360°C and 7 MPa which is equivalent to 4.62×10^{-6} mols/cm^3. The generalized modulus can again be calculated from equation II.5 where all of the parameters except D_{eff} have been discussed.

The effective diffusivity of thiophene in hydrogen is calculated by methods discussed by Satterfield (1981). Bulk gaseous diffusivity is calculated from an equation based on the kinetic theory of gases and the Leonard-Jones potential. The following parameters were used: V_b=88.1, ϵ/κ = 445.4, and $\kappa T/\epsilon_{12}$ = 3.882. The final parameter values required are σ_{12}= 4.04 and Ω_D = 0.89. The bulk diffusivity is give by

$$D_{12} = \frac{0.001858\ T^{3/2}\ [(2 + 84)/168]^{1/2}}{(70\ \text{atm})\ (4.04)^2\ \ 0.89} = 0.0208\ \text{cm}^2/\text{s} \qquad \text{(II.6)}$$

The effective diffusivity $D_{12,eff} = D_{12}\theta/\tau = 0.0042\ \text{cm}^2/\text{s}$. This value should be compared with the effective Knudsen diffuisivity to determine if Knudsen diffusion is mass transfer limiting.

Effective Knudsen diffusivity is given by the following expression:

$$D_{K,eff} = \frac{19400\ \theta^2}{\tau_m\ S_g\ \rho_p} \sqrt{\frac{T}{M}} = 0.0017\ \text{cm}^2/\text{s}. \qquad \text{(II.7)}$$

for the values θ=0.4, τ_m=2, S_g=1.76X10^6 m^2/g, T=633 K, M=84, and ρ_p= 1.4. It is surprising that Knudsen diffusion is limiting at these high pressures. However, a comparison of the calculated mean free path for gaseous thiophene at these temperatures (59 A°) to the pore radius (r_e=32 A°) shows that collisions with the walls should be important. Here the effective pore radius was calculated from:

$$r_e = \frac{2\ \theta}{S_g\ \rho_p} \qquad \text{(II.8)}$$

The overall effective diffusivity for thiophene can be calculated from the diffusional resistances using the approximate expression:

$$\frac{1}{D_{eff}} = \frac{1}{D_{12,eff}} + \frac{1}{D_{K,eff}} \qquad \text{(II.9)}$$

This leads to an overall $D_{eff} = 0.0012\ \text{cm}^2/\text{s}$. Plugging this value into the equation for the generalized modulus (eq. II.5) gives a value of $\Phi_s = 1.18$. Tabulated charts (Satterfield, 1981) indicate that the effectiveness factor for a catalyst particle having a diameter of 181 microns would be roughly greater than 0.95.

Chapter III

CATALYTIC HYDRODEOXYGENATION OF DIBENZOFURAN

Liquids derived from coal and oil shale differ from petroleum in their substantially higher oxygen contents and in the types of oxygen compounds present. Oxygen removal from coal liquids is required to ensure stability during storage (White et al., 1983) and may be required before further processing. The HDO of dibenzofuran (DBF) was chosen as a model reaction in this study since DBF is found in many coal liquids and is quite resistant to hydrotreating (see section I.E.4.b). Industrially, removal of the least reactive oxygenated compounds is the bottleneck for obtaining a high degree of conversion. Some of the effects of H_2O and H_2S on the catalytic reaction are also presented in this chapter since H_2O is formed as an HDO product and H_2S is usually present from hydrodesulfurization reactions.

III.A Experimental Section

Reactants. Dibenzofuran (99+% from Aldrich) was dissolved in a C_{16} paraffin mixture to form a solution with a concentration of 0.245 mol/L (~5.25 wt %). H_2S or H_2O were produced in situ by addition of 1-dodecanethiol or 1-decanol, respectively, to the liquid feed. These react rapidly under reaction conditions to produce the desired products. All experiments described here were performed at 350-390°C and 7 MPa total pressure, except for one study carried out to determine the reaction order with respect to hydrogen. Hydrogen was fed at the rate of 1520 mL at STP/mL liquid, equivalent to 9000 SCF/barrel, producing an initial dibenzofuran partial pressure of 24 kPa. This gas-to-liquid ratio is high

enough to ensure complete vaporization of the liquid at reactor conditions (Lin et al., 1980).

Catalyst. Several different samples of the same Ni-Mo/Al_2O_3 hydrotreating catalyst (HDS-3A) were used, and these were identified as samples number 20, 21, 22, 26, and 28. All of the catalyst samples except for number 21 were initially pre-sulfided according to the standard procedure.

The activity of this and hydrotreating catalysts in general decreases during reaction for the first 100-200 hours on stream. To achieve a steady-state activity within a reasonable length of time, the catalyst was treated with a feed containing 5 wt % quinoline at 375°C, 3 MPa, and in the absence of H_2S. A steady state with respect to the HDN of quinoline was generally observed within 150 hr on stream. In a few cases the catalyst was deactivated with dibenzofuran in the presence of H_2S. The resulting steady-state activity was higher, by approximately 30%, but there was no effect on product selectivity.

A limited number of studies were also performed on batch 21, under hydrogen pressure, but without pre-sulfiding and without addition of a sulfur compound. The relative distribution of reaction products was substantially different, as will be shown.

III.B Results: Studies of the HDO of Dibenzofuran (DBF)

III.B.1 Product distribution, sulfided catalyst.

The products isolated were essentially all hydrocarbons, with no oxygenated species other than water being detected in any significant amount. No linear paraffins were detected other than those present in the solvent or produced from the dodecanethiol. Single-ring compounds comprised the major portion of the hydrocarbons (about 75%), as shown in

the upper portion of Figure III.1. As shown in Figure III.2, cyclohexane predominated, but also present in significant but smaller amounts were methylcyclopentane, cyclopentane, benzene, methylcyclohexane, and cyclohexene. Note that cyclohexane is referred to the right-hand scale, with the others referred to the left-hand scale.

Selectivity is defined here and in subsequent figures as percent of DBF reacted that was converted to the specified product; ie., allowance is made for the fact that two molecules of single-ring products are formed from each molecule of DBF reacted in this way. Except for cyclohexene the ratios of the minor single-ring hydrocarbon products to one another did not vary with space time, suggesting that they are formed by parallel reactions. Cyclohexene would be rapidly hydrogenated to cyclohexane. It can plausibly be formed by elimination of water from phenol, via intermediate hydrogenation to form cyclohexanol, or directly from 2-cyclohexylphenol (see later).

Figure III.1 (lower portion) shows the distribution of double-ring hydrocarbon products as a function of space time. The principal species was cyclohexylbenzene (CHB). (The chemical acronyms used here are listed in Table II.2). Biphenyl also appeared, indicating that one pathway for the HDO of dibenzofuran involves direct removal of oxygen without prior ring hydrogenation. Dicyclohexyl (DCH) and (cyclopentylmethyl)-cyclohexane (CPMCH) increased with contact time, whereas cyclohexylbenzene and biphenyl decreased, indicating secondary hydrogenation. (Cyclopentylmethyl)-benzene was also believed to be present at 13% of the concentration of CHB, but it could not be detected by the analytical procedures used (see section II.D).

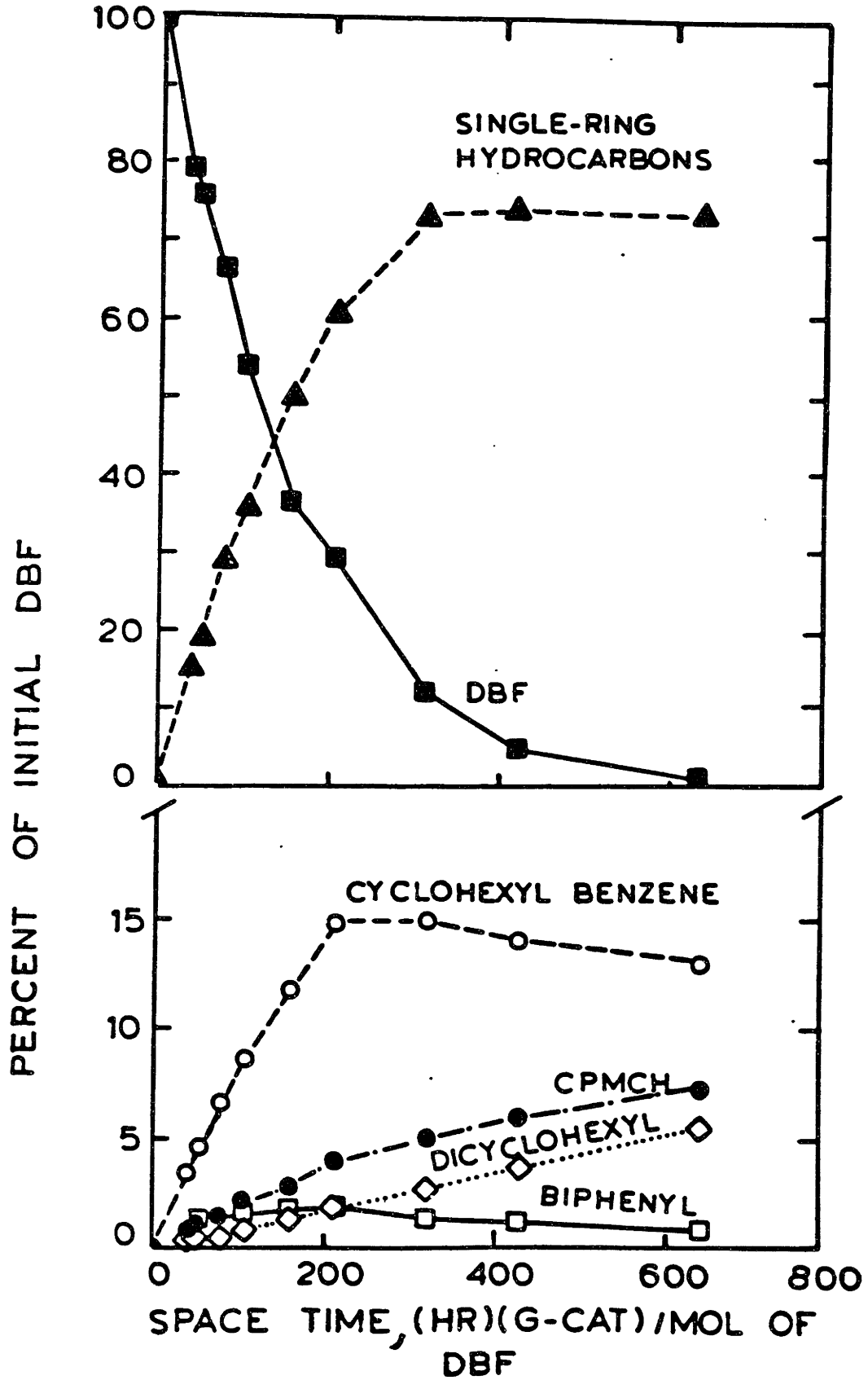

Figure III.1 Product distribution of DBF at 375 °C, 7.0 kPa of H_2S, and 7.0 MPa. Individual double-ring products are shown on the lower plot.

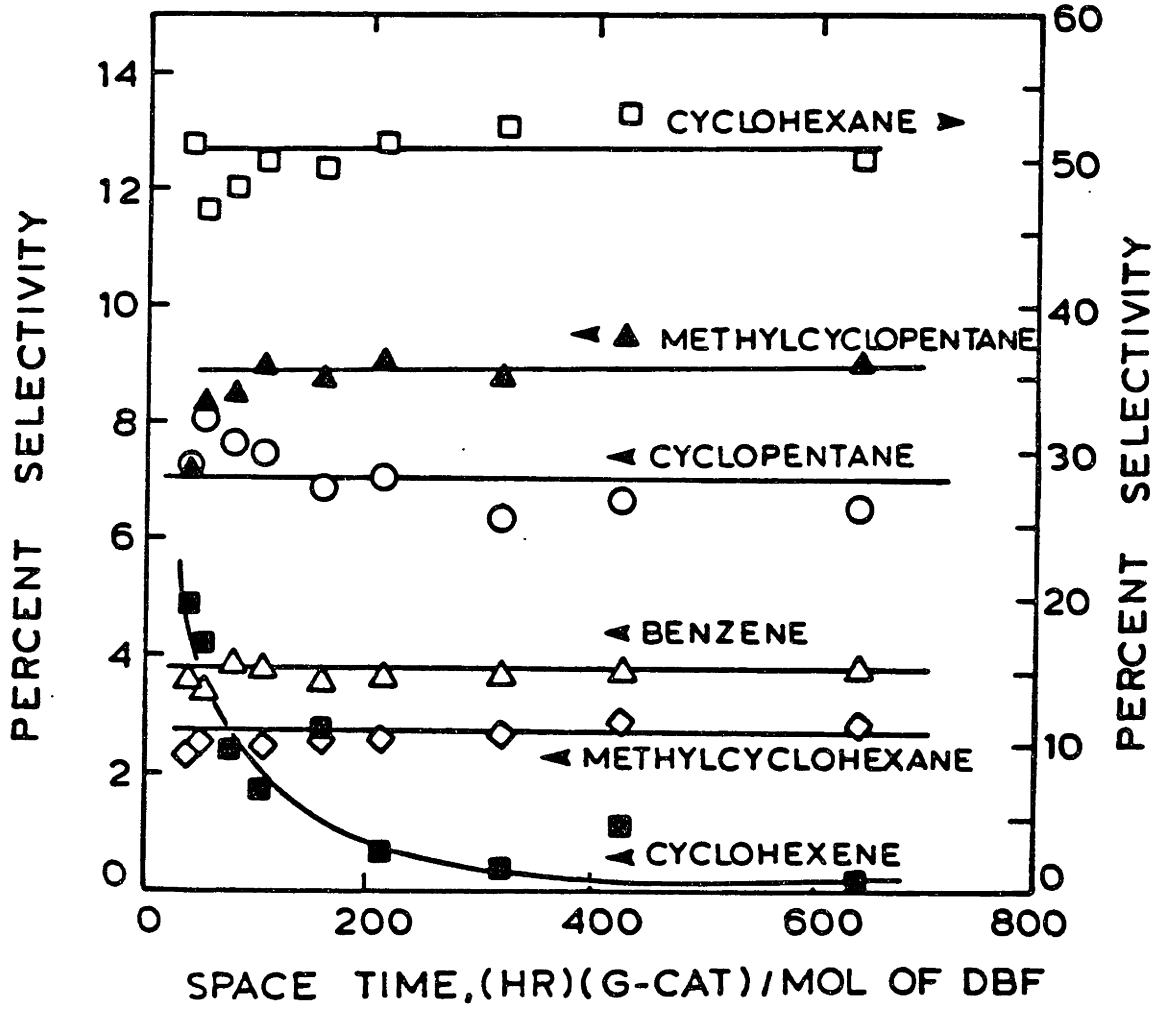

Figure III.2 Product distribution of DBF at 360 °C, 7.0 kPa of H_2S, and 7.0 MPa for individual single-ring compounds.

III.B.1.b Comparison with previous literature - Our product spectrum is similar to that of Krishnamurthy et al. (1981) in that they reported the same four double-ring compounds. Cyclohexane was found in major amounts, but they did not report any of the other single-ring compounds shown in Figure III.2. (The compound identified here as (cyclopentylmethyl)-cyclohexane is termed (cyclohexylmethyl)-cyclopentane by them.) They also reported that a phenylhexanol was present in their isolated products, but it appears that this probably was a misidentification. We compared a chromatogram of the DBF reaction products obtained with a Carbowax (polar) packed column, as reported in the thesis by Krishnamurthy (1980), to our chromatograms on a Carbowax capillary column. The elution orders of the various species were identical on the two columns. However, the product peak eluting between dicyclohexyl and cyclohexylbenzene was assigned to 6-phenyl-1-hexanol by Krishnamurthy et al. (1981), while we identified it as (cyclopentylmethyl)-benzene (CPMB), on the basis of GC/MS analysis. Furthermore, when we spiked a representative reaction sample with 6-phenyl-1-hexanol, the alcohol was found to elute after both cyclohexylbenzene and DBF on a Carbowax column.

The mass spectral data of Krishnamurthy (1980) was also compared with data from this study (appendix A6) for presumably the same GC peak. The MS results of Krishnamurthy indicate contamination by air (high intensities at mass numbers 28 and 32), but the higher mass numbers show good agreement with ours. From the high intensities at mass numbers 91 and 92 together with the parent peak at mass number 160 found in both studies, the species can be identified as CPMB rather than phenylhexanol. A phenylhexanol might conceivable be formed, but if so, it would be very reactive and unlikely to survive.

On an oxide catalyst (see later) we also found a small amount of 2-phenylphenol, the latter identified by comparing its GC retention time to that of a known standard.

III.B.2 Effect of hydrogen sulfide.

While the reactor was unattended, it was maintained at 7.0 MPa of hydrogen and 360°C, but no DBF was fed to it. Instead a solution of hexanethiol (rather than dodecanethiol) in xylene was continuously introduced along with hydrogen. This generated 13.9 kPa of H_2S in situ. With this treatment the activity of the deactivated catalyst with respect to the HDO of DBF remained stable for over 150 hours on stream when H_2S was also present during reaction (Figure III.3). Standard activity was measured at 360°C, 7.0 MPA, and a space time of 160 (hr g of catalyst)/mol of DBF.

During reaction of DBF, when the thiol was removed from the feed stream, the conversion of DBF increased dramatically and then declined fairly rapidly toward its original value as shown in Figure III.4. Reintroduction of H_2S to the system, via the thiol, caused a drop in conversion, with the catalyst requiring over 10 hr to return to normal activity. Removal of H_2S a second time again increased activity.

The same behavior was shown on another sample of the catalyst (batch 26) in which the effect of partial pressure of H_2S was determined more quantitatively. As shown in Figure III.5, increasing the H_2S partial pressure from 0 to about 5 kPa dropped the percent HDO from about 60% to about 44%, but further increases in the partial pressure to 75 kPa showed no further effect. Decreasing the H_2S partial pressure to 15 kPa from 75 kPa resulted in a substantial increase in activity, which increased further as H_2S was removed completely. These last values are transients,

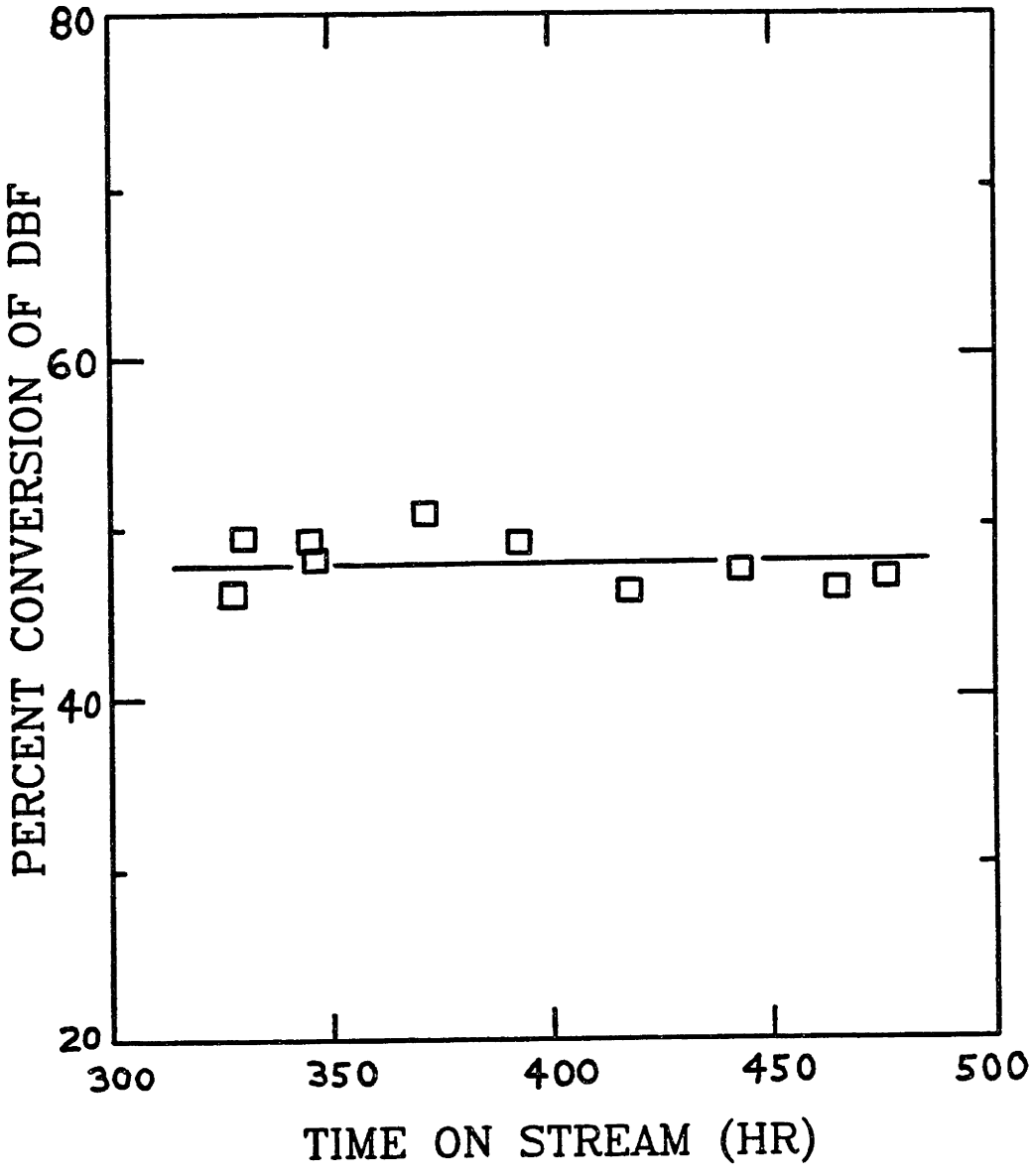

Figure III.3 Catalyst activity remains stable in the presence of H_2S.

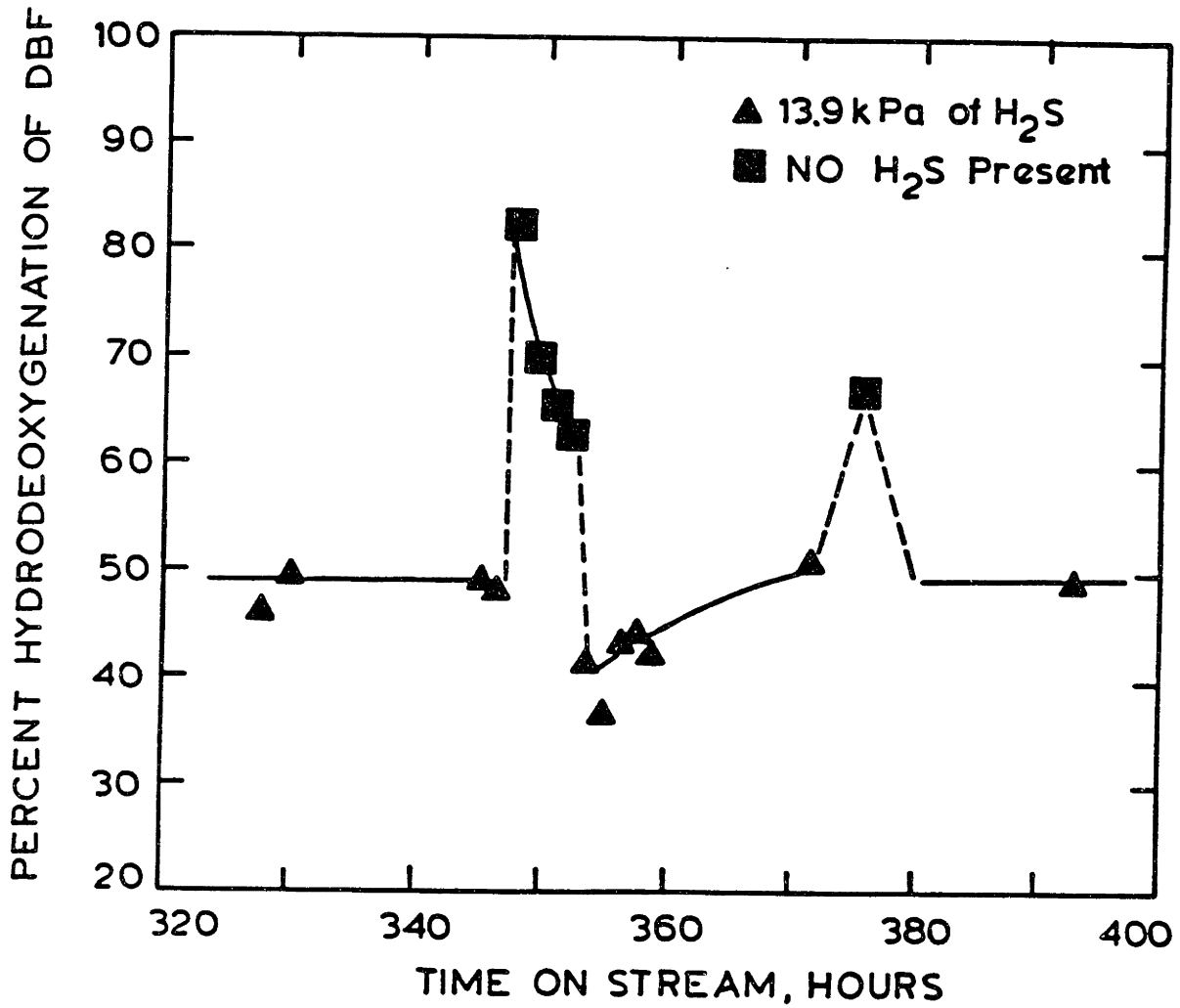

Figure III.4 Removal of H_2S increases HDO activity.

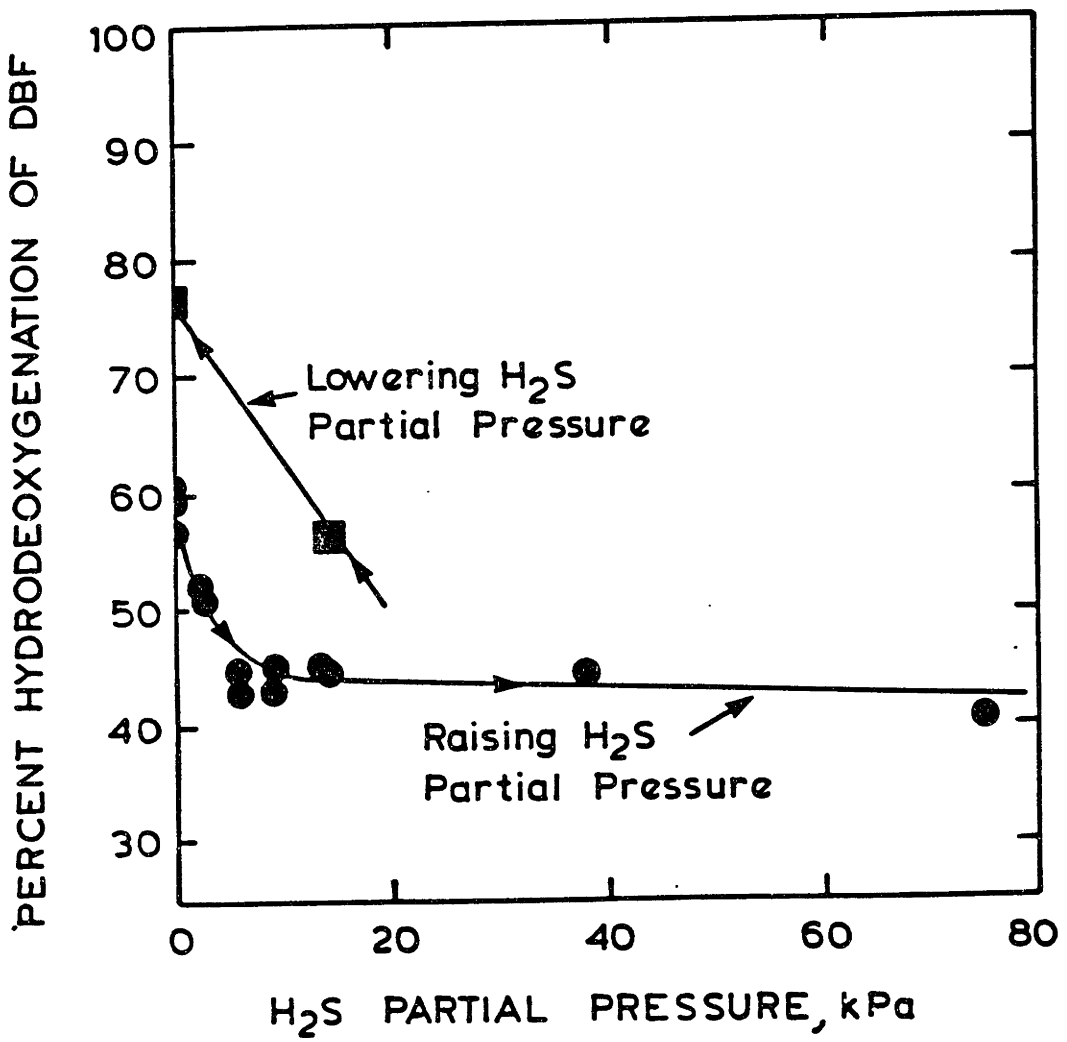

Figure III.5 Lowering of H_2S partial pressure increases HDO activity. Transient effects are observed; 24 kPa of DBF was used.

however. Judging from Figure III.4 these high levels of activity would not be maintained. This behavior is the opposite of that observed with the hydrodenitrogenation of quinoline - there the addition of H_2S to a feed stream in contact with a presulfided Ni-Mo/Al_2O_3 catalyst increased the overall nitrogen removal activity instead of decreasing it (Satterfield and Gultekin, 1981). However, the effect of H_2S on the hydrogenation reactions of the quinoline hydrodenitrogenation network are similar to the effects observed here with DBF.

Removal of H_2S increased the content of unsaturated products (benzene, biphenyl, and cyclohexylbenzene) formed per mole of DBF reacted from about 20 mol % to 30 mol %. Figure III.6 (catalyst batch 26) shows that a decrease in H_2S partial pressure also increased the percent of double-ring hydrocarbon products produced. This selectivity was not affected significantly by the length of time for which the catalyst had been previously exposed to the specified partial pressure of H_2S.

III.B.3 Effect of water.

The effect of water in the presence of H_2S was investigated by the addition of decanol to the dibenzofuran feed in a quantity that would double the partial pressure of water in the reactor (from 24 to 48 kPa) if dibenzofuran were completely reacted. The effects are minor and conversion remained essentially the same as shown in Figure III.7. The ratio of (cyclopentylmethyl)-cyclohexane to dicycloheyl increased from about 1.5 to 1.7, indicating a slight increase in isomerization activity upon the addition of water.

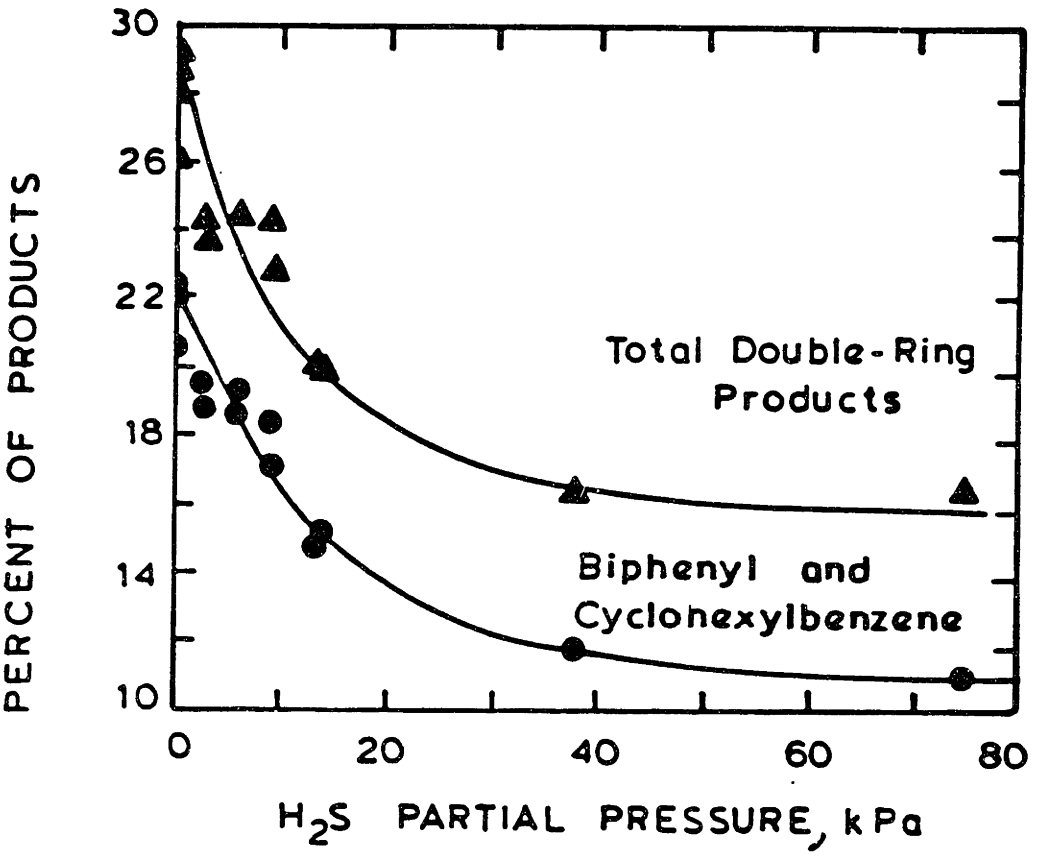

Figure III.6 Increased H_2S partial pressure decreases selectivity to double-ring products.

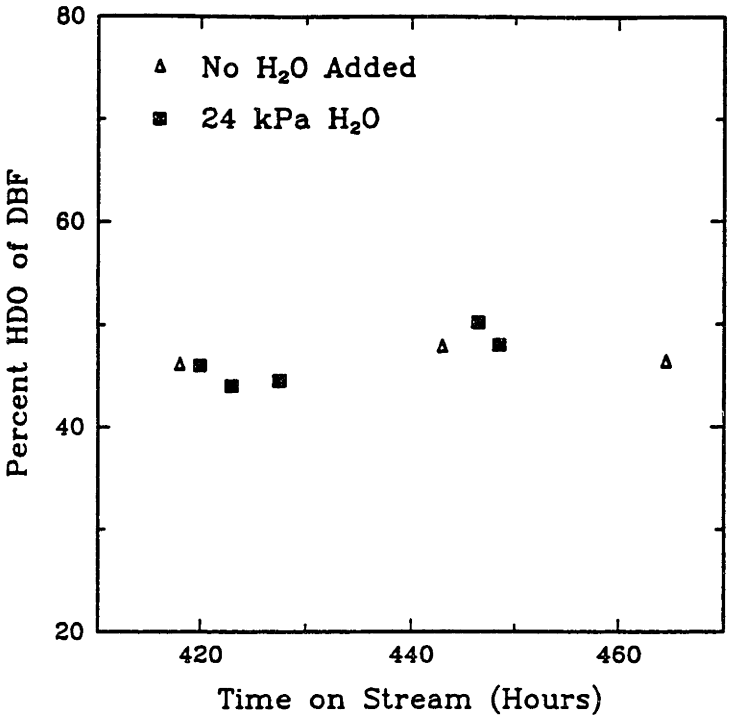

Figure III.7 Addition of water (as decanol) has no effect on the conversion of dibenzofuran.

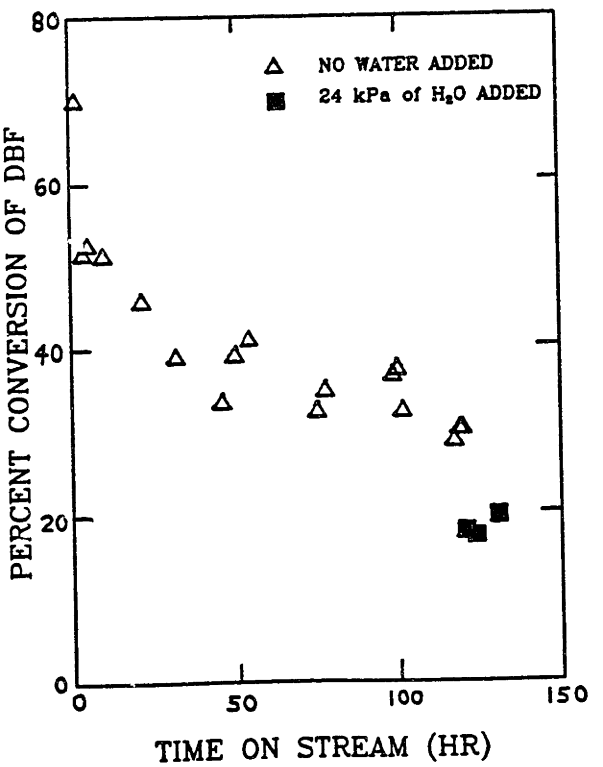

Figure III.8 "Oxide" catalyst was sensitive to water partial pressure.

III.B.4 Co-Mo catalyst.

The HDO of dibenzofuran was also studied briefly on a Co-Mo/Al_2O_3 catalyst (HDS-1442B) to see if there were any significant differences in the reaction network compared to that on a Ni-Mo catalyst. After being sulfided by the standard procedure, the catalyst was exposed to dibenzofuran (24 kPa) and H_2S (7 kPa) at a space time of 320 (hr g.of catalyst)/ mol of DBF. Total pressure and temperature were set at 7 MPa and 360°C respectively. Limited deactivation was observed, with the conversion of DBF dropping from 48 to 43 % during the first 516 hours on stream.

After a steady state was reached, the conversion of DBF was determined as a function of space time. The reaction was first order with respect to DBF as it is on a Ni-Mo catalyst (see later), but the Co-Mo catalyst was about one third as active as the Ni-Mo catalyst. Table III.1 shows that for this limited study the selectivities for single ring products were identical on the two catalysts. However, in studies of other oxygenated compounds such as phenols, significant differences have been reported over Co and Ni promoted catalysts (see section I.E.4.a)

III.B.5 Oxide catalyst.

If the Ni-Mo/Al_2O3 catalyst is not sulfided, its behavior is substantially different. Batch 21 was operated under hydrogen pressure but was not pre-sulfided, and no sulfur compound was added to the dibenzofuran feed. This catalyst will be termed "oxide catalyst", although the actual forms of the metallic elements present are not known. During 140 hours on stream at 360°C, deactivation was completed by passing a feed containing 0.245 mol/L of dibenzofuran through the reactor at a space time of 544 (hr g of cat)/ mol of DBF.

TABLE III.1

Selectivity toward Single-Ring Products on

Co-Mo and Ni-Mo Catalysts[a]

species	% selectivity Co-Mo	Ni-Mo
cyclopentane	7.1	7.0
methylcyclopentane	6.6	9.0
cyclohexane	47	50
methylcyclohexane	2.5	2.5
cyclohexene	b	b
benzene	3.3	3.6
Total single-ring products	71	72

[a]Note the the selectivities are identical for both catalysts.

[b]Varies.

HDO activity (percent removal of oxygen) was checked at a space time of 160 (hr g of catalyst)/mol, and the decline in catalyst activity is shown by the triangular symbols in Figure III.8. The fluctuations in activity after 100 hours on stream appeared to be caused by changing the space time during overnight operation. Higher space times would increase both the conversion of DBF and the partial pressure of water in the reactor.

To investigate the possible effect of water as such, 0.245 mol/L of decanol was added to the dibenzofuran feed to produce an additional 24 kPa of H_2O in situ beyond that produced by the HDO of DBF. This increase in water partial pressure dropped the conversion from 30 to 20% at 160 hr g cat/mol, as shown by the filled symbols in Figure III.8. In order to reduce the proportionate change in water partial pressure with conversion, in further experiments with the oxide catalyst, feeds were utilized which contained 0.245 mol/L of decanol.

The "oxide" form of the Ni-Mo catalyst was less active than the sulfide form. The percent of HDO over the oxide catalyst at 360°C, 7 MPa, and 160 (hr g of catalyst)/mol was only 19% (with 24 kPa of H_2O added) compared to a percent HDO of 55% (with 7 kPa of H_2S added) at the same conditions on the sulfide catalyst.

The product distribution as a function of space time for the oxide catalyst is shown in Figure III.9 (for double-ring products) and Figure III.10 (for single-ring products) for a study at 360°C and 7 MPa and with 24 kPa of water added as decanol. The distribution differed greatly from that obtained over a sulfided catalyst. The selectivity to single-ring hydrocarbons was only 25 % on the oxide catalyst, as compared to a 75% selectivity on the sulfide catalyst. The major double-ring products were

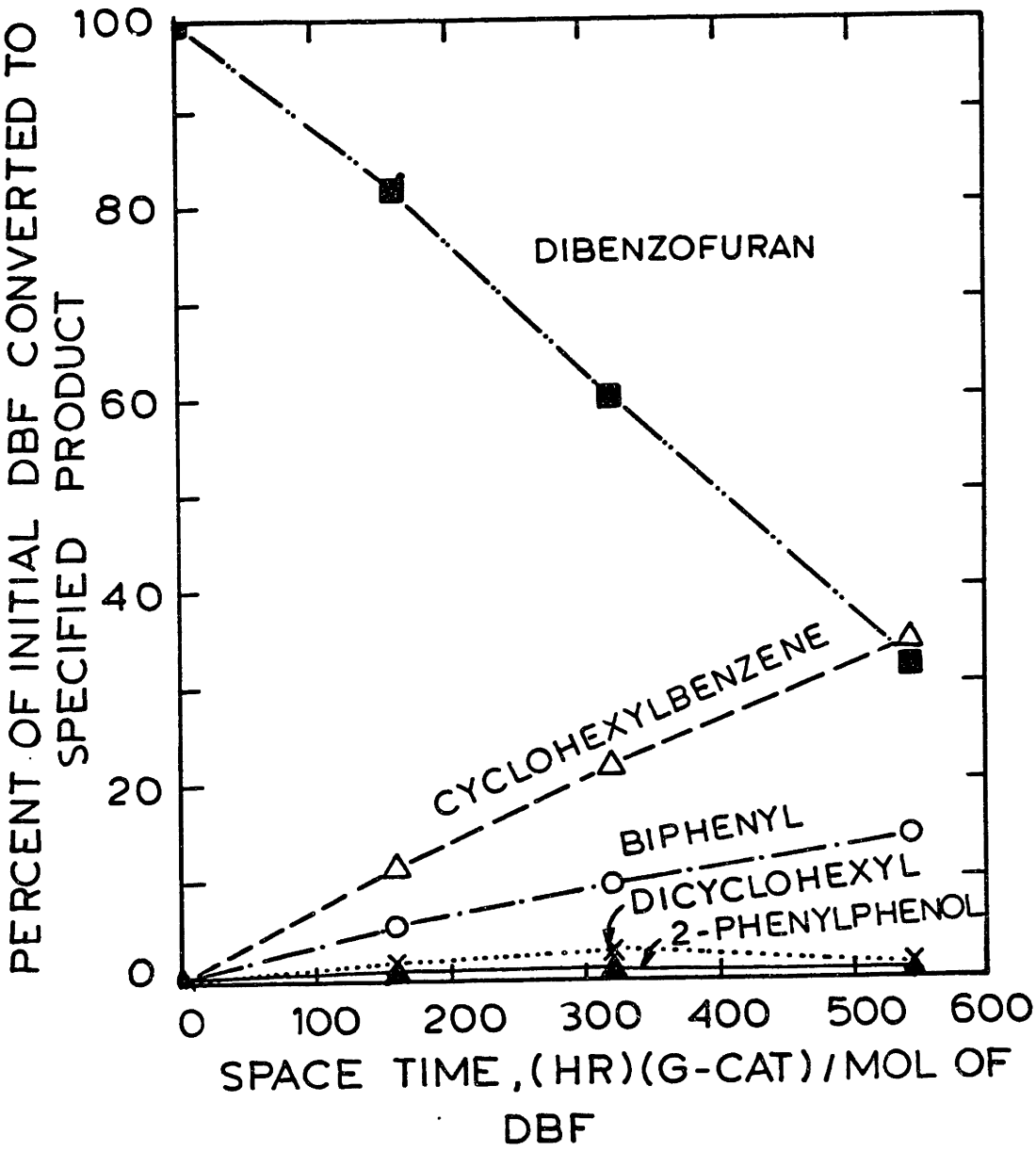

Figure III.9 Double-ring product distribution over oxide catalyst.

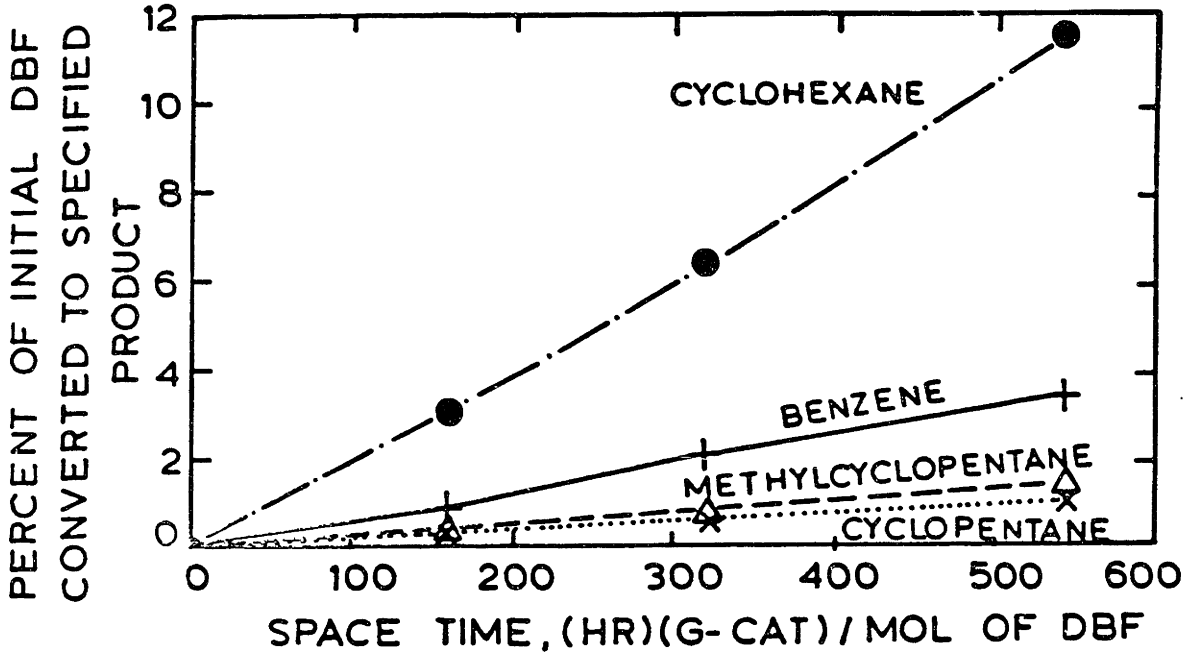

Figure III.10 Single-ring product distribution over oxide catalyst.

cyclohexylbenzene and biphenyl. 2-Phenylphenol was detected at low concentrations and appears to be an intermediate over the oxide catalyst.

Saturated products such as dicyclohexyl and CPMCH were not found to any significant extent. Among the single-ring products, cyclohexane predominated as with the sulfided catalyst; benzene, methylcyclopentane, and cyclopentane were found as before, but in somewhat different ratios. Two minor products found previously, methylcyclohexane and cyclohexene, were not found here.

Figures III.9 and III.10 also show that in the presence of 24.0 kPa of water, the rate of HDO is zero order in DBF over the oxide catalyst, indicating that adsorption of DBF may be quite strong. The curves for biphenyl, cyclohexylbenzene, and all of the single-ring products show a linear increase in concentration with time, indicating that they may be formed by parallel reactions.

III.B.5.a Sulfiding of the oxide catalyst. - After the above studies were completed at 140 hours on stream, an attempt was made to sulfide the catalyst using a liquid feed containing 30 wt % dimethyl disulfide (DMDS) in xylene. It has been reported that DMDS decomposes at a relatively low temperature, making it useful as a spiking compound (Hallie, 1982). The DMDS in xylene mixture was fed at 0.58 ml/min with a hydrogen flow rate of 250 ml at STP/min. Sulfiding was begun initially for 6 hours at 200°C at a total pressure of 0.24 MPa. The sulfiding temperature was then raised to 315°C at a rate of about 1 °C/hr and the temperature was held at 315°C for 1 hour. Conditions were therefore very similar to those used in the standard sulfiding procedure using an H_2S in hydrogen mixture.

Comparison of the activity and selectivity of the catalyst before and after exposure to the sulfiding agent indicated that only partial sulfiding had been obtained. Although the activity increased somewhat,

the product distribution resembled that found on the oxide catalyst and water still inhibited the HDO of DBF in the absence of H_2S. This resistance of the catalyst to sulfiding can probably be attributed to the reduction of MoO_3 upon exposure to high temperature hydrogen. Arnoldy et al. (1985) have shown that pre-reduction of a supported Mo catalyst shifts the required sulfiding temperature above 400°C.

The catalyst was then exposed to the DMDS/xylenes mixture for 1 hour at 360°C and and a total pressure of 7 MPa. This would produce an H_2S partial pressure of 0.7 MPa. After this severe sulfiding, the product distribution for dibenzofuran HDO closely resembled that found for a catalyst pre-sulfided in the normal manner. The only difference in selectivity observed was an increase in the CPMCH/DCH ratio from 1.5 on a normal catalyst to 2.2. However, the activity of the catalyst was slightly lower than that for a catalyst sulfided without prior exposure to hot hydrogen alone. Conversion of DBF at the standard activity condition, 160 (hr g of catalyst)/mol of DBF and 13.9 kPa of H_2S, was only 40% as compared to the expected conversion close to 50%.

III.C Results: Studies of Possible Reaction Intermediates.

Five possible intermediates in the HDO network for dibenzofuran were studied separately on either the severely sulfided form of batch 21, the catalyst originally studied as an oxide, or on batch 28 of the sulfided standard catalyst. Both catalyst samples were studied at 7.0 MPa and 360 °C, but the H_2S partial pressure was 13.9 kPa for batch 21 and 7 kPa for batch 28. The product distribution was essentially the same for both catalysts when DBF, 2-phenylphenol, or 2-cyclohexylphenol was fed, the three compounds studied on both catalysts.

Of particular interest is the extent to which single ring compounds are formed versus double-ring compounds, since this provides important evidence for determining the main reaction pathway. Also of interest is the ratio of CPMCH to DCH, which is a measure of the isomerization activity of the catalyst. Four of the possible intermediates reacted so fast over 1.6 g of catalyst that they were completely converted at the shortest space times studied. The least reactive was 2-phenylphenol, but it reacted much faster than DBF. Results discussed below were those obtained after the catalyst had reached steady-state activity.

III.C.1 2-Phenylphenol.

As shown in Figure III.11, 2-phenylphenol reacts to form mainly biphenyl and cyclohexylbenzene (CHB). Although biphenyl and CHB undergo secondary hydrogenation, the hydrogenation of biphenyl by itself proceeds much slower than the HDO of 2-phenylphenol. Thus we found that the first-order hydrogenation rate constant for biphenyl hydrogenation, measured separately, is in the range of 0.0045 mol/(hr g of catalyst) while that for 2-phenylphenol HDO is about 0.016 mol/(hr g of catalyst).

If cyclohexylbenzene were formed only from biphenyl through a series reaction of the form:

$$\text{2-phenylphenol} \xrightarrow{k_1} \text{biphenyl} \xrightarrow{k_2} \text{CHB},$$

the maximum in the concentration of biphenyl that would be observed can be calculated. Applying the mathematics discussed by Smith (1981), the maximum concentration ratio of biphenyl to the initial 2-phenylphenol is given by:

$$\left[\frac{k_1}{k_2} \right]^{k_2/(k_2 - k_1)} \qquad \text{(III.1)}$$

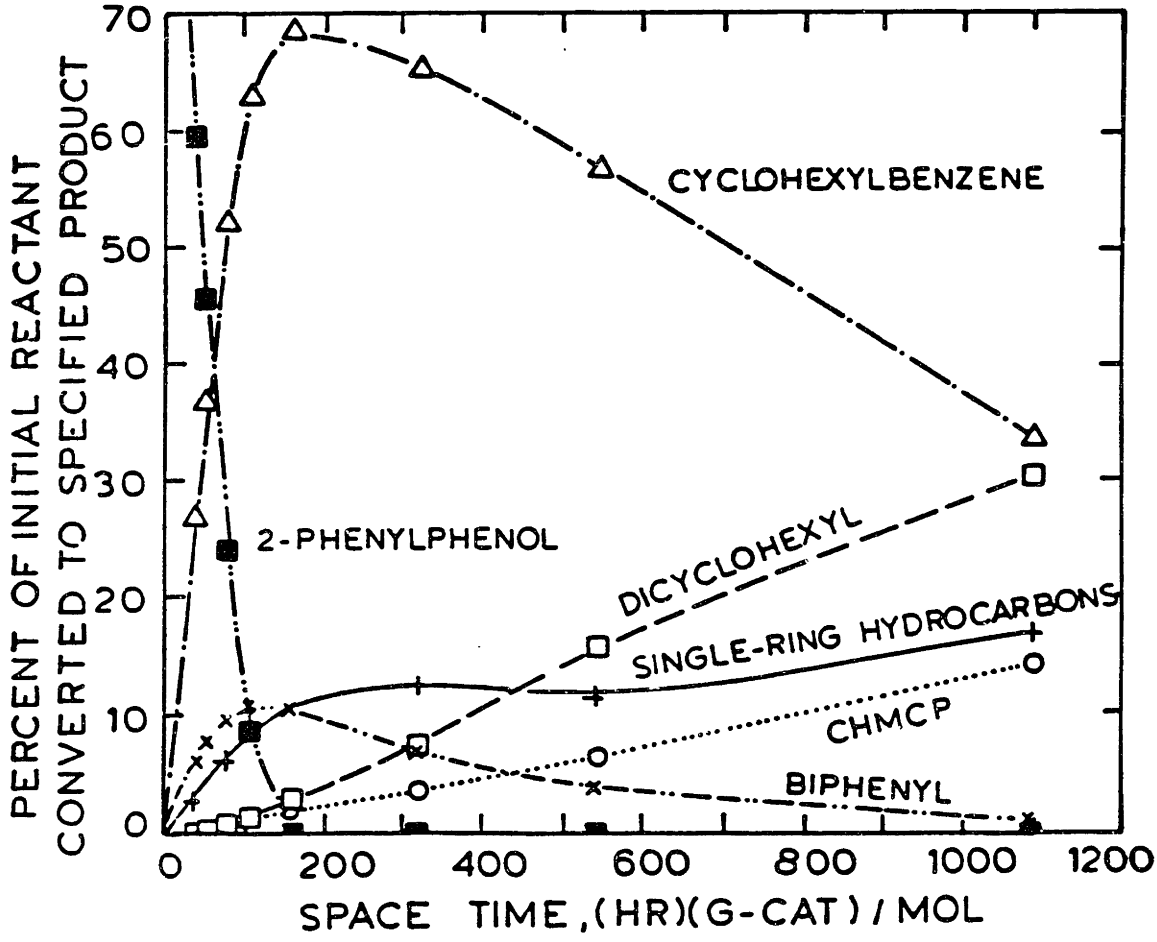

Figure III.11 Hydrodeoxygenation of 2-phenylphenol using sulfided sample 21.

From the above rate constants one can calculate that the biphenyl concentration would reach a maximum value of 61% of the initial concentration of 2-phenylphenol rather than the 10% observed. The calculation indicates that most of the cyclohexylbenzene was formed directly from 2-phenylphenol. A parallel, less important rection was the formation of CHB via biphenyl.

The ratio of CPMCH to its isomer DCH was approximately 0.5. Single-ring products comprised only 16 % of the final products.

Krishnamurthy et al. (1981) reported a study of 2-phenylphenol at 325 °C and 10.34 MPa. Cyclohexylbenzene and biphenyl were found, as here. They also reported that a phenylhexanol was isolated, but the results of this study suggest that this species was erroneously identified.

III.C.2 2-Cyclohexylphenol.

A total of 91% of the products were single-ring compounds, cyclohexane predominating (Figure III.12). The double ring compounds were CPMCH, DCH, and CHB. Cyclohexylbenzene was apparently slowly hydrogenated to DCH as a secondary reaction.

Krishnamurthy et al. (1981) studied the reaction of 2-cyclohexylphenol at 287°C in their autoclave and reported finding cyclohexylbenzene and dicyclohexyl, as here, but also phenol. Cyclohexane was a major isolated product in both studies. Since no phenol was detected here at the usual reaction conditions, a brief study was performed at 360°C and 7 MPa using only 10 mg of sulfided Ni-Mo catalyst, less than 1% of the usual catalyst loading. By changing the space time, conversions were varied from 8 to 85 %. As shown in Figure III.13, the primary products were phenol and cyclohexene, formed in nearly equal amounts. Cyclohexane appeared at higher conversions, evidently formed by hydrogenation of cyclohexene.

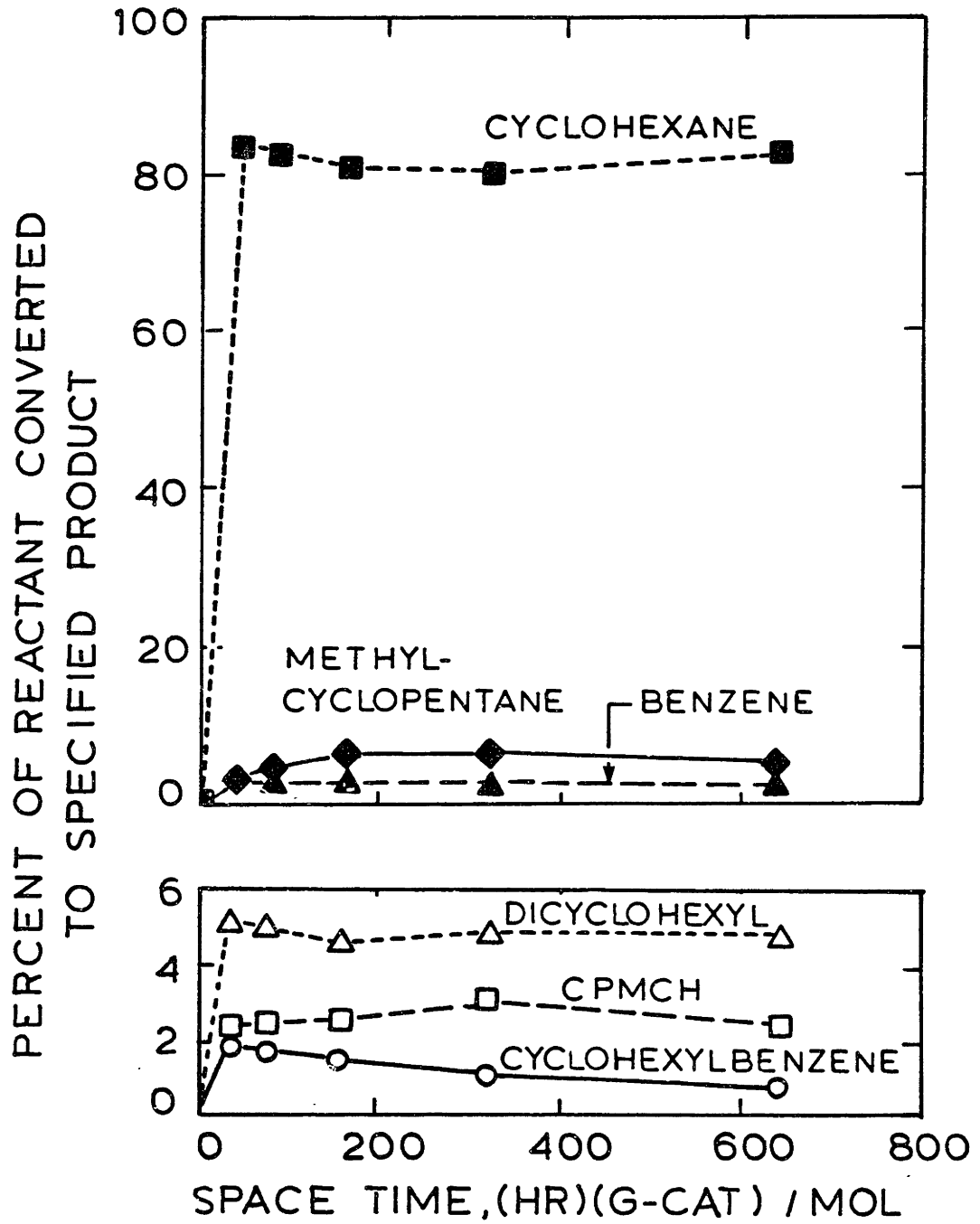

Figure III.12 Hydrodeoxygenation of 2-cyclohexylphenol using sulfided sample 28.

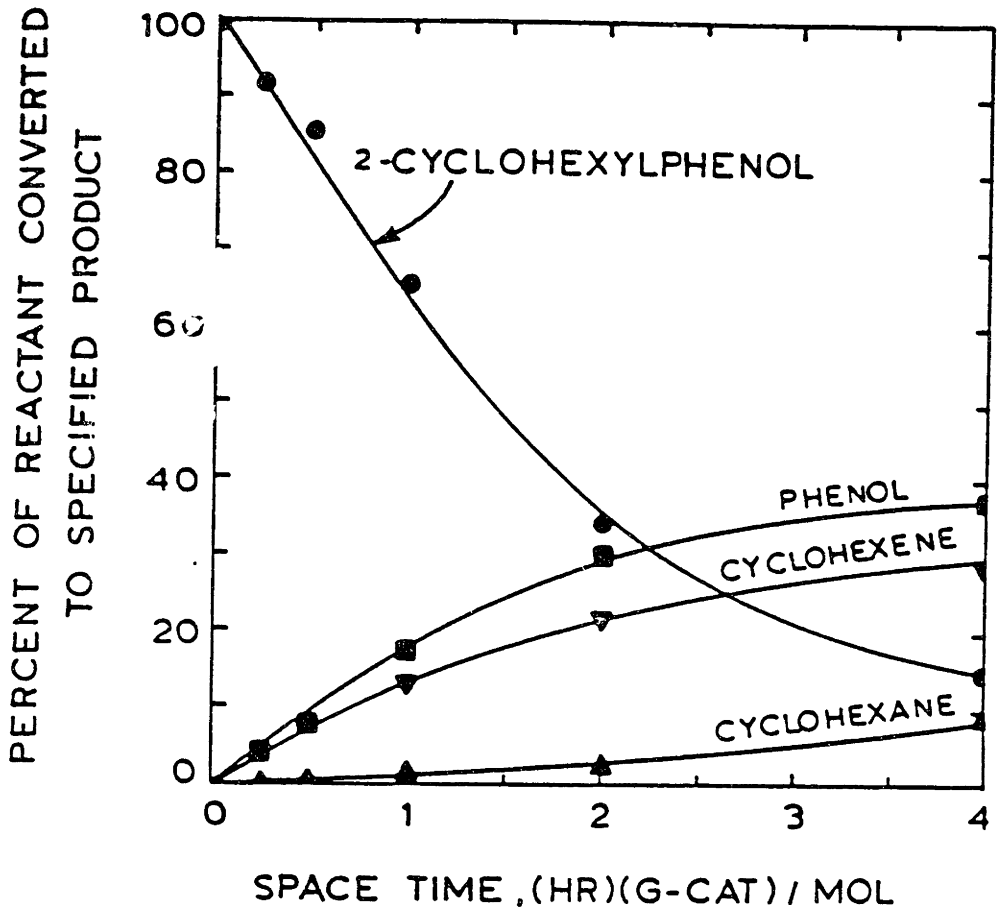

Figure III.13 Hydrodeoxygenation of 2-cyclohexylphenol at moderate conversion.

Small amounts of cyclohexylbenzene, dicyclohexyl, and 3-cyclohexylphenol were also identified (not shown). The latter species was not present in the feed and was identified by GC/MS (see Appendix A4).

Krishnamurthy et al. (1981) also concluded that even in the presence of catalyst this reaction may have been noncatalytic at least in part. To test this possibility under our conditions, the reactor was assembled in the normal configuration with the catalyst replaced by silicon carbide of approximately the same particle size. The reaction was carried out in the presence of hydrogen at a gas-to-liquid feed ratio of 1520 mL at STP/mL. Liquid feed containing 0.245 mol/L of 2-cyclohexylphenol was metered to the reactor at 0.34 mL/min.

At 390°C and 7.0 MPa total pressure, conversion of 2-cyclohexylphenol was only 2.5 %. By comparison, the catalytic reaction produced 100% conversion at 350°C over the entire range of space times tested. The greater importance of the thermal reaction in the study by Krishnamurthy and co-workers was probably due to the longer residence time in a batch autoclave as compared to a flow reactor. The products of the thermal reaction in this study were phenol and cyclohexene, as was observed for the catalytic reaction at moderate conversions.

By either mechanism the primary products thus appear to be principally phenol and cyclohexene. Hydrogenation of phenol would yield cyclohexanol, which would be expected to possess high reactivity. Removal of oxygen by elimination of water would form cyclohexene, which, produced by either route, is hydrogenated fairly rapidly to cyclohexane. This is consistent with the results for dibenzofuran shown in Figure III.2. In an earlier study of HDO of 3-ethylphenol, Satterfield and Yang (1983) also found considerable quantities of ethylcyclohexene formed as an intermediate.

III.C.3 trans-2-Phenylcyclohexanol.

Figure III.14 shows that this compound was converted rapidly and selectively to cyclohexylbenzene (CHB). The CHB became hydrogenated to DCH and isomerized to CPMCH at approximately equal rates.

III.C.4 2-Cyclohexylcyclohexanol.

The major products formed were DCH and CPMCH, as shown in Figure III-15. At low space times selectivity to DCH was high, producing a CPMCH to DCH ratio of 0.5. The DCH produced then slowly isomerized to form CPMCH. CHB was also detected, possibly formed directly during the dehydrogenation of the cyclohexanol structure, but the amounts were small.

III.C.5 1,2,3,4-Tetrahydrodibenzofuran (TH-DBF).

This compound was custom synthesized for this study by Frinton Laboratories using the method published by Ebel (1929). Figure III-16 shows that 88% of the TH-DBF reacted was converted to single-ring compounds. The cyclohexane concentration is given by the right-hand scale; those of the other species are given by the left-hand scale. Complete conversion was obtained even at the lowest space time studied.

At very short space times a new product was found to be present in small concentrations. We have identified it as hexahydrodibenzofuran by its retention order on a polar (Carbowax) GC column. For identification a small quantity of perhydrodibenzofuran was synthesized by hydrogenation of DBF over a supported Rh catalyst at 80°C and 7 MPa. On the polar column the retention order of the DBF derivatives is perhydrodibenzofuran, TH-DBF, and DBF. Since the new peak eluted between the retention times for

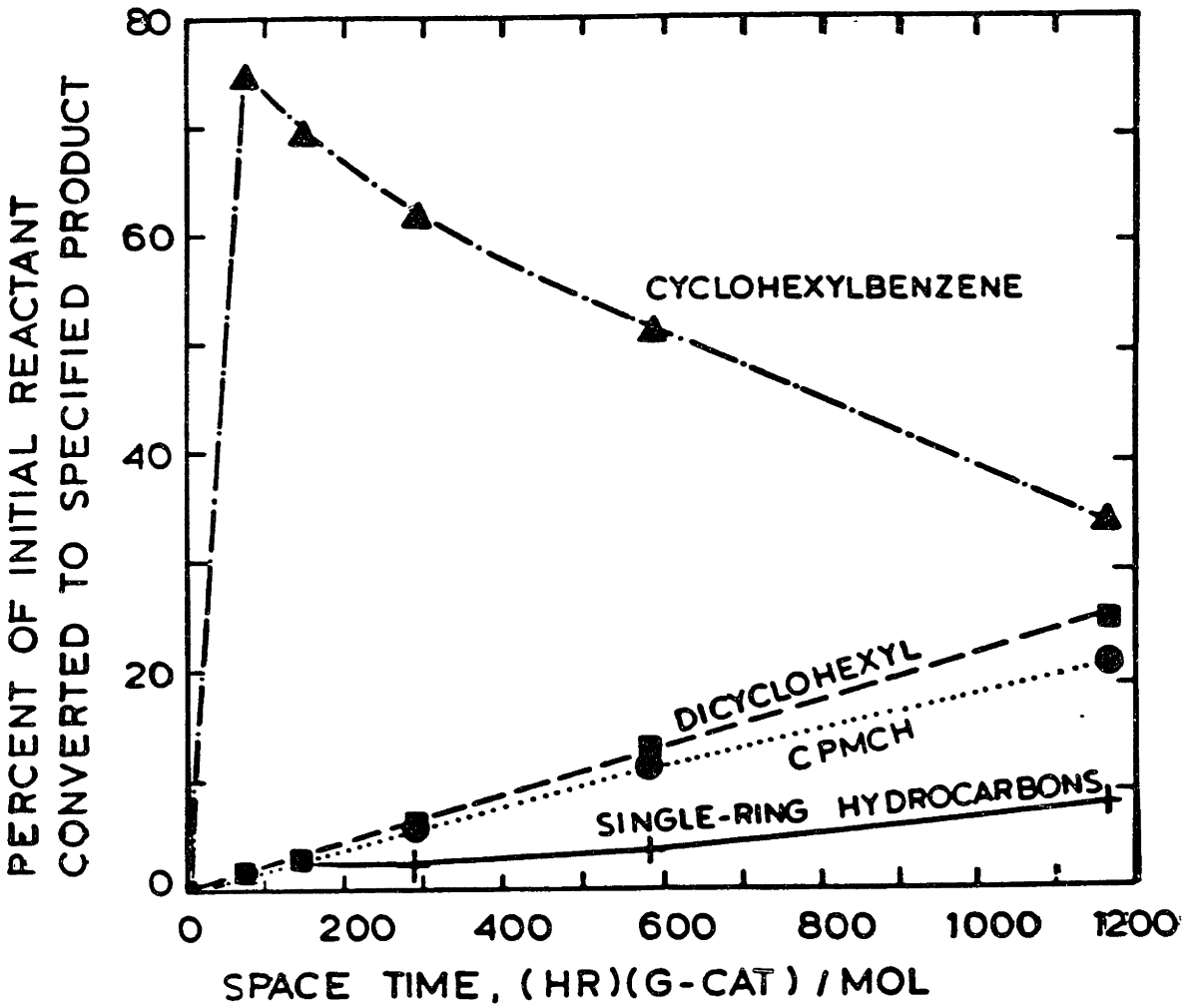

Figure III.14 Hydrodeoxygenation of trans-2-phenylcyclohexanol using sulfided sample 21.

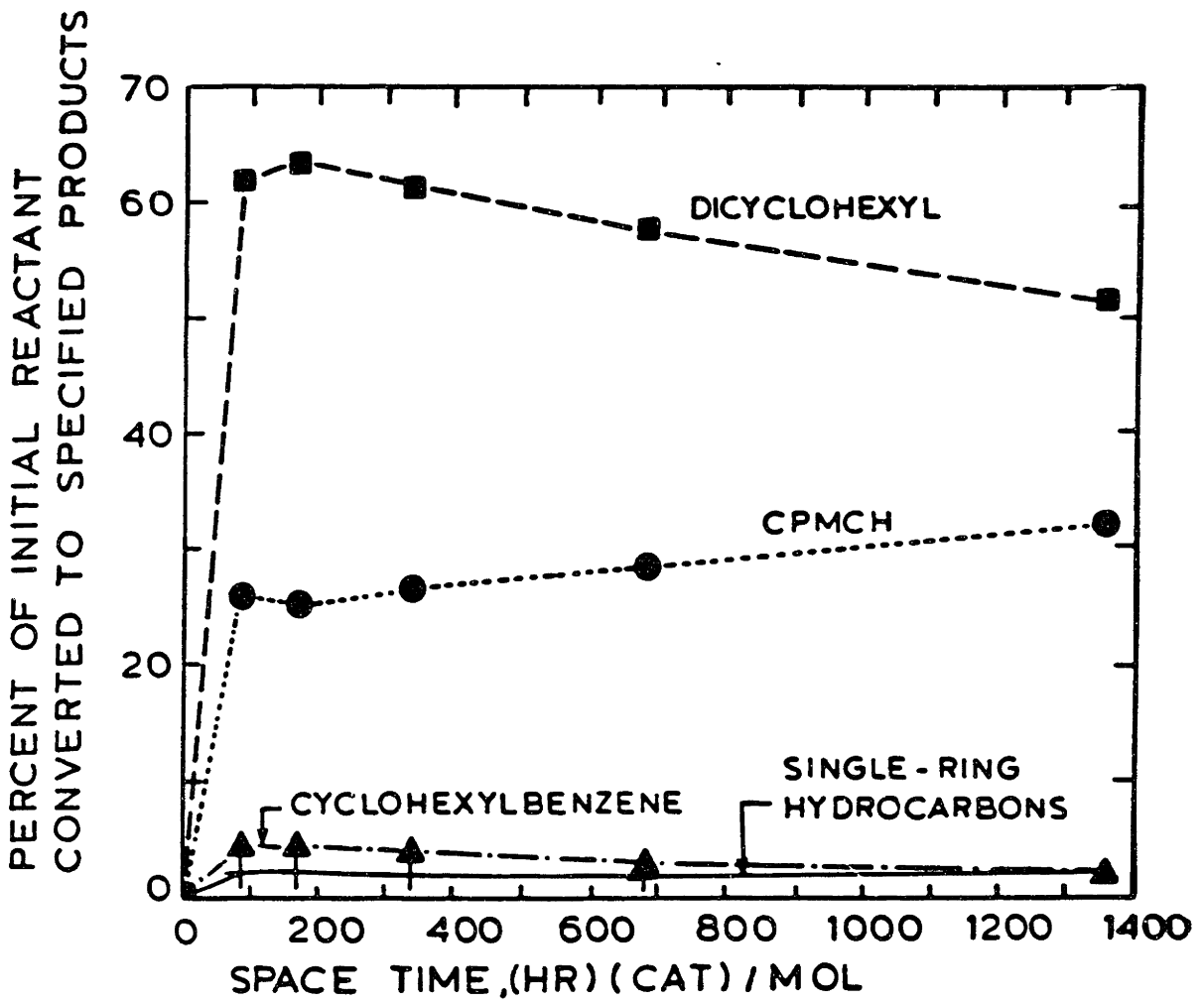

Figure III.15 Hydrodeoxygenation of 2-cyclohexylcyclohexanol using sulfided sample 21.

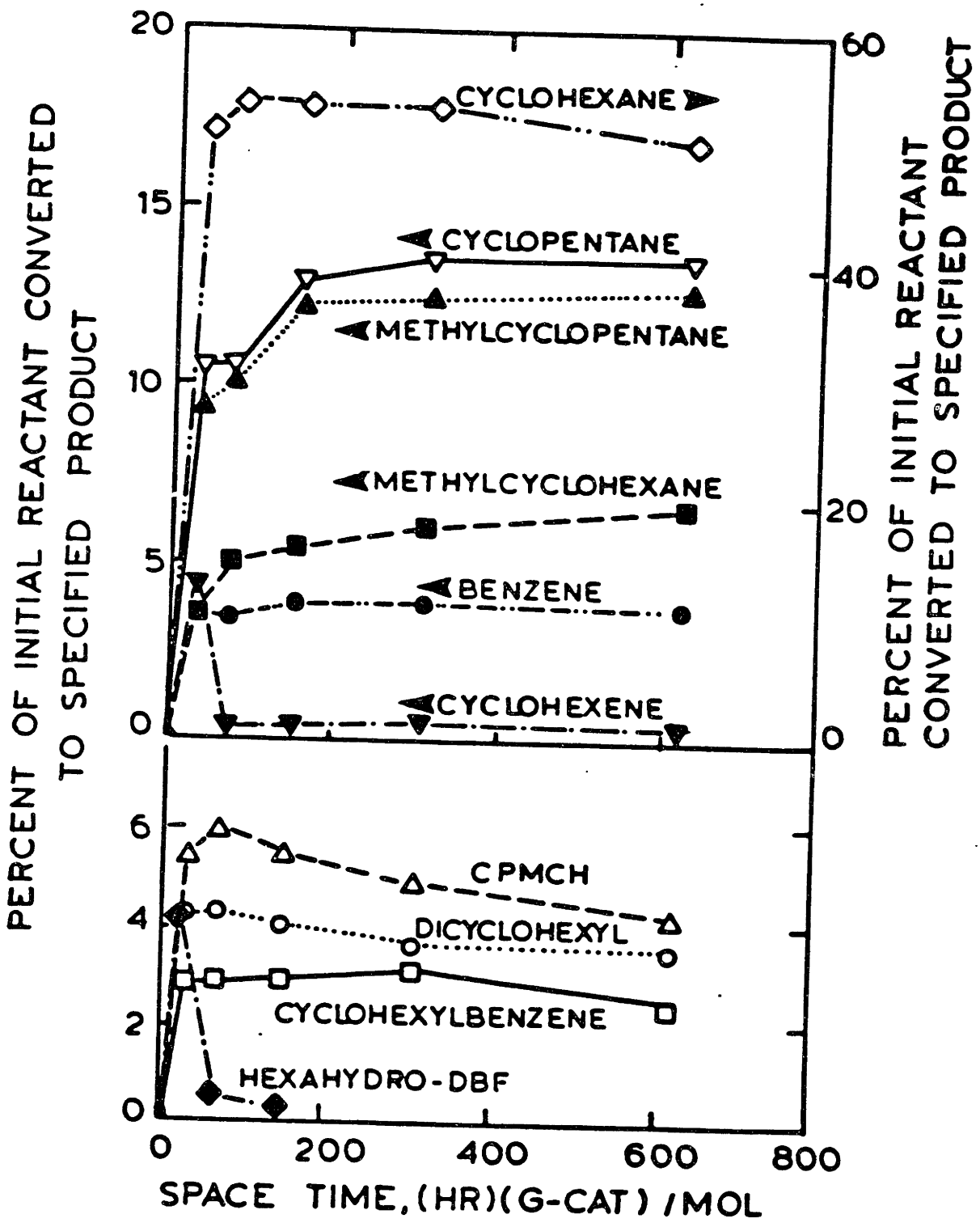

Figure III.16 Hydrodeoxygenation of 1,2,3,4-tetrahydrodibenzofuran using sulfided sample 28.

perhydrodibenzofuran and TH-DBF, it was identified as hexahydrodibenzofuran. It is plausible that hexahydrodibenzofuran can be formed from the TH-DBF and that it reacts rapidly.

III.D Reaction Kinetics

III.D.1 H_2S present.

The percent conversion of DBF was measured as a function of space time over the sulfided catalyst at each of four temperatures. The initial partial pressure of dibenzofuran was 24 kPa and the H_2S partial pressure, produced in situ, was 7.0 kPa. Semilogarithmic plots of the percent of initial DBF remaining as a function of space time are shown in Figure III.17. The linear relationships obtained establish that the overall reaction is first order with respect to DBF partial pressure over a wide range of conversions. The discrepancies in the data at zero conversion may be due to calibration error in the analysis: this would tend to shift the entire line vertically.

Least-squares regression was used to fit first-order rate constants to the data, and these are listed in Figure III.17. The rate equation was of the form:

$$\text{(III.2)} \qquad \frac{d(1 - x)}{d\tau} = -k\,(1 - x)$$

where x = conversion of DBF to hydrocarbons, τ = space time (hr g of catalyst)/(mol of DBF), and k = first-order rate constant (mol/hr g of catalyst). From the effect of temperature on the rate constant, an Arrhenius plot, shown in Figure III.18, gives an activation energy of 67 kJ/mol.

III.D.1.a Hydrogen dependence - The dependence of the rate of HDO of DBF upon the hydrogen concentration was determined in a set of two

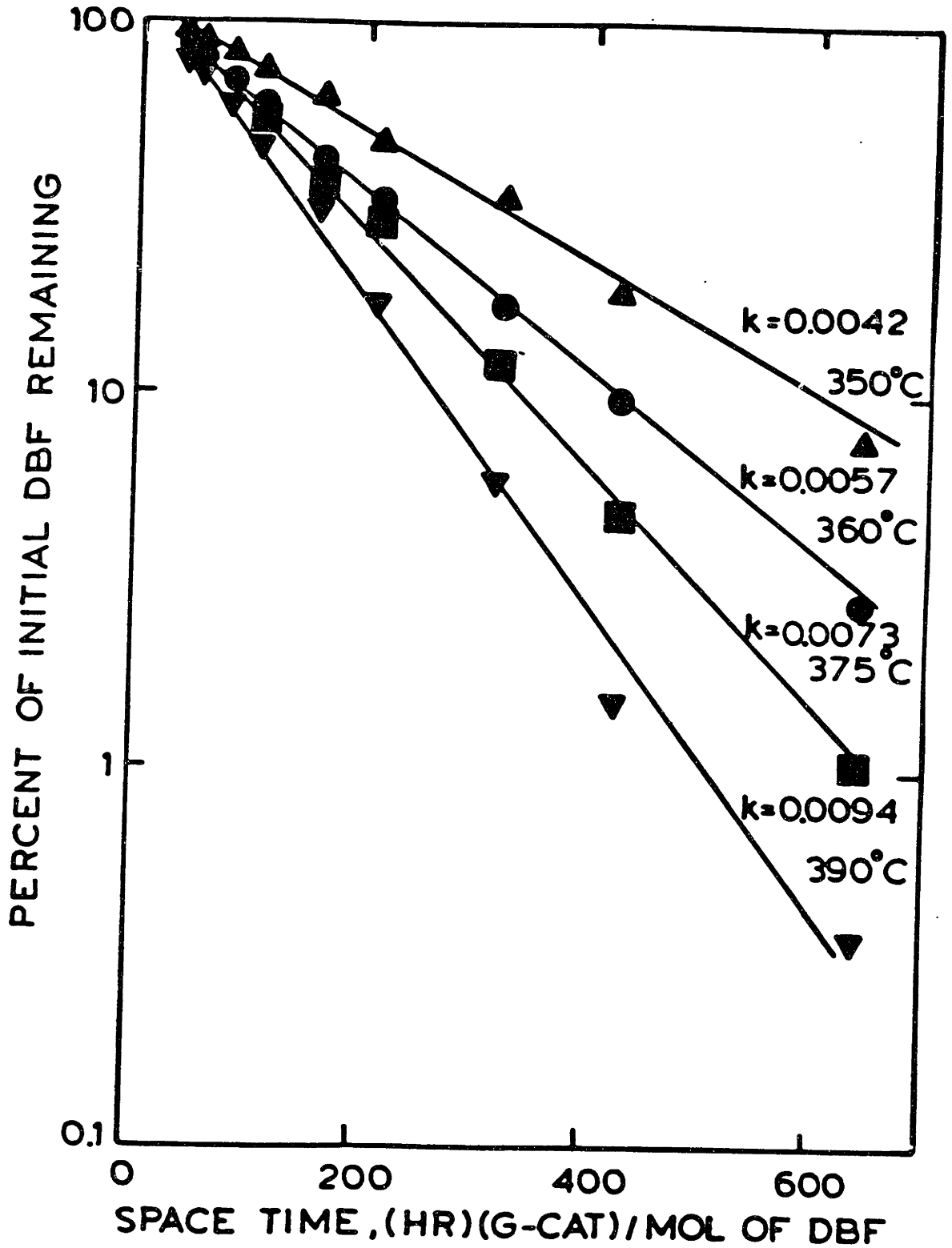

Figure III.17 Sulfide catalyst hydrodeoxygenation of dibenzofuran (DBF). The reaction is first order in DBF. Corresponding rate constants are shown in units of mols/(hr g. of catalyst).

experiments at 360°C. Hydrogen partial pressure was varied by mixing hydrogen and helium flows, which could be adjusted separately using metering valves. The hydrogen flow rate was measured with the mass flow meter, and the helium flow was determined by difference after comparing this reading to the outlet bubble flow meter measurement. This arrangement allowed the hydrogen partial pressure and total pressure to be varied independently. The partial pressures of dibenzofuran and H_2S were held constant at 24 and 13.9 kPa respectively. Space time was held constant at 160 (hr g of catalyst)/mol.

In the first experiment, the total pressure was varied at a constant H_2 partial pressure of 6.7 MPa. A constant liquid flow rate and liquid composition was maintained at all pressures. The total gas flow rate was increased as the pressure was raised in order to keep the reactant partial pressure constant. As shown in Figure III.19, total pressure has no effect upon the reaction rate. The results suggest that reaction kinetics in the vapor phase can be adequately described by partial pressure and that the use of fugacities is not required.

Another experiment was performed in which the hydrogen partial pressure was varied in the range of 2.5 to 14 MPa at a constant total pressure of 14 MPa. Here liquid and gas flow rates were held constant while only the molar ratio of hydrogen to helium was varied. The reaction rate of dibenzofuran was found to be a strong function of the hydrogen partial pressure (Figure III.20). Using this data, a first order rate constant k for the HDO of DBF was calculated from eq. III.2 at each hydrogen partial pressure. Figure III.21 shows that the rate constant is proportional to the hydrogen partial pressure. The hydrodeoxygenation of dibenzofuran is thus a second order reaction, first order in both dibenzofuran and hydrogen partial pressures.

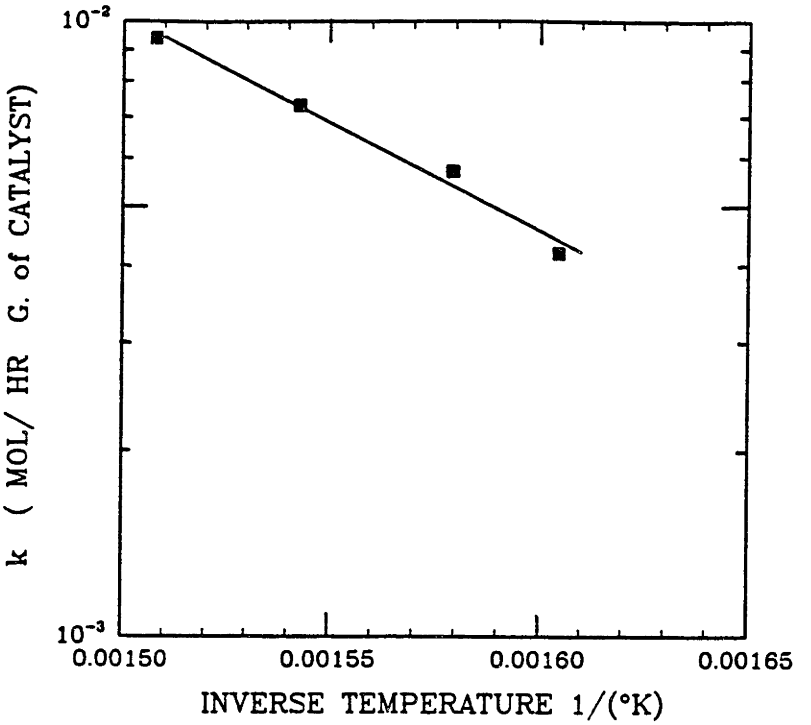

Figure III.18 Arrhenius plot for the overall rate constant.

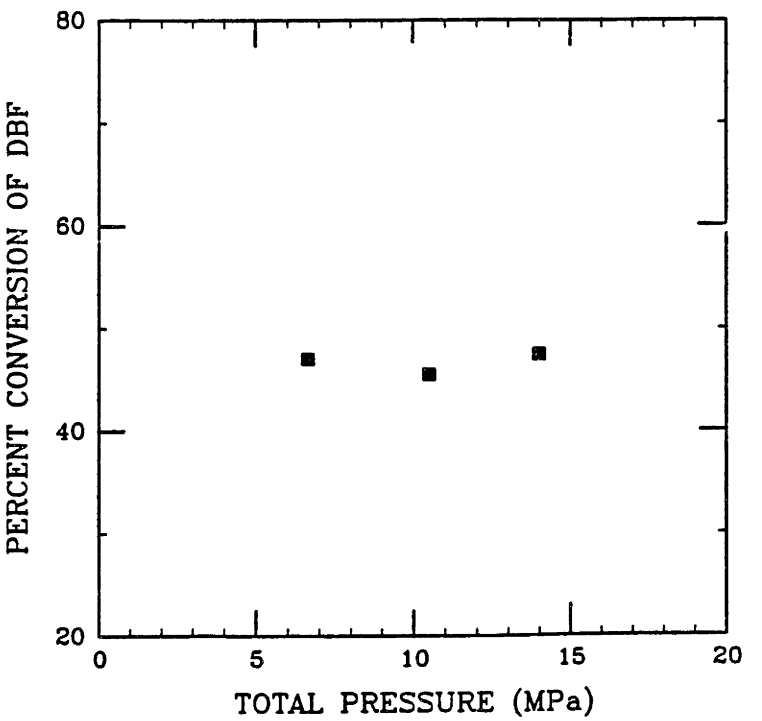

Figure III.19 Conversion of DBF is independent of total pressure.

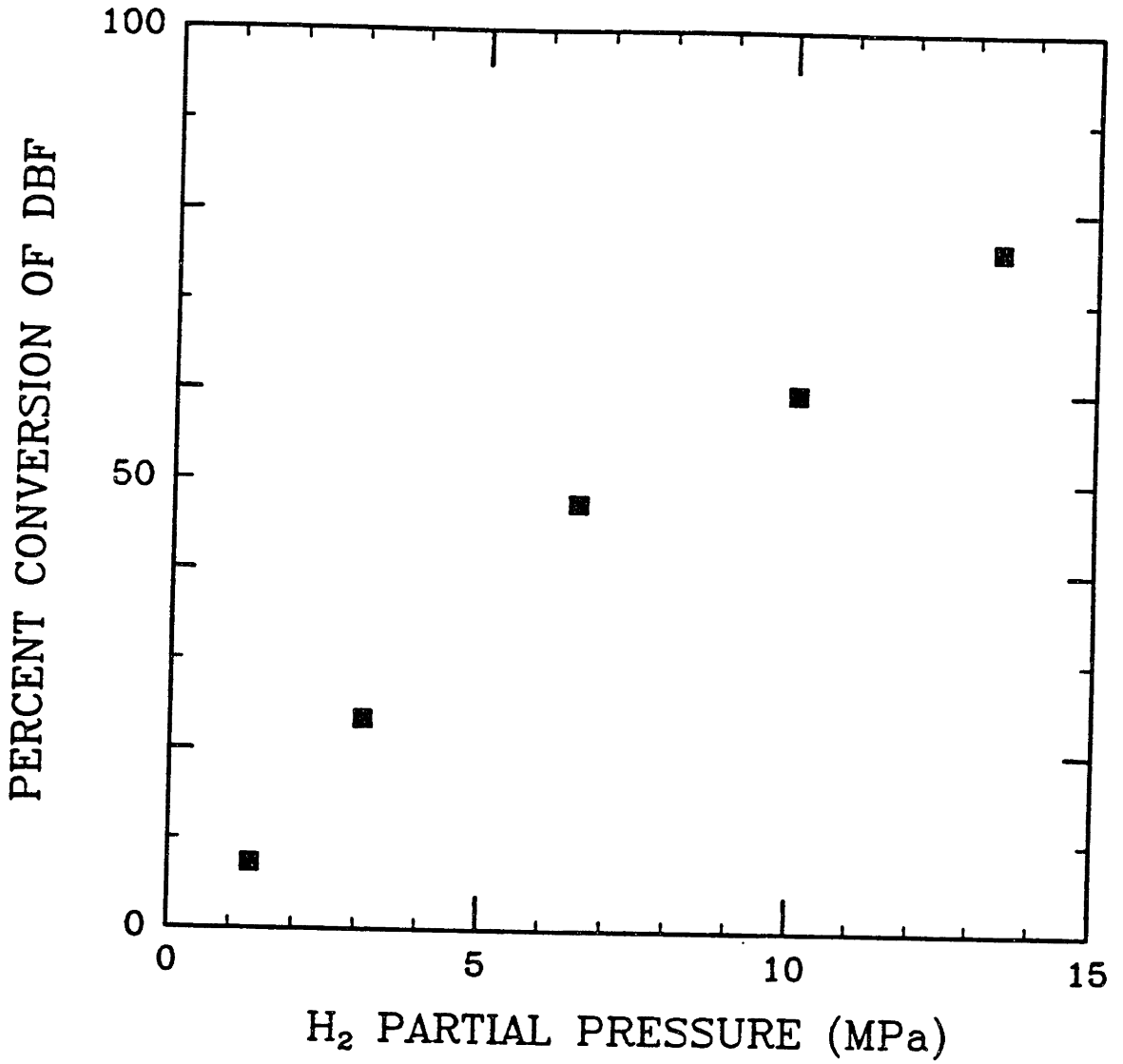

Figure III.20 The rate of dibenzofuran HDO is strongly dependent on hydrogen partial pressure.

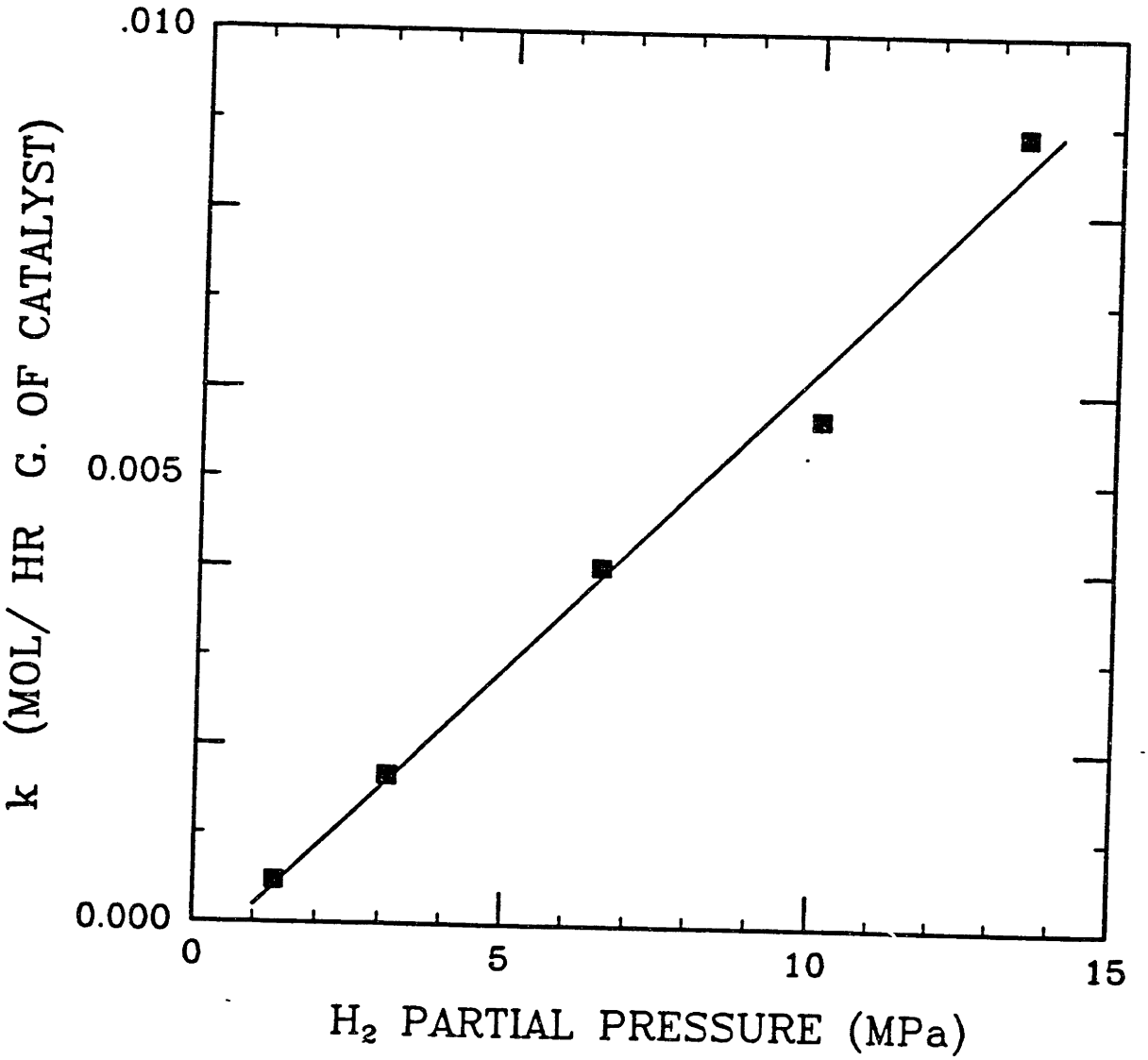

Figure III.21 The rate is first order in hydrogen partial pressure.

III.D.2 H_2S Absent.

The above study on the kinetics for DBF at 360°C was repeated, but with no sulfur compound added to the feed. Results are compared to those observed in the presence of H_2S in Figure III.22. At high space times the degree of conversion is subtantially greater when H_2S is omitted, and other data showed that water enhances the HDO of dibenzofuran in the absence of H_2S. Therefore, the deviation from first order behavior in Figure III.22 can be attributed to to a self-enhancement stemming from water formed in increasing amounts at high conversions. When H_2S is present, water has no significant effect on activity or selectivity, as discussed previously.

It appears that adsorption of H_2S onto the catalyst competes with that of H_2O and that the latter is much more weakly adsorbed. A somewhat similar effect was observed in studies on the effects of H_2S and H_2O on the hydrodenitrogenation of quinoline, on the same sulfided catalyst (Satterfield and Smith, 1986). There water vapor and H_2S, studied separately, each caused some enhancement of activity, the effects of H_2S being considerably greater than that of H_2O. In a mixture of the two, however, each at 14 kPa partial pressure, the percent conversion was essentially the same as that with 14 kPa of H_2S by itself.

In later experiments on batch 23 the addition of water, added as decanol, was found to enhance the HDO of DBF in the absence of H_2S. Figure III.23 shows that the reaction of DBF exhibited first-order behavior when only DBF and 24 kPa of decanol were fed at 360°C and 7 MPa total pressure. Addition of water moderates the change in H_2O concentraion with conversion. Evidently water had some effect on the catalyst activity which was not explored further here.

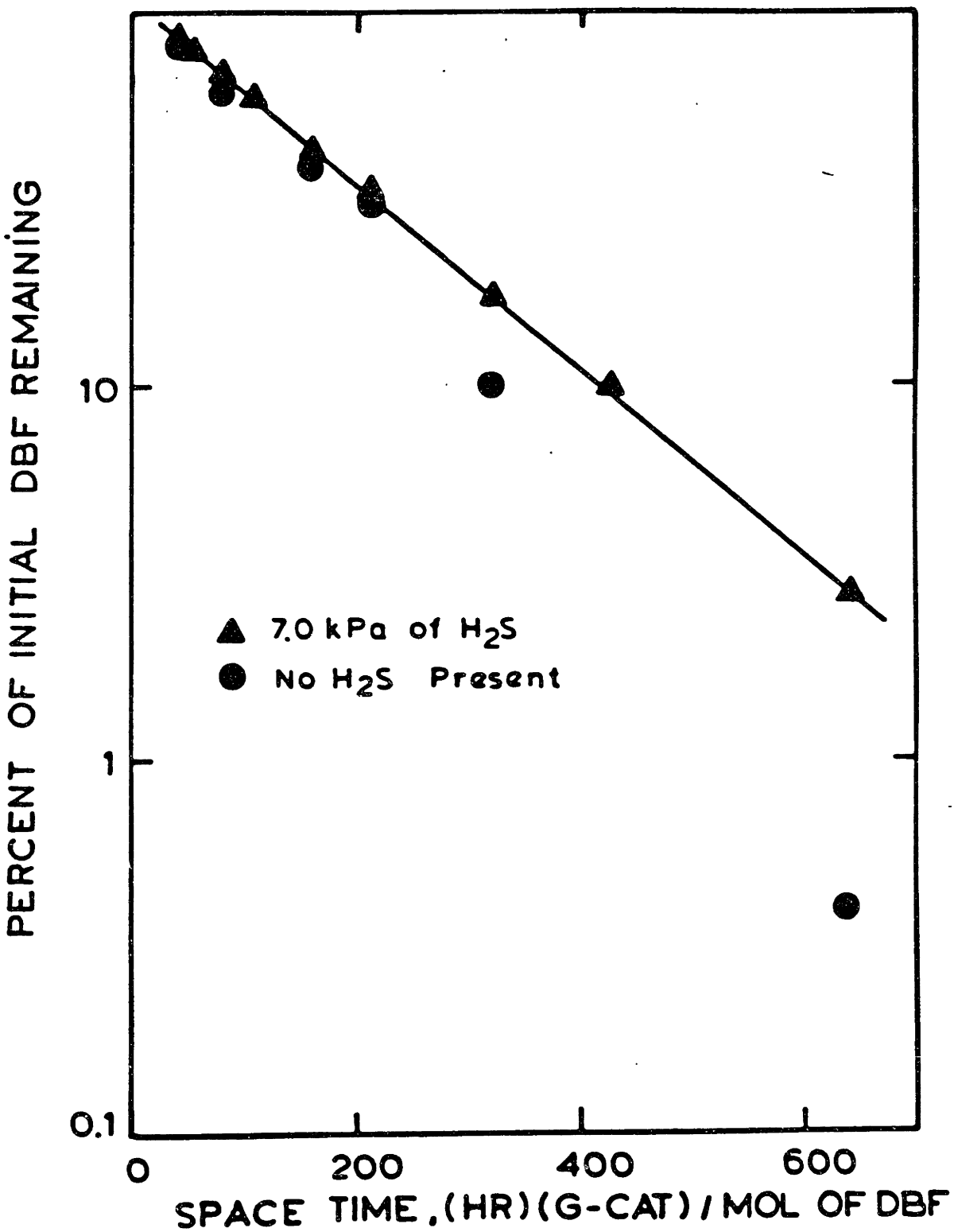

Figure III.22 The conversion at high space times is greater in the absence of H_2S.

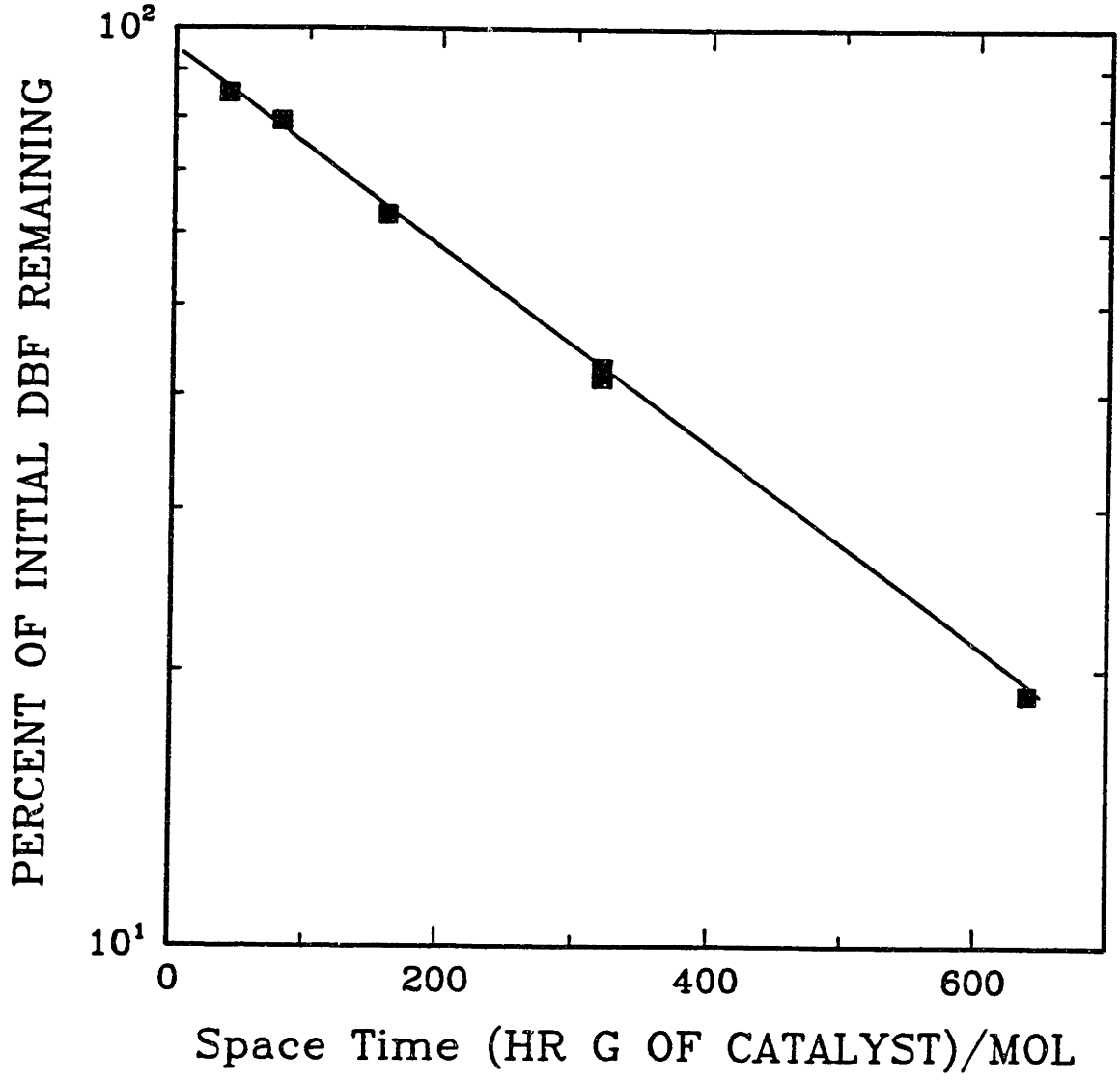

Figure III.23 The reaction of DBF is first order in the absence of H_2S and presence of 24 kPa of H_2O. (24 kPa DBF).

III.E Inhibition in the Dibenzofuran HDO Network.

The product distribution for biphenyl hydrogenation was measured separately on catalyst batch 21 at 360°C, 7 MPa, and 13.9 kPa of H_2S. Biphenyl was fed at an initial partial pressure of 24 kPa. As shown in Figure III.24, biphenyl was successively hydrogenated to cyclohexylbenzene and then dicyclohexyl. Some isomerization to CPMCH also occurred, and the formation of C_5 to C_7 single-ring hydrocarbons was limited to less than 8% of the products.

Inhibition of biphenyl hydrogenation was observed during the simultaneous HDO of dibenzofuran. In this set of experiments the biphenyl was fed at an initial partial pressure of 6 kPa (liquid feed concentration of 0.061 mols/L). Whereas a flow rate of 2.72 ml liquid/min corresponds to a spce time of 40 hr g. cat/mol in Figure III.24, the same flow rate at 6 kPa of biphenyl would now correspond to 160 hr g. cat/mol. Here space time is defined in terms of the molar feed rate of biphenyl.

Biphenyl hydrogenation was compared in the presence and absence of 24 kPa (initial) of DBF under reaction conditions of 360°C, 7 MPa, and 7 kPa of H_2S. Measured biphenyl concentrations in the samples produced during reaction of DBF were not corrected for the additional biphenyl produced from HDO. Biphenyl is normally only a minor product of dibenzofuran HDO, and the error was estimated to be unimportant. As shown in Figure III.25, the hydrogenation of biphenyl exhibited first-order kinetics, and the simultaneous HDO of DBF decreased the hydrogenation rate by approximately 60%. Figure III.26 demonstrates that the HDO of dibenzofuran was unaffected by the addition of 6 kPa of biphenyl. (Note that in Figure III.26 the space time is defined in terms of the molar flow rate of DBF rather than biphenyl.

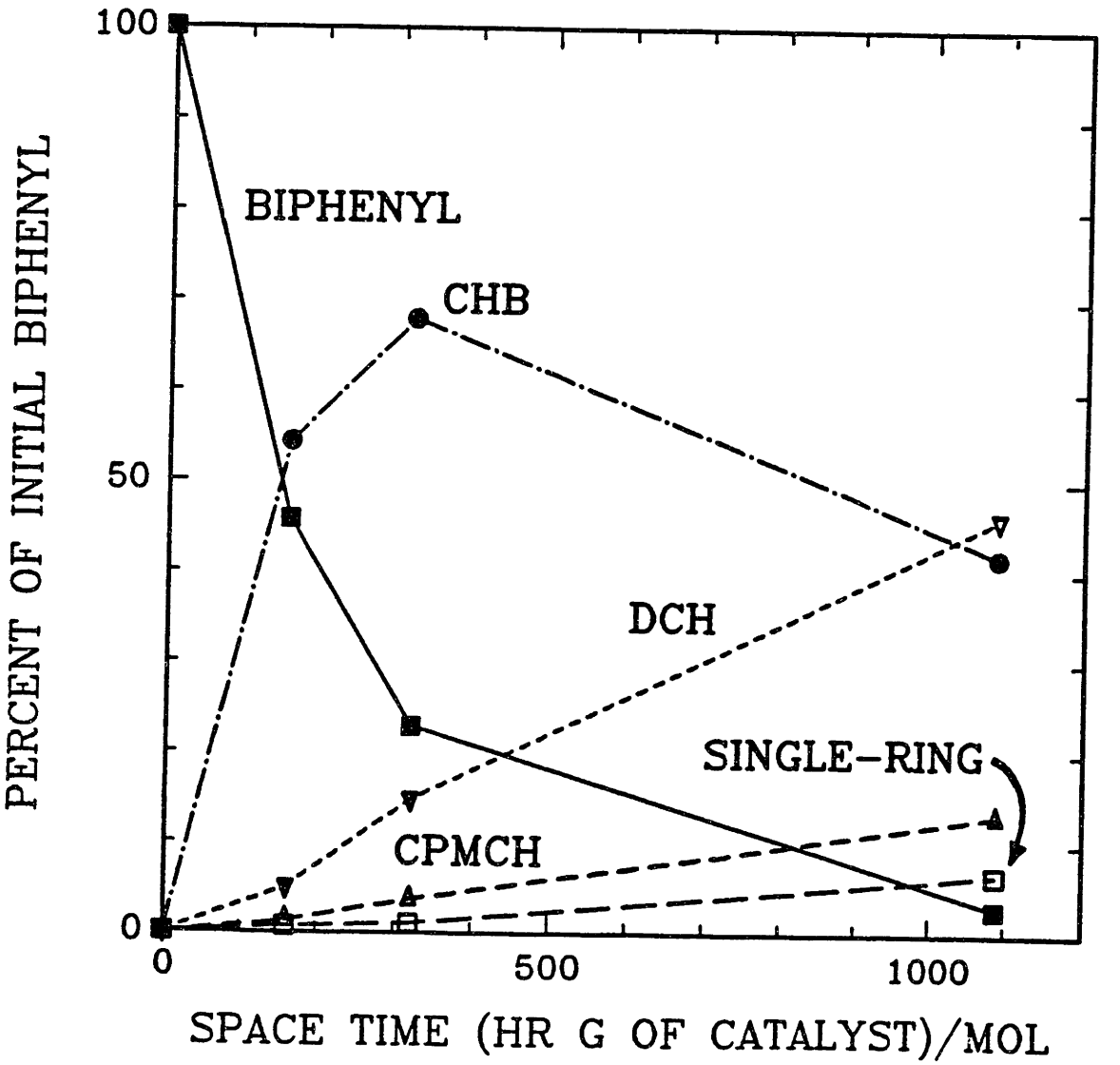

Figure III.24 Product distribution for the hydrogenation of biphenyl at 360 °C, 14 kPa H_2S, and 7 MPa on batch 20.

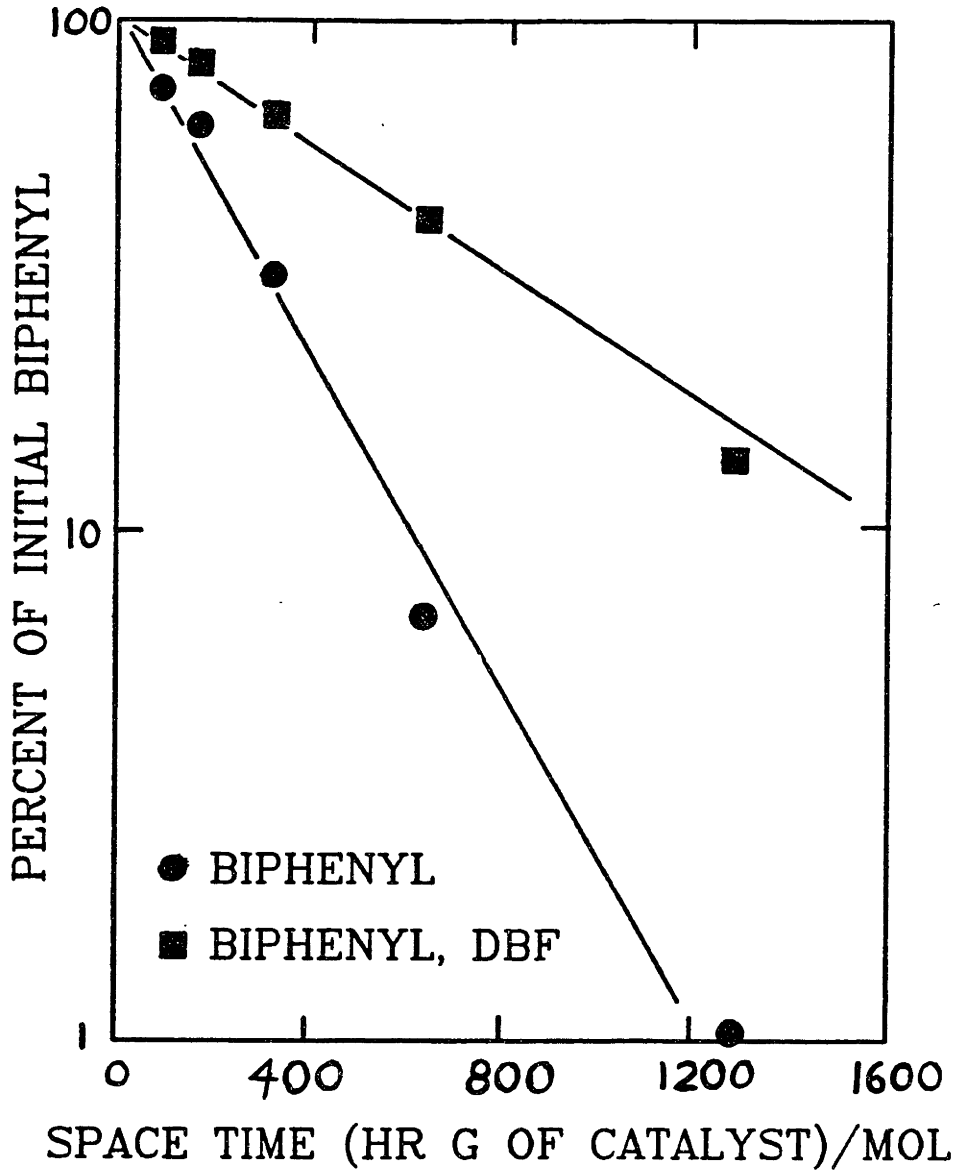

Figure III.25 24 kPa of DBF lowers the rate of biphenyl hydrogenation by 62 % at 360 °C and 7 MPa.

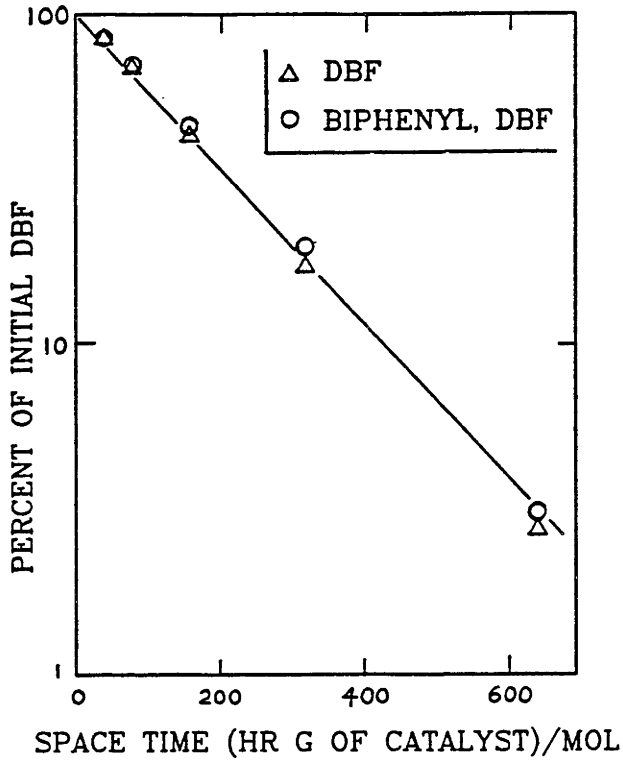

Figure III.26 HDO of dibenzofuran is unaffected by the addition of 6 kPa of biphenyl.

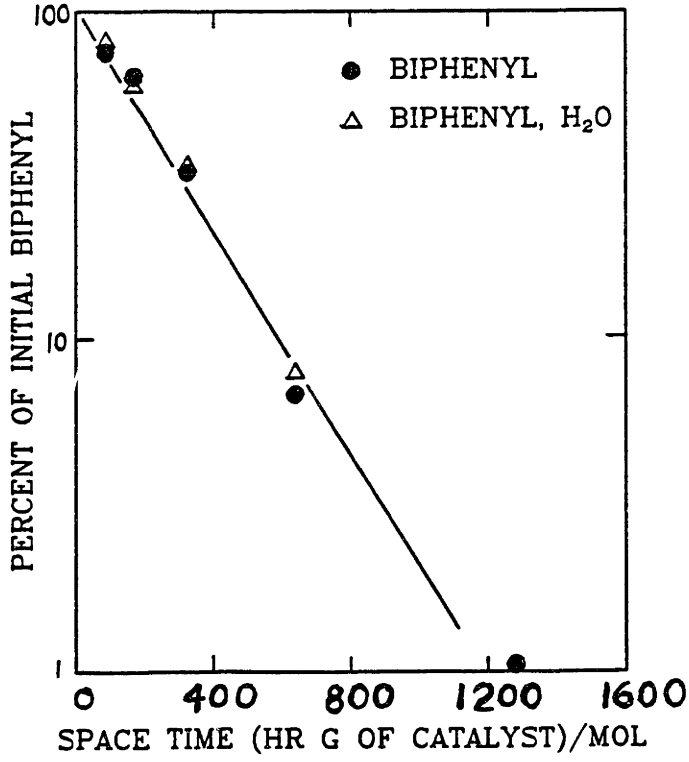

Figure III.27 Addition of 24 kPa of water has no effect upon biphenyl hydrogenation.

Inhibition of the hydrogenation reaction must result from strong adsorption of either dibenzofuran or water. Figure III.27 indicates that the addition of 24 kPa of decanol, which rapidly produces H_2O in situ, had no effect upon the hydrogenation of biphenyl. This suggests that the observed inhibition is caused by dibenzofuran. Interestingly, the observation that the hydrogenation rate for biphenyl did not increase as the DBF was converted implies that the degree of inhibition may have been independent of dibenzofuran concentration.

III.F Discussion

III.F.1 Reaction Network.

A high selectivity to single-ring products was observed for the HDO of DBF; but of the various intermediates studied, a high proportion of single-ring products occurred only from the reaction of TH-DBF or 2 cyclohexylphenol. Table III.2 compares the selectivities to various single-ring products from these three reactants to that from 2-phenylphenol. The predominance of single-ring products from DBF indicates that the major reaction pathway over the sulfide catalyst was through saturation of one ring of DBF, forming TH-DBF, hexahydrodibenzofuran, and then 2 cyclohexylphenol. This last substance reacted to form largely single-ring products.

A second, less important parallel pathway, was through direct hydrogenolysis of DBF to form 2-phenylphenol. (2-Phenylphenol was detected in the reaction of DBF over the oxide catalyst.) The 2-phenylphenol then reacts to form biphenyl and cyclohexylbenzene. One can estimate the the relative importance of the two pathways by comparing the weighted contribution from TH-DBF and 2-phenylphenol to the 72% single-ring selectivity found for DBF. By this measure, the route via TH-DBF and 2-cyclohexylbenzene accounted for about 77% of the DBF reaction and that via 2-phenylphenol, about 23%. The weighted selectivity calculated from these percentages is compared with that for DBF in Table III.3. The selectivity to single-ring compounds was not affected by temperature within the range 350-390°C, indicating that the relative importance of the two parallel pathways was not altered by temperature within this range.

At low space times the ratio of CPMCH to DCH in the products was higher for DBF than for the other species studied. At high space times this ratio was about 1.2 for DBF and TH-DBF, and it ranged from 0.5 to 0.8 for all other species.

TABLE III.2

Product Selectivity from DBF and Three Possible Reaction Intermediates

	% selectivity			
	DBF	TH-DBF	2-cyclo-hexyl-phenol	2-phenyl-phenol
total single-ring species	72	88	91	16
individual species				
cyclopentane	7.0	13	0.9	0.8
methylcyclopentane	9.0	12	5.2	1.2
cyclohexane	50	53	81.9	11.4
methylcyclohexane	2.5	5.9	0.1	0.4
benzene	3.6	3.8	2.4	1.9

TABLE III.3

Product Distribution From DBF Resembles a Weighted Distribution From Two Parallel Pathways

Species	Percent Selectivity for	
	DBF	23% 2-phenylphenol 77% TH-DBF
Cyclopentane	7.0	10.4
Methylcyclopentane	9.0	9.7
Cyclohexane	50.	43.
Methylcyclohexane	2.5	4.6
Benzene	3.6	3.4
Total Single Ring Products	72	72

The discussion above suggests a reaction network as shown in Figure III.28. The rate-limiting process for the overall hydrodeoxygenation is the reaction of DBF by the two initial parallel pathways, the sum of which is measured by the first-order rate constant. Our proposed network agrees with that of Krishnamurthy et al. (1981) in that both postulate a first step in which DBF can be converted to either 2-phenylphenol or (via TH-DBF) to 2-cyclohexylphenol. The networks differ in that here there is no evidence to suggest that 2-phenylcyclohexanol, cyclohexylcyclohexanol, or phenylhexanol are formed as intermediates.

All the oxygen-containing intermediates are more reactive than DBF and hence were not found in any significant amounts in the products when a substantial conversion of DBF occurred. These observations are thus consistent with the results of Li et al. (1985b), who studied the catalytic HDO of a number of phenolic compounds in the acidic fraction isolated from a coal liquid. They concluded that the phenols reacted one order of magnitude faster than dibenzofuran in the neutral oil fraction of the same coal liquid.

III.F.2 Sulfide versus oxide catalyst.

The sulfide form of the Ni-Mo catalyst was more active than the oxide form. The overall reaction was first order in both DBF and hydrogen, and the products were largely single-ring compounds. On the oxide catalyst, zero-order kinetics with respect to DBF were observed; double-ring compounds predominated in the products, and these were less saturated. Evidently hydrogenation functionality is much weaker on the non-sulfided catalyst than on the sulfided catalyst. The two catalysts also responded differently to water vapor. The present results emphasize the fact that a sufided catalyst can behave quite differently from its oxide precursor.

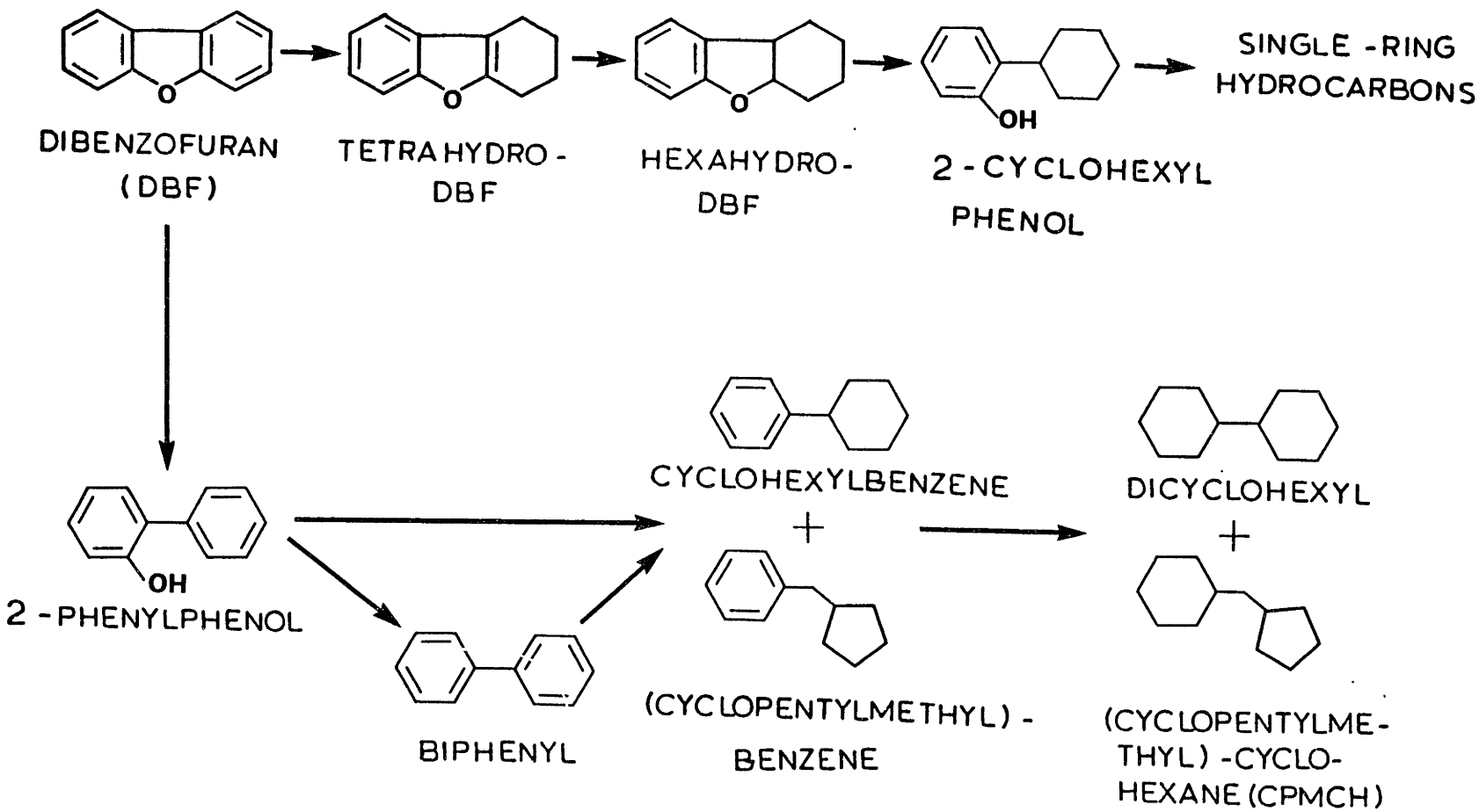

Figure III.28 Proposed hydrodeoxygenation network for dibenzofuran.

III.F.3 Effects of H_2S.

Results obtained over the sulfided Ni-Mo catalyst demonstrate that H_2S inhibits the HDO of dibenzofuran, but the cause for the changes in catalyst activity and in product distribution with H_2S partial pressure remains unclear. As shown above, with increased H_2S partial pressure, selectivity to double-ring hydrocarbons decreased (Figure III.6) and that to single-ring hydrocarbons increased. Thus the product distribution in the complete absence of H_2S shows some resemblance to that found over the oxide catalyst (Figures III.9 and .10). However, these changes in product distribution occurred immediately upon the removal of H_2S, which would not be expected if deactivation were due to oxy-sulfide formation. A more likely explanation is that labile sulfur is lost from the catalyst surface in the presence of high-temperature hydrogen and absence of H_2S.

The fact that increased H_2S concentration decreased the selectivity to double-ring products suggests that H_2S inhibits hydrogenolysis more than hydrogenation. Similar results have been reported for the hydrodesufurization of dibenzothiophene, the sulfur analog of DBF (Broderick and Gates, 1981). An increase in in H_2S concentration lowered the conversion of dibenzothiophene and lowered the biphenyl/cyclohexylbenzene product ratio. The change in selectivity was interpreted as preferential inhibition of the C-S hydrogenolysis reaction, which produces biphenyl. Likewise, Gevert and co-workers (1987) found that addition of H_2S during the HDO of phenols inhibited the formation of aromatic products. Aromatics would be formed by direct hydrogenolysis of the C-O bond.

III.F.4 Hydrogen consumption.

Hydrogen consumption is an important cost in hydroprocessing to remove heteroatoms. The consumption is determined not only by the quantity of heteroatoms to be removed but also by the reaction selectivity. Among the principal product species found here, the moles of H_2 consumed per mole of DBF reacted varies from 2 for formation of biphenyl to 9 for cyclohexane or methylcyclopentane.

The hydrogen consumed during the HDO of DBF at 360°C and 7 MPa was calculated for both the oxide and sulfided forms of a Ni-Mo catalyst. Over the oxide catalyst, in the presence of 24 kPa of water, the H_2 consumption was 5.1 mol of H_2/mol of DBF reacted. Over the sulfided catalyst in the presence of 7 kPa of H_2S, it was 7.5 mol of H_2/mol of DBF, 50% greater.

III.G Summary and Conclusions

1. In the hydrodeoxygenation (HDO) of dibenzofuran (DBF) at 360°C and 7.0 MPa on a sulfided catalyst, the major products found were single-ring hydrocarbons. Cyclohexane predominated, but also present were methylcyclopentane, cyclopentane, benzene, methylcyclohexane, and cyclohexene. Lesser quantities of double-ring products were isolated. Among them cyclohexylbenzene predominated. All oxygenated species formed as intermediates are much more reactive than DBF.

2. The major reaction pathway under our conditions appears to be hydrogenation of one ring of DBF to form hexahydrodibenzofuran, which is converted to 2-cyclohexylphenol. This in turn reacts to form phenol and cyclohexene. It is proposed that the phenol in turn is hydrogenated to cyclohexanol, which, by elimination of water, is converted to cyclohexene. Cyclohexene, formed by either path, is hydrogenated fairly rapidly to cyclohexane.

3. A second parallel pathway, of lessor importance, is direct hydrogenolysis without prior ring hydrogenation to form 2-phenylphenol, which is converted to biphenyl and cyclohexylbenzene.

4. Removal of H_2S from the mixture caused an increase in catalyst activity for HDO, which persisted for hours. Returning H_2S to the system caused a repression of catalyst activity. Removal of H_2S decreased the formation of single-ring hydrocarbons and increased the selectivity to unsaturated products in the double-ring group. In the absence of H_2S, added water (24 kPa) accelerated the HDO reaction. In the presence of H_2S, added H_2O had no effect.

5. The catalyst in the oxide form, not presulfided, behaves quite differently than the sulfided catalyst. The activity was lower, and double-ring products predominated over single-ring compounds, saturated double-ring products being minor in amount. Amoung single-ring compounds, however, cyclohexane predominated as with the a sulfided catalyst. In contrast to the sulfided catalyst, added water (24 kPa) inhibited the HDO reaction.

6. For a sulfided Ni-Mo/Al_2O_3 catalyst in the presence of H_2S at 350-390°C and at hydrogen partial pressures of 2-14 MPa, the reaction is first order in hydrogen and DBF. The activation energy is 67 kJ/mol. On the oxide form of the catalyst, not presulfided, however, the reaction is zero order with respect to DBF.

7. The observed inhibition of biphenyl hydrogenation by the simultaneous HDO of dibenzofuran agrees with the results of Krishnamurthy et al. (1981) on concentration effects in the DBF network. They found that the rection step involving the hydrogenation of biphenyl was inhibited more than the other reactions by increasing the DBF concentration. Obviously there are significant competitive reaction effects in this network which were not studied further.

Chapter IV

POISONING BY NITROGEN COMPOUNDS

IV.A Introduction

The basic nitrogen compounds found in synthetic feedstocks and heavy petroleum fractions can strongly inhibit hydroprocessing reactions through competitive adsorption. The presence of these species even at low concentrations limits the observed catalytic activity and necessitates the use of higher pressures and temperatures to obtain desired conversions. Although the significance of competitive adsorption in hydrotreating has been recognized since the 1950's (Kirsch et al., 1959), sparse quantitative information is available on the relative poisoning effect of various inhibitors. Model compound studies have provided information on the interactions between specific compounds, but these results are difficult to generalize to more complex feedstocks.

The available literature on interactions in hydroprocessing indicates that basic nitrogen compounds are the dominant inhibitors and that adsorption equilibrium constants can vary over two orders of magnitude (See sections I.C.2, I.E.5.c). The inhibiting effects of a series of nitrogen compounds follow essentially the same order of effectiveness with respect to each of several reactions. In the absence of steric effects, relative poisoning for different compounds appears to increase in the same order as the gas phase basicity. Poisoning does not correlate with aqueous pK_a values.

Thiophene was chosen as an appropriate model compound since the HDS reaction of thiophene is known to be strongly poisoned by nitrogen compounds. The high reactivity of thiophene allows the inhibition to be measured at conditions such that limited reaction of the added poison

occurs. Relative adsorption constants can thus be determined at constant inhibitor concentrations.

IV.B Experimental

All experiments described here were performed at 7.0 MPa total pressure and temperatures ranging from 300 to 400°C. Hydrogen was fed at a rate of 1520 (ml at STP)/ml liquid, equivalent to 9000 SCF per barrel, producing an initial thiophene partial pressure of 24 kPa. This gas-to-liquid ratio is high enough to ensure complete vaporization of the feed above 350°C. The gas-to-liquid ratio was doubled for operation at 300°C.

IV.B.1 Chemicals:

Thiophene (99+% from Aldrich) was dissolved in either a C_{16} paraffin mixture or a xylene mixture at a concentration of 0.245 or 0.49 mole/liter (equivalent to 1.5 or 3 wt% sulfur). Xylene was used as the solvent when compounds with low solubility in C_{16} were being fed to the reactor (ie., carbazole). No difference in conversion of thiophene was observed when operation with the two solvents was compared. H_2S was produced in situ by addition of 1-dodecanethiol to the liquid feed since thiols react rapidly at reaction conditions. Various compounds were also added to the thiophene feed as inhibitors at concentrations required to produce 0 to 24 kPa in the reactor. For the nitrogen compounds this corresponded to nitrogen levels of 0-0.44 wt% in the liquid feeds. All of the inhibitors tested were obtained from suppliers at greater than 98% purity, and reactants boiling below 250°C were redistilled to remove color and residues.

For the poisoning of dibenzofuran HDO, 1-pentylamine or 1-decylamine was added directly to the feeds to produce ammonia in the reactor.

Because of the smaller catalyst loading in the thiophene HDS system, anhydrous ammonia was pumped directly to the reactor.

When measuring the poisoning effect on the HDS reaction by an inhibitor, a series of feeds containing increasing concentrations of inhibitor was used. It was found that the catalyst attained a steady activity within 1 hour when inhibitor concentrations were increased, but overnight operation in the absence of poison was required to completely regain the initial activity. Representative samples could be collected afer passing 40 ml of feed through the reactor.

IV.B.2 Catalyst:

Several different samples of the same Ni-Mo/Al_2O_3 hydrotreating catalyst, American Cyanamid's HDS-3A (15.4 wt% MoO_3 and 3.2 wt% NiO), were used. These are identified as samples number 28, 31, 32, 36, and 37. Of the samples used at 360°C, sample 28 consisted of 1.6 grams of catalyst, while the other two samples consisted of 25 mg. Sample 36 (300°C) consisted of 2500 mg and sample 37 (400°C) consisted of 10 mg. By varying catalyst loading in this fashion similar degrees of conversion could be obtained over the substantial temperature range studied.

The catalyst pellets were crushed and sieved to a size range of 150-212 microns. The resulting effectiveness factor for the HDS reaction of thiophene would be greater than 0.95 even for the largest particles at 360 °C. Catalyst particles for operation at 400°C (sample 37) were crushed to 75-106 microns. The catalyst samples were pre-sulfided according to the standard procedure described in Section II.C.

Catalyst batch 28 was deactivated in the presence of 24 kPa of dibenzofuran and 7 kPa of H_2S until it had reached a steady activity after 150 hours. Catalyst samples 31, 32, 36, and 37, used in the thiophene

inhibition experiments, were deactivated during the HDS of thiophene until a steady activity was reached (approximately 48 hours). Catalyst activity was measured by the conversion of thiophene at a feed rate of 10.00 mmol/hr of thiophene and 5.00 mmol/hr of thiol. This standard test condition was run before the start of each set of experiments with a particular inhibitor. Catalyst activities remained stable over 100 hours even after the inhibition effects of various nitrogen compounds were studied. This indicates that the poisoning effects of nitrogen compounds are reversible. The baseline activity of catalyst batch 31 eventually declined after exposure to pyrrole, and catalyst batch 32 deactivated permanently after exposure to impure acridine. The evidence of permanent deactivation by pyrrole agrees with the results of Gutberlet and Bertolacini (1983) with 2,5-dimethylpyrrole.

IV.B.3 Analysis:

The various C_4 hydrocarbons produced from thiophene could not be separated by g.c. at 55°C and the response factor for 1-butene was used for all products. No tetrahydrothiophene was detected, and this might be expected from the high reactivity of this compound. Carbon mass balances on thiophene ranged from 94 to 101 percent.

Nitrogen compounds and polyaromatic hydrocarbons (PAH) were also analyzed by the same method. Table IV.1 lists the percent recoveries for organic inhibitors used in this study. Most of the compounds exhibited conversions of less than 30% so that inhibitor levels could be assumed to be constant. Among the more reactive species, quinoline rapidly attained equilibrium with 1,2,3,4-tetrahydroquinoline and 1,8-bis(dimethylamino)-naphthalene was subject to the partial loss of methyl groups.

TABLE IV.1 Percent Recoveries of the Compounds Fed as Inhibitors

Compound	Percent Recovery
Aniline	99
Pyridne	72
Piperidine	38
Naphthalene	100
Phenanthrene	92
1-Methylpiperidine	67
4-Methylpyridine	92
1,2,3,4-Tetrahydroquinoline	91
2-Ethylaniline	97
5,6,7,8-Tetrahydroquinoline	98
Decahydroquinoline	99
Quinoline	11
Carbazole	70
1,8-bis(N,N-dimethylamino)-naphthalene	51
2,6-dimethylpyridine	98

The saturated amines piperidine and 1-methylpiperidine exhibited low mass balances of 38 and 67% respectively. However, no significant amounts of hydrocarbon products from HDN reactions were detected. During operation with these amines, the high pressure filter downstream of the reactor would plug unless the filter temperture was maintained above 100 °C. It is possible that the amines were reacting with H_2S at low temperature to form a solid product, since similar reactions can occur between ammonia and H_2S to form ammonium bisulfide (Bucklin and Mackey, 1984).

IV.C Results for Thiophene HDS

Initial experiments on catalyst sample 31 were undertaken to establish the kinetics of thiophene HDS at 360°C and 7 MPa. Figure IV.1 shows the change in conversion of thiophene at a space time of 2.50 (hr g. cat/mol of thiophene) as increasing concentrations of 1-dodecanethiol were added to the feed as a source of H_2S. This experiment was run on an incompletely deactivated catalyst so that conversion levels are about 7% higher than baseline; however, the results clearly demonstrate product inhibition by H_2S. Inhibition of this reaction by H_2S has been shown previously by a number of studies.

Since HDS product inhibition might complicate the analysis, the proportionate change in H_2S partial pressure with conversion was reduced by adding H_2S to the system. The conversion of thiophene (24 kPa) in the presence of 12 kPa of H_2S (added to the feed as a thiol) was measured as a function of space time. The results in Figure IV.2 show that thiophene exhibits apparent first order behavior under these conditions from 0 to 75% conversion. All later experiments with thiophene were performed with

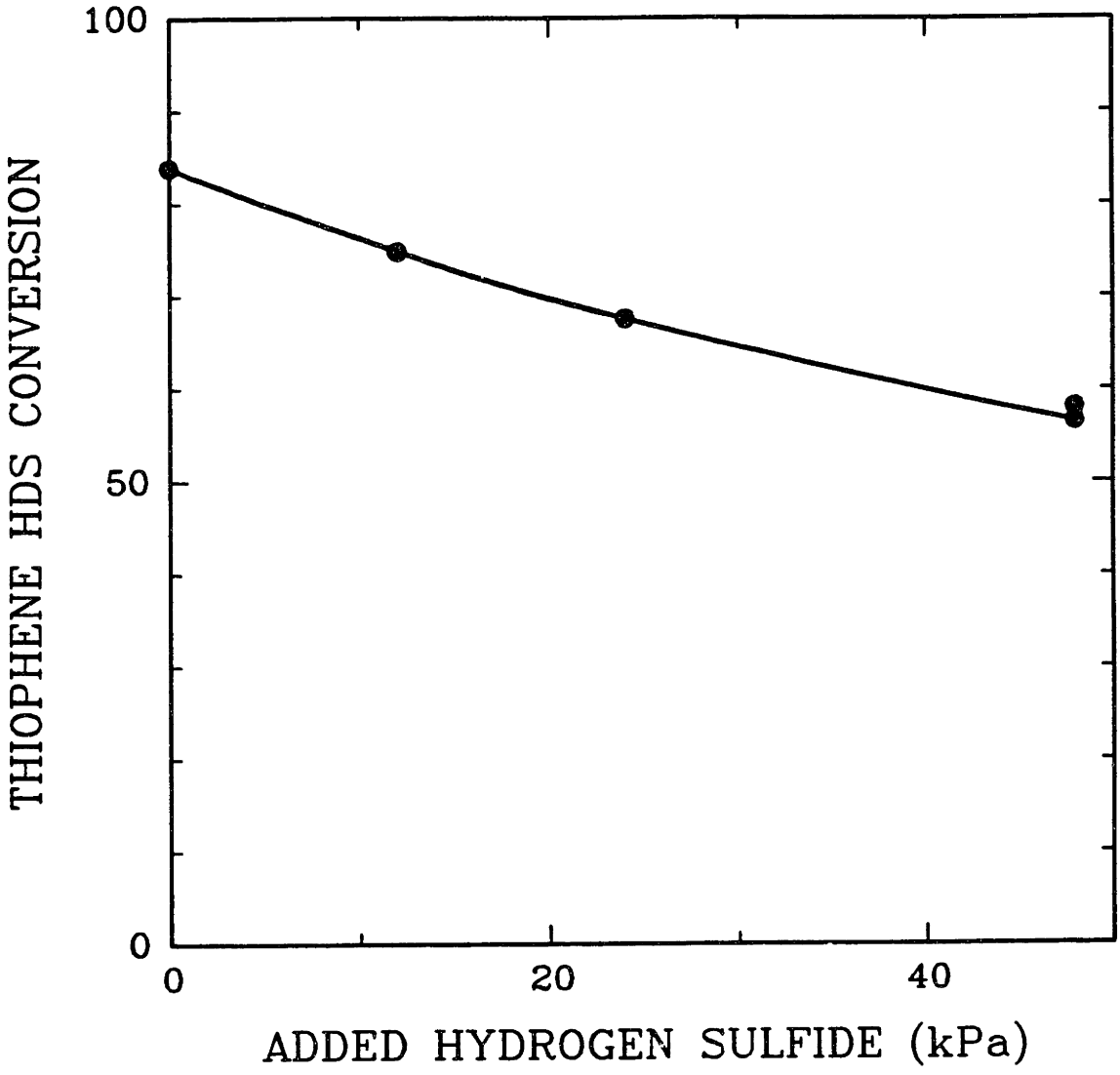

Figure IV.1 Thiophene hydrodesulfurization is inhibited by added H_2S.

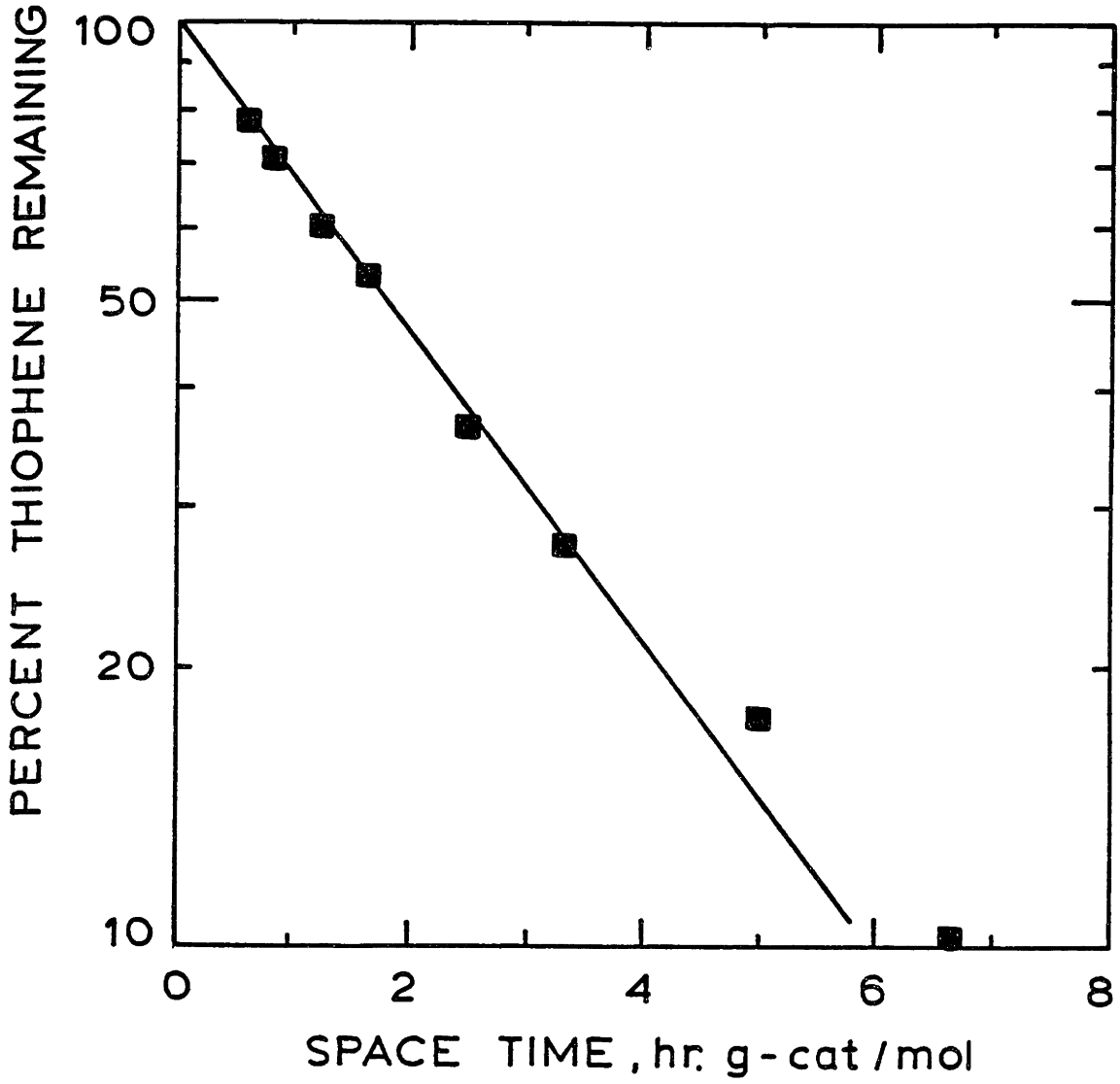

Figure IV.2 HDS of thiophene shows apparent first-order behavior in presence of added H_2S. 360 °C and 7 MPa.

the equivalent of 12 kPa added to the feeds and first order behavior was also observed at 300 and 400°C.

As an example of catalyst poisoning by nitrogen compounds, inhibition of thiophene HDS by ammonia at 360°C is shown in Figure IV.3. At a space time of 2.50 hr g. cat/mol, increasing the ammonia partial pressure from 0 to 96 kPa significantly reduced the conversion of thiophene. The raw data for the conversion of thiophene in the presence of a wide range of inhibitors is provided in Appendix A4.

The apparent first order behavior of thiophene HDS allows us to describe this poisoning with a simple Langmuir-Hinshelwood rate equation of the form:

$$\text{(IV.1)} \qquad \frac{dX}{d\tau} = \frac{k\,(1 - X)}{1 + K_I P_I} = k_a\,(1 - X)$$

where X = fractional conversion of thiophene

τ = space time (hr g. cat/mol)

k = intrinsic rate constant (mol/hr g. cat)

k_a = apparent rate constant (mol/hr g. cat)

K_I = adsorption equilibrium constant (kPa^{-1})

P_I = inhibitor partial pressure (kPa).

Inherent in this rate expression is the assumption of a one site model with competitive adsorption of thiophene and the inhibitors. Adsorption terms for thiophene and the HDS products are neglected in accordance with the observed first order behavior. More complicated kinetics expressions have been reported for thiophene HDS in the absence of poisons (Satterfield and Roberts, 1968; Massoth, 1977; Lee and Butt, 1977). However, all of these studies were conducted at amospheric pressure, making any direct comparisons with the present results difficult.

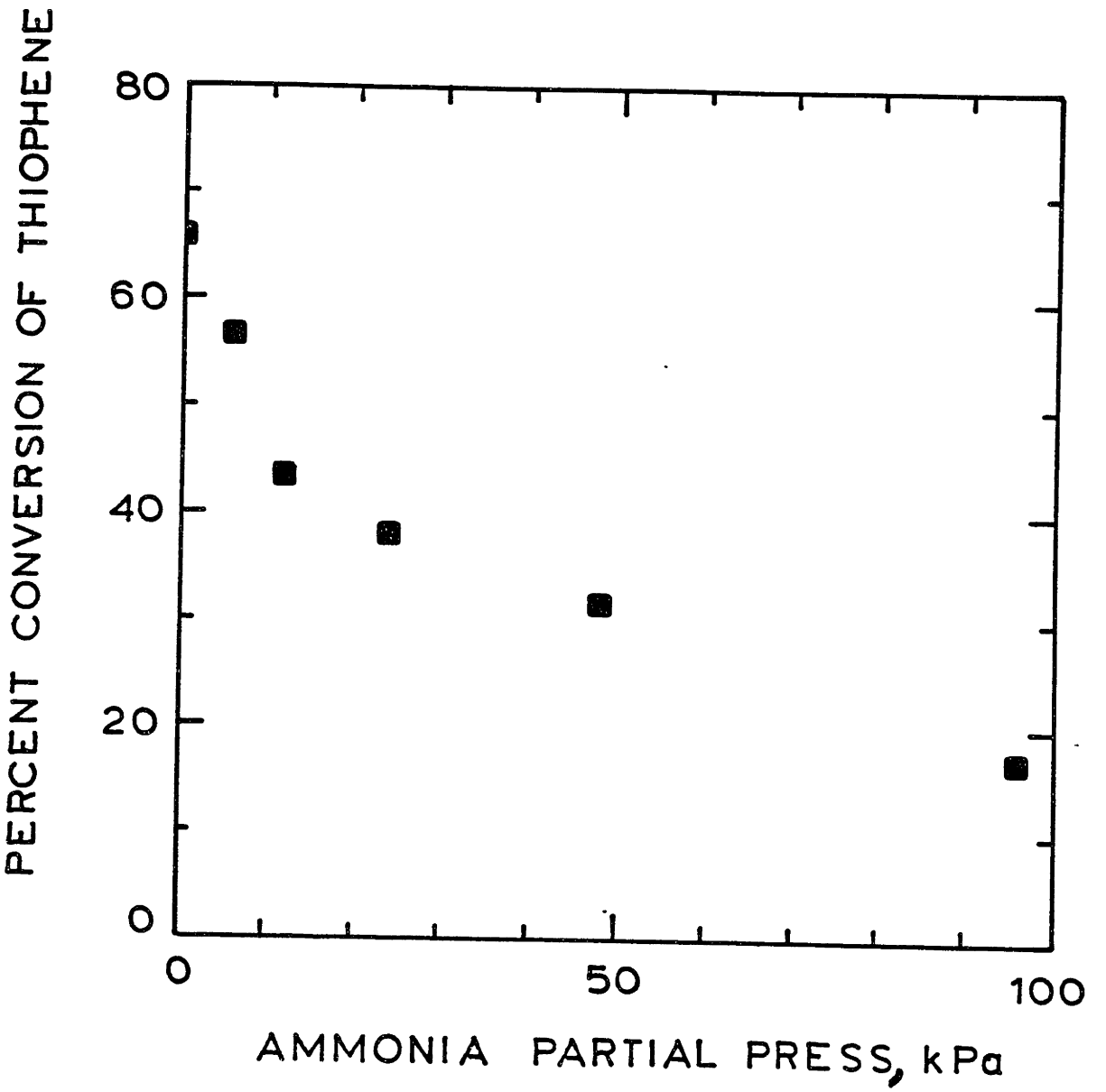

Figure IV.3

AMMONIA INHIBITS THIOPHENE HDS, 360°C

If the inhibitor partial pressure remains constant, equation IV.1 indicates that first order behavior will still be observed. At each inhibitor concentration, one can thus calculate an apparent first order rate constant k_a from the corresponding conversion. The adsorption constant can then be determined by fitting a least-squares regression line to the calculated ratio of rate constants in the form

$$\frac{k}{k_a} = 1 + K_I P_I \quad . \tag{IV.2}$$

A Langmuir isotherm plot can be derived by relating the fraction of HDS activity lost to the inhibitor partial pressure. From equation IV.1 the fraction of activity lost is given by

$$\theta = \frac{k - k_a}{k} = \frac{K_I P_I}{1 + K_I P_I} \quad . \tag{IV.3}$$

By comparison with the Langmuir isotherm, the fraction of activity lost can be thought of as a surface coverage by the inhibitor. Plotting the fraction of HDS activity lost versus the ammonia partial pressure (Figure IV.4), we see that a Langmuir isotherm with a best fit adsorption constant K_I of 0.048 kPa^{-1} describes the poisoning reasonably well. Even for a relatively weakly adsorbed poison such as ammonia, as much as 80 percent of the HDS activity can be lost.

Fitted adsorption isotherms for aniline, pyridine, and bis-1,8(N,N-dimethylamino)-naphthalene at 360°C are displayed in Figure IV.5. Calculated adsorption constants for these species ranged over two orders of magnitude, from the weakly adsorbed ammonia to the strongest inhibitor. However, it is evident that the Langmuir-Hinshelwood kinetics do not fully

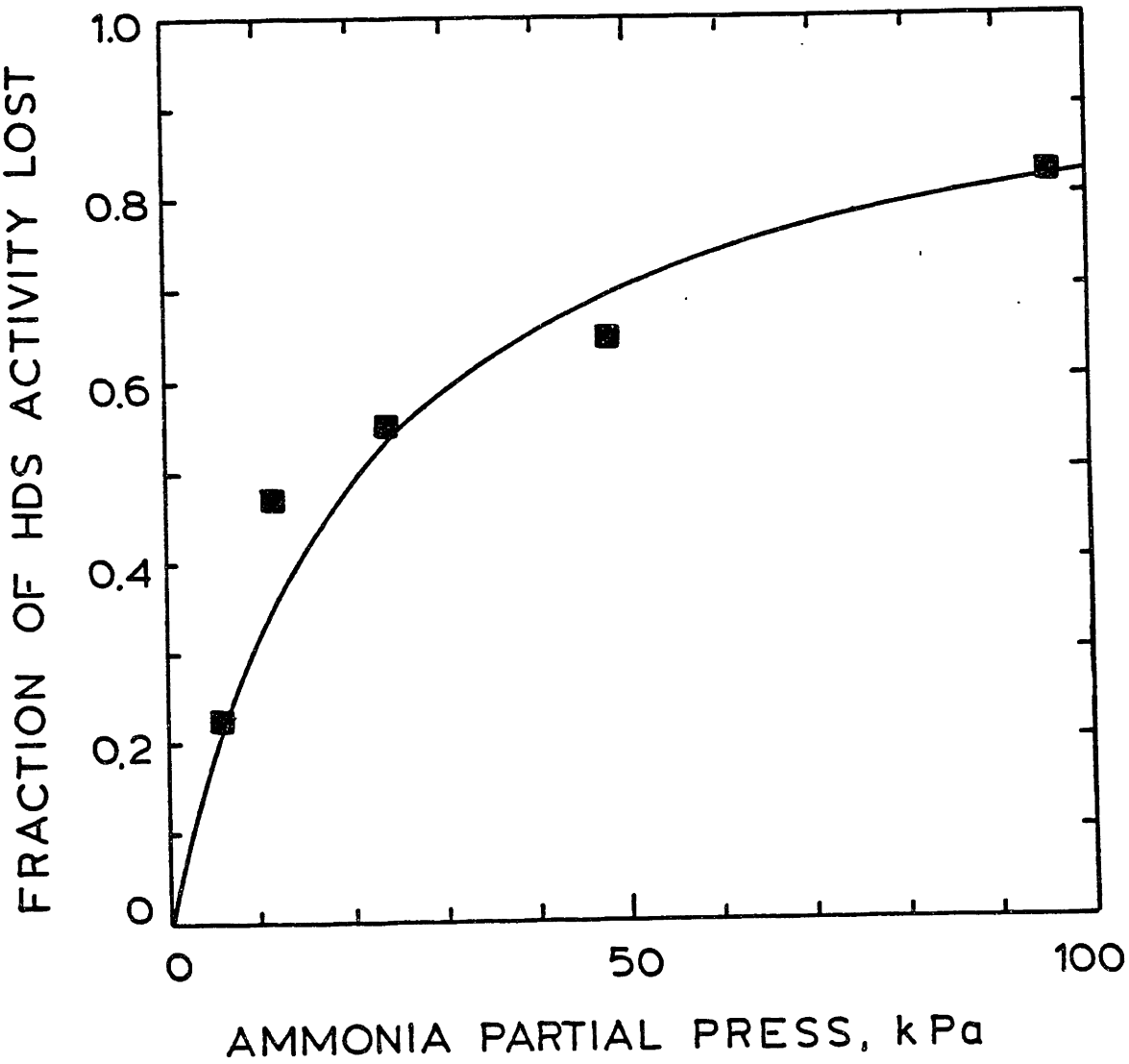

Figure IV.4 Ammonia adsorption can be described by a Langmuir isotherm.

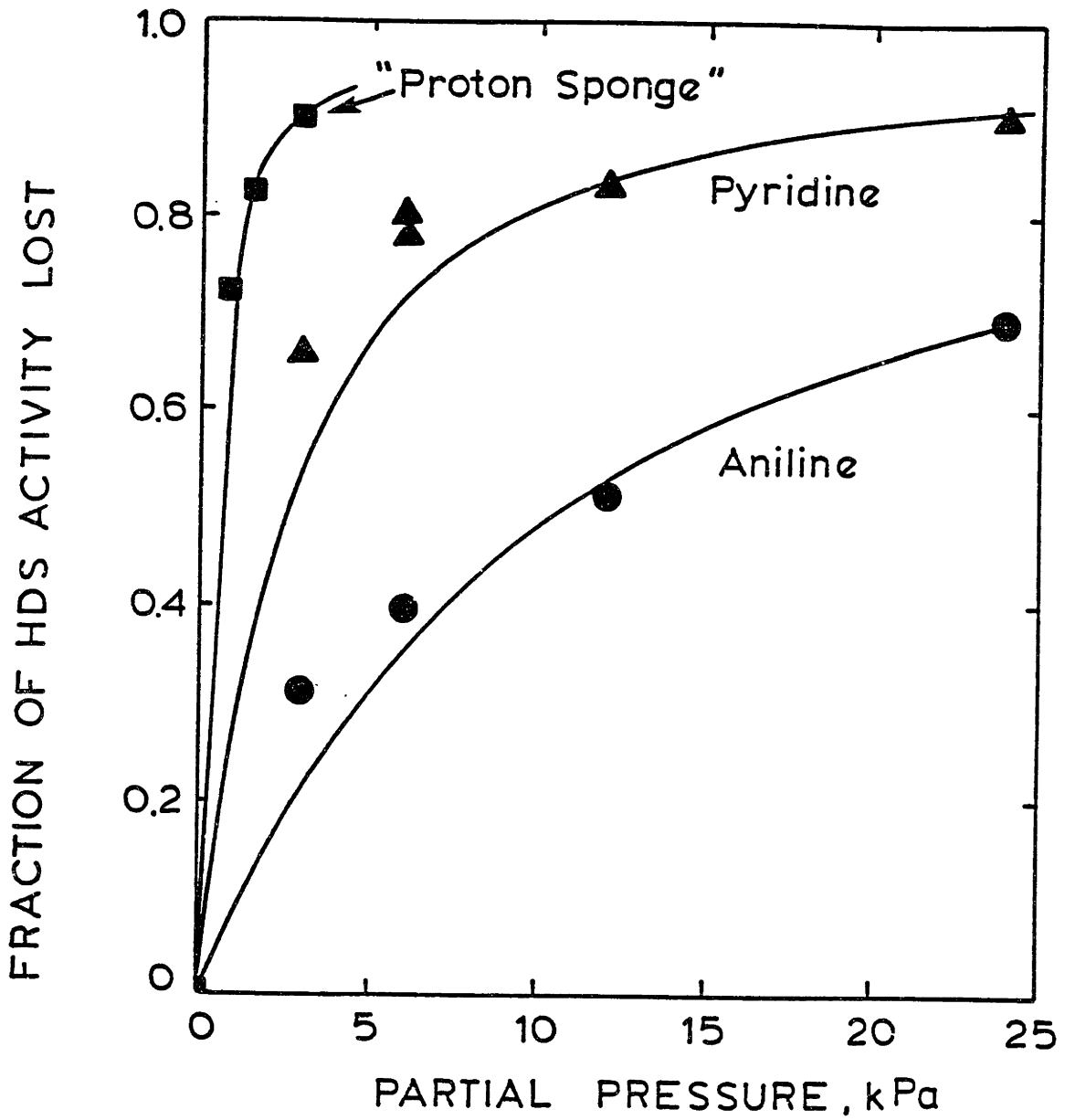

Figure IV.5 Adsorption strength varies over an order of magnitude for various nitrogen compounds.

describe the poisoning over the whole range of partial pressures for the more strongly adsorbed species. The Langmuir isotherm underestimates adsorption at lower partial pressures so that the calculated adsorption constants are only valid above approximately 1 kPa.

Massoth and Miciukiewicz (1986) reported that the Temkin adsorption isotherm more accurately described the poisoning of thiophene HDS by pyridine on a Co-Mo/Al_2O_3 catalyst. A correlation of the data in this study by the Temkin isotherm (see section IV.E) showed agreement with their findings. Although, the two parameter Tempkin isotherm can describe the poisoning by a single inhibitor over a wide concentration range, this isotherm is difficult to apply to multicomponent systems. Since hydrotreater feeds are extremely complex mixtures, Langmuir-Hinshelwood kinetics would provide more utility in modelling an industrial reactor. We therefore determined that the Langmuir isotherm would be appropriate for modelling poisoning in this study at nitrogen levels above approximately 1 kPa (~200 ppm).

Langmuir adsorption constants for all of the inhibitors successfully tested at 360°C are listed in Table IV.2 in order of increasing adsorption strength. Two of the compounds, denoted by asterisks, are sterically hindered. Figure IV.6 shows fitted adsorption isotherms for some of the intermediates and related species in the quinoline hydrodenitrogenation reaction network: o-ethylaniline, 1,2,3,4-tetrahydroquinoline (PyTHQ), and decahydroquinoline (DHQ). Naphthalene and phenanthrene, the two polyaromatic hydrocarbons, were relatively weakly adsorbed as shown in Figure IV.7.

The inhibition produced by 2-phenylphenol as a function of concentration is indicated in Figure IV.8. In this case, adsorption does not appear to follow a Langmuir isotherm, and the degree of inhibition

TABLE IV.2 Calculated Adsorption Constants, pK_a Values, and Proton Affinities for the Nitrogen Compounds Studied at 360°C

Compound	K (kPa^{-1})	pK_a (a)	PA (kcal/mol)
Naphthalene	0.011		199.8 (b)
Ammonia	0.048	9.24	207 (c)
Phenanthrene	0.064		209** (c)
Aniline	0.094	4.63	213.5 (c)
2-Ethylaniline	0.10	4.42	
2,6-Dimethylpyridine*	0.11	6.71	231.5 (f)
1-Methylpiperidine*	0.26	10.19	233.2 (d)
Pyridine	0.43	5.29	222 (c)
1,2,3,4-Tetrahydro-quinoline	0.46		225** (b)
Carbazole	0.51		
Piperidine	0.58	11.12	229.7 (d)
4-Methylpyridine	0.68	6.02	229 (e)
Quinoline	0.98	4.80	227.6 (c)
5,6,7,8-Tetrahydro-quinoline	2.0		
Decahydroquinoline	2.0		
1,8-bis(N,N-dimethylamino)-naphthalene "Proton Sponge"	3.1		246.2 (b)

* Sterically hindered

** Estimated

(a) Lang's Handbook
(b) Lau et al., 1978
(c) Meot-Ner, 1979
(d) Aue et al., 1976a
(e) Brown et al., 1980
(f) Aue et al., 1976b

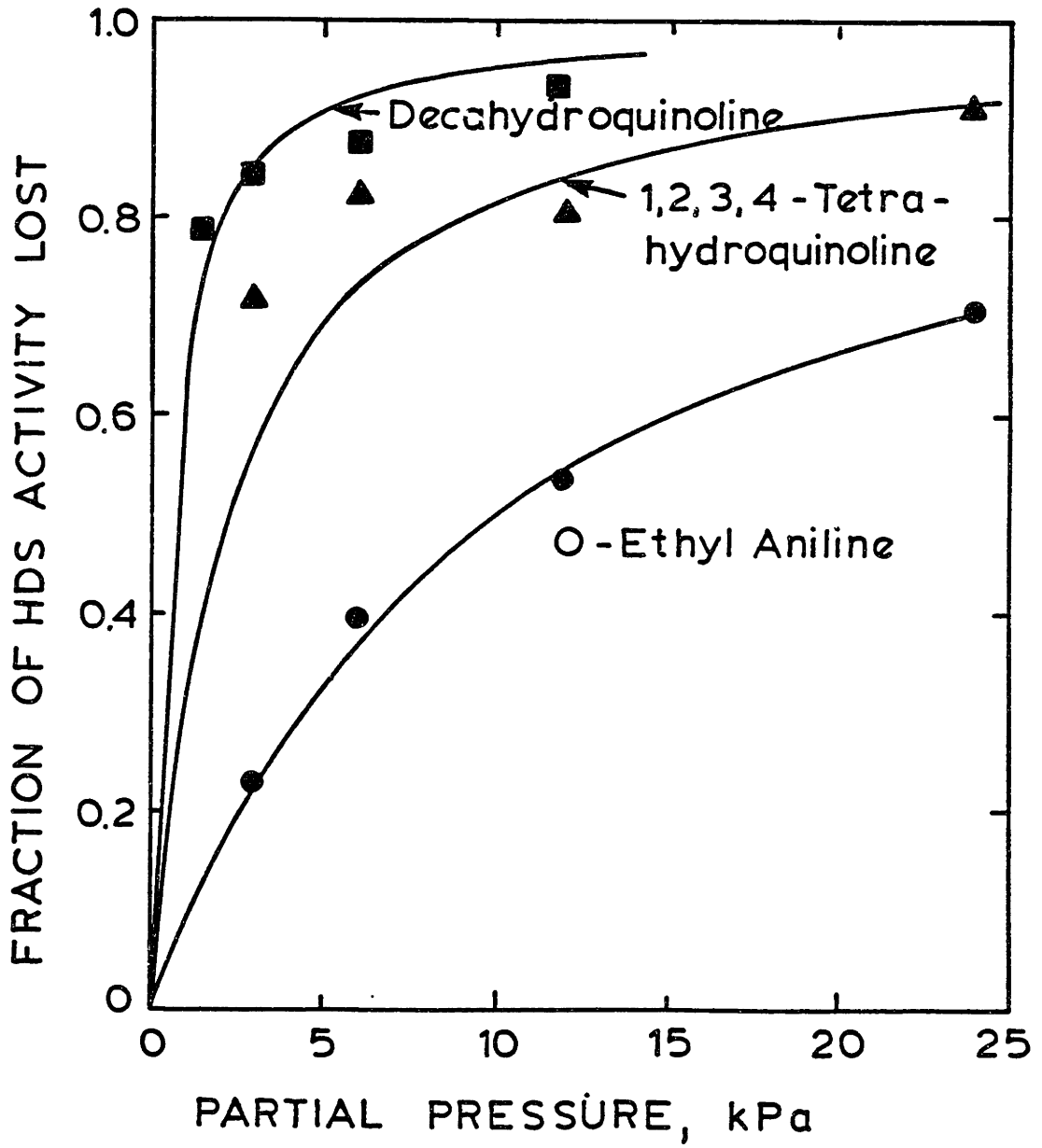

Figure IV.6 Langmuir adsorption isotherms for selected intermediates of the quinoline HDN network.

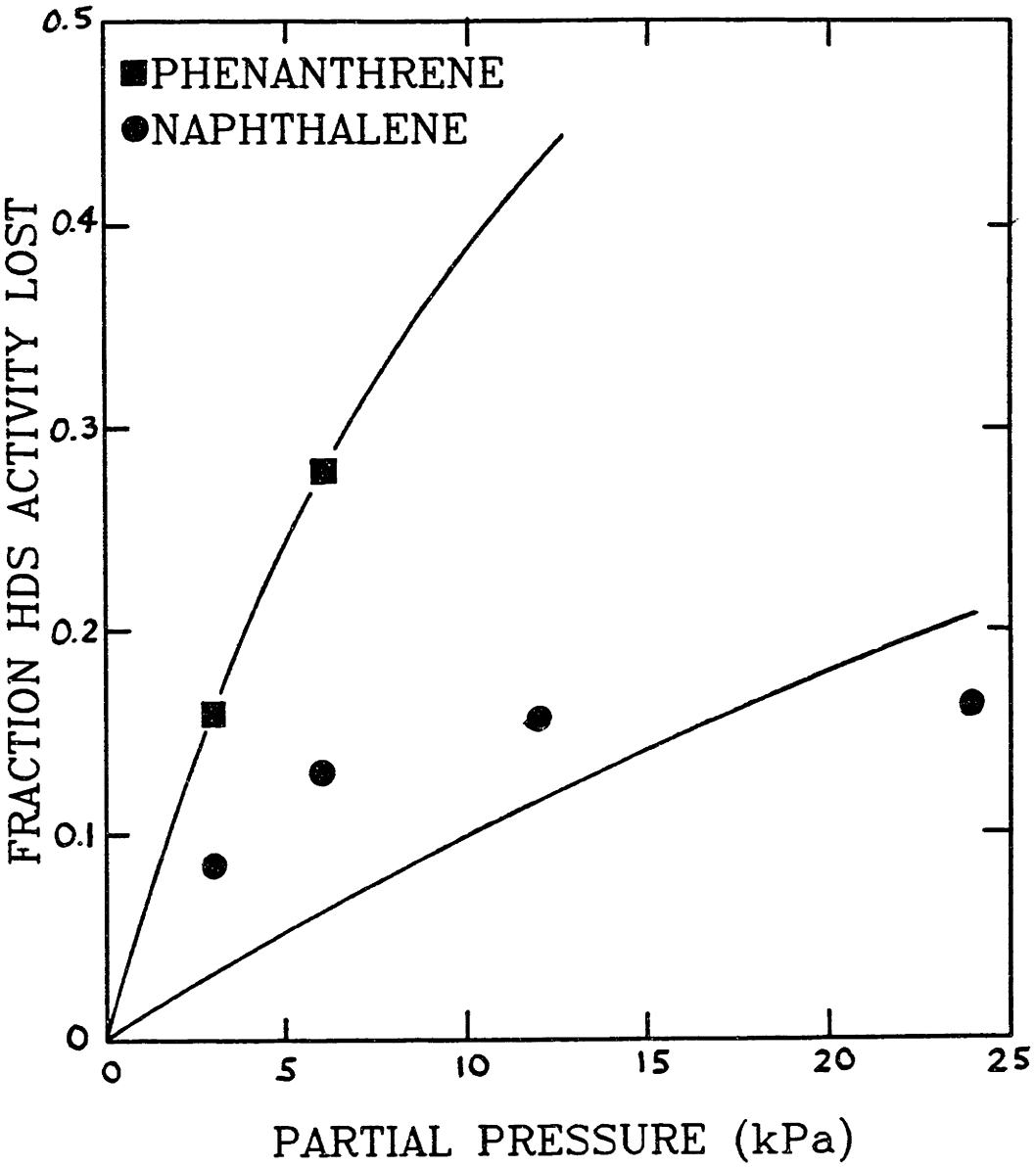

Figure IV.7 Polyaromatic hydrocarbons exhibit weak adsorption.

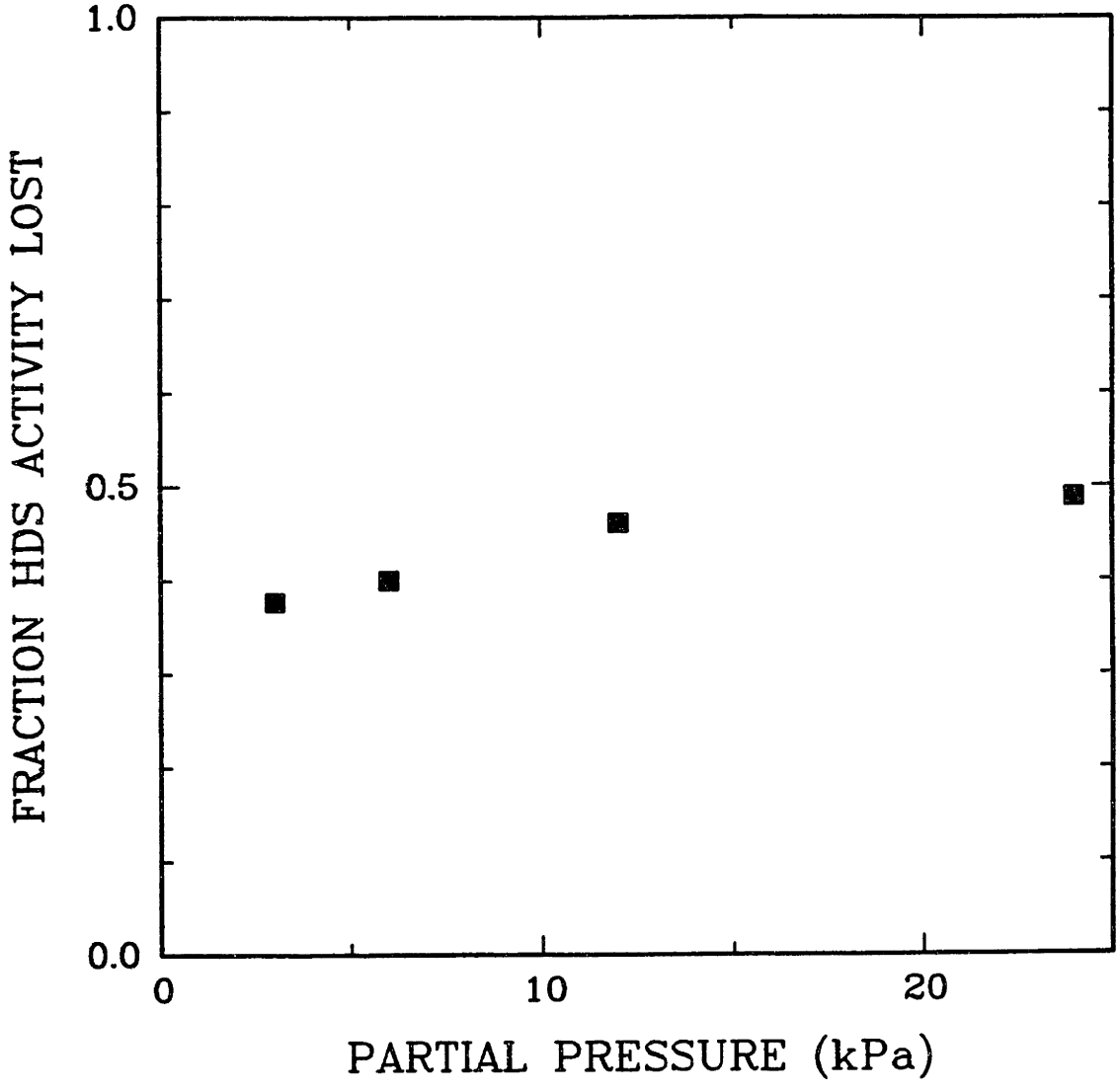

Figure IV.8 Inhibition by 2-phenylphenol is relatively independent of concentration.

produced is independent of inhibitor concentration. Similar results have been observed in the inhibition of biphenyl hydrogenation by the oxygenate dibenzofuran (see section III.E).

The results in Table IV.2 indicate that the relative adsorption strengths of different molecules at 360°C can vary over two orders of magnitude. Among the nitrogen compounds, adsorption strength increased in the order: ammonia < aniline < pyridine < quinoline. The same order was observed at 300 and 400°C. This order of inhibition is similar to that observed in studies cited in sections I.C.2 and in a study of the poisoning of cracking reactions by Fu and Schaffer (1985) (see section IV.I).

IV.D Correlation with Basicity

Although the results provide useful information on relative adsorption strength for several compound classes, what is needed is a correlation of adsorption strength against a measurable molecular property. The results suggest that, aside from steric hindrance, the basicity of the molecule may be the controlling factor in determining the strength of interaction with the catalyst surface. There is no correlation with volatility as such (Figure IV.9); for example, 5,6,7,8-tetrahydroquinoline and decahydroquinoline, with high adsorption constants (2.0 kPa^{-1}), have boiling points of about 200°C, intermediate values relative to the group as a whole. This lack of correlation is plausible since boiling point is largely determined by relatively weak van der Waals forces which are not involved in chemisorption. Table IV.2 lists the adsorption constants for the inhibitors at 360°C along with two measures of basicity: pK_a values measured in aqueous solution at 25°C and proton affinities measured in the

NO TREND WITH BOILING POINT

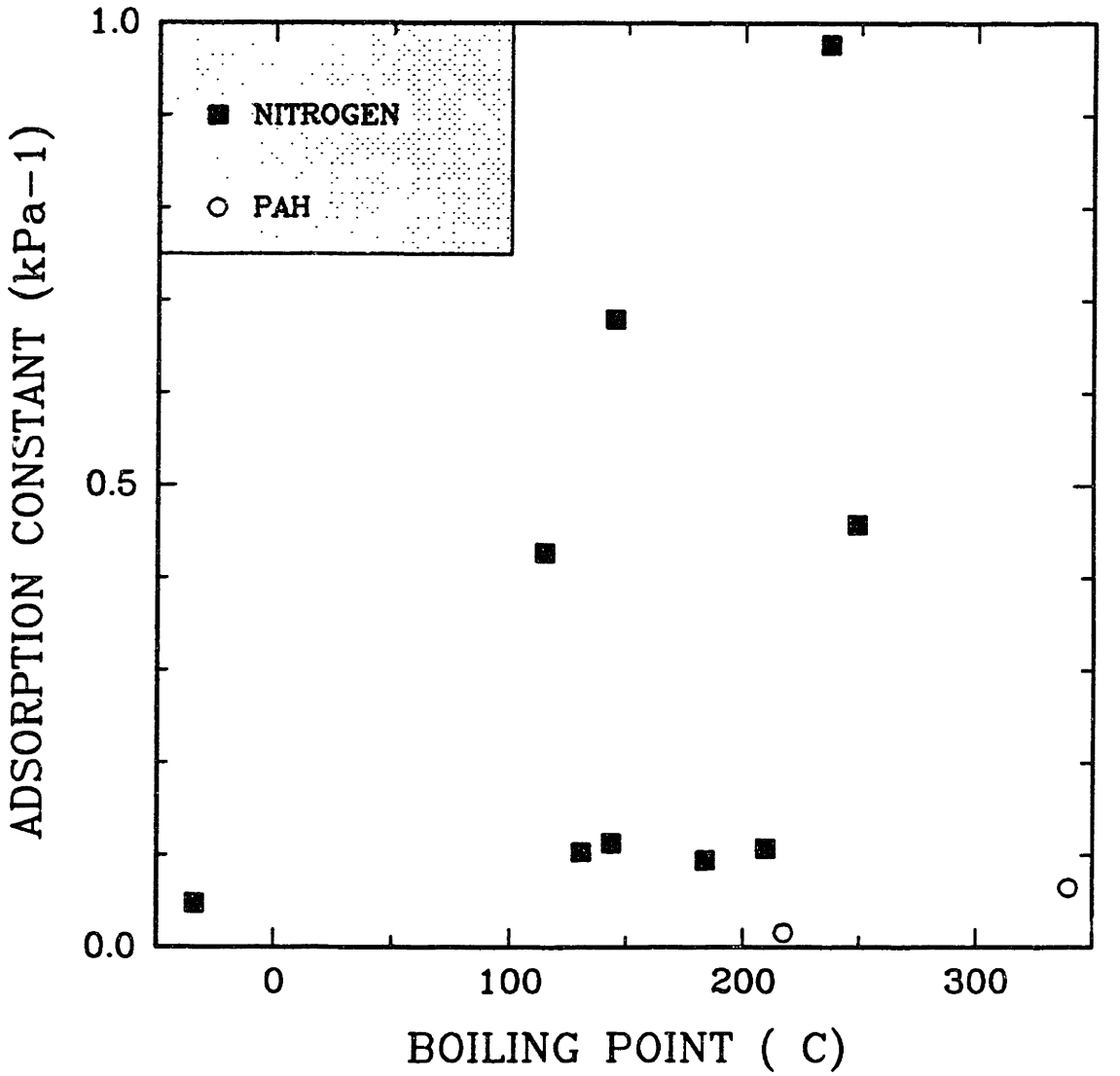

Figure IV.9 Inhibition does not correlate with boiling point.

gas phase. Higher basicity is indicated by higher pK_a values or higher proton affinity values.

A comparison of adsorption constants and corresponding pK_a values indicates that aqueous basicity is a poor predictor of adsorption strength here. Hydrolysis of ionic species in aqueous solution significantly masks the intrinsic basicity of charge localized cations and alters proton transfer equilibria (Taft, 1983).

A more appropriate measure of basicity under hydrotreating conditions is the gas phase proton affinity. This quantity represents the enthalpy change for a proton transfer reaction with all values referenced to the proton affinity of ammonia. Proton transfer equilibria between different species can be measured directly by mass spectroscopy techniques, yielding the free energy change for the reaction. A small correction is then made for the entropy term to obtain the proton affinity. Similar measurements for a large number of compound pairs allows a ladder of proton affinities to be developed. Values listed in Table IV.2 from Lau et al. (1978) and Brown and Tse (1980) actually represent ΔG values and the entropy corrections would be in the range of 1 kcal/mol. Proton affinities for 1,2,3,4-tetrahydroquinoline and phenanthrene were estimated from the values for N-ethylaniline and anthracene respectively. For 1,8-bis(dimethylamino)-naphthalene, the partial loss of the methyl groups required the estimation of an average proton affinity for the species present in the reactor (240 kcal/mol).

From Table IV.2 we see that the proton affinities of the inhibitors follow the same trend as their adsorption strengths. The better performance of gas phase basicity as a predictor of adsorption strength is reasonable, since a hydrotreating catalyst is exposed either to a hydrogen rich gas phase or a relatively inert paraffinic or aromatic liquid.

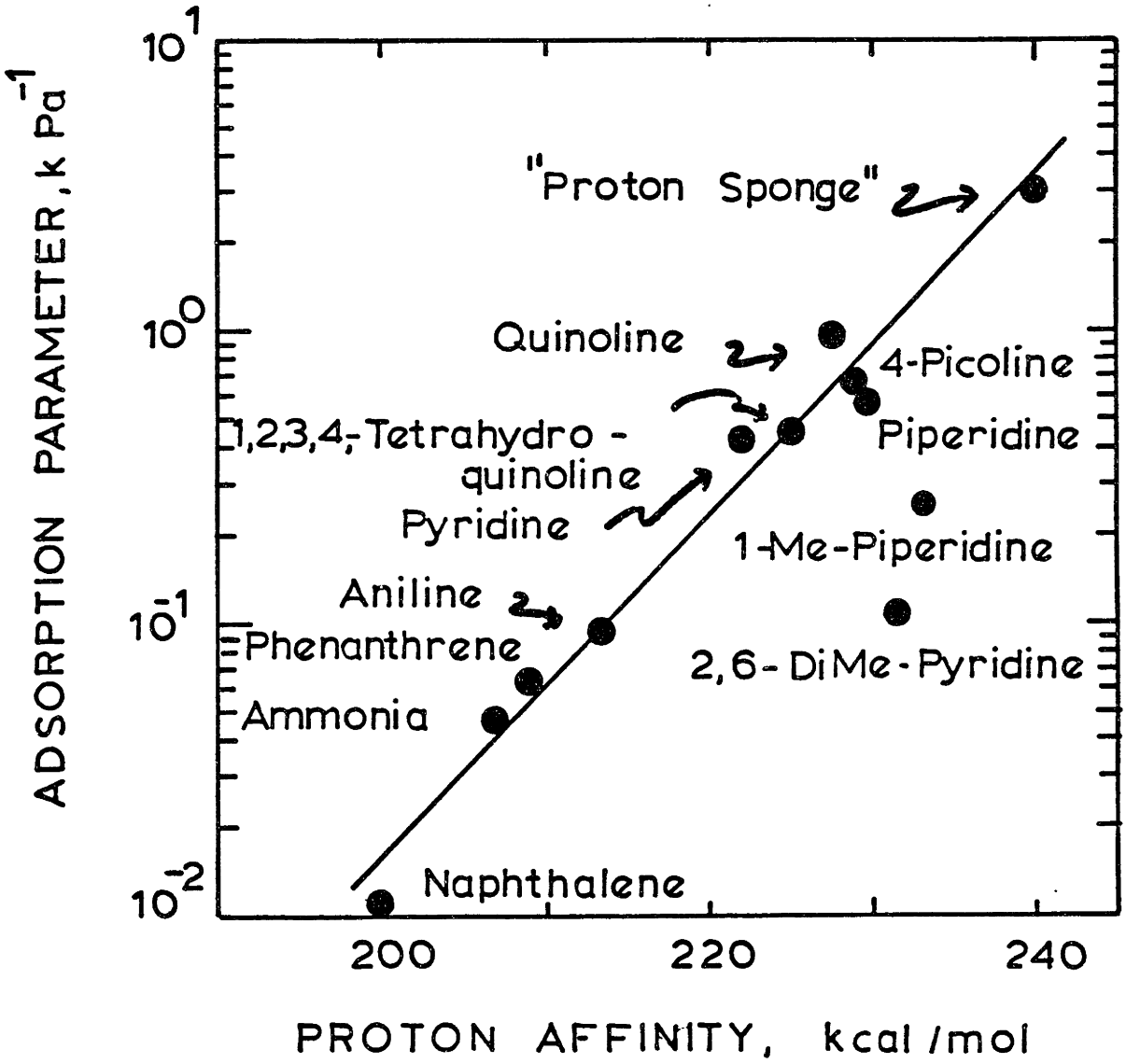

Figure IV.10 Adsorption constants correlate with proton affinity at 360 °C.

Proton affinities measured in the gas phase show good agreement with proton affinities measured in more inert liquids, such as organic solvents (Taft, 1983).

We can now consider how the adsorption equilibrium constants might correlate with proton affinity. The heat of adsorption is likely to be a controlling factor in determining the strength of adsorption, and the adsorption equilibrium constant K should be related to the heat of adsorption ΔH_a by the functional form:

(IV.4) $$K \propto \exp(\Delta H_a/RT)$$

where R = gas constant (kcal/mol K)

T = absolute temperature (K). This relation implies that differences in the entropy of adsorption between the various species are insignificant.

Assuming that acid-base interactions are responsible for adsorption, the heat of adsorption ΔH_a should then be proportional to the proton affinity (ΔH for a proton transfer reaction). Such a relation would be more appropriate for a catalyst possessing Bronsted acidity. However, following this reasoning, it appears that an appropriate form for the correlation would relate the adsorption constant of a species to its proton affinity by:

(IV.5) $$K \propto \exp(PA/RT)$$

where PA = proton affinity in kcal/mol.

Plotting the data obtained at 360°C as suggested by equation IV.5 (Figure IV.10) shows a reasonable correlation between adsorption strength and proton affinity on a semi-logarithmic scale. Large deviations from the linear correlation line are observed only for 2,6-dimethylpyridine and 1-methylpiperidine, which are presumably sterically hindered. The adsorption strength for 2,6-dimethylpyridine was six times lower than that

of 4-methylpyridine, which has a comparable proton affinity. These effects agree with the work of Gutberlet and Bertolacini (1983) with sterically hindered pyridines.

Figure IV.11 displays the same correlation at 360°C along with the best fit correlation lines at 300 and 400°C, omitting the two sterically hindered species. The form of the correlation applies over a substantial range of temperatures. The change in adsorption strength with temperature for any particular species can be examined by focusing on the particular proton affinity value for that species. As expected for an exothermic process, the strength of adsorption decreases with temperature. We also note that the slope of the correlation line decreases with temperature, so the range of relative adsorption strengths is greater at low temperature.

Equation IV.5 suggests that a more general form of the correlation should relate the log of the adsorption constant to the proton affinity divided by the absolute temperature. The data obtained at three temperatures are plotted in this form in Fiqure IV.12, where the abscissa (Proton Affinity)/RT is dimensionless. It is striking that the same slope is observed at each temperature. If we accept the assumptions discussed above, the common slope would indicate that the proportionality constant beween heat of adsorption and proton affinity is independent of temperature.

For each of those species for which adsorption constants were determined over a range of temperatures, a heat of adsorption was calculated from the best linear fit to an Arrhenius plot. The calculated heat of adsorption for each inhibitor is plotted against its proton affinity in Figure IV.13. The results show considerable scatter; however, an upward trend in ΔH_a with proton affinity is evident.

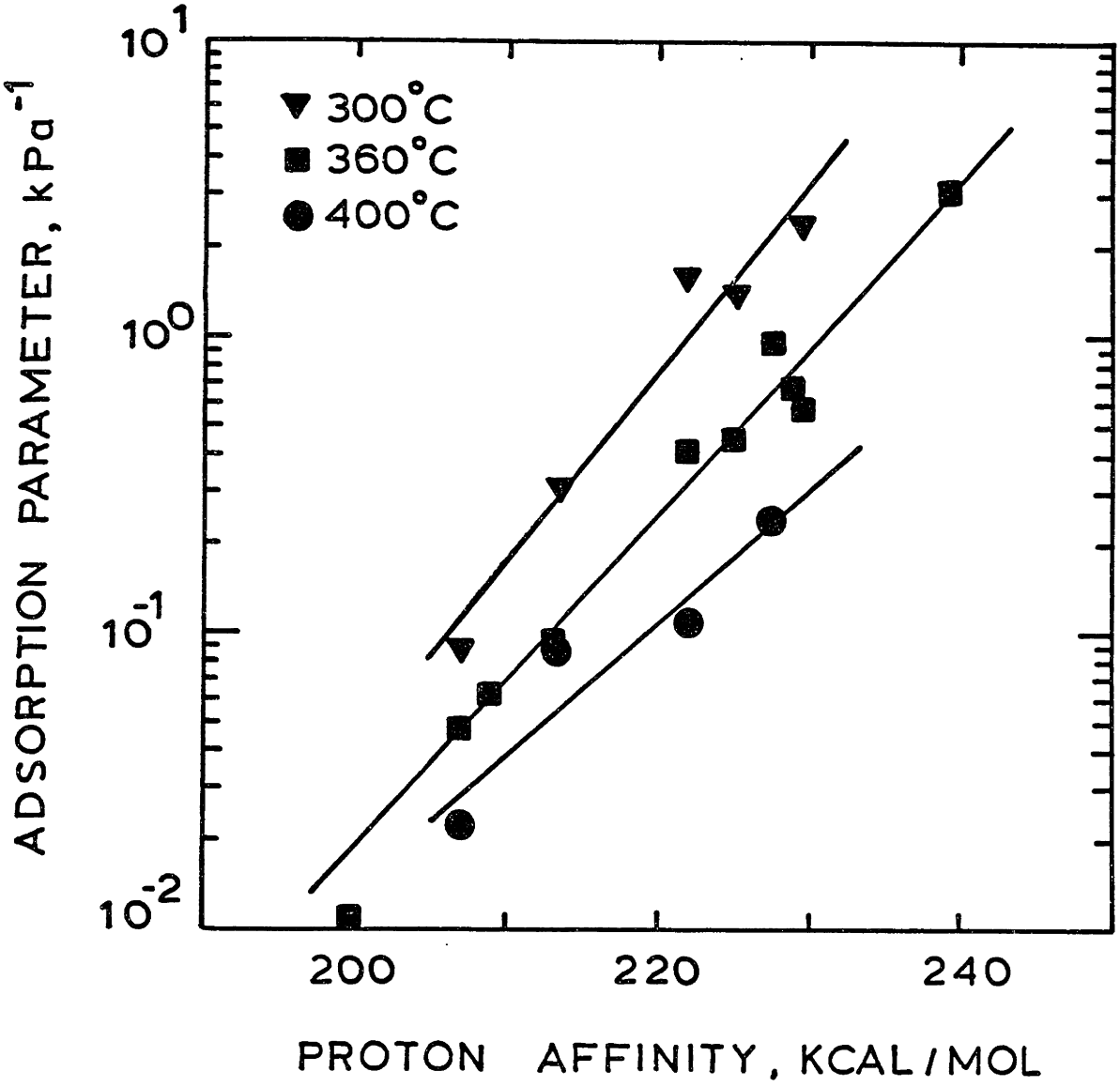

Figure IV.11 Adsorption strength decreases with temperature.

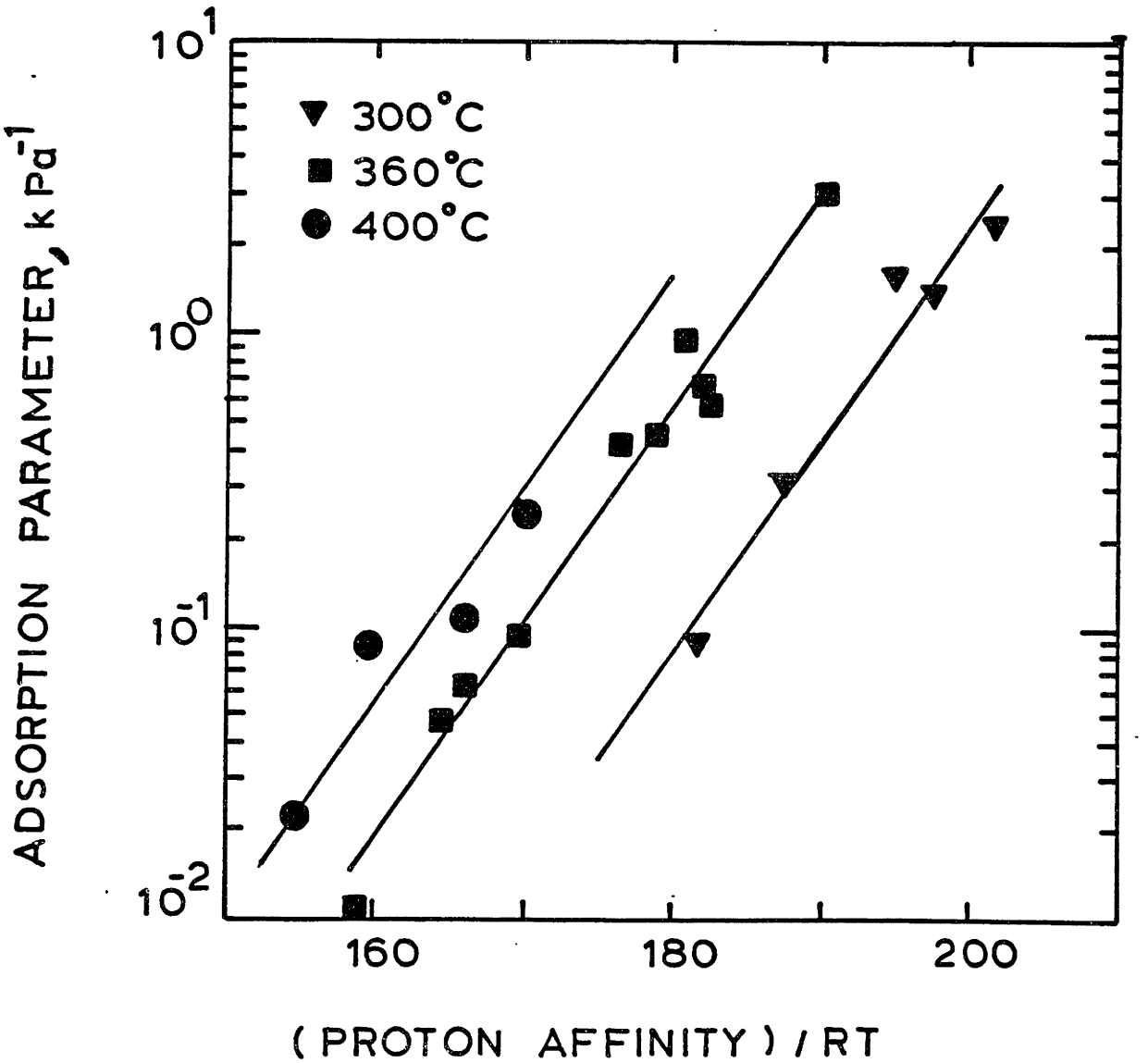

Figure IV.12 A constant slope is obtained by a correlation with the (Proton Affinity)/RT.

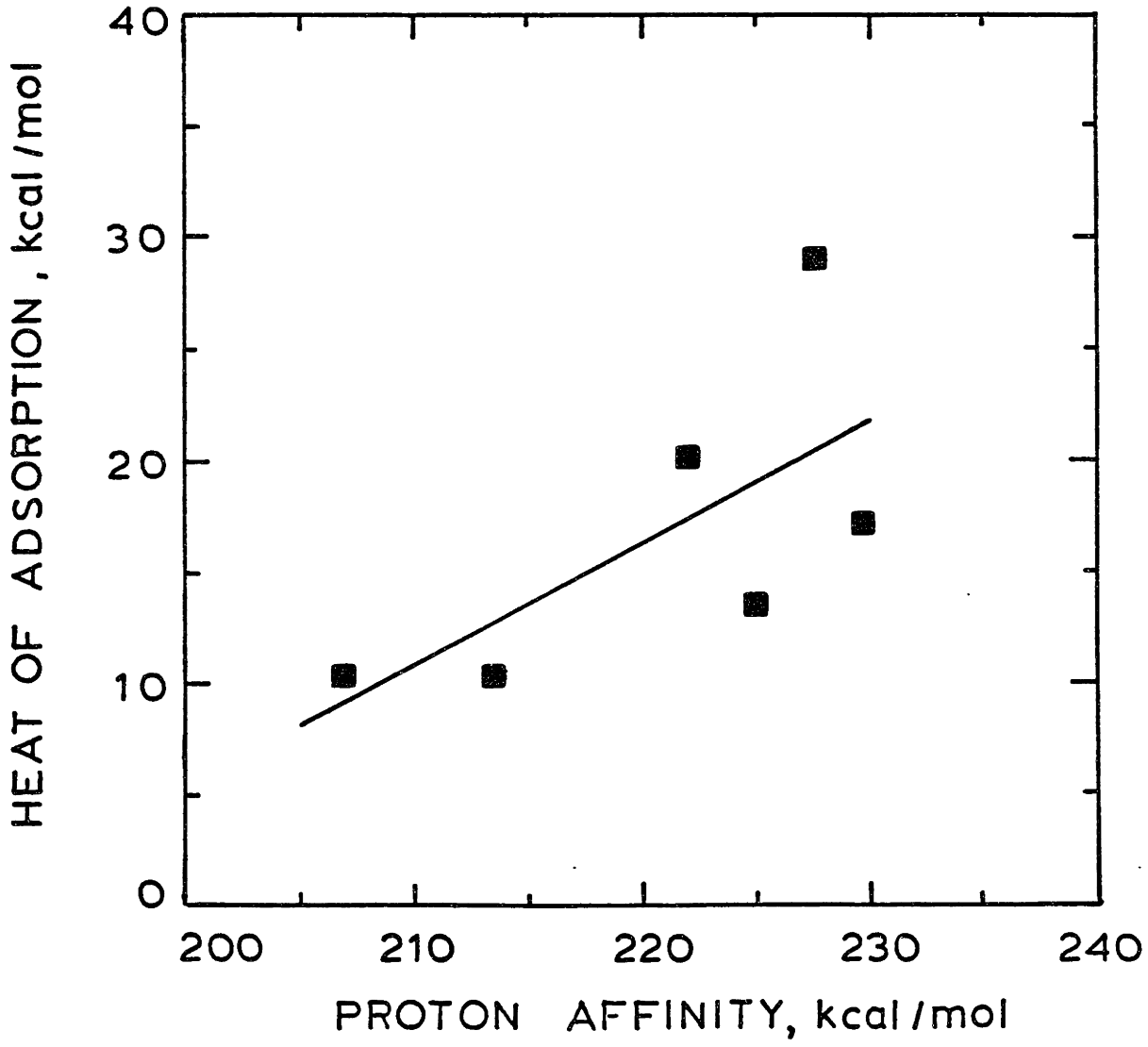

Figure IV.13 Calculated heats of adsorption exhibit an increasing trend with gas phase basicity.

IV.E Simultaneous HDN and HDO

As a test of their generality, the adsorption constants determined from the kinetics of thiophene HDS were used to predict poisoning of the hydrodeoxygenation (HDO) of dibenzofuran. Various nitrogen compounds including quinoline, intermediates of the quinoline network, and related nitrogen species were reacted simultaneously with dibenzofuran. A larger quantity of catalyst was used than in the studies with thiophene so that the nitrogen species were substantially reacted, except for NH_3. 2-Ethylaniline and aniline react to form ammonia and hydrocarbons directly. In the HDN of decahydroquinoline and quinoline, however, other organo-nitrogen compounds of considerable stability are formed and their adsorption must be considered.

Dibenzofuran is of interest since it is the major organo-oxygen compound in the neutral oil fraction of of an SRC-II coal liquid (Petrakis et al., 1983) and is relatively unreactive. The reaction network for dibenzofuran is described in Chapter III, and the overall rate is first order in DBF. No organo-oxygen intermediates are found at appreciable concentrations. Water, formed as a final product, has only a minor effect on hydrodenitrogenation reactions. The hydrodenitrogenation (HDN) network for quinoline has been studied extensively (Satterfield and Cocchetto, 1981; Shih et al., 1977).

IV.E.1 Poisoning by ammonia.

Ammonia does not react further and therefore provides a simple test to determine if the degree of inhibition of thiophene HDS and dibenzofuran HDO differs. A series of experiments was performed on catalyst sample 28 (1.6 g. HDS-3A) which had reached a steady activity. The temperature was 360°C with an H_2S partial pressure of 7 kPa and a total pressure of 7 MPa.

Ammonia was produced in situ by the addition of pentyl amine or decyl amine to the feeds, since these compounds decompose rapidly at reaction conditions to form ammonia and hydrocarbon products. The conversion of dibenzofuran was measured at 5 space times at each ammonia partial pressure. Since DBF exhibits first order behavior, an apparent first order rate constant k_a could be calculated at each level of ammonia (equation IV.1). The losses of dibenzofuran HDO activity and thiophene HDS activity at various ammonia partial pressures are comparable, as shown in Figure IV.14. This indicates that the adsorption constant for NH_3 found in the thiophene HDS system (0.048 kPa^{-1}, represented by the solid line in Figure IV.14) is equally applicable to the DBF system.

Some additional results on the poisoning of dibenzofuran HDO by ammonia are also of interest. Addition of 24 kPa of ammonia to the DBF reaction system was found to increase the apparent activation energy for the HDO of DBF in the temperature range of 360-400°C. Arrhenius plots for the apparent first-order rate constant for DBF are shown in Figure IV.15. Fed alone, the reaction exhibited an activation energy of 66 kJ/mol, while the presence of 24 kPa of ammonia lowered the rate and increased the observed activation energy to 114 kJ/mol. The increase in apparent activation energy agrees with our expectations from the form of the kinetics (equation IV.1) and the fact that adsorption of ammonia would be exothermic.

Changes in selectivity for the HDO of dibenzofuran in the presence of ammonia or organo-nitrogen bases were also observed. As shown in Figure IV.16, the presence of ammonia was found to significantly reduce the degree of isomerization found in the C_{12} (double-ring) saturated products. At 360°C the ratio of cyclopentylmethyl-cyclohexane to dicyclohexyl

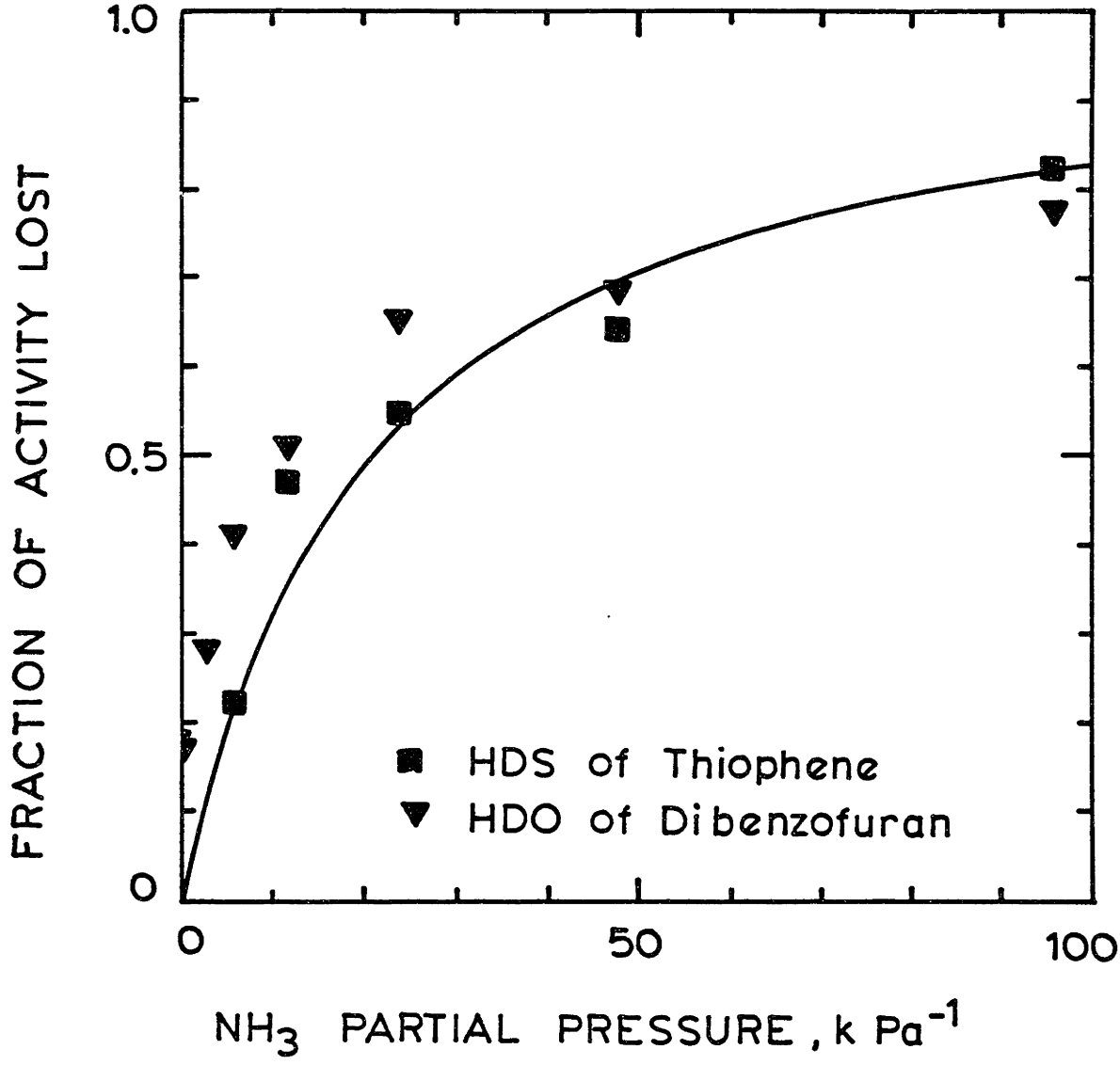

Figure IV.14 Poisoning by ammonia is similar for thiophene HDS and dibenzofuran HDO.

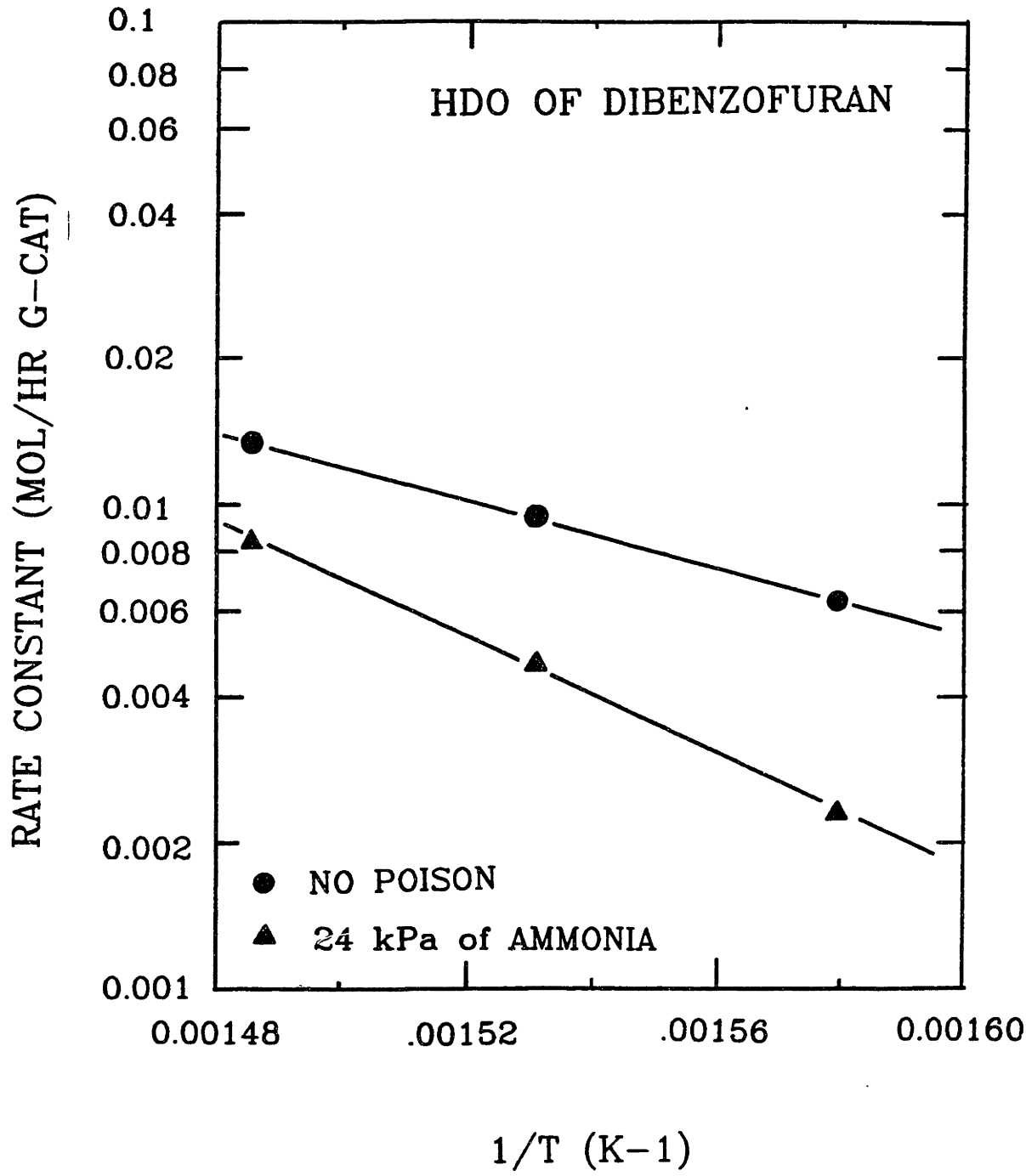

Figure IV.15 The presence of a catalyst poison increases the observed activation energy for the HDO of dibenzofuran.

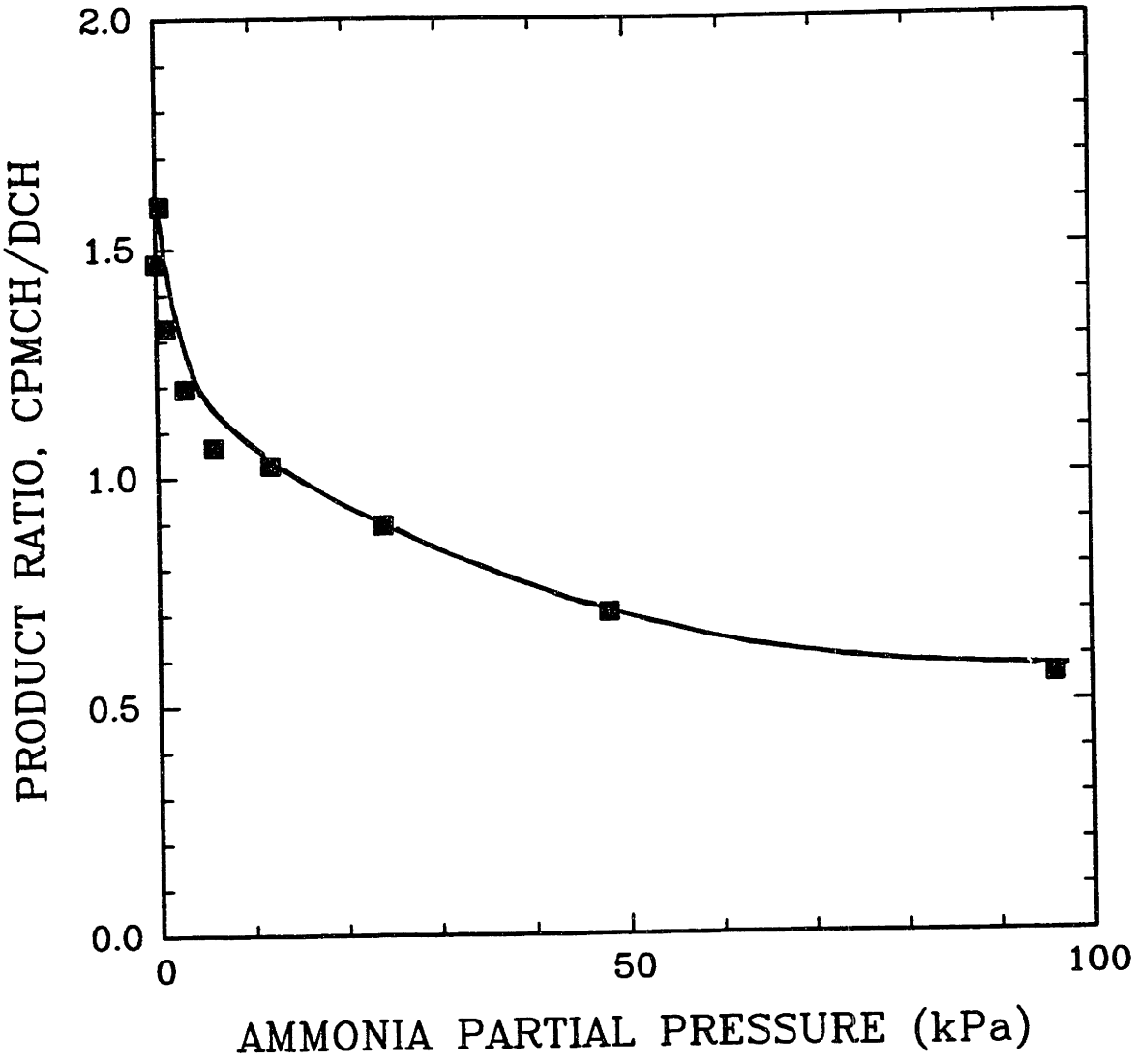

Figure IV.16 Ammonia inhibits isomerization reactions during the HDO of dibenzofuran.

dropped to one third of its inital value as the ammonia partial pressure was increased to 96 kPa.

Ammonia also had some effect upon the product distribution. Figure IV.17 shows that the percentage of double-ring products increased slightly from 28% to 35% as the ammonia concentration was raised. This small change agrees with the results of Gevert et al. (1987), in which ammonia did not affect the selectivity for the HDO of oxygenates which can react either through hydrogenation or by direct hydrogenolysis. Inhibition by ammonia was also found to increase the concentration of the partially hydrogenated oxygenates tetrahydro- and hexahydro- dibenzofuran, observed at low conversion, although these never comprised more than 3% of the initial dibenzofuran.

IV.E.2 Poisoning by organo-nitrogen compounds.

For each N-compound studied, the concentration profiles of the nitrogen species fed, ammonia, significant nitrogen intermediates, as well as dibenzofuran were determined over a range of space times. To model the kinetics of the HDO reaction, Equation IV.6 was used, in which there are adorption terms for the inhibitors I but not for DBF.

$$\text{(IV.6)} \qquad \text{Rate} = \frac{k\, P_{DBF}}{1 + \Sigma\, K_I P_I}$$

where: k = rate constant

P_{DBF} = partial pressure of reactant (DBF).

The actual first order rate constant in the absence of inhibitors, k, was measured separately on catalyst batch 28, and was found to have the value 0.00179 [mol/{hr (g of catalyst) (kPa of DBF)}]. Since catalyst batch 28 was deactivated in the presence of H_2S, this value is about 30% greater than the value listed in Figure III.17 for a catalyst deactivated with

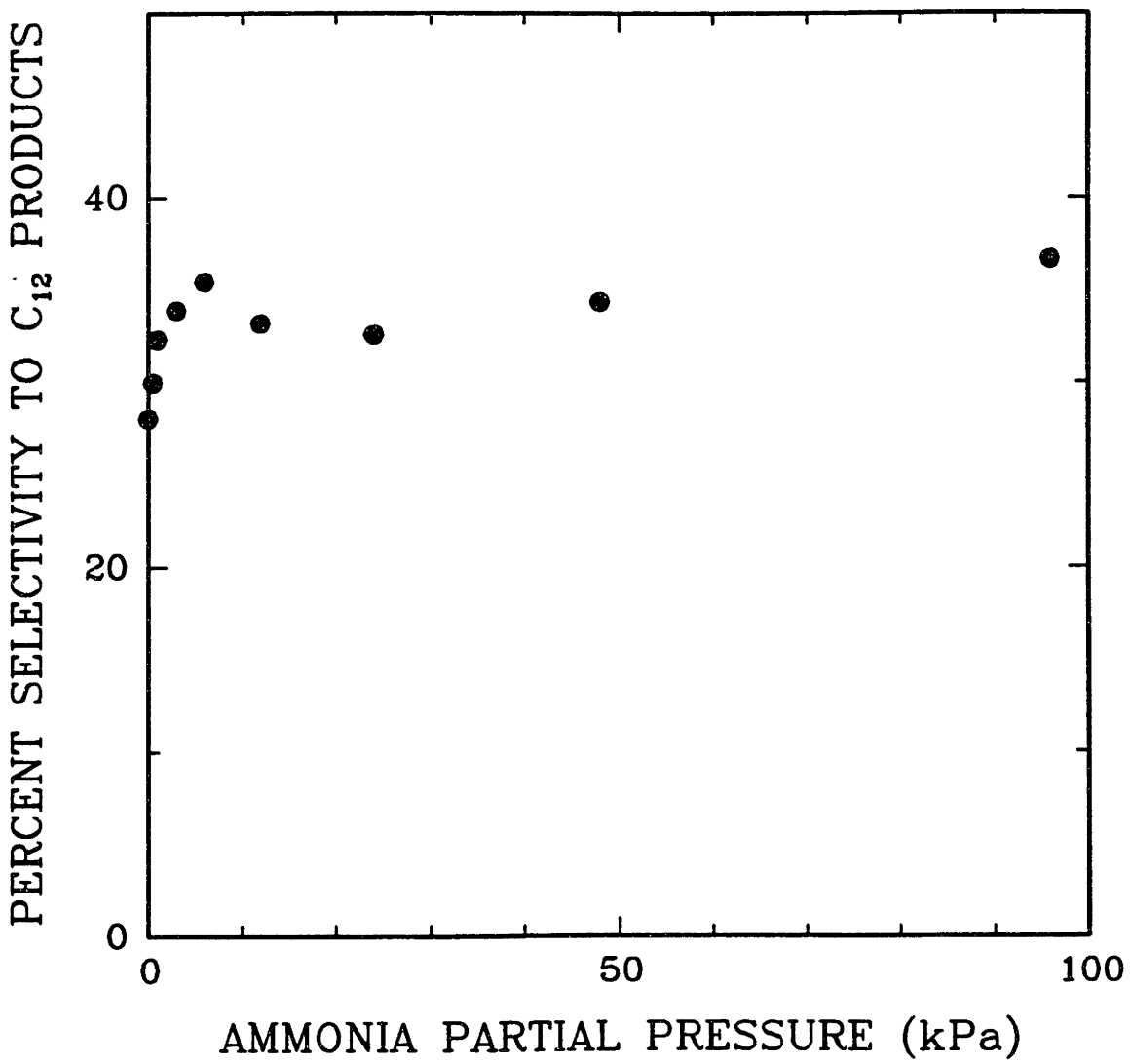

Figure IV.17 Ammonia slightly increases the selectivity toward double-ring products from DBF.

quinoline and no H_2S. The adsorption constants were set equal to those calculated from the thiophene HDS system. In consequence, there were no adjustable parameters in the poisoning model for dibenzofuran HDO.

For the simultaneous HDN reactions, kinetics were fitted to the concentration profiles of the nitrogen species over a range of space times. For each reaction i of the HDN network a Langmuir-Hinshelwood rate expression was used of the form:

$$\text{(IV.7)} \qquad \text{Rate}_i = \frac{k_i P_N}{1 + \Sigma K_I P_I}$$

where: k_i = rate constant

P_N = partial pressure of reacting nitrogen compound.

The adsorption constants were set equal to those in the thiophene HDS system, and the presence of dibenzofuran was assumed to have negligible effect upon the HDN kinetics because of its low adsorptivity (see later). Rate constants k_i were fitted to match nitrogen species concentration profiles using the HJB method (Himmelblau et al. 1967) [for computer programs see thesis of Smith, 1985].

The effect of poisoning on the HDO of dibenzofuran was modelled by simultaneously integrating the rate expressions for HDO and HDN over space time. This is approximately equivalent to fitting a smooth function through the nitrogen concentration profiles, and then using these functions to replace the P_I in Eq. IV.6. All of the rate equations were integrated through space time using a Fourth Order Runge-Kutta routine (see Appendix A8).

Measurements were made at 360°C, 7 MPa total pressure, and 7 kPa of H_2S. The DBF and nitrogen compound were fed at initial partial pressures

of 24 kPa. Concentrations of dibenzofuran and the nitrogen containing intermediates were measured as a function of space time.

IV.E.2.a Anilines - 2-Ethylaniline (OEA) reacts in one step to form ammonia and hydrocarbons, and this reaction has been studied by Olive and co-workers (1985). Figure IV.18 shows the percent of OEA and of DBF remaining as a function of space-time for reaction of an equimolar mixture of the two. The single rate constant for the HDN kinetics was determined analytically in this case (see Appendix A6) from the experimentally determined OEA conversions, using adsorption constants from the thiophene system for OEA and NH_3. The two rate equations for HDN and HDO were then integrated simultaneously. The predicted concentration profile for dibenzofuran, shown in Figure IV.18, is seen to agree closely with the experimental points.

The extent of poisoning of dibenzofuran HDO is significant. At a space time of 160 hr g cat/(mol of DBF), the conversion of DBF dropped from 68% in the absence of poison down to 32% with the simultaneous feed of OEA.

In a similar way the effect of aniline on the HDO of DBF was studied. Aniline reacts like 2-ethylaniline to form ammonia and hydrocarbons, and its adsorption constant in the inhibition of thiophene is nearly the same as that of 2-ethylaniline. The results for aniline were very similar (Figure IV.19).

IV.E.2.b Decahydroquinoline - The reaction of decahydroquinoline (DHQ) is more complicated because some dehydrogenation to form 5,6,7,8-tetrahydroquinoline (BzTHQ) also occurs. The reaction network is of the form:

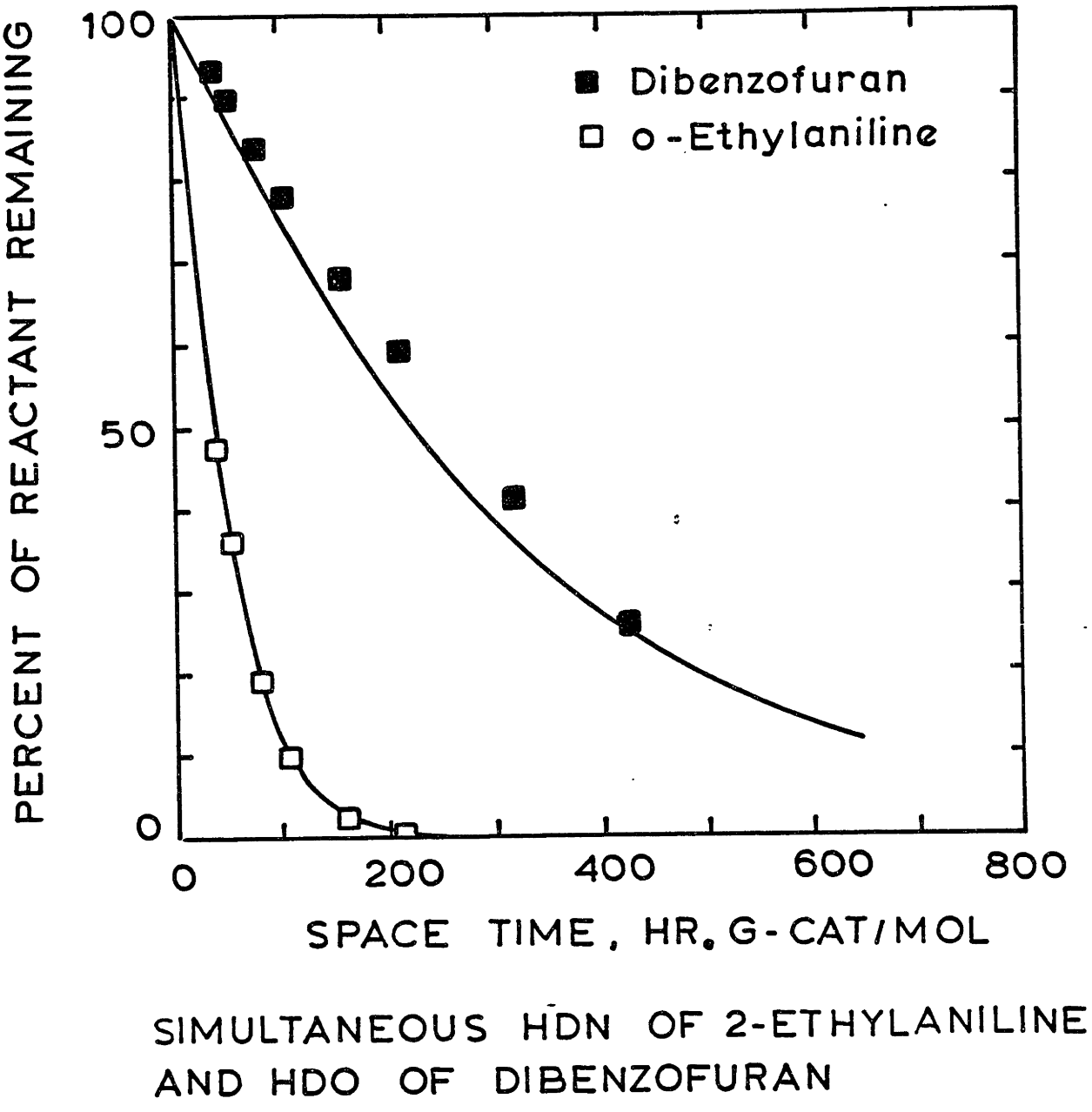

Figure IV.18 Simultaneous HDO of dibenzofuran and HDN of 2-ethylaniline.

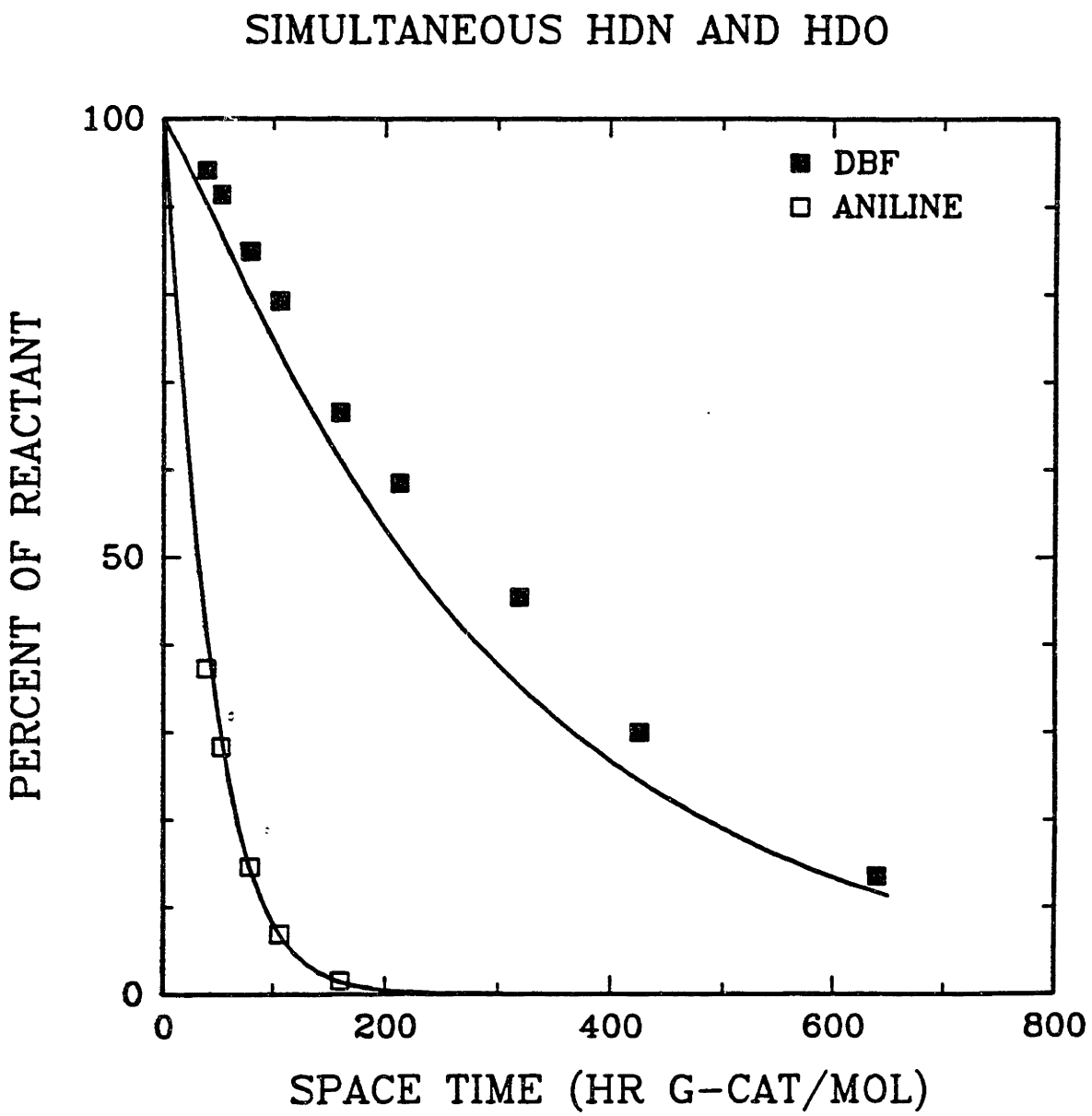

Figure IV.19 Simultaneous HDO of dibenzofuran and HDN of aniline.

$$BzTHQ \rightleftharpoons DHQ \longrightarrow NH_3 + \text{hydrocarbons}$$

No 1,2,3,4-tetrahydroquinoline (PyTHQ) was formed. Here the kinetic expression for the HDO of DBF includes adsorption constants for the three species, BzTHQ, DHQ, and NH_3. The procedure for data analysis was the same as for 2-ethylaniline, except the HDN rate constants were fitted using the HJB method (Himmelblau et al., 1967). Figure IV.20 shows the fitted concentration profiles for the organo-nitrogen species. Inhibiton of HDO is considerably stronger in this case, and the predicted profile for DBF again agrees quite well with the data, again using adsorption constants from the thiophene inhibition study. The kink in the DBF curve at a space-time of about 200, both in prediction and in actuality, is noteworthy. The disappearance of most of the BzTHQ and DHQ is accompanied by a significant increase in the rate of disappearance of DBF as these strongly adsorbed species are removed (recall that this is an integral reactor).

IV.E.2.c Quinoline - HDN of quinoline (Q) involves a significant number of intermediates of considerable stability: 1,2,3,4-tetrahydroquinoline (PyTHQ), 5,6,7,8-tetrahydroquinoline (BzTHQ), decahydroquinoline (DHQ), and 2-propylaniline (OPA), plus NH_3. The reaction network for quinoline used for analysis was identical to that used by Satterfield and Smith (1986) and is shown in Figure I.3. Rate constants for the HDN kinetics, determined by the HJB method, are listed in Table IV.3; the first order rate constant for the HDO of dibenzofuran was again 0.00179 [mol/{hr (g of catalyst) (kPa of DBF)}]. Adsorption constants obtained from the thiophene HDS study were used for the six nitrogen compounds. The hydrocarbons formed from DHQ and OPA are assumed to be weakly adsorbed and are not shown.

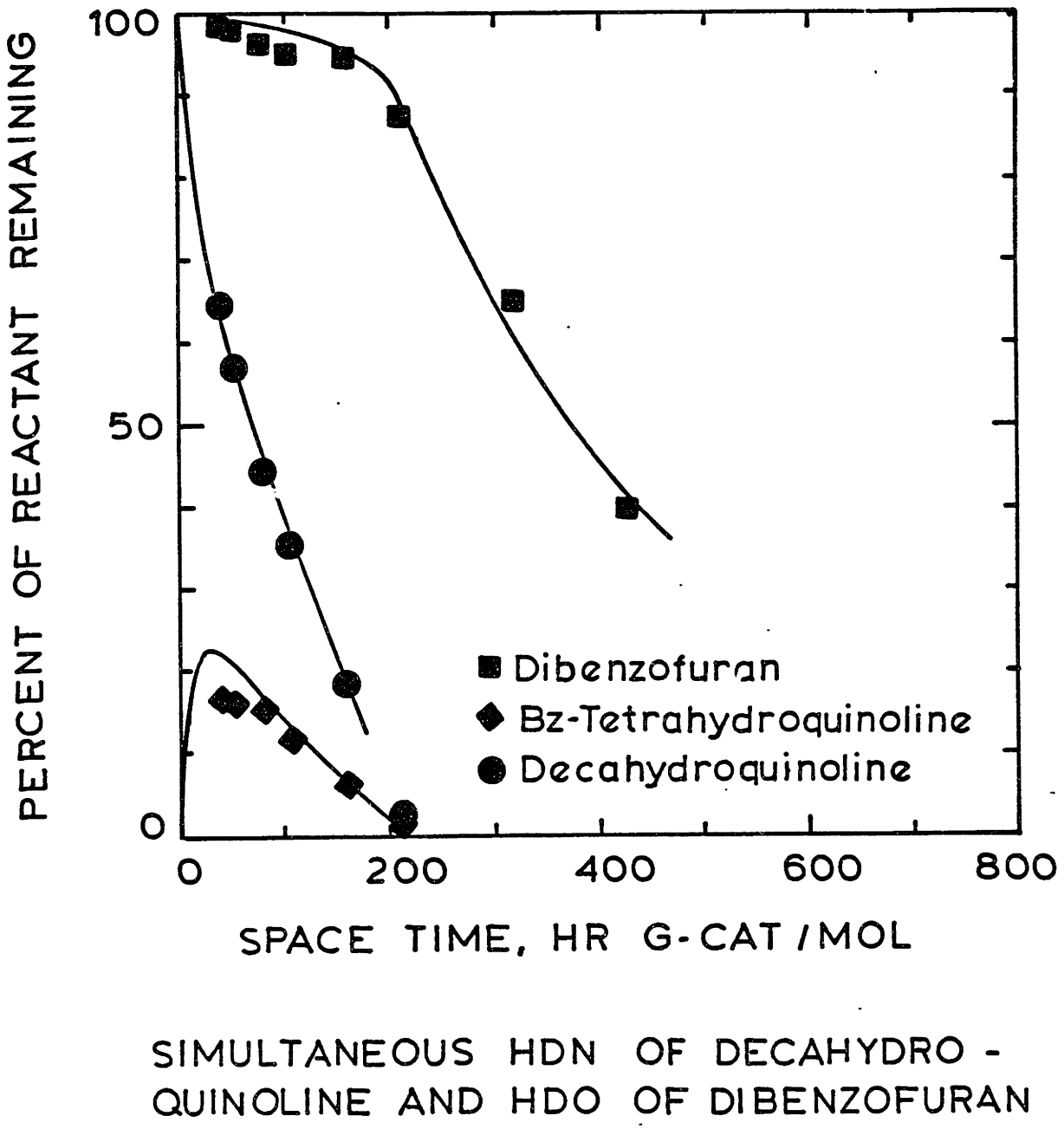

Figure IV.20 Simultaneous HDO of dibenzofuran and HDN of decahydroquinoline.

TABLE IV.3

Rate Constants Used to Model the HDN of Quinoline

Rate Constant	mol/[hr (g of catalyst) (kPa)]
k_1	0.00495
k_2	0.0157
k_3	0.0179
k_4	0.0205
k_5	0.0776
k_6	0.0
k_7	0.0668

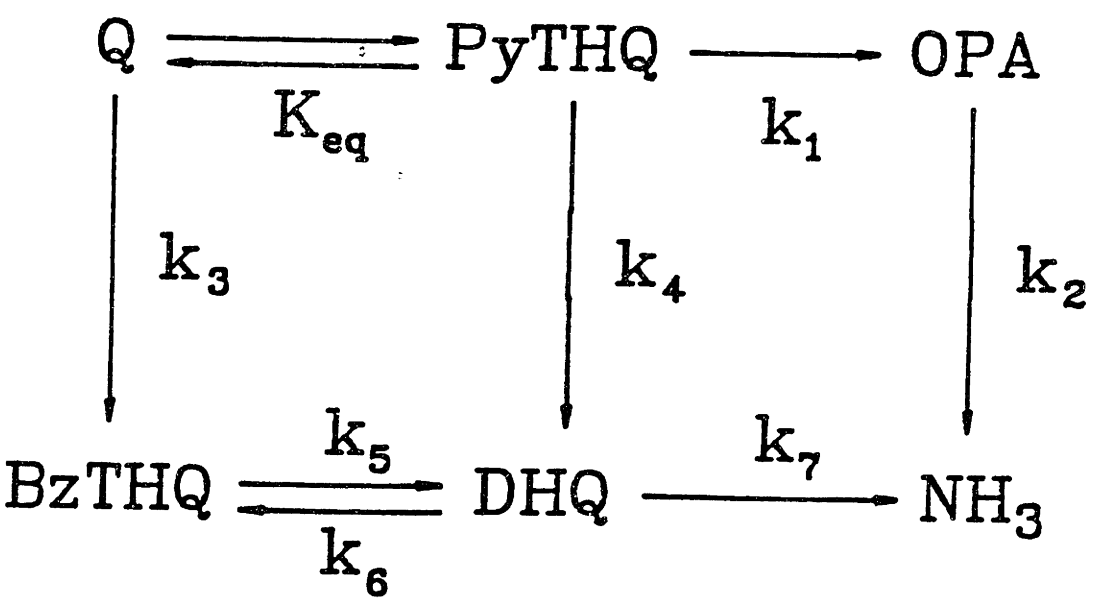

The concentrations of dibenzofuran and the nitrogen intermediates observed are plotted against space time in Figure IV.21. The solid lines represent the predictions of the kinetics model. The kink in the DBF curve is again noteworthy. Allowing for the complexity of the model and of the HDN reactions, the degree of agreement indicates that the relative inhibition produced by the nitrogen intermediates and ammonia is essentially the same for the thiophene HDS and the dibenzofuran HDO reactions. The adsorption equilibrium constants determined from the inhibition of thiophene HDS thus have more general applicability.

Although the presence of nitrogen compounds inhibits the reaction of dibenzofuran, the reactions of the nitrogen compounds are unaffected by the presence of dibenzofuran. Figure IV.22 compares the total extent of quinoline conversion to ammonia (percent HDN) with and without 24 kPa of dibenzofuran being present. The total rate of HDN appears to be identical under both conditions, and this supports the assumption that the adsorption of DBF is negligible compared to that of the organo-nitrogen compounds.

IV.F Use of Temkin Adsorption Isotherm

As noted previously, the adsorption data derived from the thiophene kinetics deviated significantly from the Langmuir isotherm at low concentrations. An alternate model for the adsorption is the Temkin isotherm, which is based on the assumption that the differential heat of adsorption decreases linearly with surface coverage θ. Because of the distribution of energies for the heat of adsorption, the isotherm takes the form:

$$\text{IV.8} \qquad \theta = \frac{RT}{q_o \alpha} \ln (A_o P)$$

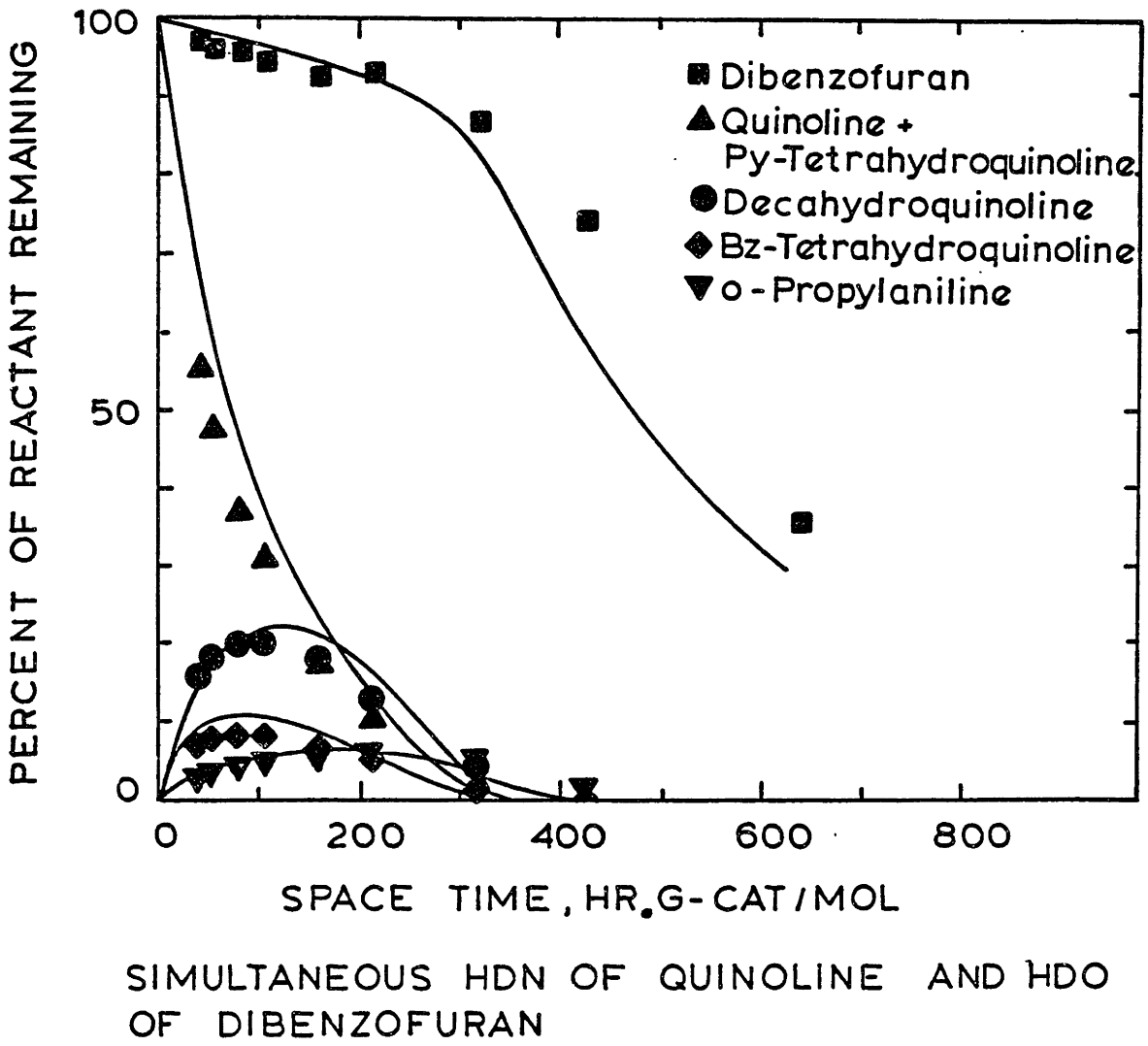

Figure IV.21 Simultaneous HDO of dibenzofuran and HDN of quinoline.

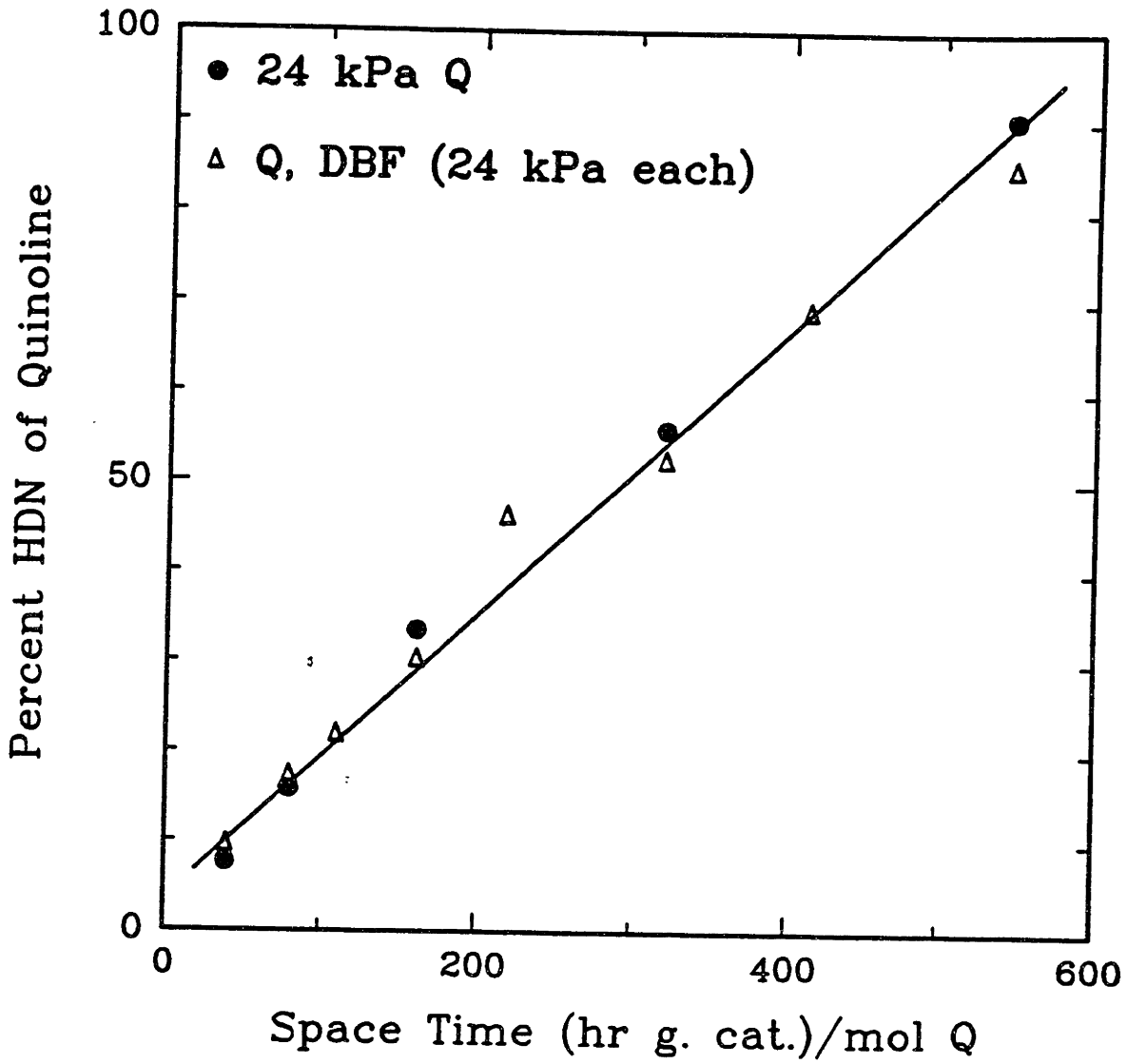

Figure IV.22 The presence of dibenzofuran has no effect upon the overall hydrodenitrogenation rate.

where q_o = differential heat of adsorption at zero surface coverage (Satterfield, 1980). The inhibition data obtained from thiophene HDS kinetics at 300°C (batch 36) are plotted in the form of the Temkin isotherm in Figure IV.23. The linearity of the data indicates that the Temkin isotherm describes the adsorption quite well here, in agreement with Massoth and Miciukiewicz (1986).

From the slope of each isotherm, determined by linear regression of equation IV.8, the quantity $q_o\alpha$ can be derived. For each species, this quantity is plotted against the proton affinity for the same compound (Figure IV.24). Since α is a constant, Figure IV.24 indicates that the differential heat of adsorption at zero coverage, derived from the Temkin isotherm, is proportional to the proton affinity.

IV.G General Discussion

The results showed that nitrogen poisoning of commercial catalysts is severe. Low levels of certain organo-nitrogen compounds poisoned off over 90% of the thiophene HDS activity. Improved catalysts for proceesing high nitrogen content feedstocks will require greater hydrodenitrogenation activity for converting organic nitrogen to ammonia. Although current catalysts have been optimized for sulfur removal, better HDN catalysts may be developed (Hirschon et al., 1987).

Adsorption constants calculated from thiophene HDS poisoning kinetics were also found to be useful in predicting inhibition for other reactions such as the HDO of dibenzofuran. The similarities in extent of poisoning suggest that these two reactions proceed on the same catalytically active site. Since the HDO of dibenzofuran has been shown to proceed mainly through a hydrogenation pathway (Chapter III), this implies that thiophene

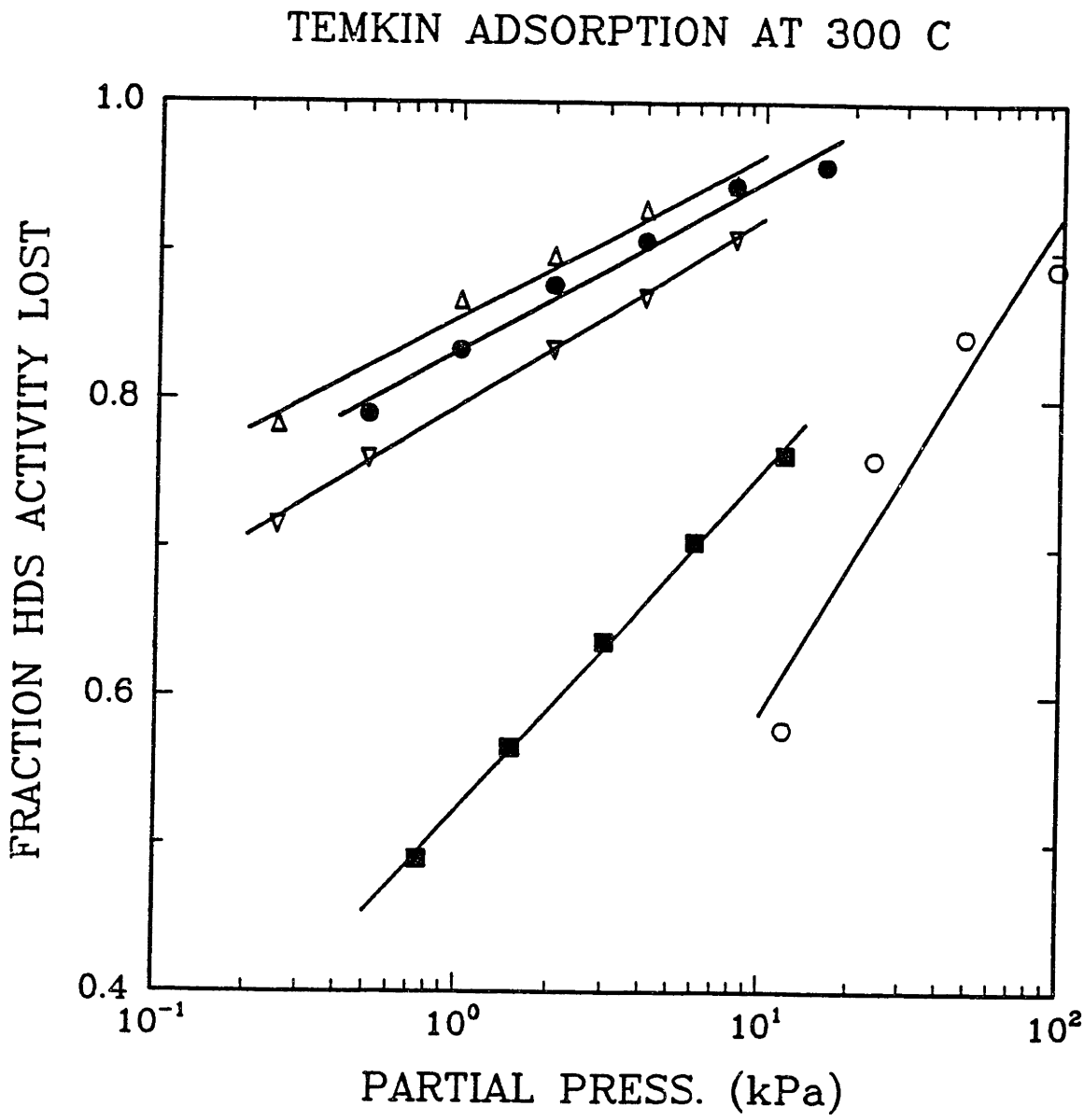

Figure IV.23 The Temkin isotherm provides a good fit for the adsorption of nitrogen compounds at 300 °C.

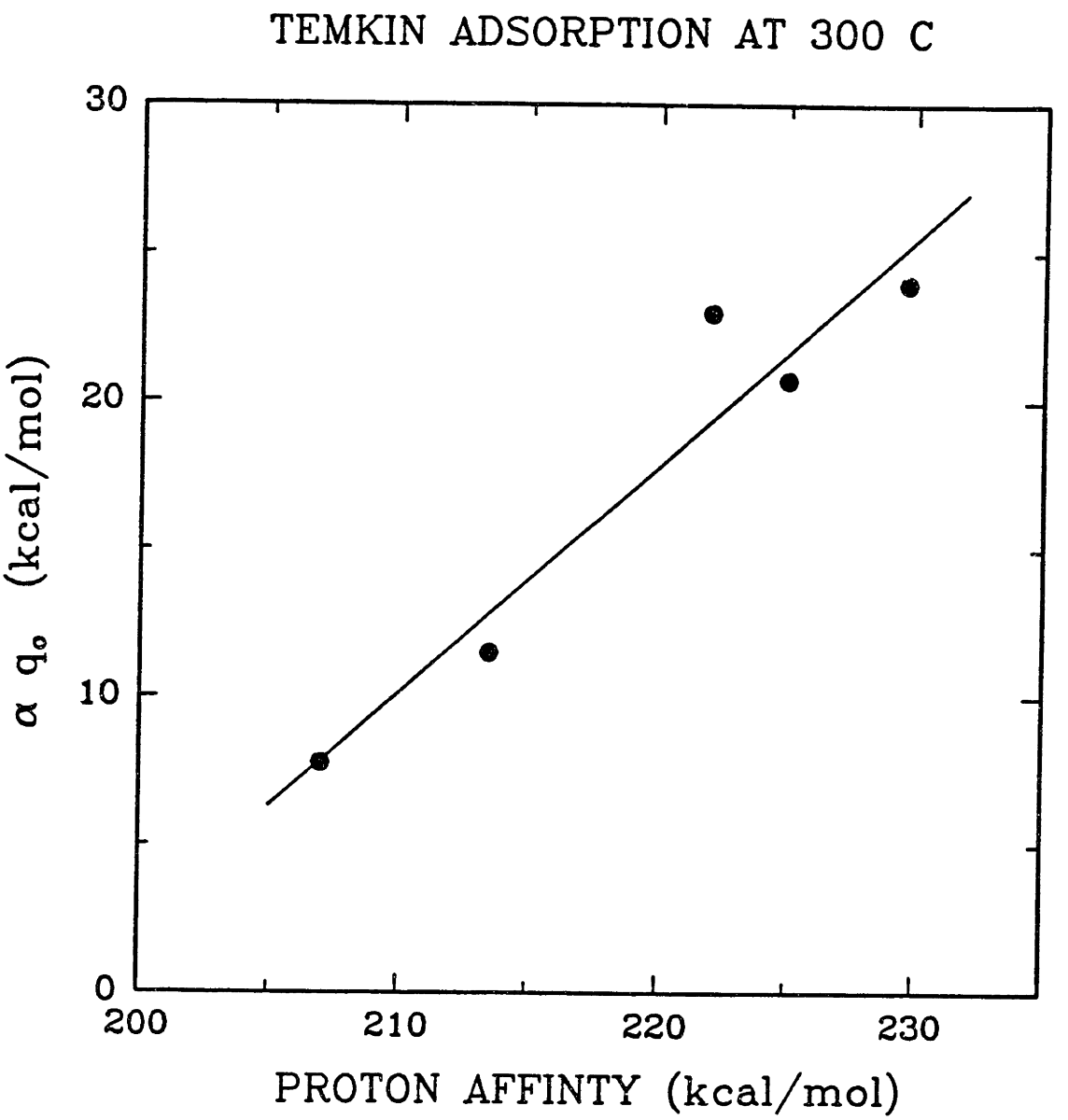

Figure IV.24 Heats of adsorption derived from Temkin isotherms at 300 °C are proportional to the proton affinity.

may also react through an initial hydrogenation. However, some precautions need to be considered before extending these results:

1. Generalization of these effects is most probable for reactions involving relatively simple kinetics and to which a single site competitive adsorption model applies.

2. The correlation of inhibition with proton affinity is most reasonable if the acidity of concern in reaction is of the Bronsted type. However, adsorption of a poison can also occur on Lewis acid sites or on other sites that may be of importance in reaction.

3. Under some conditions adsorption of nitrogen compounds can actually increase the rate of HDS. Miciukiewicz et al. (1984) report that this occurred in the HDS of thiophene when a small concentration of 2,6-dimethylpyridine was present, but not for other N-compounds and not for hydrogenation of 1-hexene. Nagai (1985) reported on enhancement of HDS of dibenzothiophene for certain catalysts and sets of conditions for several N-compounds. In the presence of quinoline, enhancement of the same reaction was observed in this study (see section V.A) at 7 MPa and 260°C, but some inhibition occurred at 360°C.

The relatively close correlation between adsorption strength and proton affinity, which appears to apply to several hydroprocessing reaction systems, suggests that it may be possible to model the inhibition effects encountered with industrial feedstocks. However, it would not be sufficient to use the total nitrogen content of the feed as a predictor of inhibition effects since the relative poisoning is dependent upon molecular structure. Quantitative predictions of reactor performance may require a detailed characterization of the compound classes present in the feed. Alternatively, it might be possible to determine an average proton

affinity for the species present in a feedstock, and to correlate this estimate of adsorption strength with expected performance.

IV.H Summary and Conclusions

1. The inhibition of thiophene HDS by various nitrogen compounds and PAH's was adequately described by Langmuir-Hinshelwood kinetics. Inhibitor adsorption equilibrium constants derived from Langmuir-Hinshelwood kinetics ranged over two orders of magnitude, with basic nitrogen compounds adsorbing most strongly.

2. Adsorption strength of the inhibitors increased in the order: ammonia < aniline < pyridine < piperidine, quinoline. This inhibition order generally agrees with previous studies on the poisoning of hydroprocessing catalysts (Lo (1981), Nagai et al. (1986)). It is interesting to note that a similar order of inhibition has been reported for the poisoning of acidic cracking catalysts (Fu and Schaffer, 1985) (see section IV.I).

3. Ammonia exhibits the weakest adsorption among the nitrogen compounds. This implies that interstage removal of ammonia in a hydrotreater should only be beneficial at relatively high HDN conversions.

4. Adsorption equilibrium constants correlated with gas phase basicity in the form:

$$\ln K \propto (\text{proton affinity}).$$

This relation appears to hold for non-sterically hindered species over a wide range of temperatures (300-400°C). The form of the correlation can be rationalized if the heat of adsorption of an inhibitor varies directly with its proton affinity.

5. Calculated heats of adsorption varied from 10 to 25 kcal/mol and showed an increasing trend with gas phase basicity. The magnitude of the

heats of adsorption indicates that raising the temperature might not be particularly effective in reducing the extent of poisoning. Total nitrogen conversion would increase; however, at the same nitrogen concentrations the adsorption constants would only drop by one half for roughly a 50°C temperature increase.

6. Similar inhibition phenomena were observed for both the HDS of thiophene and HDO of dibenzofuran. The similarities in response to poisoning suggest that these two reactions proceed on the same catalytic site. Langmuir-Hinshelwood kinetics adequately modelled simultaneous HDO and HDN reactions.

IV.I Extension of Poisoning Correlation to Cracking Catalysts

Since the proton affinity is a measure of Bronsted acidity, which involves proton transfer, it should be possible to extend the correlation of adsorption strength with proton affinity to cracking catalysts. Both silica-alumina and zeolitic cracking catalysts possess significant Bronsted acidity and are inhibited by high nitrogen content feeds.

In an early study, Mills et al. (1950) investigated the poisoning of cumene cracking at ~500°C and found that the degree of inhibition produced by the poisons decreased in the order: quinaldine ≅ quinoline > pyridine > piperidine >> decylamine >> aniline. Further experiments with ammonia showed that it was less strongly adsorbed on a silica-alumina catalyst than the organo-nitrogen bases. Voge and co-workers (1951) also reported on the poisoning of decalin cracking at 500°C. The order of inhibition over a silica-zirconia-alumina catalyst decreased in the order: acridine > quinoline >> carbazole > naphthylamine > indole > pyridine > dicyclohexylamine > pyrrole. No poisoning was observed for methylamine, dimethylamine, or ammonia.

The order of inhibition observed in these studies resembles that found here for the HDS of thiophene and shows that a trend may exist with gas phase basicity. Ammonia was found to be weakly adsorbed, and the aromatic heterocyclic nitrogen compounds were found to be the strongest poisons. For the saturated amines, such as piperidine, dicyclohexylamine, and decylamine, the relationship of adsorption strength with gas phase basicity does not appear to hold. However, these saturated molecules may have been cracking at reaction conditions.

Kinetics models of the cracking process have also been adapted to account for poisoning by nitrogen bases. Plank and Nace (1955) modelled the kinetics of cumene cracking in the presence of various poisons and

found a similar order of inhibition: imidazole >> quinaldine > quinoline >> pyridine > piperidine > indole >> butylamine. Maatman et al. (1957) reported on a detailed study of the inhibition of cumene cracking. Langmuir-Hinshelwood kinetics were used to model the poisoning by aromatics, nitrogen compounds, and oxygenates in a differential reactor at 420 and 480°C. This is one of the few studies in which adsorption equilibrium constants were determined from kinetics.

All of the previous work was conducted on amorphous silica-alumina based cracking catalysts. Of current interest is the effect of nitrogen bases on zeolite containing catalysts. Fu and Schaffer (1985) measured the changes in cracking conversion for a gas oil upon the addition of various inhibitors at the equivalent of 0.5 wt % nitrogen. Zeolitic fresh catalysts and refinery equilibrium catalysts were poisoned at 950-1050°F. Table IV.4 compares the proton affinities of the inhibitors with their effect on the conversion of a gas oil cracked over an equilibrium catalyst. The degree of inhibition is seen to increase in the same order as the proton affinity of the molecule, with the results for benzene being a notable exception.

Young (1986) reported on pulsed reaction experiments over a zeolitic cracking catalyst, poisoned with either quinoline or pyridine. Quinoline was found to inhibit the cracking of n-hexadecane significantly more than pyridine, and inhibition was found to be reversible.

Corma et al. (1987) studied the effect of nitrogen bases on the cracking of n-heptane over ultrastable Y zeolite. The order of poisoning was found to be: 2,6-dimethylpyridine (231) > quinoline (228) > pyridine (223), where the numbers in parenthesis represent proton affinities in kcal/mol. From a comparison of the poisoning by the two pyridines, basicity appears to dominate over steric factors. The contrasting low

TABLE IV.4

Inhibition of Zeolitic Cracking Catalysts

Correlates With Gas Phase Basicity

Compound	Proton Affinity (kcal/mol) a	b	c	Conversion vol. %
(none)				58.4
benzene			188.7	51.8
naphthalene			199.8	52.2
anthracene		210.0		54.3
pyrrole	211.6	210.4		54.1
pyrazine		210.8		52.6
aniline	213.5	215.5	213.9	52.7
quinoxiline		217.1		43.2
pyrrolidine	222.0			50.3
pyridine	222.8	222.0	223.6	51.4
piperidine	223.0		230.7	49.5
phenazine		224.8		42.0
quinoline	228.4	227.6		39.2
2,6-di-tert-butyl-pyridine		232.0		34.1
acridine	233.8	233.0		34.7

a (Furimsky, 1982a)
b (Meot-Ner, 1979)
c (Lau et al., 1978)

(from Fu and Schaffer, 1985)

adsorptivity of 2,6-dimethylpyridine on a hydrotreating catalyst can possibly be explained by the work of Benesi (1973). In this study, confirmed by Deeba and Hall (1979), pyridine was found to adsorb to a greater extent on alumina than on silica-alumina, while the opposite ranking of adsorptivity was observed for the sterically hindered pyridine. Benesi (1973) concluded that 2,6-dimethylpyridine was a selective probe for the strong Bronsted acid sites found on silica-alumina and did not adsorb strongly on the Lewis acid sites of alumina.

In the case of a hydrotreating catalyst, Bandyopadhyay et al. (1985) measured the infrared spectrum of quinoline adsorbed on a sulfided Mo/alumina catalyst and found no evidence for the existence of Bronsted acidity. Bronsted acid sites were observed on the oxide form of the catalyst. If the pre-sulfided Ni-Mo catalyst used here possessed only Lewis acidity, the work of Benesi would predict weak adsorption of 2,6-dimethylpyridine as was found.

The studies described above indicate that the degree of poisoning of a cracking catalyst by an inhibitor may depend upon the gas phase basicity of the inhibitor, independent of any steric effects. To determine if a correlation between adsorption strength and proton affinity exists, the data of Maatman et al. (1957) were investigated. Adsorption equilibrium constants determined at 420°C from the kinetics for cumene cracking are plotted against the proton affinites of the same species in Figure IV.25. The linear relationship indicates that a similar correlation as used for the Ni-Mo hydrotreating catalyst applies for a silica-alumina cracking catalyst. The data in Figure IV.25 refers only to nitrogen bases and polyaromatic hydrocarbons; data on the adsorption of oxygenates could not be correlated in this fashion.

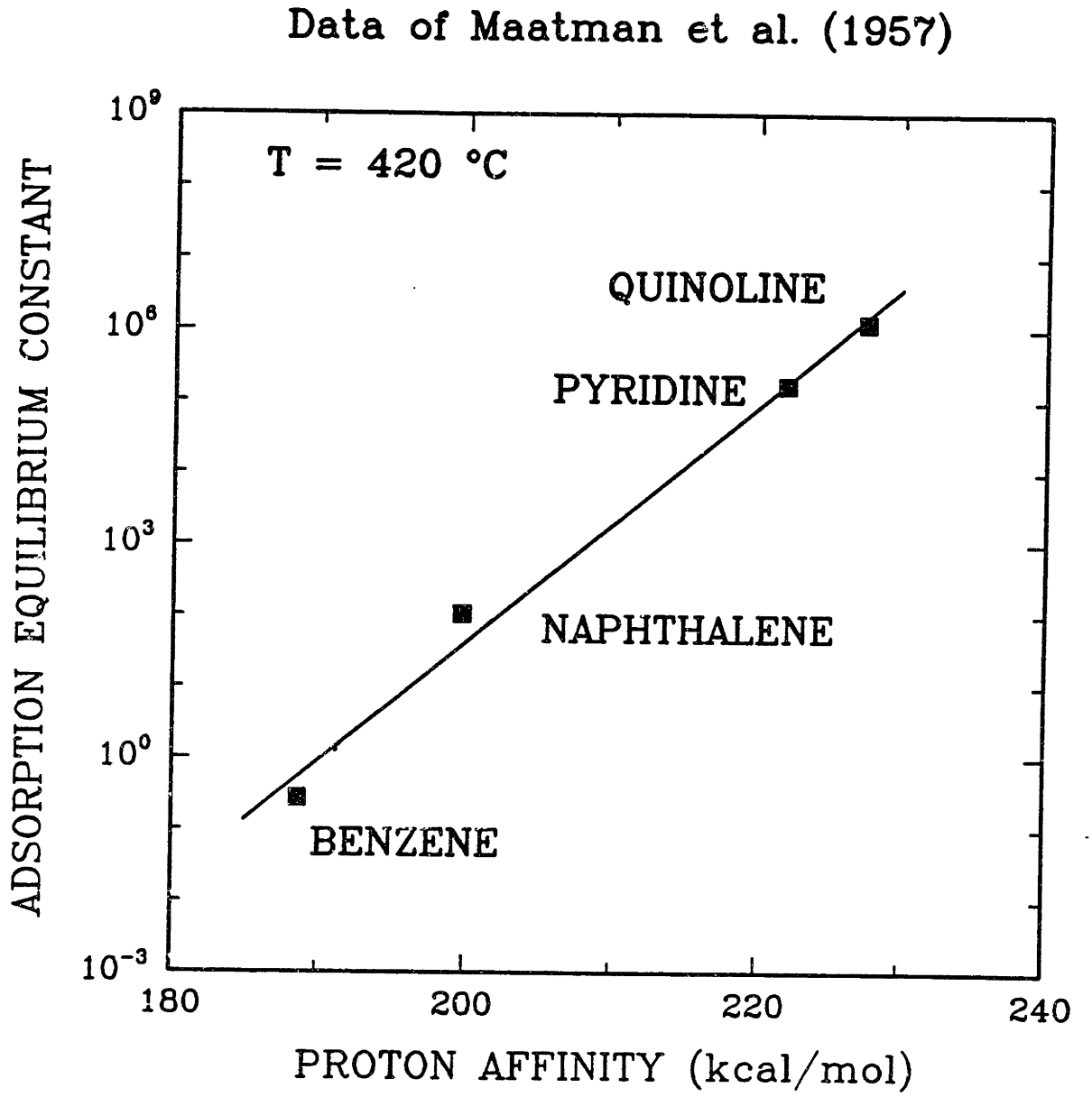

Figure IV.25 Poisoning of cumene cracking over silica-alumina can be correlated with proton affinity.

Chapter V

ADDITIONAL HYDROTREATING STUDIES

V.A Response of Dibenzothiophene Hydrodesulfurization to Presence of Nitrogen Compounds

V.A.1 Introduction

A substantial number of studies have been reported on the hydrodesulfurization (HDS) of dibenzothiophene (DBT), because it has appeared to be representative of HDS reactions of fuels in the mid-distillate range. (Section I.C.1 describes studies (Singal et al., 1981a, b; Houalla et al., 1978; Broderick and Gates, 1981) which also summarize earlier literature.) Nitrogen compounds inhibit the HDS of thiophene and also a variety of other types of reactions such as hydrogenation, hydrodeoxygenation, and cracking. In this light a recent report that nitrogen compounds increased the rate of HDS of dibenzothiophene seemed to us at first sight to be anomalous and it prompted further study.

Specifically, Nagai (1985) reported data showing that the HDS of dibenzothiophene at 220-300°C and 10.1 MPa on a sulfided Ni-Mo/Al_2O_3 catalyst was increased by addition of acridine. The same effect was reportedly obtained with quinoline, pyridine, piperidine, and dicyclohexylamine. It was also observed with a sulfided Ni-W/Al_2O_3 catalyst, but not for a sulfided Co-Mo/Al_2O_3 catalyst. On a sulfided Mo/Al_2O_3 catalyst addition of acridine decreased the HDS rate of DBT at all temperatures.

In this study, utilizing a Ni-Mo/Al_2O_3 catalyst, the addition of quinoline markedly increased the HDS of dibenzothiophene at 260°C and 7 MPa. However, at 360°C it moderately decreased the HDS reaction.

Addition of NH_3 at partial pressures up to 96 kPa had no effect on the rate of disappearance of DBT at 360°C.

V.A.2 Experimental

Two samples of the Ni-Mo/Al_2O_3 (HDS-3A) catalyst, termed batches 26 and 30, were studied at 260 and 360°C respectively. Catalyst batch 26 consisted of 1.6 grams, and prior to the experiments described here, it had been operated for over 1000 hours at 360°C for the study of hydrodeoxygenation reactions. Batch 30 consisted of 20 mg of catalyst.

Dibenzothiophene (DBT) was dissolved in a liquid carrier, either xylene for studies at 260°C or C_{16} paraffin for studies at 360°C, at a concentration of 214 mmol/liter. This produced an initial partial pressure of 21 kPa for DBT at a gas-to-liquid flow ratio of 1520 ml (at STP)/ml liquid, equivalent to 9000 SCF/bbl. All experiments were conducted at a total pressure of 7.0 MPa.

V.A.3 Results

V.A.3.a Quinoline addition at 260°C - A pure DBT solution was first fed at a space time of 580 hr g-cat/mol of DBT and several effluent samples were collected. The hydrocarbon products are biphenyl and cyclohexylbenzene, biphenyl predominating. At 1080 hours on stream (Figure V.1), the feed was switched to one containing 22 mmol/L of quinoline in addition to the DBT. Quinoline is rapidly hydrogenated to 1,2,3,4-tetrahydroquinoline (PyTHQ) in the reactor to produce an initial partial pressure of 2.2 kPa. As shown in Figure V.1, addition of quinoline raised the conversion of DBT from approximately 55% to 97%. Formation of cyclohexylbenzene was completely suppressed. These results agree with the report by Nagai of

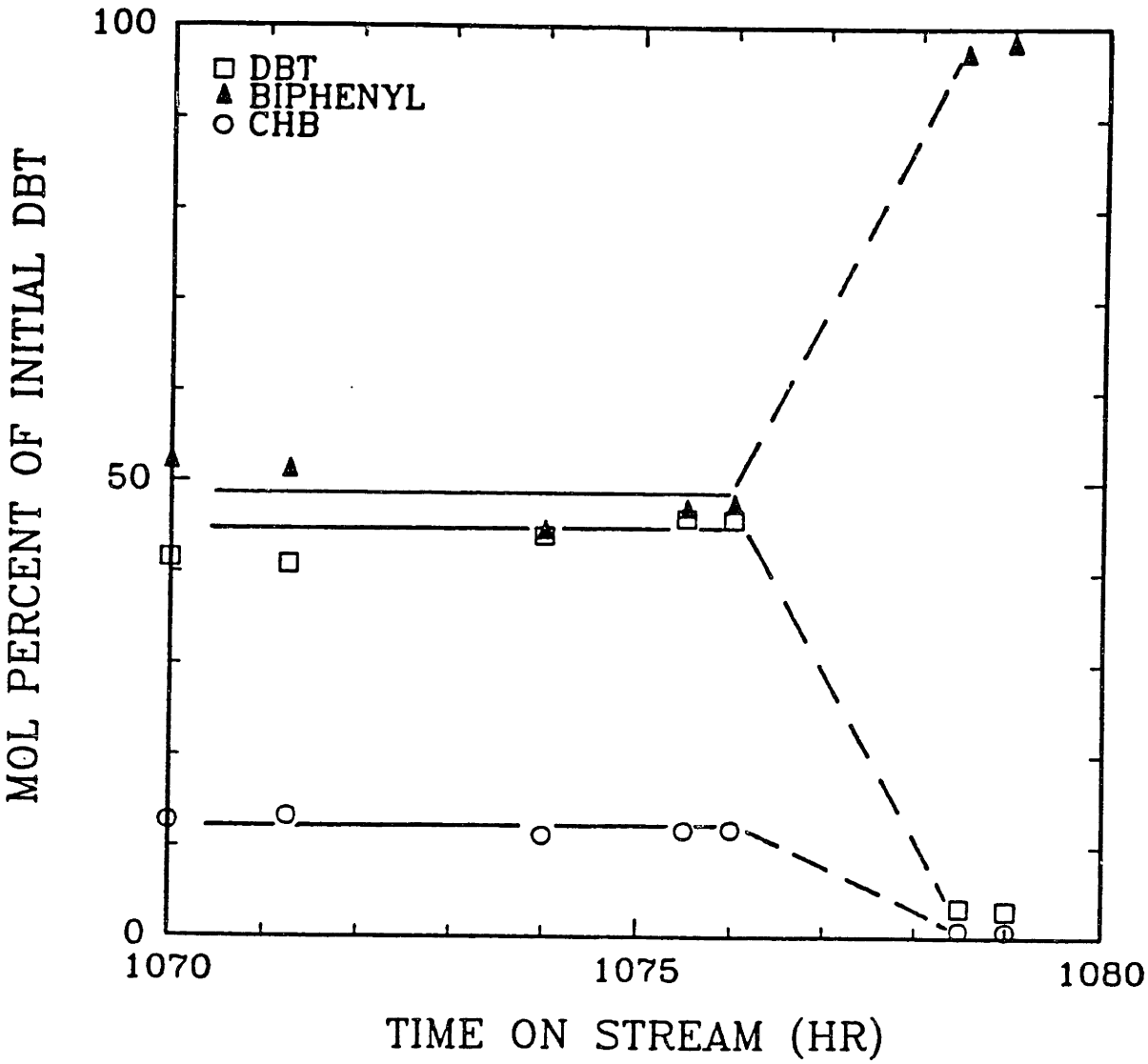

Figure V.1 At 260°C, addition of quinoline substantially increases the rate of hydrodesulfurization of dibenzothiophene. Space-time = 580 hr g. cat/mol DBT.

enhancement upon the addition of 2.2 kPa of acridine, and suppression of cyclohexylbenzene formation.

Figure V.2 shows how conversion and selectivity varied as the partial pressure of PyTHQ, added as such, was altered. The space time here was 170 hr g-cat/mol. The catalyst activity was somewhat greater here than in Figure V.1; this may be the result of raising the reactor temperature to 360°C between the two sets of experiments. The greatest enhancement in conversion was observed at the lowest PyTHQ concentration studied. However, even at 13 kPa, PyTHQ produced some enhancement.

V.A.3.b Ammonia addition at 360°C - The procedure was as before except that anhydrous ammonia was fed directly to the reactor from a high pressure metering pump. At a space time of 2 hr g-cat/mol, the disappearance of DBT remained constant at 40% as the ammonia level was varied from 0 to 96 kPa. Biphenyl comprised 95% or more of the products (Figure V.3). The two minor products identified were cyclohexylbenzene and a species tentatively identified as tetrahydro-DBT, on the basis of retention time on a G.C. column. Formation of both hydrogenated products was suppressed by ammonia.

V.A.3.c Quinoline addition at 360°C - Figure V.4 shows the conversion of DBT over a range of space times in the absence and presence of 24 kPa of added quinoline. At these reaction conditions, 50% of the quinoline was converted to PyTHQ at the shortest space time and equilibrium was attained (approximately 91% PyTHQ) at 4 hr g-cat/mol of DBT. The results indicate that PyTHQ moderately inhibits the rate of DBT hydrodesulfurization at 360°C.

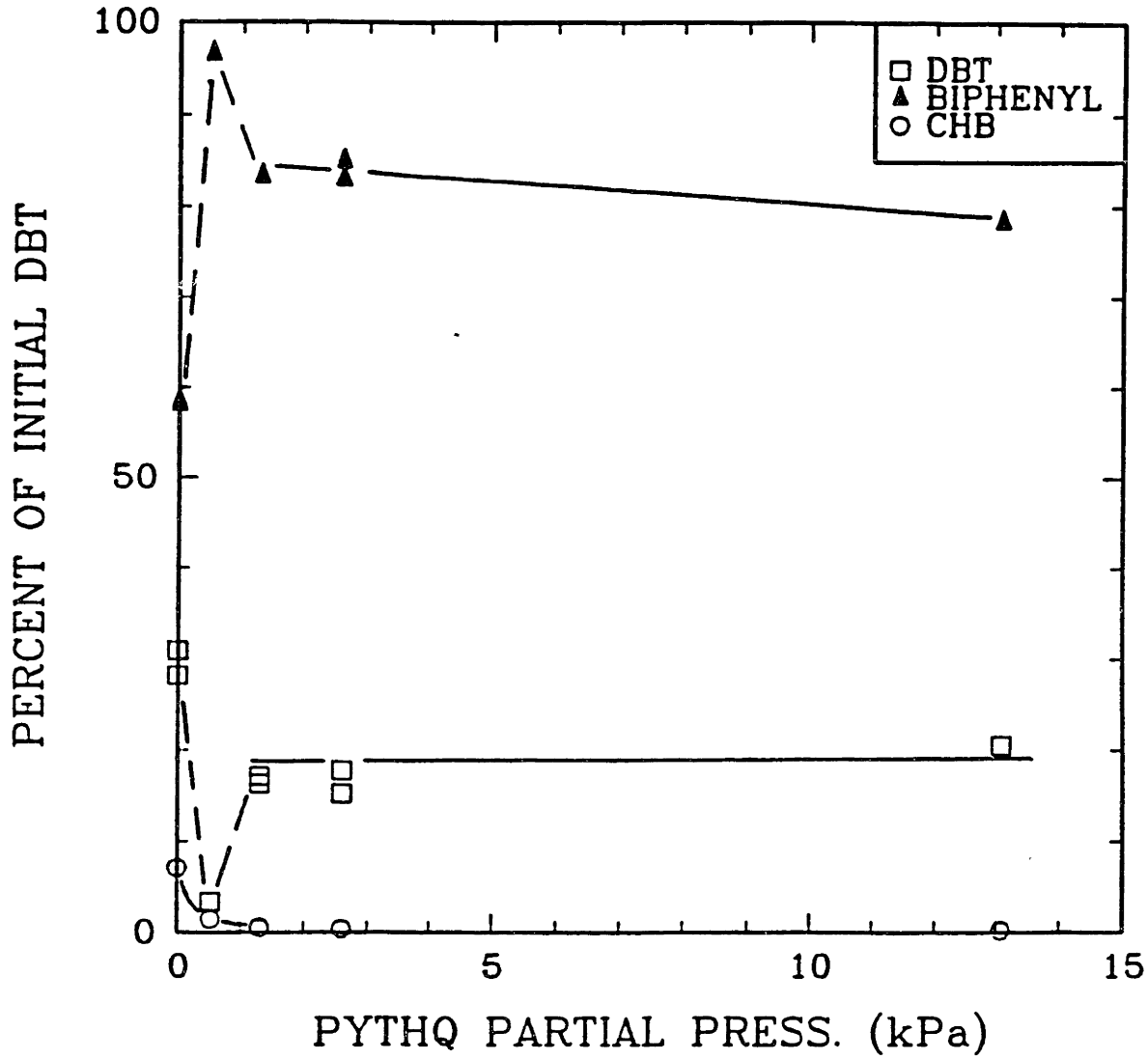

Figure V.2 Effect of partial pressure of 1,2,3,4-tetrahydroquinoline on conversion of dibenzothiophene, 260°C, space-time = 170 hr g. cat/mol DBT.

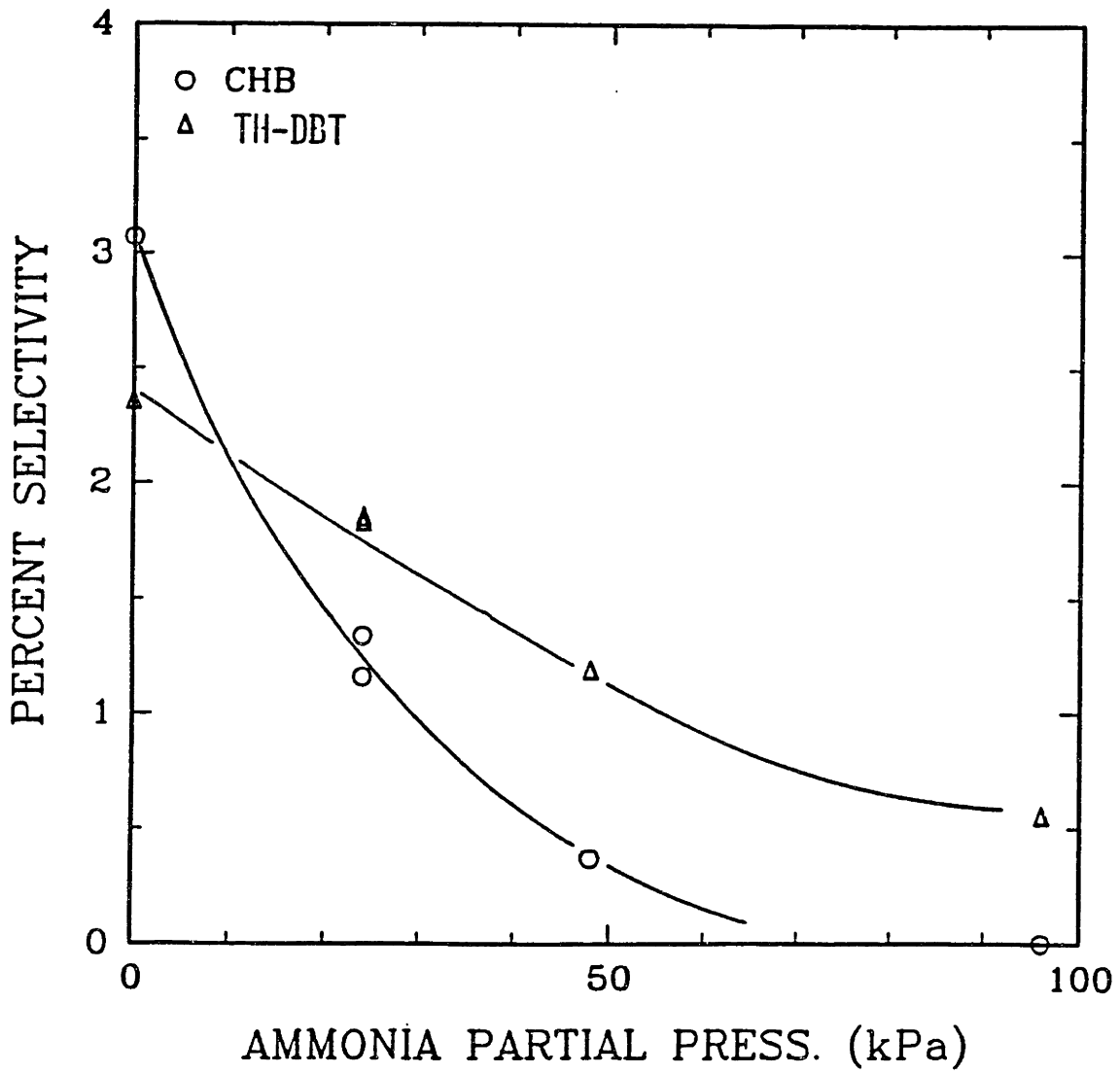

Figure V.3 Increased NH_3 concentration decreases formation of partially hydrogenated products. 360°C.

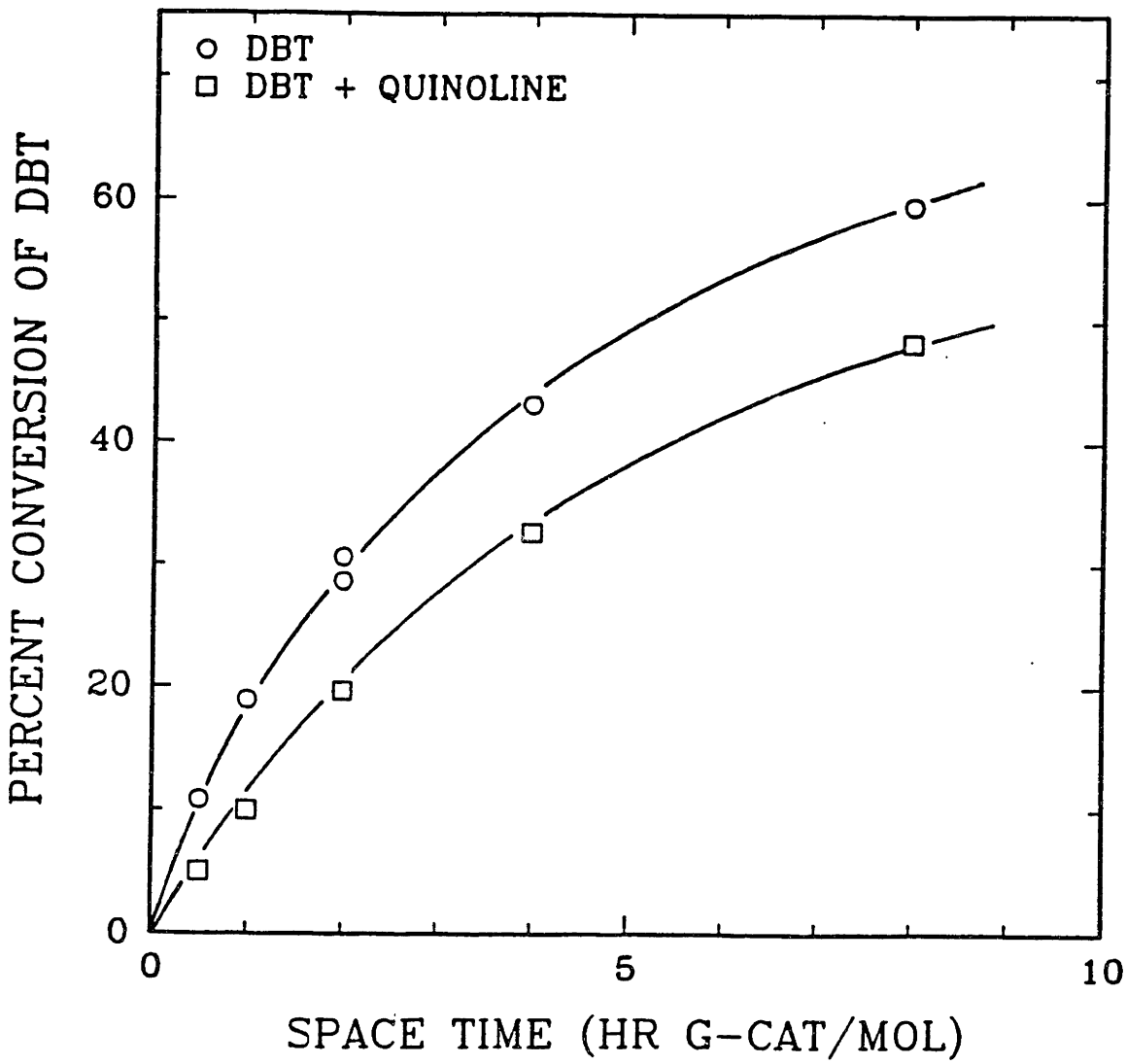

Figure V.4 At 360°C addition of quinoline moderately decreases the rate of hydrodesulfurization of dibenzothiophene.

V.A.4 Discussion

The observed enhancement of the rate of HDS of DBT agrees with the results of Nagai. The effect appears to be complex, since enhancement was observed at 260°C and inhibition at 360°C. Moreover, inhibition of thiophene HDS by various nitrogen compounds has been observed over the entire temperature range of 250-400°C. Considerably more experimentation will be needed to determine which other sulfur and nitrogen compound mixtures may behave similarly.

Clearly the nitrogen compound suppresses hydrogenation, but the mechanism whereby it enhances desulfurization is unclear. A possible explanation may proceed from the kinetic analysis of dibenzothiophene hydrodesulfurization reported by Singal et al. (181b), performed on a Co-Mo/Al_2O_3 catalyst at 285-350°C and 3.1 MPa. The rate of DBT disappearance was described best by the following Langmuir-Hinshelwood expression:

$$(V.1) \qquad -\frac{d\,(DBT)}{dt} = \frac{k\,K_{DBT}\,K_{H2}\,P_{DBT}\,P_{H2}}{(1 + K_{DBT}\,P_{DBT} + K_{prod}\,P_{prod})\,(1 + K_{H2}\,P_{H2})}$$

(See section I.C.1). Their results suggested that reactants and products adsorb strongly, ie., $K_{DBT}\,P_{DBT} + K_{prod}\,P_{prod} > 1$, that more than one product was involved and their heats of adsorption varied differently with temperature. The ratio K_{DBT}/K_{prod} varied from about 0.045 at 300°C to about 0.2 at 350°C. Plausibly the adsorption of quinoline decreases the adsorption strength of DBT products (possibly also that of DBT) thus permitting an enhanced rate of reaction. In accordance with theory, inhibition effects from competitive adsorption would be expected to diminish with increased temperature. This would account for the marked enhancement with quinoline addition observed here at 260°C and the inhibition observed at 360°C.

Among the products which might cause the inhibition, H_2S is a likely candidate. Broderick and Gates (1981) showed that inhibition of the HDS of DBT by hydrogen sulfide was quite significant and that the degree of inhibition produced decreased markedly with temperature. Figure V.5 shows that addition of H_2S as a thiol at reaction conditions of 260°C, 7 MPa, and a space time of 342 hr g-cat/mol of DBT indeed produces strong inhibition.

Aside from the mechanism, it is significant that under a limited set of circumstances a proper balance of certain nitrogen compounds to certain heterocyclic sulfur compounds may permit hydrodesulfurization to be carried out with lower hydrogen consumption and increased rate.

V.B Silica-Alumina Supported Catalyst

A few experiments were also carried out on a Ni-Mo catalyst having a silica-alumina support (Cyanamid's MHC-110) and termed Batch 29. This catalyst was pre-sulfided in the usual manner and deactivated at 360°C with a feed containing dibenzofuran and C_{12} thiol.

Over this catalyst, at 360°C and 7 MPa, a significant fraction of the C_{16} paraffin solvent cracked to lower molecular weight material. Little cracking of the solvent is observed at this temperature with a Ni-Mo/alumina catalyst. At 400°C and a liquid flow rate of 0.68 ml/min, approximately 6% of the C_{16} was cracking over MHC-110. Addition of 24 kPa of ammonia almost completely eliminated cracking of the paraffin.

The activity of MHC-110 for the HDO of dibenzofuran was compared to the activity of batch 28 (HDS-3A). Both catalysts had been deactivated with dibenzofruan in the presence of H_2S. Catalyst activity was measured at 360°C, 7 MPa total pressure, and an H_2S partial pressure of 7 kPa. On batch 29 the first-order rate constant for DBF hydrodeoxygenation

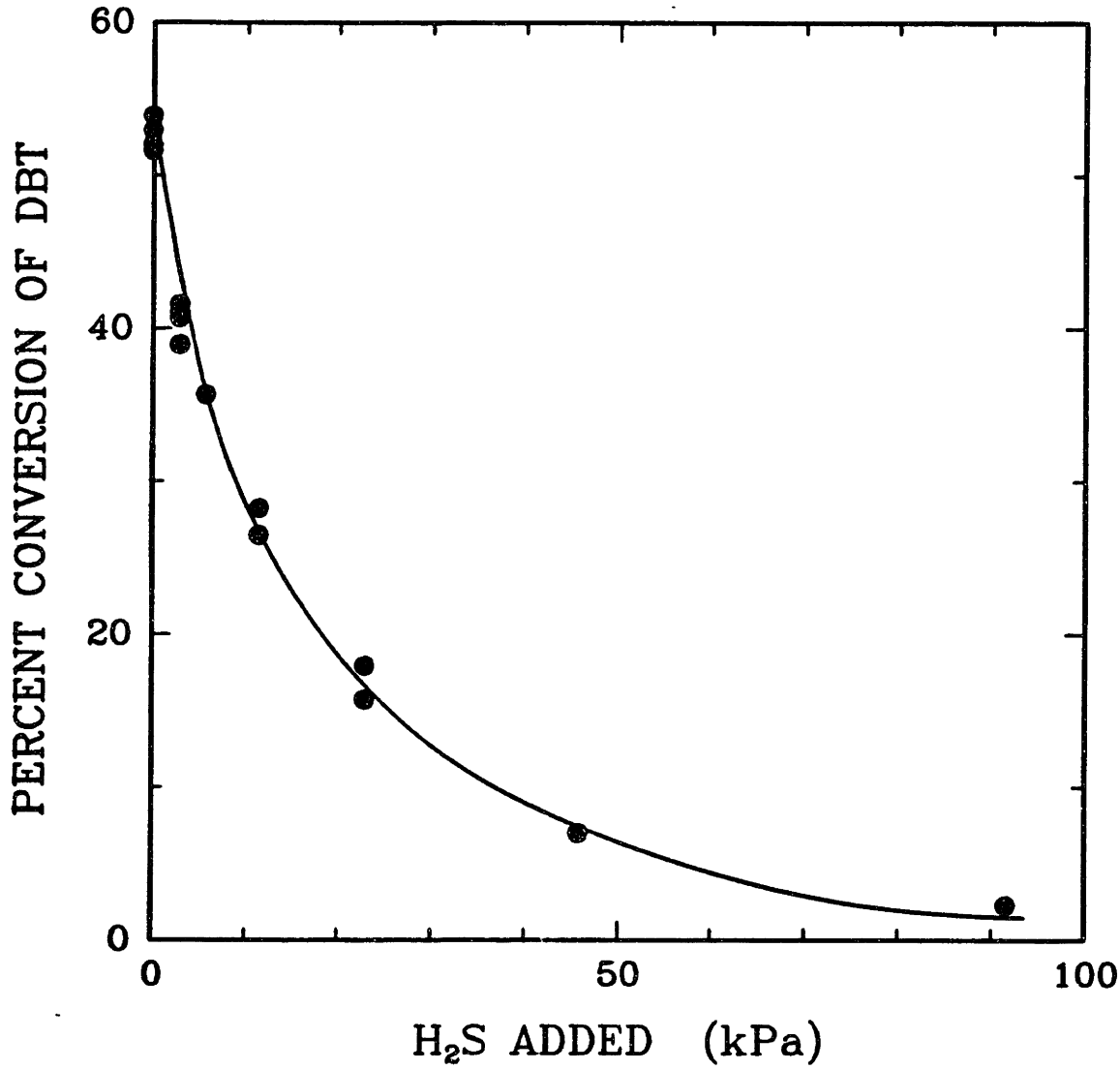

Figure V.5 Addition of hydrogen sulfide strongly inhibits the HDS of dibenzothiophene at 260°C.

(measured at 408 hours on stream) was 0.00550 mol/hr g. of catalyst. This is significantly lower than the rate constant measured on batch 28 after 330 hours on stream (0.00742 mol/hr g. of catalyst).

An experiment was also run to compare the activity of the catalyst for the hydrodenitrogenation of quinoline. Figure V.6 shows that during the simultaneous HDN of quinoline and HDO of dibenzofuran at 360°C and 7 MPa, conversion of both reactants was lower over catalyst MHC-110 than over HDS-3A. (Q + PyTHQ refers to the equilibrium mixture of quinoline and 1,2,3,4-tetrahydroquiniline which rapidly forms under reaction conditions). Similarly, under the same conditions of simultaneous HDN and HDO, the total rate of nitrogen removal from quinoline was lower over the silica-alumina supported catalyst (Figure V.7).

V.B.1 Discussion

The Ni-Mo/SiO_2-Al_2O_3 catalyst exhibited a lower activity for the HDO of dibenzofuran than did a similar alumina supported catalyst. Quinoline HDN activity in the presence of dibenzofuran was also lower over MHC-110. The results suggest the silica-alumina support does not enhance these hydrotreating reactions. This catalyst does appear to possess some cracking activity, as evidenced by the production of lower molecular weight products from paraffins. However, most of the cracking activity was poisoned by the presence of nitrogen compounds.

V.C HDN-60 Catalyst

The HDO of dibenzofuran was also studied briefly on a recently manufactured Ni-Mo/Al_2O_3 catalyst (Cyanamid's HDN-60), termed Batch 34. This "rifled" catalyst was crushed to the standard size range, and the uncrushed pellets had the properties listed in Appendix A1.

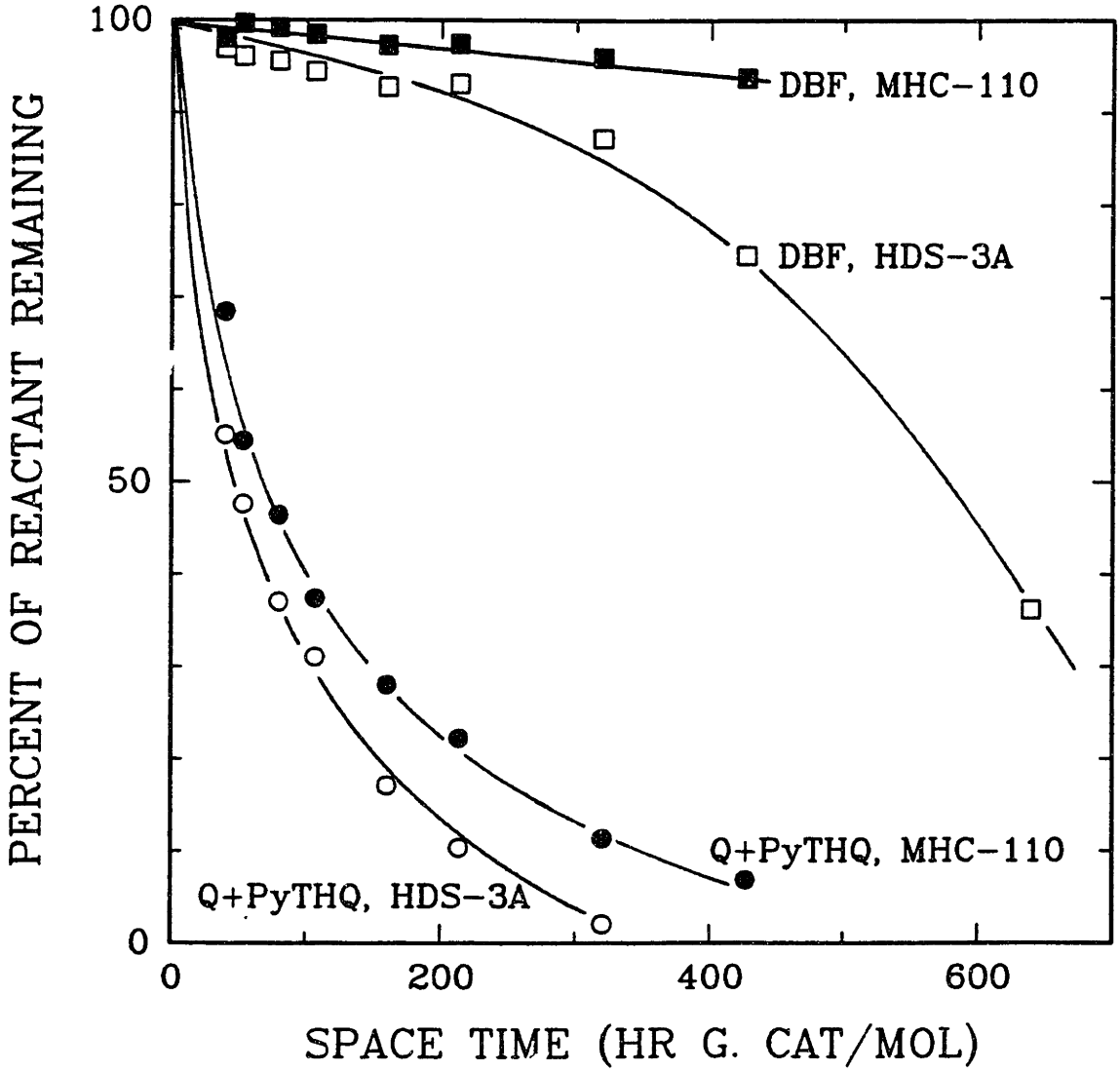

Figure V.6 HDS-3A produces higher conversions of quinoline and DBF than MHC-110.

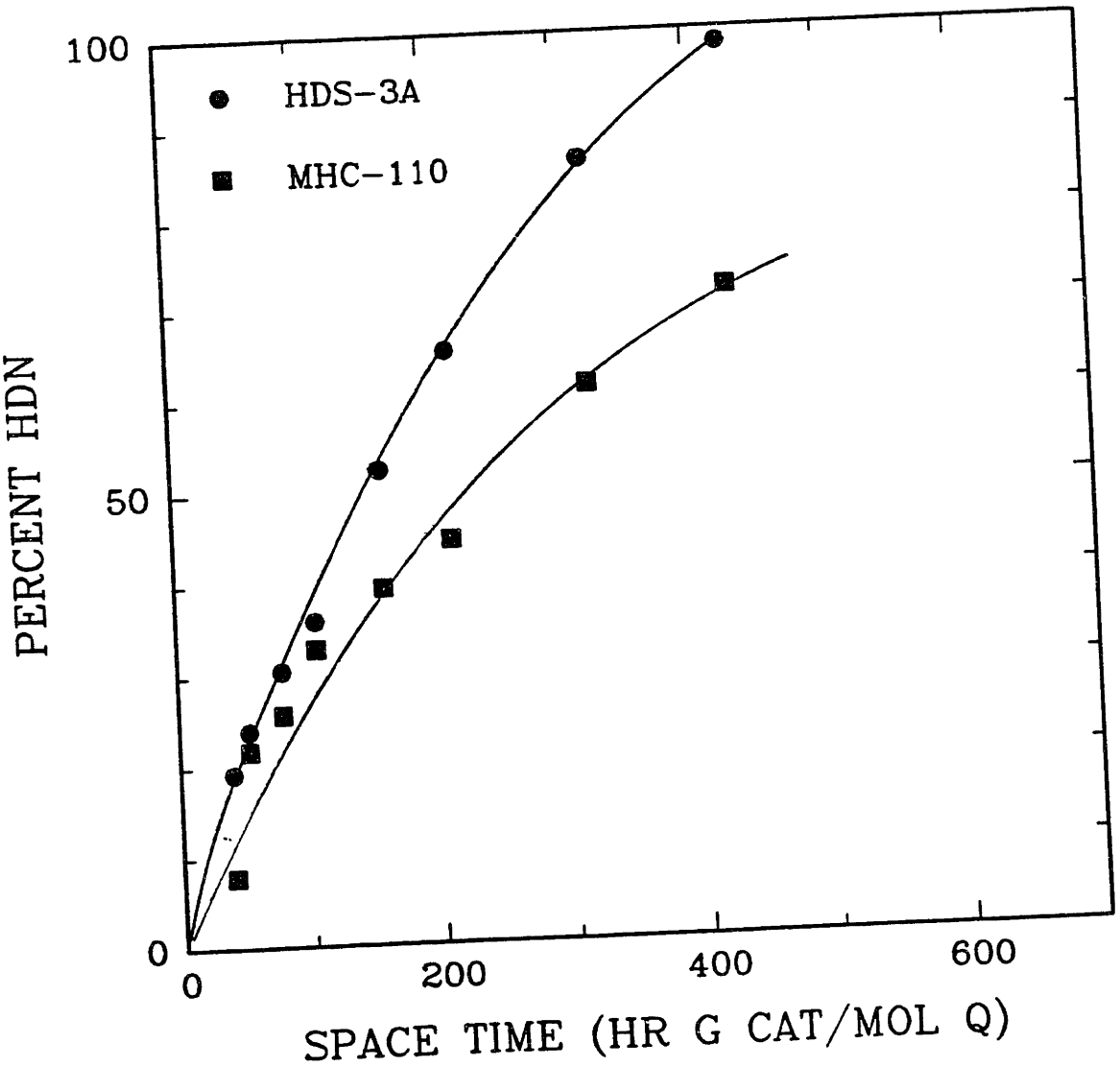

Figure V.7 Total conversion of nitrogen is lower over MHC-110 than over HDS-3A.

The HDO of dibenzofuran was measured over this catalyst at 360°C, 7 MPa total pressure, 12 kPa of H_2S, and a space time of 160 hr g. catalyst/mol of DBF. Table V.1 shows that the product distribution on this catalyst was almost identical to that found over the HDS-3A Ni-Mo/Al_2O_3 catalyst.

V.D Effect of Hydrogen Sulfide on Quinoline HDN

It has been shown in section III.B.2 that the catalytic activity and selectivity for the HDO of dibenzofuran adjusted to the H_2S concentration according to two different time scales. Removal of H_2S caused an immediate change in selectivity and enhancement in conversion, while continued reaction in the absence of H_2S resulted in a slow decline in activity lasting for hours. The experiment described here tested the response of the catalyst to H_2S as measured by the activity and selectivity for the hydrodenitrogenation of quinoline.

It has been found that higher H_2S concentrations increase the total conversion of quinoline to ammonia and hydrocarbons (see Figure V.10). Reaction selectivity also varies, with hydrogenolysis rates increasing and hydrogenation rates decreasing with higher H_2S partial pressures (Satterfield and Gultekin, 1981). This change in selectivity increases the concentration of 2-propylaniline (OPA) and decreases the concentration of decahydroquinoline (DHQ), making the ratio of these two species useful as a measure of selectivity.

Experiments were run on pre-sulfided Ni-Mo/Al_2O_3 (Batch 26) at 1050 hours on stream. Quinoline in C_{16} was fed at a space time of 40 hr g. of catalyst/mol of quinoline. Reaction conditions were 390°C, 7 MPa total pressure, and a feed ratio of 9000 SCF H_2/bbl. Hydrogen sulfide partial pressure was varied by changing the feed rate of C_{12} thiol to the reactor

TABLE V.1

Comparison of the Products from the HDO of Dibenzofuran

Produced over Two Ni-Mo/Al_2O_3 Catalysts

Product	Percent Selectivity on Catalyst HDS-3A	HDN-60
C_{12} (double-ring) products	28	28.4
biphenyl		2.6
cyclohexylbenzene		11.8
CPMB		2.6
DCH		4.3
CPMCH		7.1
Single-ring products	72	70.5
cyclopentene	7	5.8
methylcyclopentane	9	7.6
cyclohexane	50	52.6
benzene	3.6	4.5
methylcyclohexane	2.5	}not separated
cyclohexene		

using the ISCO pump, filled with pure thiol. Under these conditions representative reaction samples could be collected within 11 minutes.

Prior to the experiment pure hydrogen alone was fed over the catalyst for 2 hours. As shown in Figure V.8, varying the H_2S partial pressure rapidly from 3 to 48 kPa produced no change in the total nitrogen conversion to ammonia (percent HDN). Under steady state conditions the percent of HDN would be higher in the presence of 48 kPa of H_2S.

However, reaction selectivity was significantly affected, with the ratio of OPA to DHQ varying by almost a factor of ten (Figure V.9). We see that as in the case of dibenzofuran, the effect of H_2S follows two time scales. Product selectivity rapidly adjusts to the H_2S partial pressure. Long-term exposure of the catalyst (on the order of hours) to a specific H_2S concentration produces differences in the percent HDN.

V.E Effect of Ammonia on Quinoline HDN

A comparison of the adsorption constants for ammonia and organo-nitrogen compounds (as determined in Chapter IV) would indicate that ammonia should have little effect upon the HDN of quinoline. An experiment was therfore carried out to test this premise.

Two feeds were prepared which contained 0.122 mol/liter of quinoline in C_{16} (equivalent to 12 kPa in the reactor) and to one feed was added 0.122 mol/liter of pentyl amine. The amine reacts rapidly at reaction conditions to produce ammonia. The quinoline was fed at a space time of 640 hr g of catalyst/mol of quinoline over Batch 26. Reaction conditions were 360°C and 7 MPa total pressure. H_2S was produced in situ by feeding C_{12} thiol directly to the reactor using the ISCO pump. H_2S partial pressure was varied over a substantial range from 0 to 96 kPa.

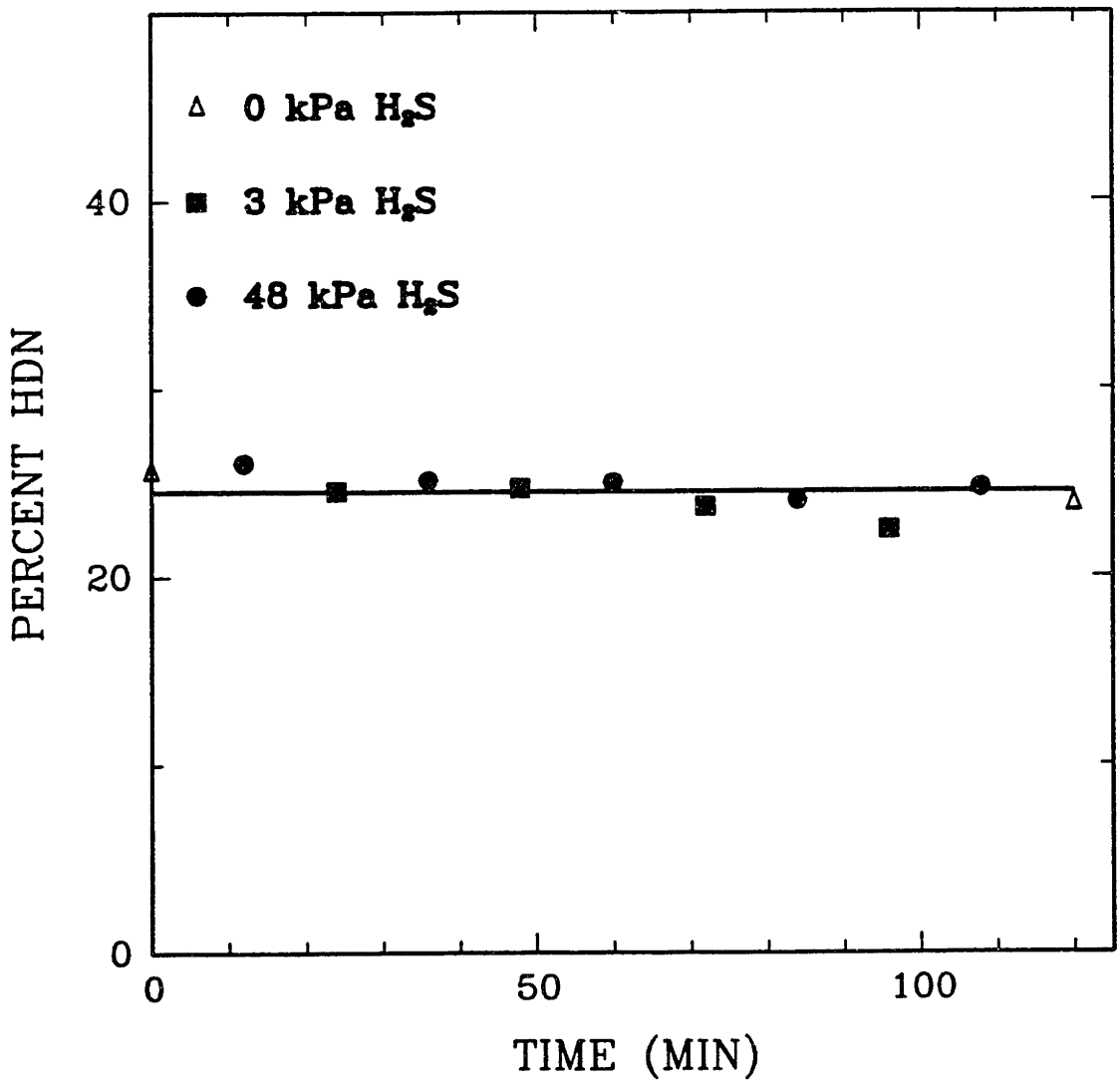

Figure V.8 Conversion of quinoline is unaffected by rapid changes in H_2S concentration.

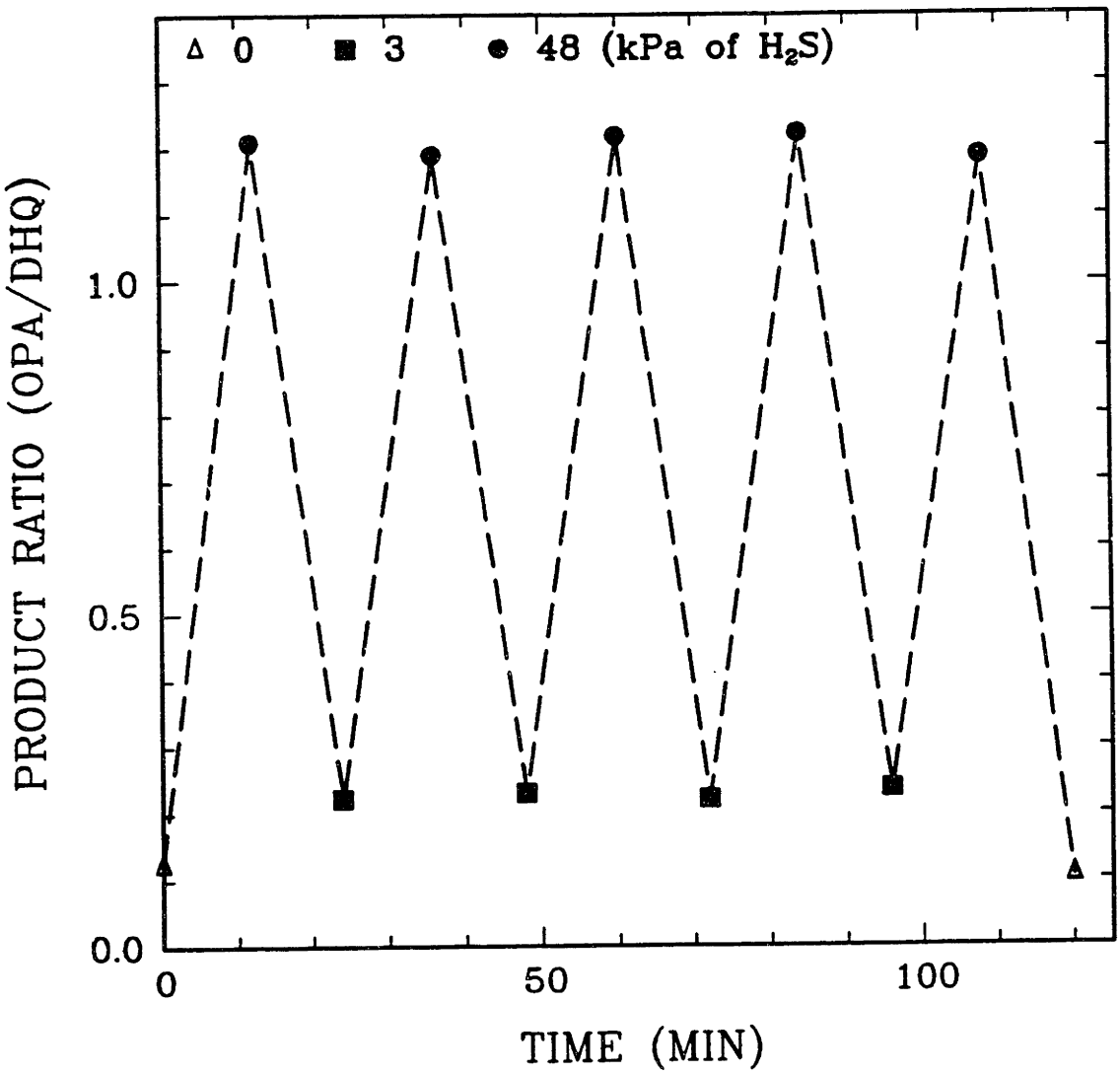

Figure V.9 Catalyst selectivity in the HDN of quinoline responds rapidly to H_2S partial pressure.

Figure V.10 shows that increasing the H_2S partial pressure increased the percent HDN with quinoline fed alone and with an equimolar feed of amine. As expected the addition of relatively weakly adsorbed ammonia has very little effect upon the conversion of quinoline.

V.F Purification of Phenanthrene

The phenanthrene available from chemical supply houses is produced from coal tar and generally contains dibenzothiophene as the chief impurity. Use of the phenanthrene as a reaction solvent would be unacceptable where the the sulfur compound could deactivate the catalyst (as in slurry Fischer-Tropsch synthesis). A brief study was therefore carried out to determine if selective reaction could remove the dibenzothiophene at a reasonable cost.

Purification of the phenanthrene is difficult because of the similar physical properties of phenanthrene (m.p. 99-101°C, b.p. 340°C) and dibenzothiophene (m.p. 97-100°C, b.p. 332-333°C). Purification can be achieved with zone refining but at a prohibitive cost. An alternative method of purification involves hydrodesulfurization of dibenzothiophene (DBT) over a conventional hydrotreating catalyst. This would convert the DBT to higher volatility hydrocarbons which can be removed by distillation. Unfortunately, significant hydrogenation of phenanthrene also occurs. However, previous experiments with a pre-sulfided Ni-Mo/Al_2O_3 catalyst have shown that nitrogen poisoning can inhibit the hydrogenation of phenanthrene and enhance the hydrodesulfurization of DBT under certain conditions (see sections V.A and VII.C.3).

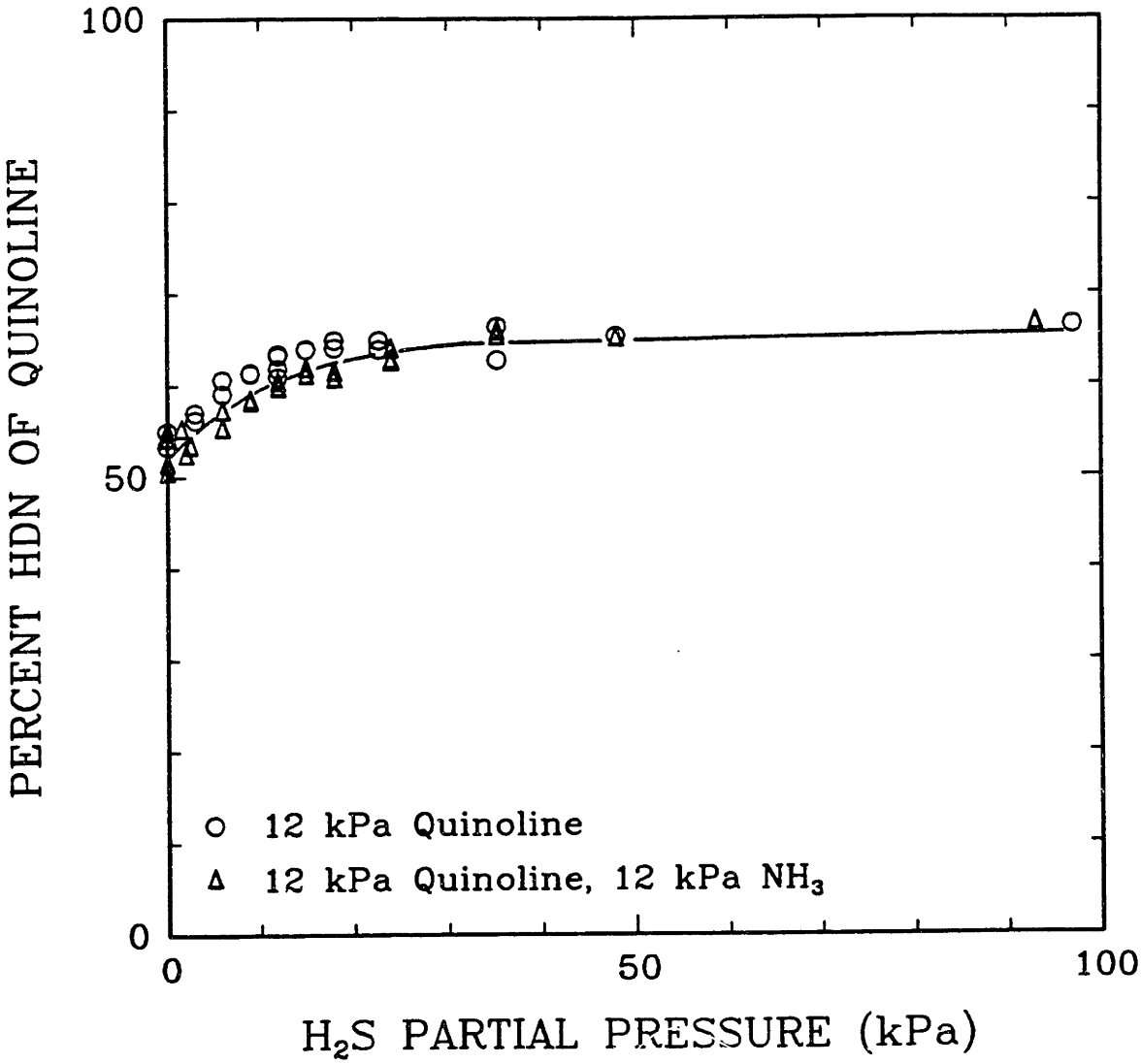

Figure V.10 Ammonia addition does not affect quinoline conversion; H_2S addition increases total HDN conversion.

V.F.1 Experimental results

The phenanthrene (98%) was purchased from Aldrich Chemical Company, and it contained approximately 1 wt% dibenzothiophene (1700 ppm of sulfur). Purification was carried out over a sample of HDS-3A at 250°C and 3.5 MPa of hydrogen. The phenanthrene was dissolved in C_{14} paraffin at a concentration of 50 g/liter. (C_{16} paraffin appeared to form an azeotrope with the phenanthrene when a distillation of their mixture was attempted.) The catalyst was poisoned by adding 24.2 ml/liter of piperidine to the phenanthrene feed. Feeds to the reactor consisted of 0.68 ml/min of liquid and 1030 ml at STP/min of hydrogen.

In the absence of a nitrogen poison, 80% of the phenanthrene was hydrogenated under these conditions. Addition of piperidine to the system kept the conversion of phenanthrene below 2.5%. Both with and without a nitrogen compound no dibenzothiophene was detected in the products by gas chromatography. For this specific case poisoning of the catalyst with a nitrogen compound greatly improved the reaction selectivity.

Chapter VI

SOME EFFECTS OF VAPOR-LIQUID EQUILIBRIA ON PERFORMANCE OF A TRICKLE BED REACTOR

VI.A Introduction

Trickle bed reactors utilized in the petroleum industry for hydrotreating and hydrocracking are commonly operated under conditions in which the liquid feed partially vaporizes. The resulting distribution of reactants, products and inert species between the liquid and vapor phases can affect reaction selectivity, mask the intrinsic kinetics and alter the observed activation energy. Thus the common practice industrially of gradually increasing the operating temperature of a trickle bed reactor to compensate for catalyst deactivation, so as to maintain a constant conversion at fixed LHSV, alters vapor-liquid equilibria and can have consequences on reactor performance not immediately obvious. Likewise, changing the hydrogen recycle rate can alter the extent of feed vaporization and the exit conversion. These effects may also be seen when feed physical properties are changed or when laboratory results in a trickle bed reactor are compared to those in an autoclave.

Some of the consequences of varying reactor operating conditions are investigated here using two different model reactions carried out in a laboratory trickle bed reactor. Data are presented for reactants and liquid feeds of different volatilities, and the results are compared to theoretical predictions obtained from a reactor model which explicitly accounts for the distribution of species between phases.

The two reactions studied were the hydrodeoxygenation of dibenzofuran (b.p. 285°C) and the hydrogenation of n-butylbenzene (b.p. 183°C),

dissolved in either n-hexadecane (b.p. 287°C) or in squalane (b.p. 350°C). The reaction of dibenzofuran (DBF) exhibits overall second order kinetics in the vapor phase, first order in both reactant and hydrogen, and all oxygenated intermediates are more reactive than DBF so that a one step reaction model can be used (LaVopa and Satterfield, 1987). For the reaction of butylbenzene (BBz), the analogous reaction of propylbenzene has been reported to exhibit first order kinetics in the vapor phase with propylcyclohexane as the only product (Gultekin et al., 1984). Here the reactions of DBF and BBz in the liquid phase were also found to be first order in reactant. As shown in Figure VI.1, first-order kinetics describe the reaction of BBz in C_{16} under two-phase conditions (350°C, 7 MPa, and a feed ratio of 380 ml H_2/ ml liquid). Likewise, Figure VI.2 demonstrates that first-order kinetics apply for the reaction of DBF in C_{16} under the same conditions.

Since reactant concentrations in the reactor would vary with H_2/liquid feed ratio, the kinetics should also be independent of reactant concentration. Figure VI.3 shows that the conversion of DBF was independent of feed concentration up to 0.245 mols DBF/liter. Here the conversion of DBF was measured under two-phase condtions at a constant LHSV, 350°C, 7 MPa, and a feed ratio of 190 ml H_2/ml liquid.

VI.B Reactor Model

The starting point for analysis is the ideal trickle bed reactor model (Satterfield, 1975) which assumes plug flow of the liquid, complete wetting of the catalyst particles, and absence of heat or mass transfer limitations. The model also assumes that the gaseous reactant is present in great excess and that no vaporization or condensation occurs. For a purely catalytic reaction, the conversion attained in an ideal trickle

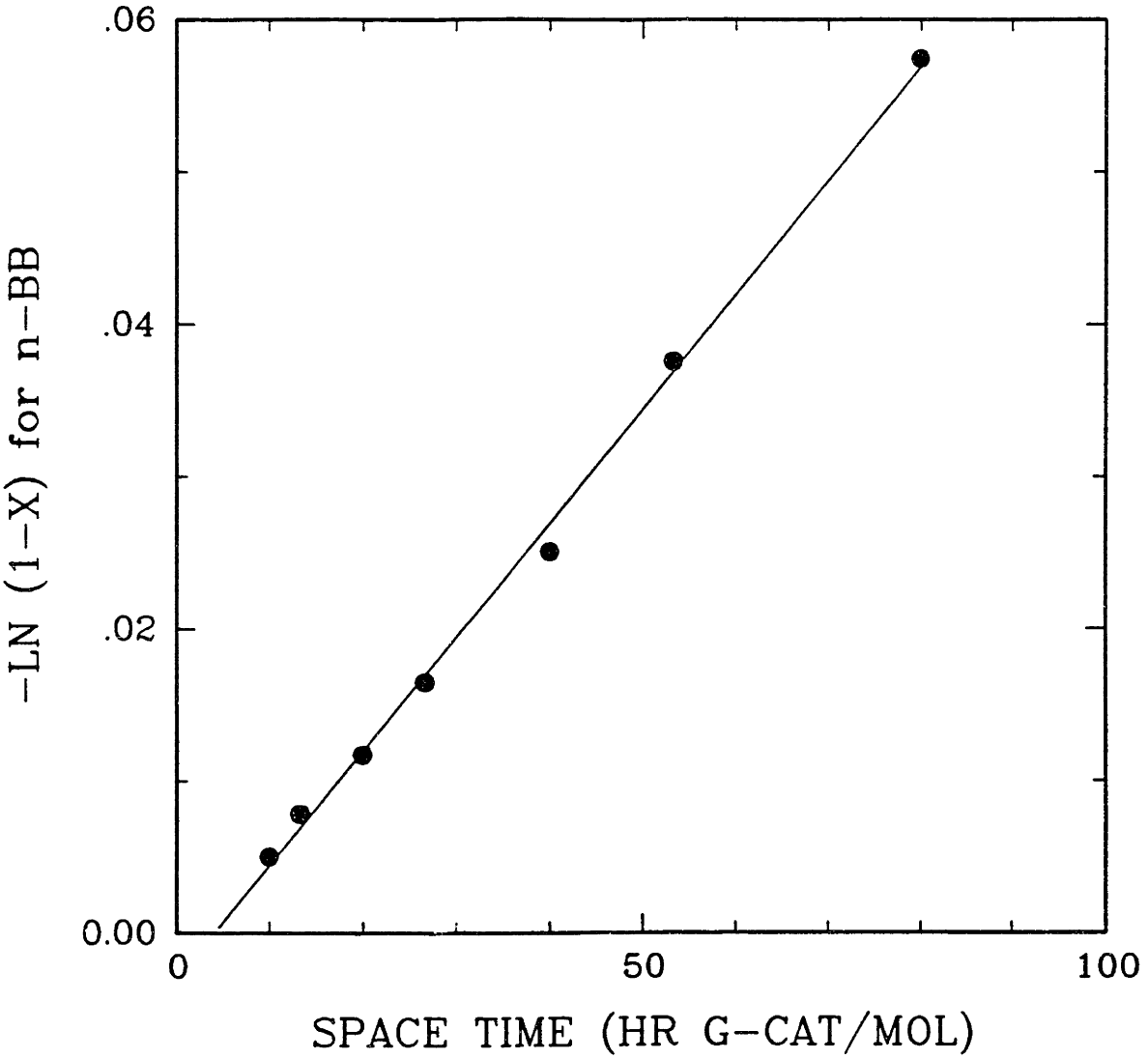

Figure VI.1 Hydrogenation of butylbenzene exhibits first-order behavior under mixed phase conditions.

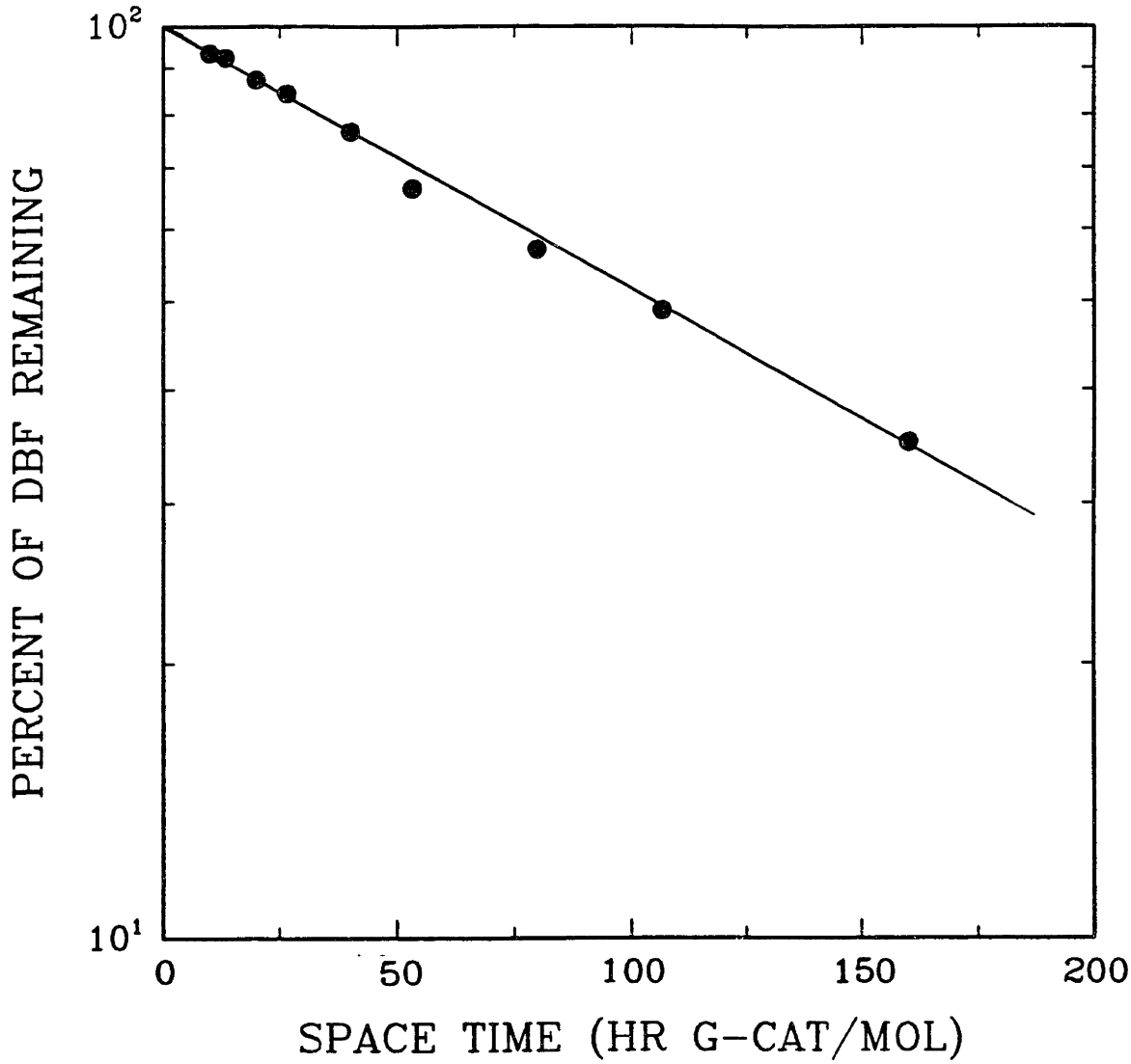

Figure VI.2 HDO of dibenzofuran exhibits first-order behavior under mixed phase conditions.

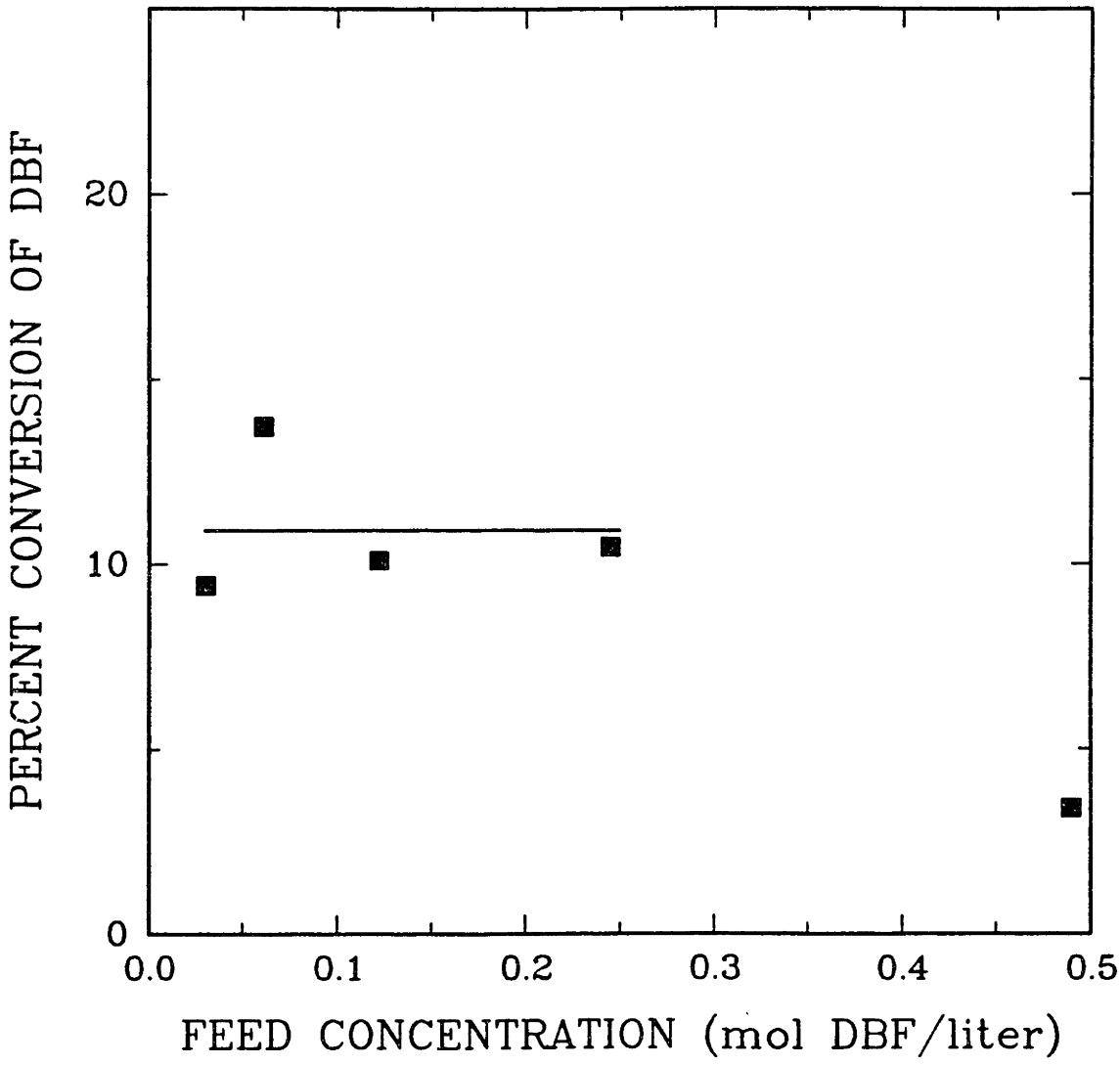

Figure VI.3 Reaction rate for DBF is independent of feed concentration up to 0.245 mol DBF/liter.

bed reactor should depend only upon liquid feed composition, LHSV (ratio of liquid volume fed per hour to catalyst volume), intrinsic kinetics, and concentrations at the catalyst surface.

Vaporization and condensation, which must be allowed for in a more general model, affect conversion by altering the concentrations of species within the reactor. The problem now becomes one of estimating fugacity, the correct thermodynamic driving force for reaction, for each reactant species throughout the reactor. Component partial pressures, which approximate fugacities, can be estimated by assuming that vapor liquid equilibrium is established at all points in the catalyst bed. With this assumption, which is valid if mass transfer resistances are small, an appropriate vapor-liquid equilibrium model can be used in a flash calculation to determine species mole fractions.

Mathematically the reactor is modelled as N stages in series with each stage containing an equilibrium flash and a differential reactor modelled as a CSTR. In Figure VI.4, which represents any of the stages from 1 to N, liquid feed L_{i-1} and vapor stream V_{i-1} enter stage i with known compositions. A flash calculation determines the equilibrium mole fractions which satisfy the mass balance equation

$$\text{VI.1} \qquad L'_i x'_{i,j} + V'_i y'_{i,j} = L_{i-1} x_{i-1,j} + V_{i-1} y_{i-1,j}$$

for each component j. Using the calculated equilibrium partial pressures y'_{ij} and the vapor phase reaction kinetics, the conversion in reaction zone i can now be determined. Since vapor phase kinetics are being used, the unreacted vapor stream V'_i is then adjusted for reactant conversion and product formation to yield V_i and $y_{i,j}$.

For the experimental studies here, relatively low concentrations of reactant were used and hydrogen consumption was kept below 5%. Thus

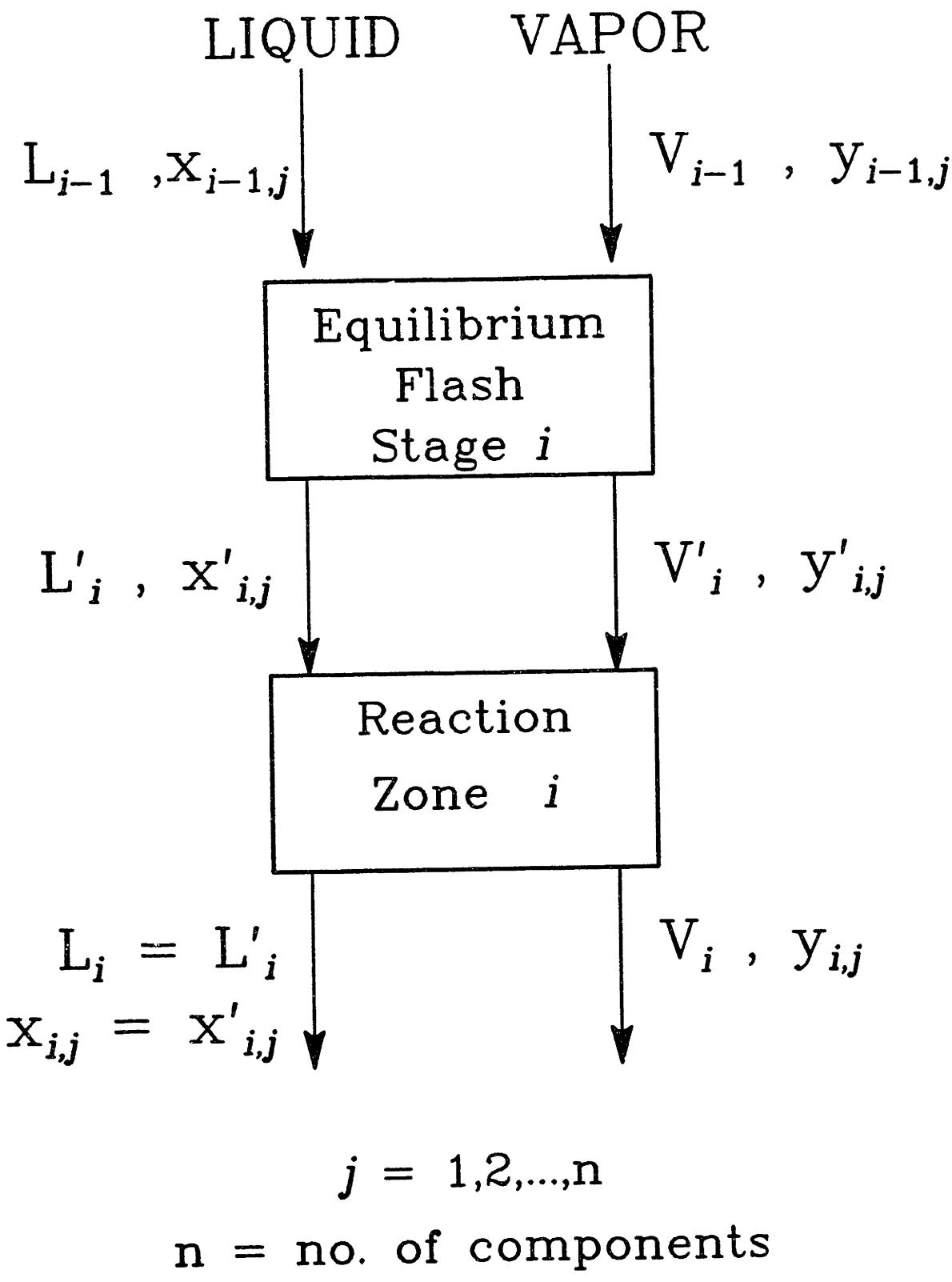

Figure VI.4 The model divides the trickle bed reactor into stages, each containing an equilibrium flash and a reaction zone.

vapor-liquid distribution coefficients could be taken to be independent of conversion and the theoretical model could be simplified further to include only the initial stage. The reaction rate was given by:

$$\text{VI.2} \qquad \frac{d(1-X)}{d\tau} = -k\, p_O\, (1-X)\, p_H$$

and the equilibrium flash calculation was used only to determine the initial partial pressures of reactant (p_O) and hydrogen (p_H) for each set of reactor conditions.

Computer programs provided by Prausnitz and co-workers (1980) were used to estimate the vapor-liquid equilibrium. Thermodynamic equilibrium requires that the fugacity of species i is the same in both phases according to

$$\text{VI.3} \qquad \gamma_i\, x_i\, f_i^{OL} = \phi_i\, y_i\, P$$

where: γ_i = activity coefficient for species i

f_i^{OL} = fugacity of pure liquid i at system temperature T (bars)

ϕ_i = fugacity coefficient for species i

P = system total pressure (bars).

Fugacity coefficients were calculated from the truncated virial equation of state, and activity coefficients were predicted by the UNIFAC contribution of groups method. Pure liquid fugacities for condensable species were estimated from published vapor pressure data (Reid et al., 1987; Sivaraman and Kobayashi, 1982), and a Henry's law constant was used for hydrogen (Lin et al., 1980). Details of the calculations are presented in Appendix A7, and the computer programs are documented in the thesis of Smith (1985). Table VI.1 lists the calculated vapor-liquid distribution coefficients for the major species for conditions of 350°C and a H_2/feed ratio of 2250 SCF/bbl.

Table VI.1 Vapor-Liquid Distribution Coefficients for Major Species at 350°C, 7 MPa, and 380 ml H_2/ml liquid

	Solvent	
Component	Squalane	Hexadecane
hydrogen	2.64	5.50
solvent	0.025	0.080
dibenzofuran	0.078	0.078
n-butylbenzene	0.233	

Kinetics were based upon vapor phase partial pressures since the calculated fugacity coefficients did not deviate significantly from unity. Use of kinetics based upon liquid phase mole fractions would be less accurate as the liquid phase is less ideal and activity coefficients vary more widely.

VI.C Approximate Reactor Model

An expression is developed which can be used to predict the change in inlet reactant concentration that will be produced by changing the gas-to-liquid feed ratio in a trickle bed reactor. For this simplified model, the following assumptions were required in addition to those of the more general model:

1. Negligible absorption of hydrogen occurs in the liquid phase.
2. The overall liquid volatility is a constant. This implies that the solvent volaility can be described by K_S.
3. Mole fraction of the reactant in the liquid feed is small, $z \ll 1$.

In actuality the first assumption may not be valid since the mole fraction of H_2 in the liquid phase can be significant even when the fraction of total hydrogen that is dissolved in the liquid phase is small. However, using these assumptions, the liquid and gas flow rates in the reactor (L and G respectively) can be expressed in terms of feed flow rates (L_f and G_f). L and G are constant through the reactor by assumptions (1) and (2) respectively. Ignoring assumption (3) for the present:

VI.4 $(1-z)L_f = x^S L + y^S G = x^S L + x^S K^S G$. Also, from assumption (1),

VI.5 $G_f = (1-y^S)G = (1-x^S K^S)G$, which can be rearranged to:

VI.6 $G = G_f/(1-x^S K^S) = L_f R/(1-x^S K^S)$.

From equation VI.4 and VI.6,

VI.7 $L = [(1-z)L_f - x^S K^S G]/x^S = [(1-z)L_f - x^S K^S L_f R/(1-x^S K^S)]/x^S$.

Using the expressions for the flow rates L and G, it is now possible to derived an expression for the mole fraction of reactant in the vapor phase. From a mass balance on the reactant:

VI.8 $zL_f = \frac{y}{K} L + y G$, which can be written in terms of feed flow rates using equations VI.5 and VI.6:

VI.9
$$N = \frac{y}{K}\left[[(1-z)L_f - x^S K^S G]/x^S \right] + y G$$

$$= y \left[\frac{(1-z)L_f}{K x^S} + G\left[1 - \frac{K^S}{K}\right] \right]$$

$$= y L_f \left[\frac{1-z}{K x^S} + \frac{R}{1 - x^S K^S}\left[1 - \frac{K^S}{K}\right] \right]$$

This can be rearranged to:

VI.10
$$y = z \frac{K}{\left[\frac{1-z}{x^S} + \frac{R}{(1 - x^S K^S)} (K - K^S) \right]}$$

Using assumption (3) above ($x^S \simeq 1$ and $1-z \simeq 1$), equation VI.10 can be simplified to:

VI.11
$$y = z \frac{K}{\left[1 + \frac{R}{(1 - K^S)} (K - K^S) \right]}$$

Equation VI.11 thus gives the vapor phase mole fraction of the reactant in terms of its feed mole fraction, the volatilities of reactant and solvent, and the gas-to-liquid flow ratio R.

VI.D Experimental

All experiments discusssed here were run at 7 MPa total pressure and temperatures ranging from 350 to 390°C. Pressure drop in the laboratory trickle bed reactor was negligible.

The catalyst consisted of 0.8 grams of a pre-sulfided commercial Ni-Mo/alumina catalyst, crushed and sieved to a size range of 150-212 microns. Calculations indicated that mass transfer limitations in the liquid phase were negligible for this size of catalyst particle. The catalyst was diluted with 8 times its volume of inert SiC with an average diameter of 406 microns in order to reduce dispersion (Van Klinken and van Dongen, 1980). Unfortunately, over long term use the activity of this catalyst sample declined so that only data obtained in the same set of experiments can be compared. This deactivation may have been caused by exposure of the catalyst to a high boiling point white oil (Kaydol).

The reactant, either dibenzofuran or n-butylbenzene, was dissolved in a liquid carrier at a concentration of 0.245 moles per liter. Dodecanethiol, a sulfur compound which rapidly reacts to form hydrogen sulfide in situ, was also fed in the liquid at a constant molar ratio with the hydrogen feed so as to produce 7 kPa of H_2S in all experiments. At standard conditions the liquid flow rate was 0.68 ml/min which corresponds to a LHSV based on reactor volume of 3.8 hr^{-1}. In terms of the catalyst volume, calculated from the compacted bulk density for pellets, the equivalent LHSV was 37 hr^{-1}.

Use of the paraffins n-hexadecane (b.p. 287°C) and squalane, a branched C_{30} with a boiling point (b.p.) of 350°C, allowed the overall feed volatility to be varied. The predicted extent of vaporization for these two liquids is shown in Figure VI.5 for a range of gas to liquid flow ratios at 350°C and 7 MPa. Here the feed ratios are shown in ml of H_2 at STP per ml of liquid, where 1000 ml at STP per ml liquid is approximately 6000 standard cubic feet per barrel. The difference in boiling points for DBF and BBz , 285 and 183°C respectively, also allowed the effect of reactant volatility to be investigated.

VI.E Results

An initial experiment was carried out to establish the effect of the presence of an inert liquid on conversion. For a reactant of moderate volatility an increase in the quantity of liquid phase relative to vapor phase would be expected to reduce the reactant partial pressure, and thus conversion. In Figure VI.6 data are shown for the HDO of DBF at 350°C and a constant space time of 80 hr g-cat./mol.

To obain these data, a series of feeds were prepared such that the molar flow rates of hydrogen, thiol, and DBF were kept constant as the solvent flow rate was increased. All vapor phase reaction with C_{16} and trickle bed operation with squalane are compared by the two data points at 0.68 ml liquid/min (1520 ml H_2/ml feed). Percent conversion is essentially the same. For trickle bed operation conversion drops as the squalane feed rate is increased. The reactor model, using an equilibrium flash calculation, predicts the conversions shown by the solid line in Figure VI.6. The differences reflect the accuracy with which vapor-liquid equilibrium can be predicted.

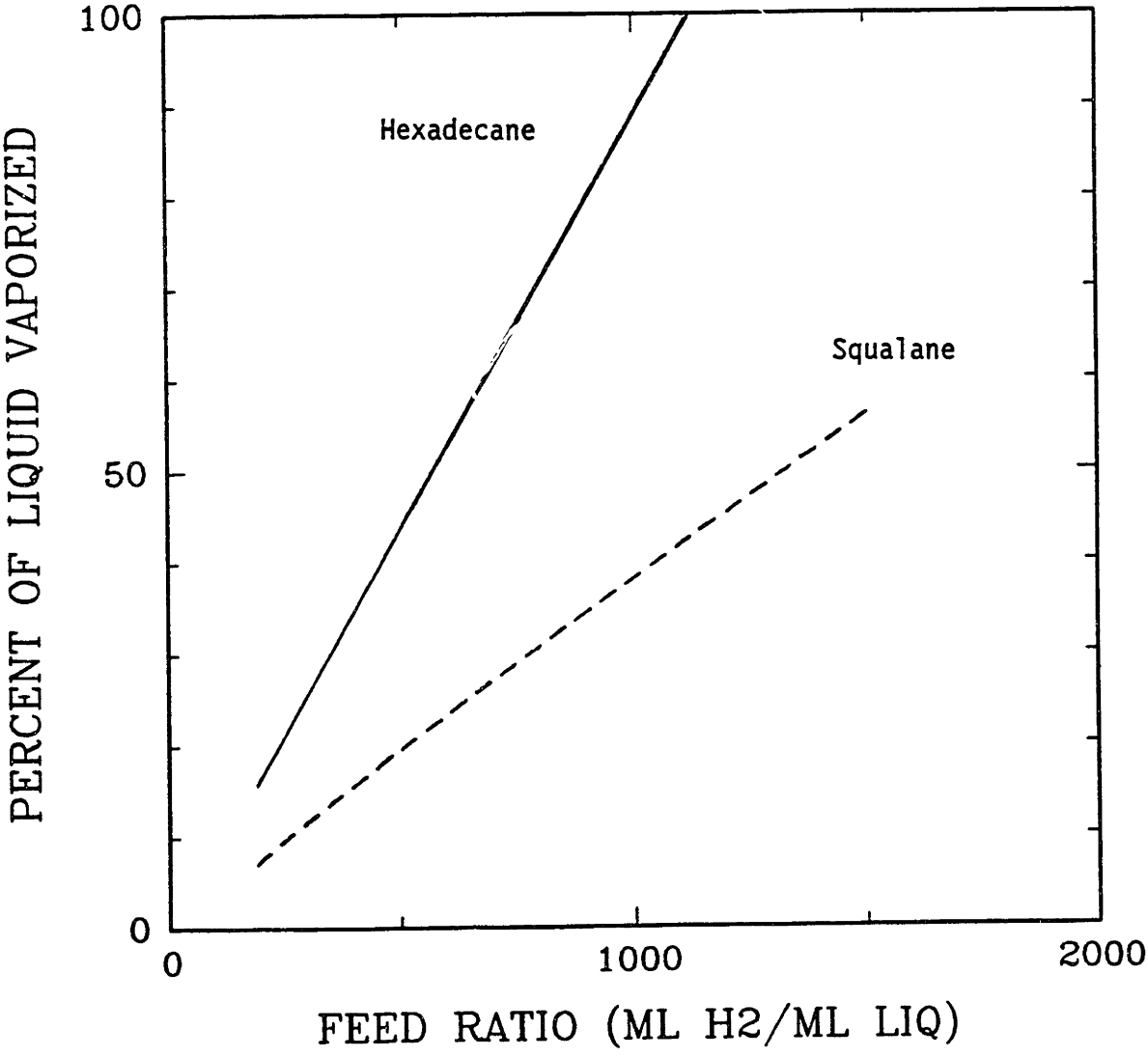

Figure VI.5 The fraction of feed vaporized could be varied over a wide range at 350°C and 7 MPa by changing the feed ratio.

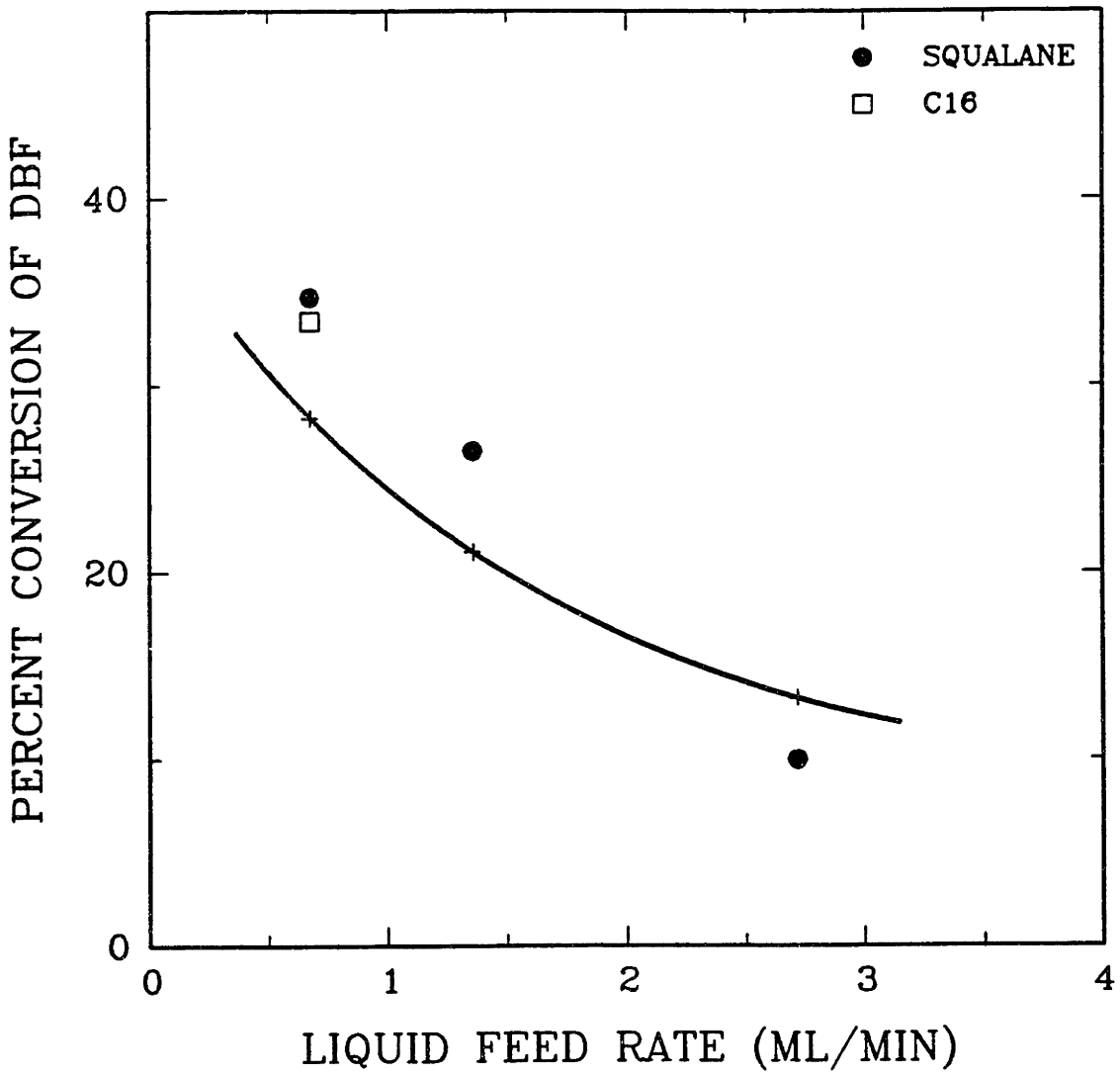

Figure VI.6 Increased solvent flow rate reduces conversion.

Although the results of the previous experiments are instructive, an operation closer to industrial practice involves changing the gas flow rate at constant LHSV and feed composition. A series of experiments was therefore carried out to determine how solvent and reactant volatility would affect conversion when the hydrogen feed rate was varied.

Figure VI.7 shows the change in conversion, as gas flow rate was varied, of DBF dissolved in squalane, at 350°C and a space time of 80 hr g-cat/mol. The reactant is more volatile than the solvent, and complete vapor phase operation is attained above 3000 ml H_2/ml. This ratio is significantly higher than industrial practice, but was used here to show the effect of transition from all-vapor to mixed phase behavior. An increase in conversion occurred as the gas to liquid flow rate was reduced since reactant partial pressure has increased. The dashed line in the figure is the prediction from first order vapor phase kinetics assuming that no condensation occurs. The trickle bed reactor model (solid line) predicts moderately higher conversions than those observed experimentally. As the feed ratio is decreased from 1520 to 190 ml H_2/ml, the model predicts an increase in partial pressure of DBF from 19.6 to 36.4 kPa, a 90% increase.

The effect of feed ratio on the hydrogenation of butylbenzene dissolved in squalane is shown in Figure VI.8 for the same space time. Butylbenzene is more volatile than DBF and the effect of feed ratio is more dramatic. The model (solid line) fits the data quite well and predicts an increase in partial pressure for BBz from 23 to 85 kPa (270% increase) as the feed ratio is decreased from 1520 to 190 ml H_2/ml.

In a similar set of experiments with DBF at 350°C, the effect of having a more volatile liquid was studied by using $C_{16}H_{34}$ as the carrier. Above a feed ratio of 1100 ml at STP/ml liquid, the reaction is all vapor

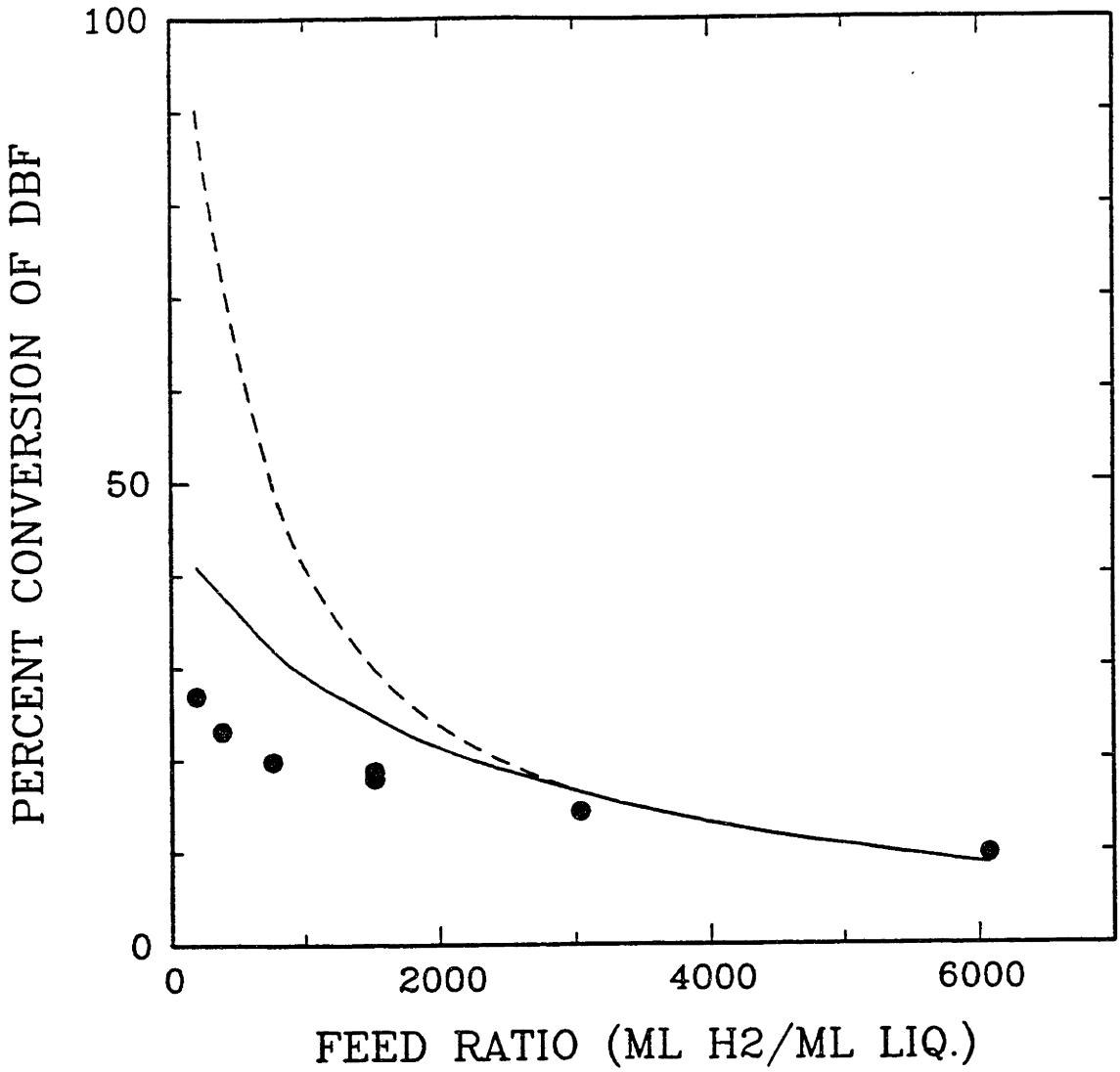

Figure VI.7 Conversion of DBF in squalane at 350°C increases as the feed ratio is reduced.

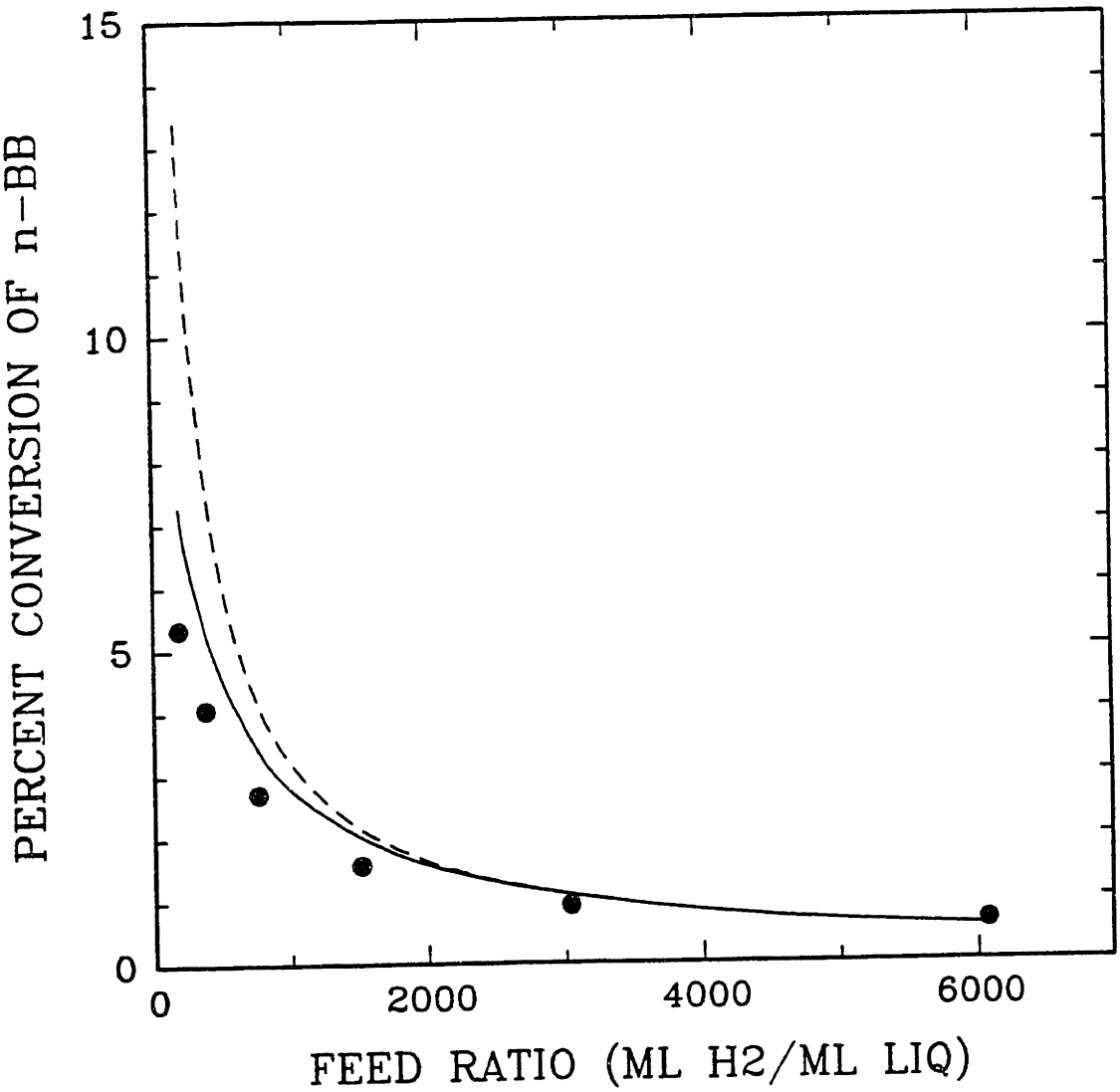

Figure VI.8 Conversion of butylbenzene in squalane increases sharply as the feed ratio is reduced.

phase and vapor phase kinetics describes the results in Figure VI.9. Once a liquid phase forms as the gas flow rate is decreased, conversion in this case becomes independent of gas to liquid flow ratio. The volatilities of the solvent and reactant are comparable and the vapor-liquid equilibrium model predicts that reactant partial pressure will be constant.

The final set of experiments compares the effect of temperature on the HDO reaction under gas phase and trickle bed operation. The change in phase conditions was obtained by using $C_{16}H_{34}$ as the solvent at gas to liquid feed ratios of 1520 and 380 ml H_2/ml respectively. Recall that DBF and $C_{16}H_{34}$ have the same volatility. First order rate constants were calculated directly from conversion in the temperature range of 350 to 390°C, and are displayed as Arrhenius plots on Figure VI.10. In trickle bed reactors reaction rate constants are frequently calculated based on inlet and outlet condensed phase concentrations, regardless of the true vapor and liquid concentrations in the reactor, which are usually unknown. Figure VI.10 illustrates how this may lead to confusing interpretations. Although the DBF concentration in the feed was the same in both cases, with the lower H_2/feed ratio used for trickle bed operation, the DBF partial pressure is higher and a greater conversion is obtained. Thus first-order rate constants calculated by the above procedure are higher than they would be if based on true vapor phase concentration. In the same low fixed H_2/feed ratio, increased temperature increases the DBF partial pressure as the system moves towards an all vapor reaction and hence higher conversion. Correspondingly the calculated activation energy for purely vapor phase reaction is 76 kJ/mol while it is 89 kJ/mol with a mixed phase present, under the particular conditions studied here.

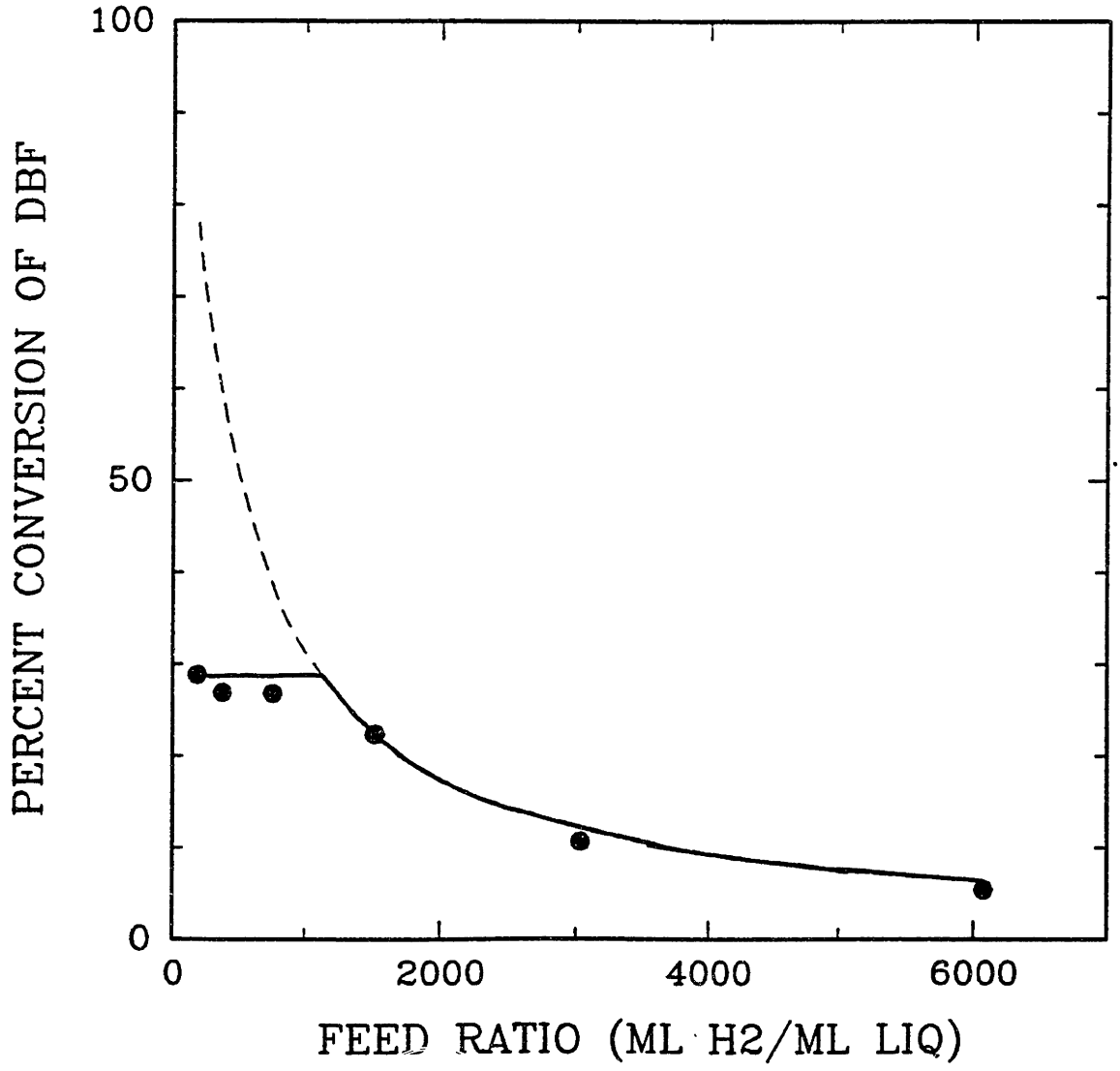

Figure VI.9 Conversion of DBF in hexadecane is unaffected by feed ratio under two-phase conditions.

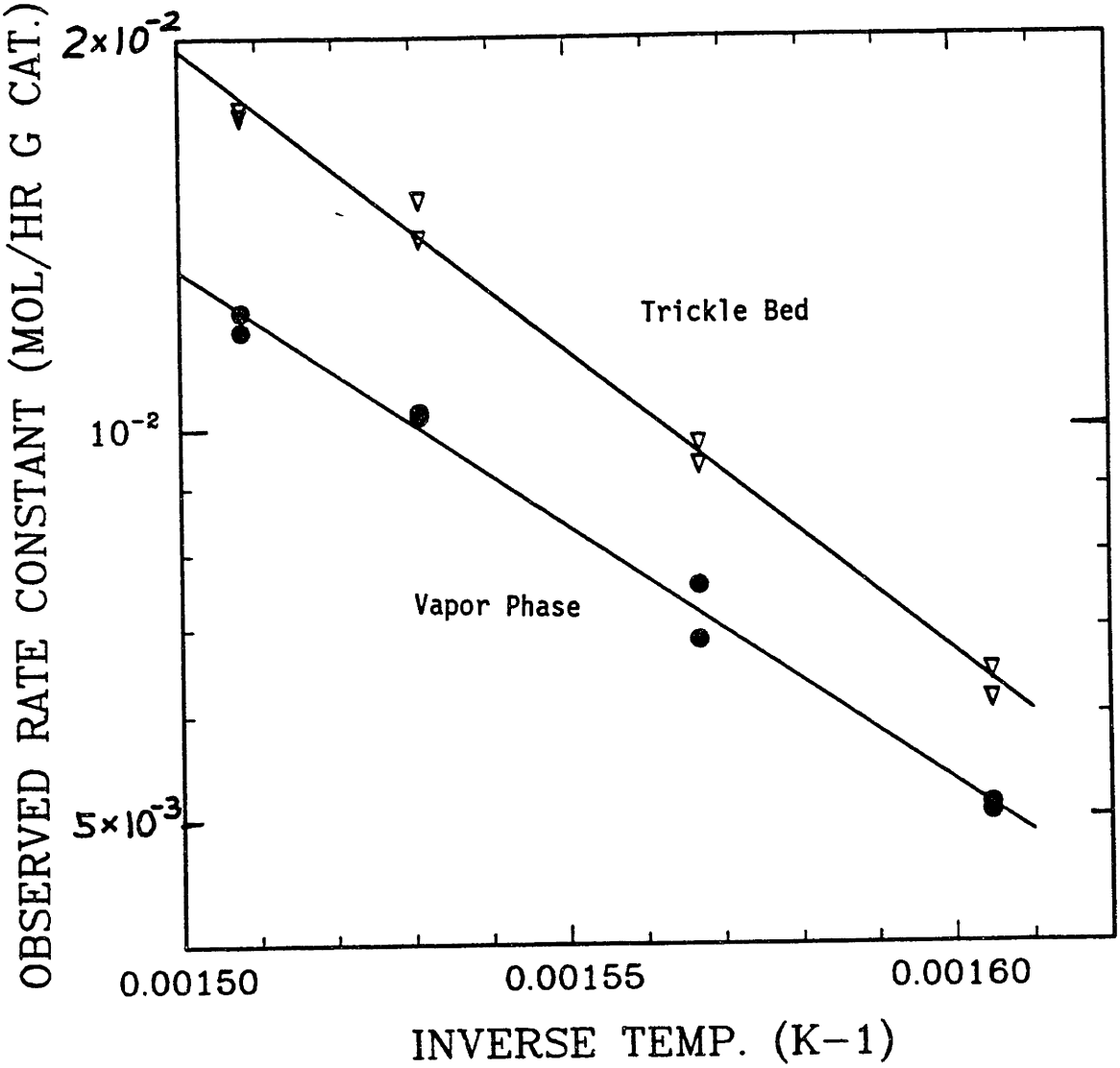

Figure VI.10 Observed effect of temperature is greater under trickle bed operation.

VI.F Discussion

The results suggest that the effect of changing gas to liquid flow ratio in a trickle bed reactor can lead to quite varied behavior, depending upon the relative volatility of the reactant compared to that of the overall feed. Almost no effect was observed for DBF in a solvent of similar volatility (C_{16}), while significant changes occurred with squalane as the solvent. In comparing the effect of reactant volatility, butylbenzene responded more to changes in gas flow rate than DBF.

One can analyze the results in terms of the approximate reactor model which describes the observed trends. Using the assumptions described previously, an approximate expression for the mole fraction of reactant in the vapor was derived for a single stage:

$$\text{VI.11} \qquad y = z \; \frac{K}{\left[1 + \frac{R}{(1 - K^S)} \; (K - K^S) \right]}$$

In this expression the $1-K_S$ does not approach zero since $K_S \ll 1$ for the solvent used here and for typical hydrotreating conditions. Equation VI.11 indicates that analysis of trickle bed reactor data in terms of entrance and exit liquid phase mole fractions is justified only if the expression in brackets is constant. Under these conditions the initial vapor phase mole fraction is proportional to the feed concentration. However, analysis based upon exit mole fractions would cause significant errors if temperature or hydrogen feed ratio were varied.

From equation VI.11 we see that the effect of gas flow rate is negligible only if the expression

$$\left\{ \frac{K - K_S}{1 - K_S} \right\} \ll 1$$

A specific case is for $K = K_S$, whereupon the vapor phase mole fraction of the reactant becomes independent of gas-to-liquid flow ratio. This behavior was observed for the reaction of DBF in C_{16} where both species had similar volatilities.

This simple analysis suggests that the observed effect of changing gas to liquid feed ratio would be greatest when:

1. The feed ratio R is large.

2. The solvent volatility is low, $K_S \ll 1$.

3. The absolute difference in volatilities between reactant and solvent $|K - K_S|$ is large.

The last condition indicates that trickle bed reactor feeds having a narrow boiling distribution would exhibit a conversion relatively insensitive to feed ratio at constant LHSV.

The results also demonstrate that a trickle bed reactor model which includes vapor-liquid equilibrium calculations can describe the observed trends in conversion as operating conditions are changed. Although these experiments have been carried out with simple first order systems, the same type of model would be expected to apply where adsorption or inhibition effects are important. In the extreme case of a zero order system, as with quinoline hydrodenitrogenation, gas-to-liquid flow ratio would not affect conversion.

The results on the effect of temperature indicate that the activation energy observed for a reaction in a trickle bed reactor would depend upon the volatilities of reactant and solvent and the gas-to-liquid feed ratio.

VI.G Conclusions

In general both theory and experiment show that the greatest effect on conversion of changing gas/liquid feed ratio occurs when liquid volatility is low and when the absolute difference in volatilities between reactant and unreacted liquid is large.

In fuels processing, a liquid feed of fairly narrow boiling point range is usually used. However if reaction causes intermediates or products of considerable volatility to be formed, analyses such as those performed here may help to interpret effects observed.

VI.H Nomenclature

f_i^{oL} = fugacity of pure liquid i at system temperature T (bars)

K = vapor-liquid distribution coefficient for reactant (y/x)

K_S = vapor-liquid distribution coefficient for solvent (y^S/x^S)

L = molar flow rate of liquid

p_O = initial reactant partial pressure

p_H = initial hydrogen partial pressure

P = total pressure

R = feed ratio, moles H_2 per mole of liquid

V = molar gas flow rate

X = fractional conversion of reactant

x = mole fraction of reactant in liquid phase

y = mole fraction of reactant in gas phase

z = mole fraction of reactant in liquid feed

γ_i = activity coefficient for species i

τ = space time, hr g-cat/mol

ϕ_i = fugacity coefficient for species i

Chapter VII

CONTROL OF CATALYST DEACTIVATION WITH AMMONIA

VII.A Introduction

As discused in section I.F, deactivation of hydrotreating catalysts is an important limitation in the processing of heavier feedstocks which contain high concentrations of heteroatoms and polyaromatic hydrocarbons. The observation, early in this thesis, that exposure of a deactivated catalyst to ammonia could enhance its activity for the HDO of dibenzofuran was therefore noted with some interest. Several brief studies were carried out to investigate the usefulness of this technique and to test possible explanations for the phenomenon.

VII.B Experimental

All of the experiments were conducted on several samples (20,22, and 23) of the same Ni-Mo/Al_2O_3 catalyst (HDS-3A), pre-sulfided before use. Each batch consisted of 1.6 grams of catalyst. Batches 20 and 22 were deactivated with a feed containing quinoline in the absence of H_2S, followed by experiments on the HDO of dibenzofuran. Batch 23 was started up with the HDO of DBF in the presence of H_2S and then was immediately coked with anthracene.

Ammonia was fed to the reactor using the ISCO pump and the ammonia feed system. During operation with 1:1 mixtures of ammonia and hydrogen it was found that expansion of the mixture through the back-pressure regulator (BPR) caused appreciable cooling. This would tend to freeze any C_{16} solvent passing through the system unless the BPR was wrapped with heating tape. The standard ammonia treatment (as used in batches

20,22,and 23) involved feeding an equimolar NH_3/H_2 mixture to the reactor at 1090 ml at STP/min and a liquid flow rate of 0.68 ml/min. Liquid feeds consisted of either C_{16} paraffin or Kaydol, a high boiling point mineral oil (white oil). Dodecanethiol was present in the feed to produce 12 kPa of H_2S in situ, and the ammonia exposure lasted for one hour at 360°C and 7 MPa total pressure. Variations of this standard treatment were also used and are described below.

The coking procedure (Batch 23) involved feeding a 1 wt% anthracene in xylene mixture to the reactor at 390°C under helium flow. Anthracene has been found to coke under these conditions more readily than other polyaromatics such as phenanthrene or acridine (Scaroni and Jenkins, 1985). During coking, helium was fed at 300 (ml at STP)/min at a total pressure of 7.0 MPa. Liquid was fed at 0.34 ml/min to produce a space time of of 9.1 hr g-cat/(g of anthracene), and coking conditions were maintained for 3 hours.

All tests of catalyst activity for the HDO of dibenzofuran were performed with the DBF dissolved in a C_{16} paraffin carrier at 0.245 mol of DBF/liter. Dodecanethiol was added to the liquid feeds to produce H_2S in the reactor. The hydrogen-to-liquid flow ratio was set at 9000 SCF/bbl.

When the catalyst was not undergoing activity testing or other procedures, it was operated continuously with a feed of CS_2 or thiol in xylenes, and hydrogen flow was also maintained. Temperature and pressure were kept at 360°C and 7 MPa respectively, and a constant H_2S partial pressure of 12 kPa was produced from the sulfur compound added to the feed.

VII.C Results

IV.C.1 Effect of Ammonia Upon a Deactivated Catalyst.

While operating catalyst batch 20 it was first noted that exposure of the catalyst to relatively high concentrations of ammonia could affect the activity of a deactivated Ni-Mo catalyst. Experiments were conducted using the HDO of dibenzofuran as a test reaction at reaction conditions of 360°C, 7.0 MPa total pressure, and an H_2S partial pressure of 13.9 kPa. With the catalyst at a steady activity, producing 55% conversion of dibenzofuran (DBF) at a space time of [160 hr (g. of catalyst)/(mol of DBF)], the gas flow to the reactor was switched from hydrogen to a 1:1 mixture of ammonia and hydrogen. The H_2S concentration, produced in situ by the addition of dodecanethiol to the feed, remained constant. Conversion of DBF immediately dropped from 55% to approximately zero at the same space time once the NH_3 entered the system. After one hour the NH_3/H_2 flow was replaced with pure hydrogen, and it was found that the catalyst activity had increased substantially. The activity (as measured by the HDO of DBF) remained high for the next few days, although it exhibited some decline during this period.

It was decided that the effect of ammonia deserved further study, and the experiment was reproduced on catalyst batch 22. After deactivation of this catalyst with quinoline as described above, experiments were performed on the HDO of dibenzofuran in the temperature range of 350-390°C. During these experiments no further deactivation of the catalyst was observed. Figure VII.1 shows that the conversion of DBF remained constant at approximately 55% from 250 to 500 hours on stream. Here conversion of DBF was measured at a standard condition of 160 hr g-cat/mol, 360°C, 7.0 MPa total pressure, and an H_2S partial pressure of 7 kPa.

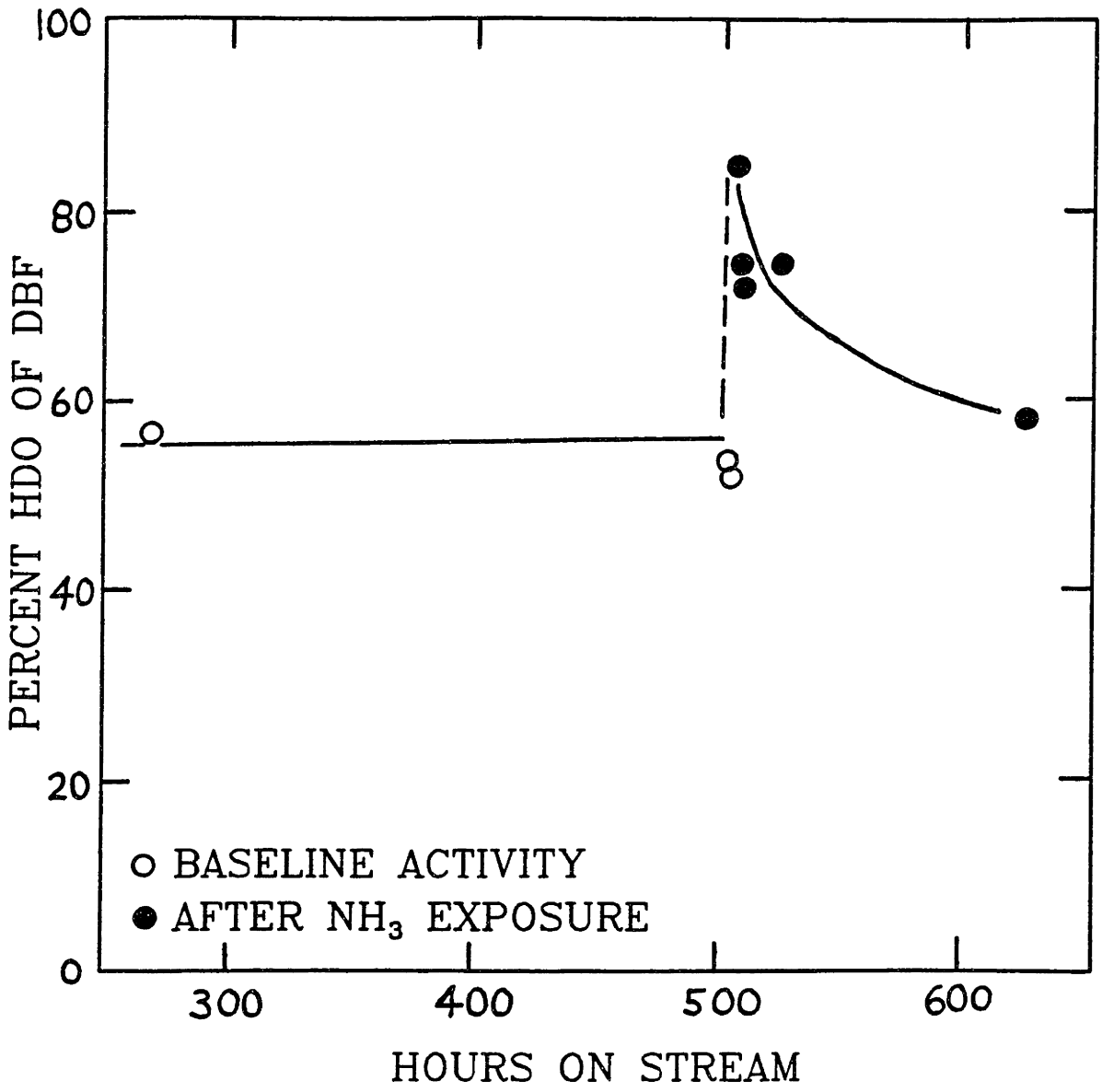

Figure VII.1 Activity for the HDO of Dibezofuran is enhanced after exposure to ammonia.

At 506 hours on stream, the feed containing DBF and C_{12} thiol was maintained at a flow rate of 0.68 ml/min, while the hydrogen flow was replaced by a 1:1 mixture of NH_3 and H_2 at the same total gas flow. Upon addition of ammonia the percent HDO of DBF dropped markedly, and the ammonia flow was stopped after one hour. A sample collected one hour after returning the gas feed composition to hydrogen showed that the conversion of DBF had increased from 55 to 85% (Figure VII.1). The corresponding conversion on a fresh pre-sulfided catalyst which had been on stream for only one hour (batch 23) was 96% of the DBF.

Since the reaction of DBF can be described by first order kinetics, the enhancement in activity upon exposure to ammonia can be equated with a 140% increase in the first-order rate constant. The catalyst activity for the HDO of DBF declined towards its previous level during the next 122 hours following ammonia exposure. Between 625 and 631 hours on stream the HDO of DBF was then measured as a function of space time. These results are compared with the baseline activity of batch 22 (264-287 hours on stream) in Figure VII.2. The catalyst activity still exhibited a 20% greater first-order rate constant 122 hours after exposure to ammonia.

VII.C.2 Coking Studies with Anthracene

These experiments were carried out to determine if process conditions affected the reactivation by ammonia. Important process variables would include: duration of ammonia exposure, pressure, temperature, and gas composition. The presence or absence of H_2S, H_2O, or a liquid phase could also affect the process. In order to rapidly screen these process conditions, the catalyst was repeatedly coked with anthracene under helium. Following each accelerated deactivation, the catalyst could then be exposed to ammonia under various test conditions listed in Table VII.1.

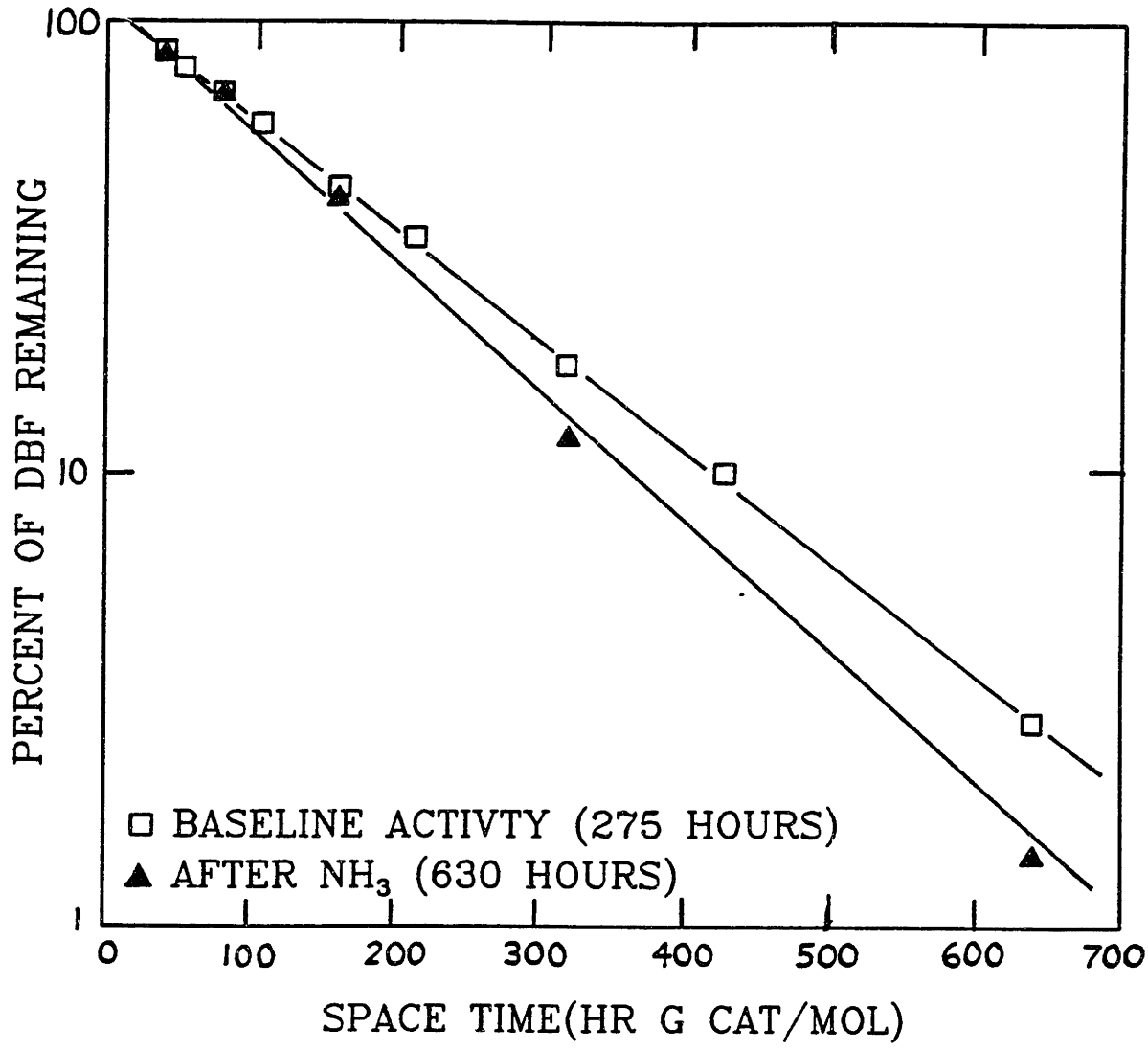

Figure VII.2 Catalyst activity remains higher than normal 120 hours after ammonia treatment.

Table VII.1 Reactivation Procedures Used to Produce Activity Identified by Letter

Procedure	Gas	Press (MPa)	Temperature (°C)	H_2S(kPa)	Liquid	Time
Standard	NH_3/H_2	7	360	12	C_{16}	1 hr
b	--	--	--	0	--	--
c	--	--	--	--	--	--
d	--	--	--	O, H_2O	--	--
e	--	--	--	--	--	2 hr
f	NH_3/He	--	--	0	--	--
g	NH_3/He	--	--	0	tetralin	--
h	--	--	--	0	--	--
i	--	--	--	--	--	--
j	--	14	400	--	--	--
k	--	--	--	--	Kadol	--
l	H_2	--	--	--	Kadol	--
m	--	--	--	--	Kadol	--
n	--	--	--	Intermittent	--	--

Note: -- signifies standard condition.

VII.C.2.a The effects of H_2S and H_2O on reactivation. - The initial experiments on catalyst batch 23 were designed to establish if hydrogen sulfide or water had any influence upon the activity enhancement by ammonia. The initial activity of the catalyst decreased after coking with anthracene, with conversion of DBF dropping from 96% (a) to 50%. Letters in parenthesis refer to data points in Figure VII.3, which shows the activity history of batch 23 for the HDO of dibenzofuran at standard conditions. Treating the catalyst with a 1:1 mixture of NH_3 in H_2 increased the conversion of DBF to 59% (b), while coking the catalyst a second time reduced the conversion of DBF further to 38%. Re-exposure of the catalyst to ammmonia, this time in the presence of 12 kPa of H_2S, increased the conversion to 72% (c). Conversion of DBF declined to 47% during the following 42 hours on stream.

The catalyst was coked a third time, and then exposed to ammonia in the presence of 12 kPa of decanol. Conversion of DBF increased from 32 to 41% (d). However, under these conditions less than 10% of the decanol reacted to form water. Some decylamine was detected in the reactor effluent, formed from the reaction of decanol with ammonia.

Since the HDO of dibenzofuran exhibits first-order kinetics, rate constants have been calculated at each activity level and are plotted in Figure VII.4. Treatment with ammonia alone is seen to have increased the the activity by 26%, while NH_3 treatment in the presence of H_2S increased activity by 170%. Results for ammonia treatment in the presence of water are inconclusive due to the low conversion of decanol.

VII.C.2.b Comparison of operating conditions. - Experiments were also run on catalyst batch 23 to examine the effect of the duration of ammonia exposure, gas composition, presence of a liquid phase, and severity of

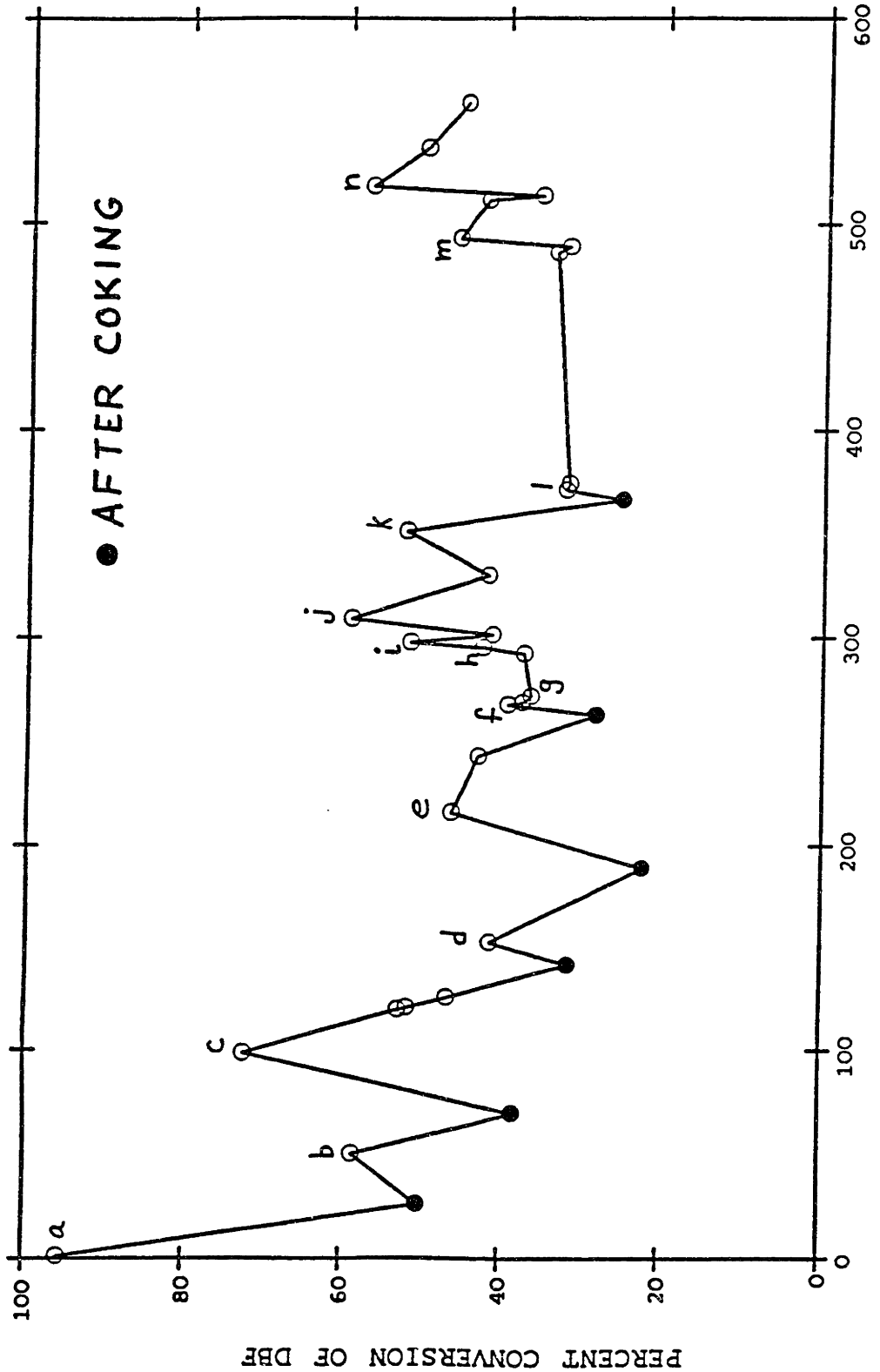

Figure VII.3 Activity history of catalyst batch 23.

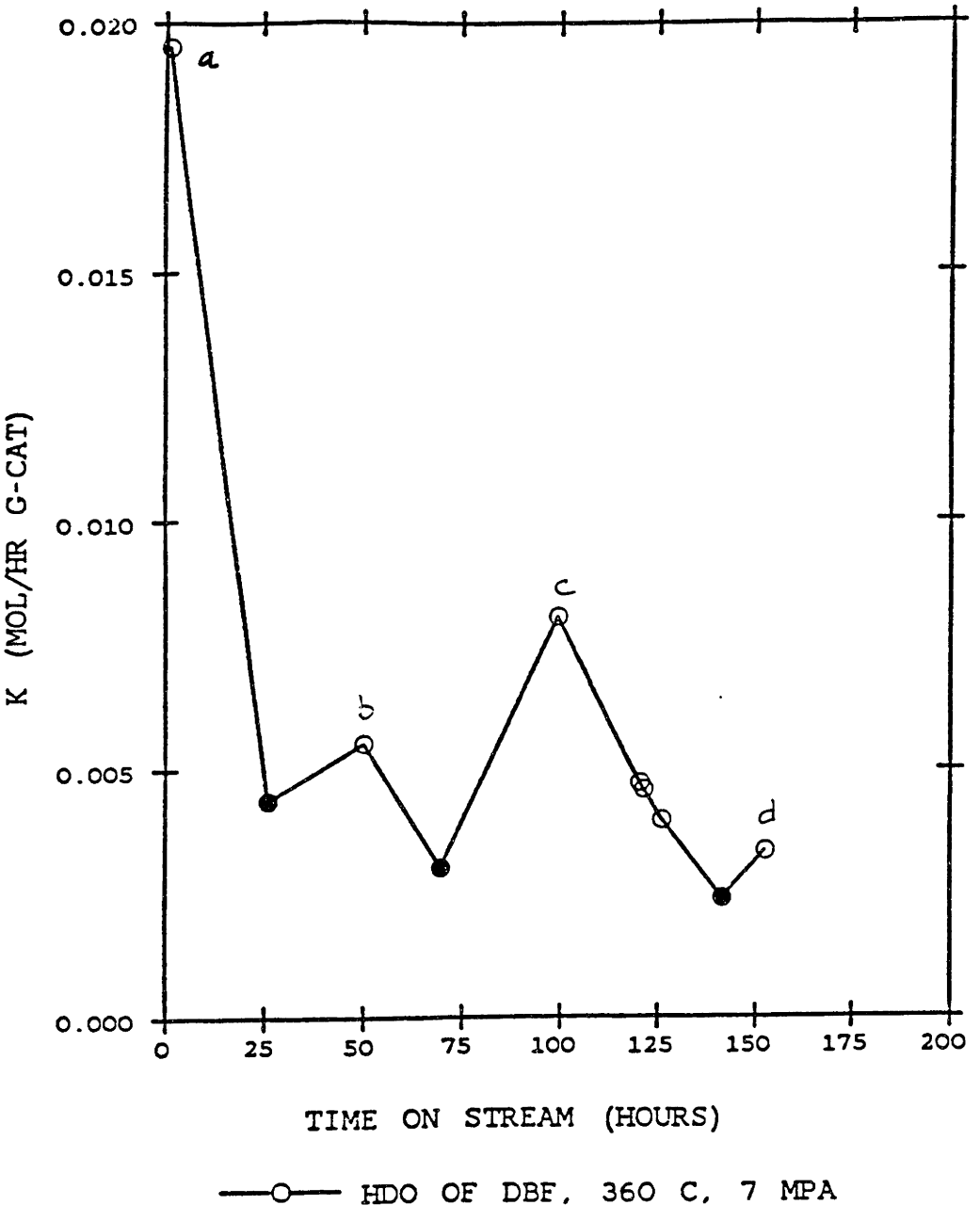

Figure VII.4 Activity of catalyst batch 23 in terms of first-order rate constants.

operation on the efficacy of ammonia treatment. The catalyst was coked at the start of the experiments, and the conversion of DBF measured subsequently was only 22%. The catalyst was then exposed to ammonia and 12 kPa of H_2S for two hours rather than one hour. Flow rates were reduced by 50% so that the same quantity of ammonia was passed over the catalyst, and HDO conversion increased to 47% (e) in Figure VII.3. This corresponds to a 150% increase in the first-order rate constant.

Subsequent coking lowered the HDO rate conversion to 28%, and experiments were performed to determine if hydrogen aids in reactivation of the catalyst. Exposure of the catalyst to a 1:1 mixture of NH_3 and helium for one hour raised the conversion level to 39% (f). Repeating the ammonia/helium treatment in the presence of a hydrogen donor (tetralin) produced a similar HDO activity (37% conversion (g)). The catalyst was then subjected to ammonia treatment in the presence of hydrogen and the conversion of DBF rose slightly to 43% (h). An additional exposure to NH_3/H_2 in the presence of 12 kPa of H_2S increased conversion further to 52% (i). Conversion rapidly declined to 41% within 4 hours.

The effect of increasing the severity of operating conditions during ammonia exposure was studied next. Temperature was increased from 360 to 400°C and the total pressure was doubled to 14 MPa. The conversion of DBF increased to 59% (j) immediately after ammonia exposure and then declined to 42% after 20 hours on stream. Higher severity operation does not appear to significantly alter the effect of ammonia.

Ammonia treatment was then repeated in the presence of a liquid phase and 12 kPa of H_2S. The liquid feed consisted of dodecanethiol dissolved in Kaydol. Previous treatments with ammonia had utilized C_{16} as the liquid carrier, and operating conditions were such that complete vaporization of the C_{16} occurred. With a liquid phase present, the

conversion of DBF rose and remained at 52% (k) even 19 hours after ammonia exposure.

VII.C.2.c Effect of a liquid phase. - The apparent benefit of having a liquid phase present during NH_3 exposure was studied in the third set of experiments on batch 23. The catalyst was coked after 366 hours on stream and attained an activity level at which 25% conversion of DBF occurred at standard conditions. Following the coking procedure, the catalyst bed was flushed with Kaydol for one hour in the presence of hydrogen and 12 kPa of H_2S. This procedure raised the conversion of DBF to 32% (l) in Figure VII.3. Repeating the Kaydol flush with a NH_3/H_2 mixture flowing over the catalyst raised the activity to 46% conversion of DBF (m). Conversion of DBF declined to 36% after 20 hours.

In the last experiment in this series the catalyst was exposed to NH_3/H_2 for one hour with a C_{16} carrier flowing through the reactor. In this case the liquid feed was alternated every 10 minutes between pure C_{16} and a solution of dodecanethiol in C_{16}. Conversion of DBF increased to 57% and remained higher at 45% conversion of DBF over 40 hours after NH_3 exposure.

VII.C.3 Desorption of 1,2,3,4-Tetrahydroquinoline at 250°C.

The desorption of 1,2,3,4-tetrahyroquinoline (PyTHQ) from a Ni-Mo hydrotreating catalyst was studied at 250°C. Low levels of PyTHQ reduced the hydrogenation of phenanthrene from 83% to 20%, and the poisoned catalyst required over 20 hours to recover its initial activity after the PyTHQ was removed from the feed. Exposure of a PyTHQ poisoned catalyst to either 100 kPa of ammonia or 4 kPa of decylamine greatly decreased the length of time required for full recovery of activity. The presence of

NH_3 or decylamine apparently enhances the desorption of PyTHQ. This work is included here since it may provide some insight into the effect of higher levels of NH_3 in enhancing the activity of a deactivated catalyst.

VII.C.3.a Experimental. - The experiments were performed under vapor phase conditions on a single sample of pre-sulfided Ni-Mo catalyst (batch 41) at 250°C and 3.5 MPA total pressure. The liquid feed consisted of phenanthrene and hexanethiol dissolved in C_{12} paraffin at 0.204 and 0.143 mols/l respectively. The gas-to-liquid flow ratio of 9000 SCF/bbl produced a phenanthrene partial pressure of 10 kPa and an H_2S concentration of 7 kPa. All experiments were run at a liquid flow rate of 0.34 ml/min. Organo-nitrogen poisons were added to the liquid feeds, while ammonia was pumped directly to the reactor.

VII.C.3.b Results. - The conversion of phenanthrene in the presence of H_2S is indicated by the (a) in Figure VII.5. Percent conversion of phenanthrene is defined here as the percent of disappearance of phenanthrene. No attempt was made to identify the hydrogenated products. At (b) in Figure VII.5 the feed was switched to one containing phenanthrene, hexanethiol, and the equivalent of 0.25 kPa of PyTHQ. The conversion dropped dramatically and reached a steady state value of 20% after 4 hours.

At the time represented by (c) the PyTHQ was removed from the feed and a slow recovery of activity was observed. However, after 16 hours the conversion had only increased to 62%, indicating slow desorption of the nitrogen poison. At time (d) the equivalent of 4 kPa of 1-decylamine was added to the phenanthrene feed and conversion fell to about 2%. The

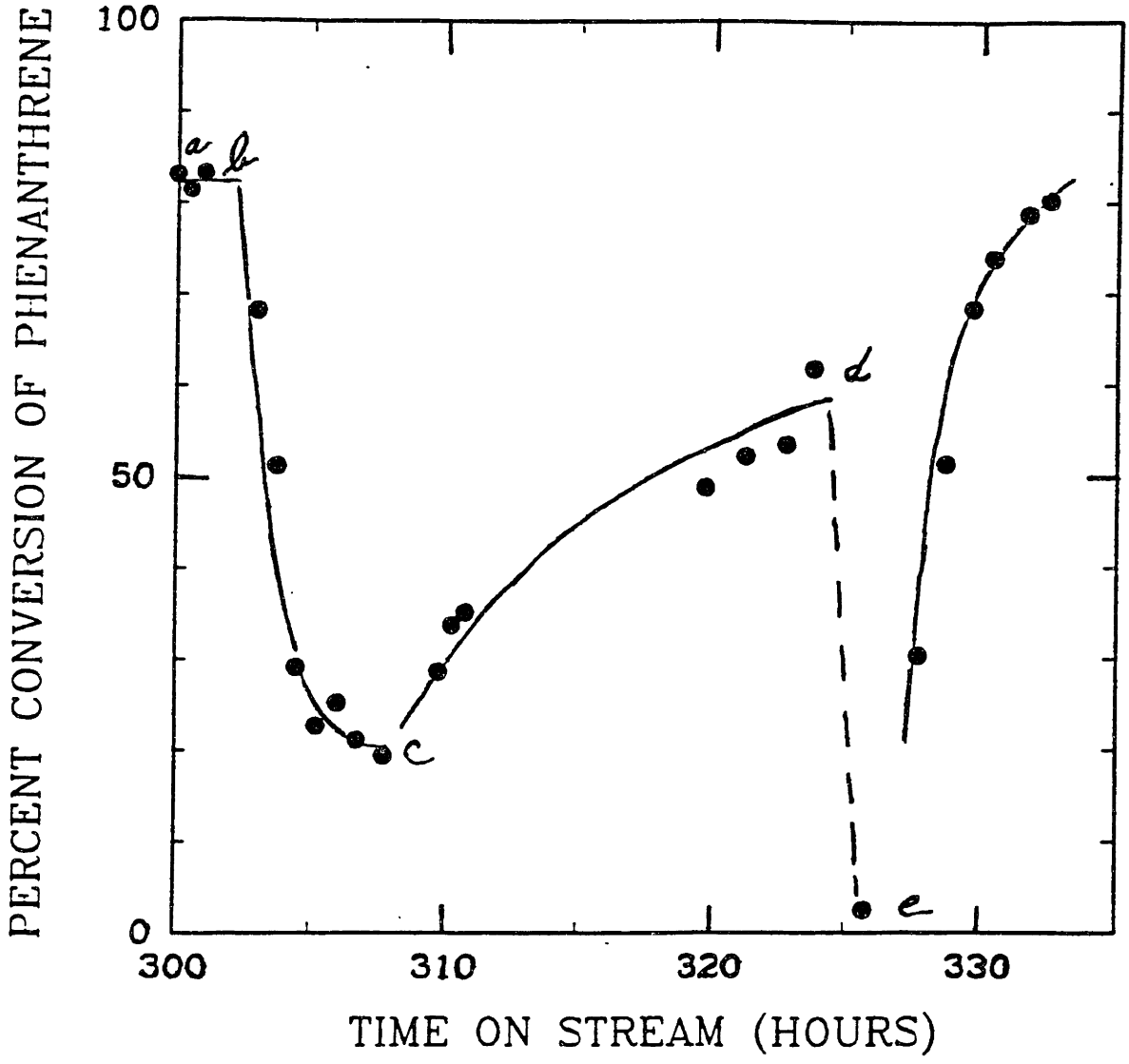

Figure VII.5 PyTHQ and decylamine strongly inhibit phenanthrene hydrogenation at 250°C. Recovery of activity is slow after PyTHQ exposure.

decylamine was removed from the feed at (e), and this time the catalyst regained its initial activity within 7 hours.

Figure VII.6 shows an additional experiment with decylamine, this time with a pre-poisoned catalyst. A feed containing the equivalent of 0.25 kPa of PyTHQ was run overnight and the corresponding conversion of phenanthrene at (a) had dropped to the range of 23-32%. At the time represented by (b) the PyTHQ was removed from the feed and 4 kPa of decylamine was added. The amine was removed from the feed at (c), and the conversion of phenanthrene rose above 80% within 5 hours.

Figure VII.7 shows the effect of ammonia upon the catalyst which has again been pre-poisoned by exposure to PyTHQ. Time (a) here represents the unpoisoned activity, and (b) represents the time at which PyTHQ at 0.25 kPa was added to the feed. The PyTHQ was fed overnight and the conversion of phenanthrene dropped to 20%.

At time (c) in Figure VII.7 the PyTHQ was removed from the feed, and the equivalent of 100 kPa of ammonia was pumped to the reactor for the following 2.5 hours. At time (d) the ammonia feed was stopped and conversion rapidly increased to over 80% within 2 hours. Ammonia thus also increases the rate of activity recovery of the PyTHQ poisoned catalyst.

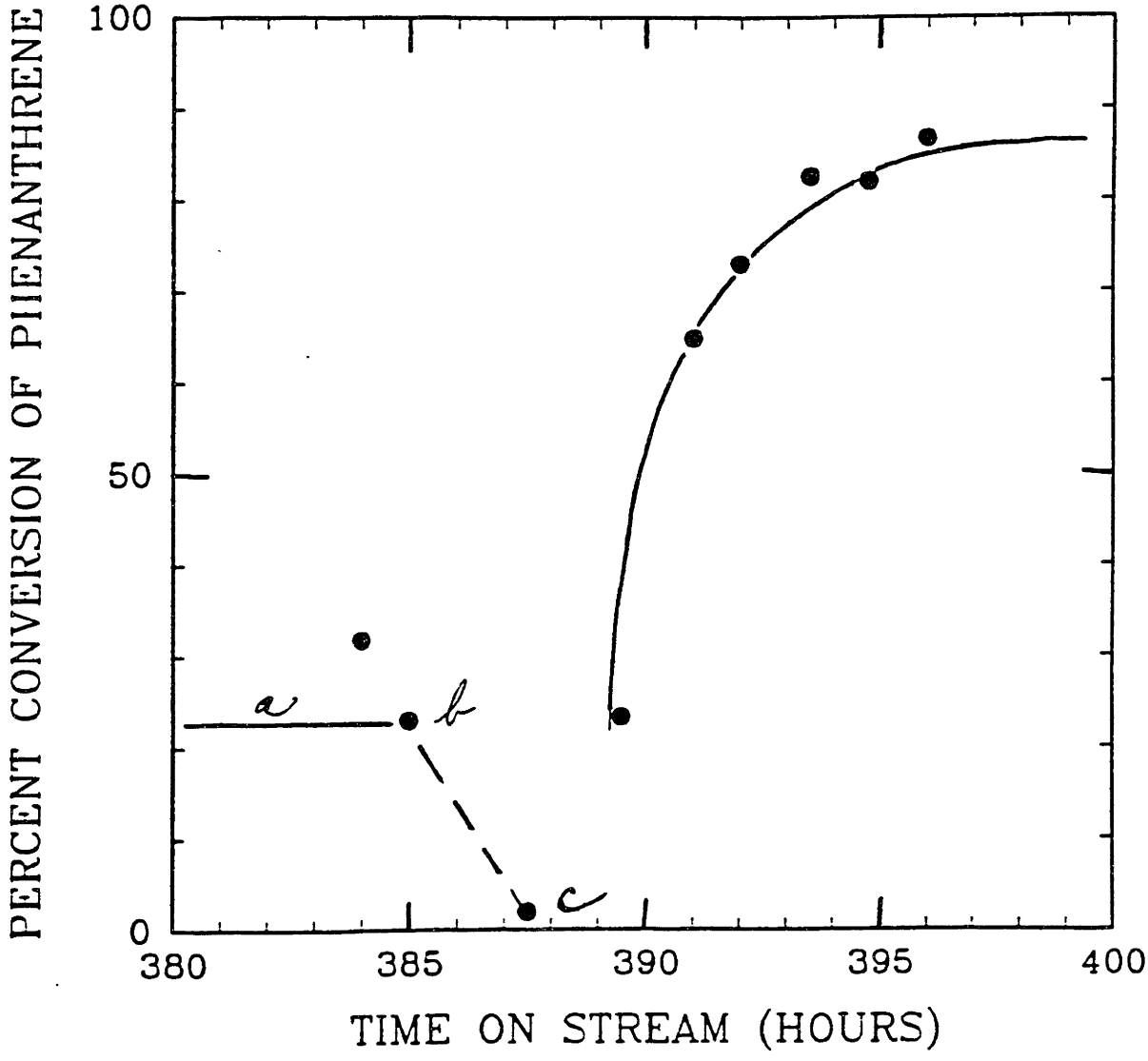

Figure VII.6 Decylamine exposure increases rate of activity recovery.

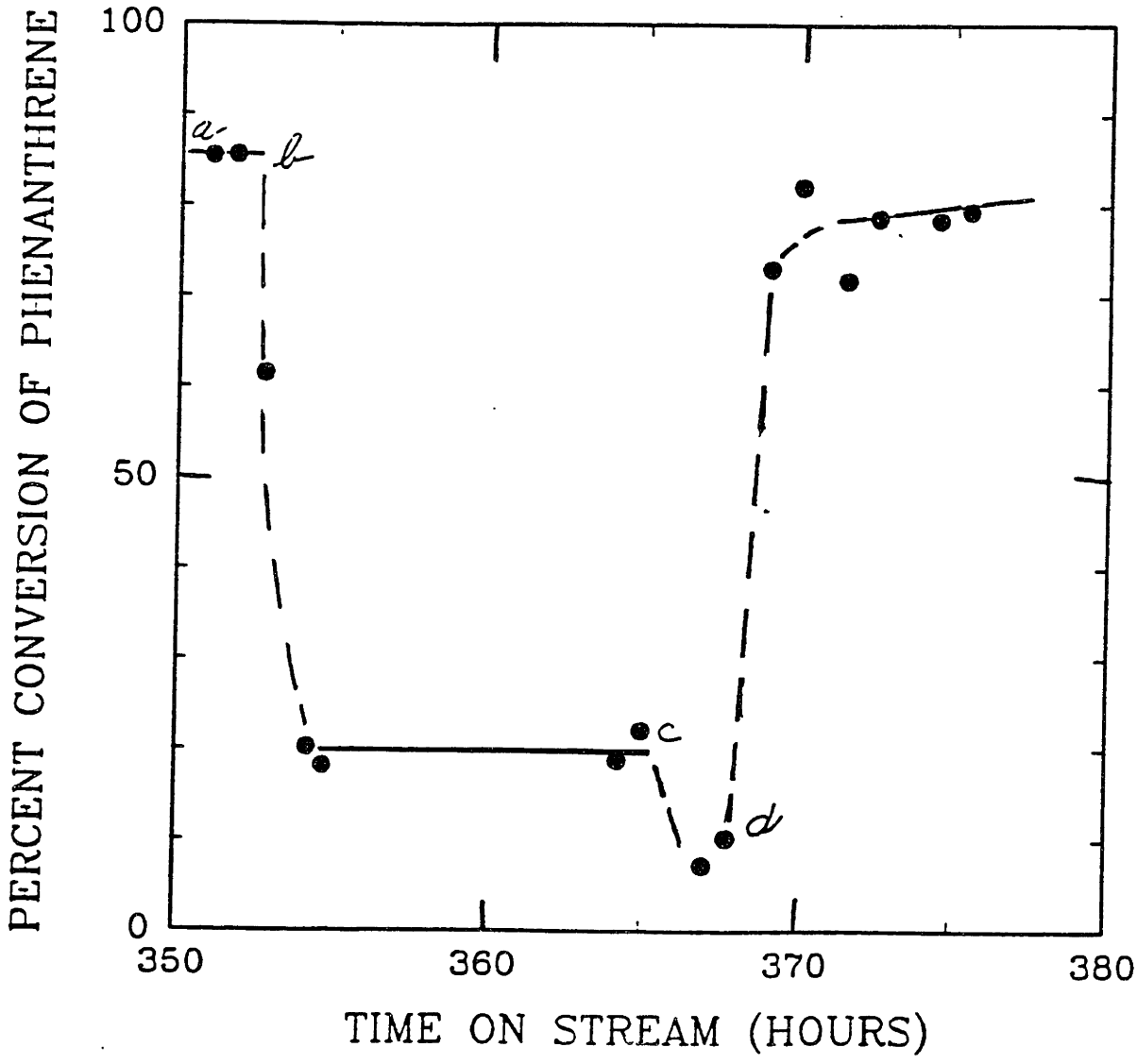

Figure VII.7 Ammonia exposure increases rate of activity recovery.

VII.D Discussion

Brief exposure of an aged Ni-Mo catalyst to an equimolar mixture of NH_3 and H_2 at 7 MPa was found to enhance the catalyst activity for the HDO of dibenzofuran for roughly 150 hours. Almost no conversion of the reactant actually occurred while the ammonia was being fed. Catalyst activity reached a maximum immediately after the NH_3 was removed from the system; the catalyst activity then slowly declined towards its previous deactivated level.

It is interesting to note that the time required for the catalyst to return to its level prior to ammonia exposure is on the same order as the time required for a fresh catalyst to deactivate to a stable activity. Since the initial deactivation period is thought to be due to coke formation, this suggests that ammonia may enhance the activity by removing the adsorbed coke or coke precursors from the catalyst surface. An equilibrium level of coke then may reform on the catalyst surface, returning the activity to its previous level.

Coking experiments (batch 23) also provided information on the operating conditions which produce the greatest enhancement in catalytic activity. Exposure of the Ni-Mo catalyst to ammonia was capable of increasing the activity for the HDO of dibenzofuran from conversions as low as 22% up to 57%. The latter activity was not stable, but deactivated to 45% conversion after 40 hours on stream. Under identical conditions, the conversion of DBF obtained on a catalyst deactivated in a normal manner is approximately 50-55 %. Ammonia treatment may thus be able to recover the activity lost by severe coking under helium and return the catalyst activity close to its equilibrium level.

Treatment with ammonia was found to have the greatest effect in the presence of 12 kPa of H_2S. It is possible that a high partial pressure of

ammonia can remove sulfur from the catalyst (it is known that pure hydrogen can), and the hydrogen sulfide may serve to re-sulfide the surface. It is interesting to note that intermittent exposure to H_2S during ammonia treatment was also effective. Removal of sulfur from the surface could also help to dislodge adsorbed coke precursors.

Flushing the catalyst with a liquid was found to increase the catalytic activity even in the absence of ammonia. It is possible that the liquid flow over the particles aids in the removal of high molecular weight coke precursors from the catalyst surface. This implies that catalyst life should be greater in a trickle-bed or slurry reactor than in a vapor phase fixed-bed reactor.

The studies on catalyst poisoning by PyTHQ at 250°C may also provide an explanation for the effect of ammonia. PyTHQ strongly inhibited the hydrogenation of phenanthrene, and desorption of this poison proceeded at a very slow rate. Exposure of the PyTHQ poisoned catalyst to 4 kPa of decylamine or 100 kPa of NH_3 produced even greater inhibition; however, complete recovery of activity occurred more rapidly in this case.

The results indicate that NH_3 and decylamine enhance the desorption of PyTHQ. From the strong inhibition of hydrogenation produced by NH_3 and decylamine, it is clear that these species adsorb strongly. It is also plausible that they could adsorb competitively and could displace the pre-adsorbed PyTHQ. Since NH_3 and decylamine desorb rapidly, a rapid recovery of activity is observed after they are removed from the system. Possibly a similar effect is occurring when ammonia is passed over the catalyst at 3.5 MPa, with ammonia aiding in the desorption of coke precursors.

VII.E Summary and Conclusions

1. Exposing a Ni-Mo catalyst which has been deactivated in model compound experiments to an ammonia/hydrogen mixture enhances the activity of the catalyst for dibenzofuran HDO. Enhancement of activity is greatest if some H_2S is also present (12kPa). The enhancement appears to be temporary, with the activity returning to its previous stable level after several days.

2. Passing a liquid over a catalyst which has been deactivated by coking in the vapor phase also produces an enhancement in activity. The presence of a liquid phase also appears to increase the effectiveness of ammonia exposure. The activity of a severely coked catalyst could be returned almost to a normal activity by ammonia exposure.

3. Low levels of ammonia can aid in the removal of a strongly adsorbed poison (PyTHQ) from the catalyst at 250°C.

4. The results are consistent with ammonia aiding in the desorption of coke precursors from the catalyst surface. The presence of a liquid phase may also help to flush away the high molecular weight material.

5. If the preceding explanation is correct, the enhancement of activity is only temporary since coke levels return to normal levels once the NH_3 is removed. Ammonia treatment of catalyst may still be useful if it can prevent long-term deactivation of the catalyst. Any benefits could only be established with long-term studies using real feeds.

OVERALL SUMMARY AND CONCLUSIONS

1. The HDO of dibenzofuran, studied separately, occurred at approximately the same rate as the hydrodenitrogenation of quinoline over a sulfided $NiMo/Al_2O_3$ catalyst at 360°C and 7 MPa. DBF was the least reactive of a number of oxygenates including 2-phenylphenol and 2-cyclohexylphenol.

2. Dibenzofuran was found to react by two parallel pathways; through 2-phenylphenol, a hydrogenolysis pathway, and through 1,2,3,4-tetrahydrodibenzofuran, a hydrogenation pathway. The initial disappearance of DBF was the rate limiting step.

3. Nitrogen poisoning of commercial NiMo catalysts is severe. This suggests that improved catalysts for the processing of heavy feeds will require greater hydrodenitrogenation activity. Current catalysts have been developed and optimized for hydrodesulfurization, not for HDN.

4. The inhibition of thiophene HDS by various nitrogen compounds and PAH's was adequately described by Langmuir-Hinshelwood kinetics. Inhibitor adsorption equilibrium constants derived from Langmuir-Hinshelwood kinetics ranged over two orders of magnitude, with basic nitrogen compounds adsorbing most strongly.

5. Adsorption strength of the inhibitors increased in the order: ammonia < aniline < pyridine < piperidine, quinoline. This inhibition order generally agrees with previous studies on the poisoning of hydroprocessing catalysts.

6. Ammonia exhibits the weakest adsorption among the nitrogen compounds. This implies that interstage removal of ammonia in a hydrotreater should be beneficial only at relatively high HDN conversions.

7. Adsorption equilibrium constants correlated with gas phase basicity in the form: $\ln K \alpha$ (Proton Affinity)/RT.
This relation appears to hold for non-sterically hindered species over a wide range of temperatures (300-400°C). The form of the correlation can be rationalized if the heat of adsorption of an inhibitor varies directly with its proton affinity.

8. Calculated heats of adsorption varied from 10 to 25 kcal/mol and showed an increasing trend with gas phase basicity. The magnitude of the heats of adsorption indicates that raising the temperature might not be particularly effective in reducing the extent of poisoning but might increase nitrogen conversion.

9. Similar inhibition phenomena were observed for both the HDS of thiophene and HDO of dibenzofuran, and this suggests that these two reactions proceed on the same catalytic site. Langmuir-Hinshelwood kinetics adequately modelled simultaneous HDO and HDN reactions.

10. With feeds containing both aromatic nitrogen and DBF, the reaction rate for DBF hydrodeoxygenation increased dramatically at a position in the reactor at which a high conversion of the nitrogen had been achieved. Similar behavior in a commercial reactor could produce a hot zone within the catalyst bed.

11. The results suggest that the low reactivity of HDO observed industrially may be caused by catalyst poisoning.

12. A trickle bed reactor model which accounts for vapor-liquid equilibrium can describe observed trends in conversion resulting from changes in operating conditions. Both theory and experiment show that the greatest effect on conversion of changing gas/liquid feed ratio occurs when liquid volatility is low and when the absolute difference in volatilities between reactant and liquid is large.

REFERENCES

Akgerman, A., Collins, G.M., and Hook, B.D., Ind. Eng. Chem. Fund., 24, 398 (1985).

Anderson, E.V., Chem. & Eng. News, 65(27), 7-13 (1987).

Arnoldy, P., van den Heijkant, J.A.M., De Bok, G.C., and Moulin, J.A., J. Catal., 92, 35 (1985).

Aue, D.H., Webb, H.M., and Bowers, M.T., J. Am. Chem. Soc., 98, 318 (1976a).

Aue, D.H., Webb, H.M., Bowers, M.T., Liotta, C.L., Alexander, C.J., and Hopkins, H.P.Jr., J. Am. Chem. Soc., 98, 854 (1976b).

Badilla-Ohlbaum, R. and Chadwick, D., Fuel, 58, 834 (1979a).

Badilla-Ohlbaum, R., Pratt, K.C., and Trimm, D.L., Fuel, 58, 309 (1979).

Bandyopadhyay, S., Massoth, F.E., Pons, S., and Eyring, F.E., J. Physical Chem., 89, 2560 (1985).

Benesi, H.A., J. Catal., 28, 176 (1973).

Bhinde, M.V., "Quinoline Hydrodenitrogenation Kinetics and Reaction Inhibition", thesis, U. of Delaware, Newark (1979).

Bogdanor, J.M. and Rase, H.F., Ind. Eng. Chem. Prod. Res. Dev., 25, 220 (1986).

Bredenberg, J.B., Huuska, M., Raty, J., and Korpio, M., J. Catal., 77, 242 (1982).

Broderick, D.H. and Gates, B.C., A.I.Ch.E. J., 27, 663 (1981).

Brown, F.R. and Karn, F.S., Fuel, 59, 431 (1980).

Brown, R.S. and Tse, A., J. Am. Chem. Soc., 102, 5222 (1980).

Bucklin, R. and Mackey, J.D., Chem. Eng. Progr., 80, 63 (1984).

Cocchetto, J.F. and Satterfield, C.N., Ind. Eng. Chem. Proc. Des. Dev., 15, 272 (1976).

Cocchetto, J.F. and Satterfield, C.N., Ind. Eng. Chem. Proc. Des. Dev., 20, 49 (1981).

Collins, G.M., Hess, R.K., and Akgerman, A., Chem. Eng. Comm., 35, 281 (1985).

Corma, A., Forres, V., Monton, J.B.,and Orchilles, A.V., Ind. Eng. Chem. Res., 26, 882-886 (1987).

Cronauer, D.C., Jewell, D.M., Shah, Y.T., and Modi, R.J., Ind. Eng. Chem. Fund., 18(2), 153 (1979).

Cusumano, J.A., Dalla Betta, R.A., and Levy, R.B., Catalysis in Coal Conversion, Academic Press (1978).

Dalling, D.K., Haider, G., Pugmire, R.J., Shabtai, J., and Hull, W.E., Fuel, 63, 525 (1984)

Deeba, M. and Hall, W.K., J. Catal., 60, 417 (1979).

Delmon, B., ACS Div. Petr. Chem., Prepr., 22, 503 (1977).

Desikan, P. and Amberg, C.H., Can. J. Chem., 42, 843 (1964)

Ebel, F., Helv. Chim. Acta, 12, 3 (1929).

Elliott, D.C., ACS Div. Petr. Chem., Prepr., 28, 667 (1983).

Fishel, N.A., Auvil, S.R., and Gross, D.E., in Catalysis in Organic Synthesis, W.H. Jones, ed., Academic Press, New York, p. 119 (1980).

Fu, C. and Schaffer, A.M., Ind. Eng. Chem. Prod. Res. Dev., 24, 68 (1985).

Furimsky, E., Erdol Kohle, 35, 455 (1982a).

Furimsky, E., Fuel Proc. Tech., 6, 1 (1982).

Furimsky, E., "Chemistry of Catalytic Hydroprocessing", Catl. Rev. - Sci. Eng., 25(3), 421 (1983a)

Furimsky, E., App. Catal., 6, 159 (1983b).

Furimsky, E., Ind. Eng. Chem. Prod. Res. Dev., 22, 426 (1983c).

Furimsky, E., Mikhlin, J.H., Jones, D.Q., Adley, T., and Baikowitz, H., Can. J. Chem. Eng., 64, 982 (1986).

Gevert, B.S., Otterstedt, J.E., and Massoth, F.E., Applied Catal., 31, 119 (1987).

Grandy, D.W. and Petrakis, L., ACS Div. Fuel Chem., Prepr., 29(6), 40 (1984).

Gultekin, S., Ali, S.A., and Satterfield, C.N., Ind. Eng. Chem. Proc. Des. Dev., 23, 179 (1984).

Gutberlet, L.C. and Bertolacini, R.J., Ind. Eng. Chem. Prod. Res. Dev., 22, 246 (1983).

Haider, G., "Catalytic Hydrogenation of Coal Derived LIquids and Related Oxygen Containing Compounds", thesis, Univ. of Utah, Univ. Microfilms Int. no. DA8203386, p. 252 (1981).

Hall, C.C. and Cawley, C.M., J. Soc. of Chem. Ind., 58(7), 7 (1939).

Hallie, H., Oil Gas J., 80, 69 (1982).

Hara, T., Jones, L., Li, N.C., and Tewari, K.C., Fuel, 60, 1143 (1981).

Harvey, T.G., Matheson, T.W., Pratt, K.C., and Stanborough, M.S., Ind. Eng. Chem. Proc. Des. Dev., 25, 521 (1986).

Heller, S.R. and Milne, G.W.A., EPA/NIH Mass Spectral Data Base; NSRDS-NBS 63, Suppl., U.S. Govt. Printing Office, Washington, D.C. (1980).

Hertz, H.S., Brown, J.M., Chesler, S.N., Guenther, F.R., Hilpert, L.R., May, W.E., Paris, R.N., and Wise, S.A., Anal. Chem., 52(11), 1650 (1980).

Himmelblau, D.M., Jones, C.R., and Bischoff, K.B., Ind. Eng. Chem. Fund., 6, 539 (1967).

Hirschon, A.S., Laine, R.M., and Wilson, R.B., Jr., Prepr. - ACS Div. Petrol. Chem., 32(2), 268 (1987).

Hirschon, A.S., Wilson, R.B., Jr., and Laine, R.M., ACS Div. Fuel Chem., 30(2), 298 (1985).

Ho, T.C.,'Hydrodenitrogenation Catalysis', unpublished (1987).

Ho, T.C., Montagna, A.A., and Steger, J.J., Proc., 8th Int. Congr. on Catalysis, Berlin (West), vol. II, p. 257, Verlag Chemie, Weinheim (1984).

Hoffman, H.L., Hydrocarbon Proc., 2, 41 (1987).

Houalla, M., Nag, N.K., Sapre, A.V., Broderick, D.H., and Gates, B.C., A.I.Ch.E. J., 24, 1015 (1978).

Huttinger, K.J. and Kirrman, H., Erdol Kohle, 36(1), 17 (1982).

Kamiya, Y., Yao, T., and Oikawa, S., ACS Div. Fuel Chem., Prepr., 24(2), 116 (1979).

Kirsch, F.W., Shalit, H., and Heinemann, H., Ind. Eng. Chem., 51, 1379 (1959).

Kocis, G.R. and Ho, T.C., Chem. Eng. Res. Dev., 64, 288 (1986).

Krishnamurthy, S., Ph.D. Thesis, University of Pittsburgh (1980).

Krishnamurthy, S., Panvelker, S., and Shah, Y.T., A.I.Ch.E. J., 27, 994 (1981).

Krishnamurthy , S. and Shah, Y.T., Chem. Eng. Comm., 16, 109 (1982).

Lange's Handbook of Chemistry, 13th Ed., J.A. Dean, ed., McGraw-Hill (1985).

Lau, Y.K., Saluja, P.P.S., Kebarle, P., and Alder, R.W., J. Am. Chem. Soc., 100, 7328 (1978).

Lee, H.C. and Butt, J.B., J. Catal., 49, 320 (1977).

Lee, C. and Ollis, D.F., J. Catal., 87, 325 (1984a).

Lee, C. and Ollis, D.F., J. Catal., 87, 332 (1984b).

Levenspiel, O., Chemical Reaction Engineering, John Wiley & Sons, New York p. 287 (1972).

Li, C.-L., Katti, S.S., Gates, B.C., and Petrakis, L., J. Catal., 85, 256 (1984).

Li, C.-L., Xu, Z.-R., Cao, Z.-A.,and Gates, B.C., A.I.Ch.E. J., 31, 170 (1985a).

Li, C.-L., Xu, Z.-R., Gates, B.C., and Petrakis, L., Ind. Eng. Chem. Proc. Des. Dev., 24, 92 (1985b).

Lin, H., Sebastian, H.M., Chao, K., J. Chem. Eng. Data, 25, 252 (1980).

Lo, H., Ph.D. thesis, Univ. of Delaware (1981).

Maatman, R.W., Lago, R.M., and Prater, C.D., Advances in Catalysis, 9, 531, Academic Press, New York (1957).

Mallinson, R.G., Chao, K.C., and Greenhorn, R.A., ACS Div. Fuel Chem., Prepr., 25(4), 120 (1980).

Massoth, F.E., J. Catal., 47, 316 (1977)

Massoth, F.E. and Miciukiewicz, J., J.Catal., 101, 505 (1986).

McClennen, W.H., Meuzelaar, H.L.C., Metcalf, G.S., and Hill, G.R., Fuel, 62(12), 1422 (1983)

McIlvried, H.G., Ind. Eng. Chem. Proc. Des. Dev., 10, 125 (1971)

Meot-Ner, M.J., J. Am. Chem. Soc., 101, 2396 (1979).

Messenger, L. and Attar, A., Fuel, 58, 655 (1979).

Miciukiewicz, J., Zmierczak, W., and Massoth, F.E., Proc., 8th Int. Congr. on Catal., vol. II, p. 671, Verlag Chemie, Weinheim (1984).

Mills, G.A., Boedeker, E.R., and Oblad, A.G., J. Amer. Chem. Soc., 72, 1554 (1950).

Mitchell, T.O., Coal Proc. Tech., 6, 28 (1980).

Nagai, M., Ind. Eng. Chem. Prod. Res. Dev., 24, 489 (1985).

Nagai, M. and Kabe, T., J. Catal., 81, 440 (1983).

Nagai, M., Sato, T., and Aiba, A., J. Catal., 97, 52 (1986).

Nalitham, R.V., Guin, J.A., Tarrer, A.R., and Curtis, C.W., Ind. Eng. Chem. Proc. Des. Dev., 24, 598 (1985).

Odebunmi, E.O. and Ollis, D.F., J. Catal., 80, 56-64 (1983a).

Odebunmi, E.O. and Ollis, D.F., J. Catal., 80, 65-75 (1983b).

Odebunmi, E.O. and Ollis, D.F., J. Catal., 80, 76-89 (1983c).

Olive, J.-L., Biyoko, S., Moulinas, C., and Geneste, P., Applied Catal., 19, 165 (1985).

Owens, P.J. and Amberg, C.H., Advan. Chem. Ser., 32, 182 (1961).

Petrakis, L., Young, D.C., Ruberto, R.G., and Gates, B.C., Ind. Eng. Chem. Proc. Des. Dev., 22, 298 (1983).

Plank, C.J. and Nace, D.M., Ind. Eng. Chem., 47, 2374 (1955).

Pratt, K.C. and Christoverson, V., Fuels Proc. Tech., 8, 43 (1983).

Prausnitz, J.M., Anderson, T., Grens, E., Eckert, C., Hsieh, R. and O'Connell, J., Computer Calculations for Mulicomponent Vapor-Liquid and Liquid-Liquid Equilibria, Prentice-Hall, New Jersey, (1980).

Ramaswamy, A.V., Sharma, L.D., Singh, A., Singhal, M.L., and Sivasanker, S., Appl. Catal, 13, 311 (1985).

Reid, R.C., Prausnitz, J.M., and Poling, B.E., The Properties of Gases and Liquids, 4th ed., McGraw-Hill, New York (1987).

Rollmann, L.D., J. Catal., 46, 243 (1977).

Sapre, A.V. and Gates, B.C., Ind. Eng. Chem. Proc. Des. Dev., 21, 86 (1982).

Satterfield, C.N., A.I.Ch.E. J., 21, 209 (1975).

Satterfield, C.N., Heterogeneous Catalysis in Practice, McGraw-Hill, New York (1980).

Satterfield, C.N., Mass Transfer in Heterogeneous Catalysis, Robert E. Krieger Publishing Co., Huntington, N.Y. (1981).

Satterfield, C.N. and Cocchetto, J.F., Ind. Eng. Chem. Proc. Des. Dev., 20, 53 (1981).

Satterfield, C.N. and Gultekin, S., Ind. Eng. Chem. Proc. Des. Dev., 20, 62 (1981).

Satterfield, C.N., Modell, M., and Mayer, J.F., A.I.Ch.E. J., 21, 1100 (1975).

Satterfield, C.N., Modell, M., and Wilkens, J.A., Ind. Eng. Chem. Proc. Des. Dev., 19, 154 (1980).

Satterfield, C.N. and Roberts, G.W., A.I.Ch.E. J., 14, 159 (1968).

Satterfield, C.N. and Smith, C.M., Ind. Eng. Chem. Proc. Des. Dev., 25, 942 (1986).

Satterfield, C.N. and Yang, S.H., J. Catal., 81, 335 (1983).

Satterfield, C.N. and Yang, S.H., Ind. Eng. Chem. Proc. Des. Dev., 23, 11 (1984).

Scaroni, A.W. and Jenkins, R.G., A.C.S. Div. Petr. Chem. - Prepr., 30(3), 544 (1985).

Schuit, G.C.A. and Gates, B.C., A.I.Ch.E. J., 19, 417-438 (1973).

Schuman,S.C. and Shalit, H., Catal. Rev., 4(2), 245 (1970).

Schwager, I., Farmanian, P.A., and Yen, T.F., Adv. Chem. Ser., 170, 67 (1978).

Shah, Y.T. and Cronauer, D.C., Catal. Rev. - Sci. Eng., 20, 209 (1979).

Shih, S.S., Katzer, J.R., Kwart, H., and Stiles, A.B., ACS Div. Petr. Chem., Prepr., 22, 919 (1977)

Schulz, H., Rahman, N.M., Kordokuzis, G., and Sharma, L.D., Proc. Int. Conf. on Coal Science, Maastricht, 1987, ed. K.A. Nater, Elsevier Scince, New York, to be published.

Shukla, Y.V., Ph.D. thesis, Univ. of Utah (1985).

Singhal, G.H., Espino, R.L., Sobel, J.E., J. Catal., 67, 446 (1981a).

Singhal, G.H., Espino, R.L., Sobel, J.E., and Huff, G.A., Jr., J. Catal, 67, 457 (1981b).

Sivaraman, A. and Kobayashi, R., J. Chem. Eng. Data, 27, 264 (1982).

Smith, C.M., Ph.D. thesis, MIT (1985).

Smith, C.M. and Satterfield, C.N., Chem. Eng. Sci., 41, 839 (1986).

Smith, J.M., Chemical Engineering Kinetics, 3rd ed., McGraw-Hill, New York, p. 88 (1981).

Snyder, L.R., ACS Div. Petr. Chem., Prepr., 15(2), C44-C62 (1970).

Taft, R.W., in Progress in Physical Organic Chemistry, R.W. Taft, ed., John Wiley and Sons, 14, 247 (1983).

Tamm, P.W., Harnsberger, H.F., and Bridge, A.G., Ind. Eng. Chem. Proc. Des. Dev., 20, 262 (1981).

Thakkar, V.P., Baldwin, R.M., and Bain, R.L., Fuel Proc. Tech., 4, 235 (1981).

Thakur, D.S. and Thomas, M.G., Ind. Eng. Chem. Prod. Res. Dev., 23, 349 (1984).

Thakur, D.S. and Thomas, M.G., Appl. Catal, 15, 197 (1985).

Topsoe, H. and Clausen, B.S., Catal. Rev. - Sci. Eng., 26, 395 (1984).

Van Klinken, J. and van Dongen, R.H., Chem. Eng. Sci., 35, 59 (1980).

Weigold, H., Fuel, 61, 1021 (1982).

Weisser, O. and Landa, S., Sulphide Catalysts, Their Properties and Applications, Pergamon, New York (1973).

White, C.M., Jones, L., and Li, N.C., Fuel, 62, 1397 (1983).

White, C.M. and Li, N.C., Anal. Chem., 54, 1564 (1982a).

White, C.M. and Li, N.C., Anal. Chem., 54, 1570 (1982b).

Yang, S.H. and Satterfield, C.N., Ind. Eng. Chem. Proc. Des. Dev., 23, 20 (1984).

Yoshimura, Y., Shimada, H., Sato, T., Kubota, M., and Nishijima, A., Appl. Catal., 29, 125 (1987).

Young, G.W., J. Phys. Chem., 90, 4894 (1986).

Appendix A1 Catalyst Specifications (Manufacturer's Data)

	American Cyanamid Catalyst		
	HDS-3A	HDS-1442B	MHC-110
Support	alumina	alumina	55 % Al_2O_3 45 % SiO_2
MoO_3 (wt %)	15.4	15.9	23.8
NiO (wt %)	3.2	0	3.7
CoO (wt %)	0	3.2	0
P (wt %)	1.4	—	3.6
Compacted bulk density (g/cm^3)	0.72	0.56	0.83
Surface area (m^2/g)	176	282	223
Pore volume (cm^3/g)	0.60	0.83 (H_2O)	—

Appendix A1 Catalyst Properties (Manufacturer's Data)

American Cyanamid's HDN-60

Composition	wt %
MoO_3	22.1
NiO	3.2
P	3.3
Na_2O	0.006
SO_4	0.16
Al_2O_3	balance
Porosity	
Surface area (N_2)	157 m^2/g
Pore volume (H_2O)	0.44 ml/g
Pore volume (Hg)	0.36 ml/g
Compacted bulk density	0.81 g/ml
particle density	1.504 g/ml

Appendix A2 Brief Description of Catalyst Batches

Batch 20 - (1.6 g. HDS-3A) Deactivation with quinoline and no H_2S. Initial experiments on HDO of DBF: effects of H_2S, H_2O, and hydrogen pressure. Catalyst replaced after exposure to high levels of ammonia.

Batch 21 - (1.6 g. HDS-3A) Catalyst initially operated as the oxide. Deactivated with DBF and no H_2S.
After sulfiding: experiments on intermediates in HDO of DBF.

Batch 22 - (1.6 g. HDS-3A) Deactivated with quinoline and no H_2S. Determined the kinetics for DBF at four temperatures. Catalyst exposed to high levels of ammonia and replaced.

Batches 23-25 - Coking experiments with anthracene under He pressure.

Batch 26 - (1.6 g. HDS-3A) Deactivated witth quinoline and no H_2S. Investigated effect of H_2S on DBF hydrodeoxygenation in detail. Experiments with DBF/biphenyl mixtures.
Initial experiments with dibenzothiophene and quinoline at 260°C.

Batch 27 - (1.6 g. Co-Mo catalyst) Deactivated in presence of DBF and H_2S. Experiments on HDO of DBF.

Batch 28 - (1.6 g. HDS-3A) Deactivated with DBF and H_2S. Experiments with HDO intermediates. Study on the poisoning of dibenzofuran HDO by nitrogen compounds.

Batch 29 - (1.6 g. MHC-110) Deactivated with DBF and H_2S. Experiments on the reactions of quinoline and DBF.

Batch 30 - (20 mg HDS-3A) Initial experiments on the poisoning of thiophene HDS at 360 °C and with no sulfur compound added to the feed. Interactions between dibenzothiophene and nitrogen

compounds also studied at 360 °C.

Batch 31 - (25 mg HDS-3A) Effect of H_2S on thiophene HDS. Poisoning of thiophene HDS by nitrogen compounds at 360 °C. 24 kPa of additional sulfur compoound added

Batch 32 - (25 mg HDS-3A) Poisoning of thiophene HDS by nitrogen compounds at 360 °C; 24 kPa of sulfur compound added.

Batch 33 - (1.6 g. HDS-3A) Catalyst disposed of after one week.

Batch 34 - (1.6 g. HDN-60 Catalyst; Ni-Mo/Al_2O_3 rifled catalyst). Brief experiment on the HDO of dibenzofuran. Simultaneous reaction studies on the HDN of 2-ethylaniline and the HDO of 2-phenylphenol.

Batch 35 - (2 g. HDS-3A) Poisoning of thiophene HDS at 250 °C. Poor reproducibility of poisoning results.

Batch 36 - (0.25 g. HDS-3A) Poisoning of thiophene HDS at 300 °C.

Batch 37 - (10 mg HDS-3A; crushed to 75-106 microns) HDO of 2-cyclohexylphenol at moderate conversions. Poisoning of thiophene HDS at 400 °C.

Batch 38 - (2 g. HDS-3A) Check on batch 35 on poisoning of thiophene HDS by nitrogen compounds. Poor reproducibility; probably due to irreversible adsorption of catalyst poisons.

Batch 39,40 - Purification of phenanthrene (removal of dibenzothiophene) using HDS-3A.

Batch 41 - (HDS-3A) Studies on irreversible poisoning by nitrogen compounds at 250 °C. Poisoning of phenanthrene hydrogenation.

Batch 42 - (0.8 g. HDS-3A) Trickle-bed reactor experiments on the HDO

of DBF and the hydrogenation of butylbenzene. Varied gas-to-liquid flow rate and liquid carrier. Comparison of vapor and trickle-bed operation.

Appendix A3 Mass Spectra for the Identified Products of Dibenzofuran

Retention Time (min)	Component
1.78	methylcyclopentane

Lower Abundance Cutoff Level = 10.0%

MASS	ABUNDANCE (%)	MASS	ABUNDANCE (%)	MASS	ABUNDANCE (%)
18.05	13.1	39.05	37.9	52.95	10.1
27.05	43.6	41.05	82.9	55.05	28.5
27.95	31.8	42.05	39.6	56.05	100.0
29.05	12.3	42.95	16.7	69.05	37.1

2.08	benzene

Lower Abundance Cutoff Level = 10.0%

MASS	ABUNDANCE (%)	MASS	ABUNDANCE (%)	MASS	ABUNDANCE (%)
27.05	11.6	51.05	30.8	77.05	33.5
39.05	21.8	52.05	28.1	78.05	100.0
50.05	26.9				

2.20 cyclohexane

Lower Abundance Cutoff Level = 10.0%

MASS	ABUNDANCE (%)	MASS	ABUNDANCE (%)	MASS	ABUNDANCE (%)
27.05	41.3	41.05	82.4	56.05	100.0
28.05	17.4	42.05	35.0	69.05	26.9
29.05	15.2	43.05	13.9	84.05	52.1
39.05	38.8	55.05	40.5		

2.46 cyclohexene

Lower Abundance Cutoff Level = 10.0%

MASS	ABUNDANCE (%)	MASS	ABUNDANCE (%)	MASS	ABUNDANCE (%)
11.55	20.1	28.05	23.0	54.05	54.5
12.95	12.8	28.85	11.4	67.05	100.0
17.15	12.0	38.95	54.8	77.05	10.5
17.95	30.9	40.95	44.6	79.05	11.4
24.15	10.8	42.25	12.8	80.95	10.2
26.05	10.5	49.95	20.1	82.05	40.2
27.05	44.9	50.95	17.2		

3.42 methylcyclohexane

Lower Abundance Cutoff Level = 10.0%

MASS	ABUNDANCE (%)	MASS	ABUNDANCE (%)	MASS	ABUNDANCE (%)
26.15	14.2	41.05	79.1	56.05	32.0
27.05	43.9	42.05	38.1	68.95	17.2
27.95	21.1	43.05	12.0	70.05	21.9
28.95	21.5	53.15	13.3	83.05	82.8
30.25	11.4	55.05	100.0	98.05	33.8
39.05	28.6				

33.32 cyclopentylmethyl-cyclohexane

Lower Abundance Cutoff Level = 10.0%

MASS	ABUNDANCE (%)	MASS	ABUNDANCE (%)	MASS	ABUNDANCE (%)
27.05	10.4	54.15	18.4	82.05	76.0
28.05	17.0	55.05	100.0	83.05	67.4
29.05	17.2	67.05	58.6	96.05	39.0
38.95	22.8	68.05	24.3	97.05	14.1
41.05	69.6	69.05	21.9	109.15	12.3
53.05	12.0	81.05	27.5	166.15	14.2

34.10 cyclopentylmethyl-benzene

Lower Abundance Cutoff Level = 10.0%

MASS	ABUNDANCE (%)	MASS	ABUNDANCE (%)	MASS	ABUNDANCE (%)
27.95	11.3	69.05	18.7	92.05	100.0
41.05	28.9	91.05	54.8	160.05	22.3
67.05	10.2				

34.72 dicyclohexyl

Lower Abundance Cutoff Level = 10.0%

MASS	ABUNDANCE (%)	MASS	ABUNDANCE (%)	MASS	ABUNDANCE (%)
16.05	11.0	54.05	12.7	82.05	100.0
27.95	14.8	55.05	67.3	83.05	41.8
38.95	16.1	67.05	54.2	166.05	15.8
41.05	38.1	81.15	10.7		

34.94 cyclohexylbenzene

Lower Abundance Cutoff Level = 10.0%

MASS	ABUNDANCE (%)	MASS	ABUNDANCE (%)	MASS	ABUNDANCE (%)
27.05	11.4	78.05	13.2	115.05	17.0
39.05	14.7	91.05	56.3	117.05	70.3
41.05	13.0	92.05	17.6	118.05	12.3
51.05	11.4	104.05	100.0	160.15	51.1
77.05	12.2	105.05	12.7		

37.46 biphenyl

Lower Abundance Cutoff Level = 10.0%

MASS	ABUNDANCE (%)	MASS	ABUNDANCE (%)	MASS	ABUNDANCE (%)
50.05	11.2	76.05	23.2	153.15	46.3
50.95	11.0	151.15	10.0	154.05	100.0
62.85	11.2	152.15	31.5	155.05	13.1

44.28 1,2,3,4-tetrahydro-dibenzofuran

Lower Abundance Cutoff Level = 10.0%

MASS	ABUNDANCE (%)	MASS	ABUNDANCE (%)	MASS	ABUNDANCE (%)
14.95	18.9	45.65	10.9	115.05	26.1
19.25	16.8	46.55	10.9	119.35	10.9
22.05	16.4	51.15	11.3	128.15	13.9
25.25	13.4	57.45	13.4	132.95	13.0
30.65	11.8	63.05	10.1	144.05	100.0
32.95	12.6	63.55	13.9	145.05	16.8
33.45	12.2	65.05	12.0	171.15	17.2
34.65	11.8	75.95	11.8	172.15	48.3
35.45	12.2	82.95	11.8	173.05	10.9
36.95	10.1	85.85	10.5	207.05	12.2
42.95	17.6	96.05	10.1	208.95	12.2
44.65	11.3	102.85	11.3		

Appendix A4 Mass Spectral Data for 2- and 3-Cyclohexylphenol

(Detected in the Products From 2-Cyclohexylphenol)

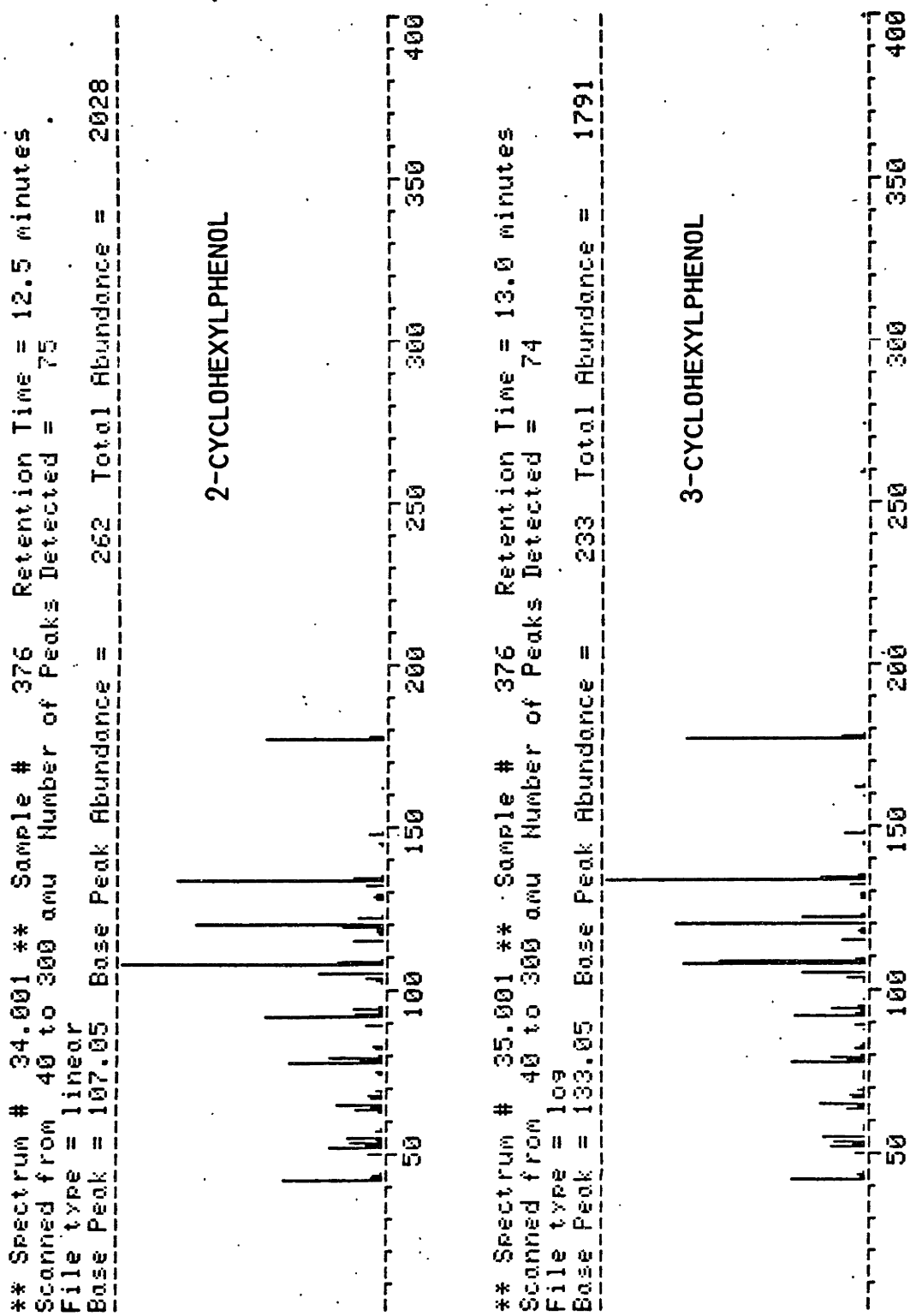

Appendix A5 Conversion Data for the Poisoning of Thiophene HDS

Tables A5.1 through A5.4 list the conversion of thiophene observed in the presence of various catalyst poisons, measured over a range of concentrations. The numbering of the inhibitors corresponds to the order in which the experiments were performed on each catalyst batch.

Table A5.1 Poisoning of Thiophene HDS on Catalyst Batch 36

The experiments were carried out at 7 MPa, 300 °C, and 18,000 SCF/bbl.

Inhibitor Partial Pressure (kPa)	% HDS of Thiophene	Inhibitor Partial Pressure (kPa)	% HDS of Thiophene
1. Ammonia		2. Aniline	
0	94.3	0	95.4
12	70.2	0.75	79.2
24	49.7	1.5	73.7
48	36.3	3.0	67.2
96	27.2	6.0	59.7
		12.0	51.7
3. Pyridine		4. PyTHQ	
0	94.5	0	94.5
0.5	45.5	0.25	55.0
1.0	38.3	0.5	48.9
2.0	30.0	2.0	37.1
4.0	23.6	4.0	30.6
8.0	14.9	8.0	22.4
16.0	11.5		
5. Piperidine			
0	93.4		
0.25	44.9		
1.0	30.8		
2.0	24.9		
4.0	18.2		
8.0	14.3		

Table A5.2 Poisoning of Thiophene HDS on Catalyst Batch 37

The experiments were carried out at 7 MPa, 400 °C, and 9,000 SCF/bbl.

Inhibitor Partial Pressure (kPa)	% HDS of Thiophene	Inhibitor Partial Pressure (kPa)	% HDS of Thiophene
1. Ammonia		2. Aniline	
0	31.7	0	26.3
6	23.5	0.75	19.0
12	19.8	1.5	16.5
24	17.9	3.0	15.3
48	14.5	6.0	13.8
96	12.5	12.0	12.2
		24.0	10.7
3. Pyridine		4. Quinoline	
0	16.4	0	16.4
0.5	13.7	0.5	10.9
2.0	10.5	1.0	10.1
4.0	10.0	2.0	7.6
8.0	8.0	4.0	6.3
16.0	6.9	8.0	4.9
		16.0	4.0

Table A5.3 Poisoning of Thiophene HDS on Catalyst Batch 31

The experiments were carried out at 7 MPa, 360 °C, and 9,000 SCF/bbl.

Inhibitor Partial Pressure (kPa)	% HDS of Thiophene
1. Ammonia	
0	64.7
0	67.4
6	56.7
12	43.5
24	38.4
48	31.7
96	17.2
2. Aniline	
0	66.6
3.0	52.9
6.0	48.4
12.0	41.3
24.0	28.6
3. Pyridine	
0	66.6
3	31.1
6	21.2
6	19.2
12	16.7
24	9.8
4. Piperidine	
0	67.2
3	20.5
6	15.4
6	14.4
12	11.7
24	8.0
5. Naphthalene	
0	59.3
3	56.1
6	54.2
12	53.1
24	52.9
6. Pyrrole	
0	57.8
6	27.7
12	20.6
24	17.5
0	45.9
7. Pyrrolidine	
0	45.8
3	14.2
6	11.9
12	11.0
24	8.8
8. Phenanthrene	
0	47.1
3	41.5
6	36.8

Table A5.4 Poisoning of Thiophene HDS on Catalyst Batch 32

The experiments were carried out at 7 MPa, 360 °C, and 9,000 SCF/bbl.

Inhibitor Partial Pressure (kPa)	% HDS of Thiophene
1. 4-Picoline	
0	70.3
3	21.9
6	13.4
12	14.1
24	10.9
3. 2-Ethylaniline	
0	64.3
3	54.7
6	46.1
0	66.1
12	37.9
24	26.0
5. BzTHQ	
0	66.2
1.5	20.4
3.0	15.8
6.0	12.7
12.0	9.2
7. Carbazole	
0	61.4
1.5	40.9
3.0	31.6
9. 2-phenylphenol	
0	66.9
3	49.8
6	48.5
12	44.9
24	43.2
11. 2,6-lutidine	
0	65.3
1.5	43.6
3.0	36.9
6.0	34.8
12.0	33.8
24.0	27.8

Inhibitor Partial Pressure (kPa)	% HDS of Thiophene
2. 1-Methylpiperidine	
0	73.9
3	34.7
6	23.6
12	26.0
24	18.7
4. PyTHQ	
0	66.1
3	26.0
6	17.0
12	18.8
24	8.6
6. DHQ	
0	65.5
1.5	20.0
3.0	15.2
6.0	12.4
12.0	7.2
8. bis 1,8-(dimethylamino)-naphthalene	
0	64.6
0.75	25.0
1.0	16.5
3.0	9.7
10. Quinoline	
0	66.5
1.5	25.5
3.0	21.1
6.0	15.9
12.0	10.4
12. acridine	
0	67.7
0.75	23.5
1.5	21.3
3.0	12.9
6.0	7.6
0	48.3

Appendix A6 Analytical Solution of the Rate Expression for Aniline

The Langmuir-Hinshelwood rate expression for the HDN of aniline is

$$\text{Rate} = \frac{dx}{d\tau} = \frac{k\ P\ (1-X)}{1 + K_{NH3} P\ X + K_A P\ (1-X)}$$

where: K_A = adsorption equilibrium constant for aniline (kPa^{-1})

K_{NH3} = adsorption equilibrium constant for ammonia (kPa^{-1})

k = rate constant (mol/[hr {g. of catalyst} kPa])

P = inlet partial pressure of aniline (kPa)

X = fractional conversion of aniline.

Rearranging this equation gives:

$$\left[\frac{1}{P\ (1-X)} + \frac{K_{NH3}\ X}{(1-X)} + K_A \right] dX = k\ d\tau$$

Separating the differential equation by terms gives

$$\int \frac{dX}{P\ (1-X)} + K_{NH3} \int \frac{X\ dX}{(1-X)} + K_A \int dX = K_A \int d\tau$$

which can be integrated to

$$\frac{-\ln(1-X)}{P} + K_{NH3} \int \frac{X\ dX}{(1-X)} + K_A\ X = k\ \tau\ .$$

Using the integration $\int \frac{X\ dX}{(1-X)} = -\ln(1-X) - X$

gives: $$\frac{-\ln(1-X)}{P} - K_{NH3} \left[-\ln(1-X) + X \right] + K_A X = k\ \tau$$

From this linear form the rate constant can be determined.

Appendix A7 Thermodynamic Data for Modelling Vapor-Liquid Equilibrium

Computer programs provided by Prausnitz and co-workers (1980) were used to estimate the vapor-liquid equilibria for the two reaction systems. Thermodynamic equilibrium requires that the fugacity of species i is the same in both phases according to

$$\gamma_i \, x_i \, f_i^{oL} = \phi_i \, y_i \, P$$

where: γ_i = activity coefficient for species i

f_i^{oL} = fugacity of pure liquid i at system temperature T (bars)

ϕ_i = fugacity coefficient for species i

P = system total pressure (bars).

Fugacity coefficients were estimated from the truncated virial equation of state, which required the following physical properties for each component:

T_c = critical temperature (K)

P_c = critical pressure (bars)

Z_{RA} = Rackett equation parameter

RD = mean radius of gyration (A°)

DM = dipole moment (D)

association and solvation parameters

Values were estimated for all of the major species present in the system; hydrocarbon products, and the reaction products of the thiol (H_2S, and C_{12}) were neglected. Critical properties were obtained from Reid et al. (1987) or were estimated by the Joback modification of Lyderson's method, a group contribution technique (Reid et al., 1987). The values used in this study are listed in Table A7.1.

Table A7.1 Physical Properties Used in the Estimation of Fugacity Coefficients for Each Species

Compound	T_c (K)	P_c (bars)	Z_{RA}	RD	DM
n-Hexadecane	722	14.0	0.239	8.32	0.0
Squalane	764	6.10	0.23	13.0	0.0
Hydrogen	33.2	13.0		0.371	0.0
Dibenzofuran	800.	36.2	0.274	6.	0.5
n-Butylbenzene	660.	28.9	0.26	4.6	0.4

The Rackett compressibility parameter was obtained from tables in Reid et al. (1987) or the compressibility factor at the critical point Z_c was used as a rough estimate. The Rackett parameter was set equal to zero to identify non-condensable species such as hydrogen.

If unavailable, dipole moments were estimated from known values for similar molecular structures. Likewise, the radius of gyration was estimated from molecular size. Values for these parameters are also listed in Table A7.1. Solvation and association parameters were estimated from values provided by Prausnitz and co-workers (1980) for similar pairs of interacting species. Since only hydrocarbons and aromatics dominated the system, all of the solvation and association parameters were set equal to zero.

Fugacity coefficients determined from the computer programs of Prausnitz et al. are listed in Table A7.3.

Condensable Species - Pure Liquid Fugacities

Pure liquid fugacities were calculated for the condensable species in the system. Saturation vapor pressures at the sytem temperature and molar liquid volumes were required. Experimental vapor pressures weere used if these were available as for dibenzofuran (Sivaraman and Kobayashi, 1982). Unknown vapor pressures could be estimated by the methor of Lee and Kesler (Reid et al., 1987, p. 207). Reference state fugacities were calculated from the equation:

$$f_i^{oL} = p_i^s \phi_i^s \quad \exp \int_{p_i^s}^{p^r} \frac{v_i^L}{R\,T} \, dP$$

where: p_i^s = saturation (vapor) pressure of pure liquid i at temp. T

ϕ_i^s = fugacity coefficient of pure saturated vapor i at temperature T and pressure p_i^s

v_i^L = molar liquid volume of pure i at temperaure T

p^r = refernce pressure for fugacity

For convenience the reference pressure is taken as $p^r = 0$ and the molar liquid volume is assumed to be a function only of temperature. ϕ_i^s was set equal to one since the vapor pressures are fairly low and the system temperature is high. Liquid molar volumes were estimated from the modified Rackett technique (Reid et al., 1987, p. 67).

Vapor pressures at 350°C and pure liquid fugacity coefficents at 350°C and 7 MPa are listed in Table A7.2. Significant differences occur only for the more volatile species n-butylbenzene.

The final equation of equilibrium for each species at pressure P and temperature T becomes:

$$\phi_i \, y_i \, P = \gamma_i^{p^r} \, x_i \, f_i^{oL} \exp \int_{p^r}^{P} \frac{v_i^L}{R \, T} \, dP$$

Here again the same reference pressure of $p^r = 0$ was used. f_i^{oL} was a requuired value, with all other values being estimated by subroutines. The liquid molar volume in the integral was calculated from the Rackett equation.

Non-condensable Species - Hydrogen was the only non-condensable species present in major amounts in the reactor. A Henry's Law constant was used for this species in the form: fugacity $f_i^V = H_i \, x_i$, and the Henry's Law constant was derived from data by Lin et al. (1980) for the hydrogen/C_{16} system. The Henry's Law constant for hydrogen in n-hexadecane was 385 bar at 350°C and 7 MPa. A Henry's Law constant of H = 192 was estimated for H_2 in squalane at the same conditions.

Table A7.2 Vapor Pressures at 350° and Pure Liquid Fugacities at 350°C and 7 MPa

Component	Vapor pressure (bars)	f_i^L (bars)
n-Hexadecane	3.293	3.20
Squalane	0.956	0.956
Dibenzofuran	3.636	3.60
n-Butylbenzene	18.11	16.46

Table A7.3 Calculated Activity and Fugacity Coefficients at 350°C, 7 MPa, and a Gas-to-Liquid Flow Ratio of 380 ml H_2/ ml Liquid.

Component	Fugacity Coefficient ϕ_i	Activity Coefficient γ_i
Hydrogen	1.00	-
n-Hexadecane	1.00	1.00
Squalane	1.100	1.106
Dibenzofuran	0.998	1.297
n-Butylbenzene	1.062	0.772

Activity coefficients for the non-condensable species were estimated by the Unifac contribution of groups method. The Unifac data file contained the group-group interaction parameters, and it was necessary only to specify the groups present in each compound. The characterization of the molecules is listed below in Table A7.4.

Table A7.4 Molecular Information Required by UNIFAC

Compound	Group Number	Quantity of such groups in molecule
n-Hexadecane	1	2
	2	14
Squalane	1	8
	2	16
	3	6
Dibenzofuran	10	8
	11	3
	18	1
n-Butylbenzene	10	5
	13	1
	2	2
	1	2

Appendix A8 Selected Computer Programs

Program 1 - Program generates species concentrations as a function of space time for the simultaneous HDO of dibenzofuran and HDN of quinoline. A fourth order Runga-Kutta routine integrates the Langmuir-Hinshelwood reaction kinetics, with concentrations based on the percent of initial reactant remaining. Program reads in HDN rate constants from file RTCONS.DAT and reads in adsorption constants for nitrogen compounds. The rate constant for the HDO of DBF is fixed.

```
C*      PROGRAM GENERATES CONCENTRATION VERSUS TIME FOR THE
C*      SIMULTANEOUS HDO OF DBF AND HDN OF QUINOLINE

        DIMENSION C0(5)
        COMMON AK(10)
        DATA C0/100.0,0.0,0.0,0.0,0.0/
C*
        OPEN(UNIT=22,ACCESS='SEQUENTIAL',STATUS='FRESH',
                FILE='COMP.DAT')
        OPEN(UNIT=23,ACCESS='SEQUENTIAL',STATUS='OLD',
                FILE='RTCONS.DAT')

        WRITE(5,160)
160     FORMAT(1X,'INPUT ADS. CONST. FOR OPA,BZ,DHQ,Q,PY,NH3')
        READ(5,*)A1,A2,A3,A4,A5,A6
C*
        READ(23,*)AK
        RK=0.00742
C*
        T=0.0
        H=10.006
        C1=C0(1)
        C2=C0(2)
        C3=C0(3)
        C4=C0(4)
        C5=C0(5)
        CDBF=100.
        WRITE(22,100)T,C0(1),C0(2),C0(3),C0(4)
C*      ENTER LOOP TO CALCULATE CONCENTRATIONS
        DO 10 I=1,65
        D=A1*C1+A2*C2+A3*C3+(.091*A4+.909*A5)*C4+A6*C5+1.
        V11 = F1(C1,C4,D)
        V12 = F2(C2,C3,C4,D)
        V13 = F3(C2,C3,C4,D)
        V14=F4(C4,D)
        V15=F5(C1,C3,D)
        RDBF1=-RK*CDBF/D
C*
```

Set up for Aniline, Should be /0.0,0.0,0.0,100.0,0.0/

```
      G=H/3.0
      XC1 = C1 + G*V11
      XC2 = C2 + G*V12
      XC3 = C3 + G*V13
      XC4=C4+G*V14
      XC5=C5+G*V15
      XDBF=CDBF+G*RDBF1
      D=A1*XC1+A2*XC2+A3*XC3+(.091*A4+.909*A5)*XC4+A6*XC5+1.
      V21=F1(XC1,XC4,D)
      V22=F2(XC2,XC3,XC4,D)
      V23=F3(XC2,XC3,XC4,D)
      V24=F4(XC4,D)
      V25=F5(XC1,XC3,D)
      RDBF2=-RK*XDBF/D
C*
      XC1 = C1 - G*V11 + H*V21
      XC2 = C2 - G*V12 + H*V22
      XC3 = C3 - G*V13 + H*V23
      XC4=C4-G*V14+H*V24
      XC5=C5-G*V15+H*V25
      XDBF=CDBF-G*RDBF1+H*RDBF2
      D=A1*XC1+A2*XC2+A3*XC3+(.091*A4+.909*A5)*XC4+A6*XC5+1.
      V31=F1(XC1,XC4,D)
      V32=F2(XC2,XC3,XC4,D)
      V33=F3(XC2,XC3,XC4,D)
      V34=F4(XC4,D)

      V35=F5(XC1,XC3,D)
      RDBF3=-RK*XDBF/D
C*
      XC1 = C1 + H*(V11 - V21 + V31)
      XC2 = C2 + H*(V12 - V22 + V32)
      XC3 = C3 + H*(V13 - V23 + V33)
      XC4=C4+H*(V14-V24+V34)
      XC5=C5+H*(V15-V25+V35)
      XDBF=CDBF+H*(RDBF1-RDBF2+RDBF3)
      D=A1*XC1+A2*XC2+A3*XC3+(.091*A4+.909*A5)*XC4+A6*XC5+1.
      V41=F1(XC1,XC4,D)
      V42=F2(XC2,XC3,XC4,D)
      V43=F3(XC2,XC3,XC4,D)
      V44=F4(XC4,D)
      V45=F5(XC1,XC3,D)
      RDBF4=-RK*XDBF/D
C*
      C1 = C1 + H/8.*(V11 + 3.*V21 + 3.*V31 + V41)
      C2 = C2 + H/8.*(V12 + 3.*V22 + 3.*V32 + V42)
      C3 = C3 + H/8.*(V13 + 3.*V23 + 3.*V33 + V43)
      C4= C4 + H/8.*(V14 +3.*V24 + 3.*V34 + V44)
      C5= C5 + H/8.*(V15 +3.*V25 + 3.*V35 + V45)
      CDBF=CDBF+H/8.*(RDBF1+3.*RDBF2+3.*RDBF3 +RDBF4)
      T= T + H
C*    IF(I/4*4.NE.I)GOTO 10
      WRITE(22,100)T,C1,C2,C3,C4,CDBF
10    CONTINUE
```

```
99        FORMAT(1X,6F10.6)
100       FORMAT(1X,7E12.6)
          STOP
          END
C*
C*FUNCTION TO CALCULATE VALUE OF DERIVATIVE
          FUNCTION F1(C1,C4,D)
          COMMON AK(10)
          F1=(AK(1)*C4 -AK(2)*C1)/D
          RETURN
          END
C*
C*        FUNCTION
          FUNCTION F2(C2,C3,C4,D)
          COMMON AK(10)
          F2=(AK(3)*C4 -AK(5)*C2 )/D
          RETURN
          END
C*
C*
          FUNCTION F3(C2,C3,C4,D)
          COMMON AK(10)
          F3=(AK(4)*C4+AK(5)*C2-AK(6)*C3)/D
          RETURN
          END
C*
C*        FUNCTION
          FUNCTION F4(C4,D)
          COMMON AK(10)
          F4=-(AK(1)+AK(3)+AK(4))*C4/D
          RETURN
          END
C*
C*        FUNCTION

          FUNCTION F5(C1,C3,D)
          COMMON AK(10)
          F5=(AK(2)*C1 +AK(6)*C3)/D
          RETURN
          END
```

Program 2 - Program was used to fit adsorption equilibrium constants to the poisoning data using Langmuir-Hinshelwood kinetics. The fitted equation was of the form Y = 1 + Ax, where Y = ratio of poisoned/poisoned first order rate constants, A = adsorption constant (kPa^{-1}), and x = inhibitor partial pressure (kPa).

```
C       PROGRAM FITS X, Y DATA TO THE EQUATION Y=1 + AX BY
C* LEAST-SQUARES REGRESSION
C*
        DIMENSION X(10),Y(10)
        OPEN (UNIT=22,ACCESS='SEQUENTIAL',STATUS='OLD',FILE=
        READ(22,*)N
C*      N IS THE NUMBER OF DATA POINTS
        READ (22,*)XK0
C*      XK0 IS THE UNPOISONED RATE CONSTANT
        DO 100 I=1,N
        READ(22,*)X(I),Y(I)
        Y(I)=XK0/Y(I)
100     CONTINUE
        XSUM=0.0
        X2SUM=0.0
        XYSUM=0.0
        DO 200 I=1,N
        XSUM=XSUM+X(I)
        X2SUM=X2SUM+X(I)**2
        XYSUM=XYSUM+X(I)*Y(I)
200     CONTINUE
        SLOPE=(XYSUM-XSUM)/X2SUM
        WRITE(5,300)SLOPE
300     FORMAT(1X,'ADSORPTION CONSTANT=',2X,F8.5)
        RES2SUM=0.0
        XDIFSUM=0.0
        XBAR=XSUM/FLOAT(N)
        DO 400 J=1,N
        RES2SUM=RES2SUM+(Y(J)-1.0-SLOPE*X(J))**2
        XDIFSUM=XDIFSUM+(X(J)-XBAR)**2
400     CONTINUE
        XMSE=RES2SUM/FLOAT(N-1)
        S2B1=XMSE/XDIFSUM
        SB1=SQRT(S2B1)
        WRITE(5,500)SB1
500     FORMAT(1X,'STAND. DEV. OF ADSORP. CONSTANT +',3X,F8.5)
        END
```